

**PELVIC NEUROVISCERAL PLASTICITY FOLLOWING
COMPLETE SPINAL CORD INJURY**

by

Diana V. Hunter

B.Sc., Simon Fraser University, 2010

A THESIS SUBMITTED IN PARTIAL FULFILLMENT OF
THE REQUIREMENTS FOR THE DEGREE OF

DOCTOR OF PHILOSOPHY

in

THE FACULTY OF GRADUATE AND POSTDOCTORAL STUDIES
(Neuroscience)

THE UNIVERSITY OF BRITISH COLUMBIA
(Vancouver)

November 2018

© Diana V. Hunter, 2018

The following individuals certify that they have read, and recommend to the Faculty of Graduate and Postdoctoral Studies for acceptance, the dissertation entitled:

Pelvic neurovisceral plasticity following complete spinal cord injury

submitted by **Diana V. Hunter** in partial fulfillment of the requirements for
the degree of **Doctor of Philosophy**
in **Neuroscience**

Examining Committee:

Dr. Matthew Ramer

Supervisor

Dr. Tim O'Connor

Supervisory Committee Member

Dr. Brian Cairns

University Examiner

Dr. Colleen Nelson

University Examiner

Additional Supervisory Committee Members:

Dr. Stacy Elliott

Supervisory Committee Member

Dr. Chris Maxwell

Supervisory Committee Member

Abstract

Spinal cord injury (SCI) interrupts communication between the brain and peripheral organs resulting in profound and long-lasting effects, including clinically important dysfunction of the pelvic viscera (PV). Sensory and autonomic peripheral neurons innervating the PV are contained in the dorsal root ganglia (DRG) and pelvic ganglia (PG), respectively. Previous studies have identified changes in these neurons after SCI, but questions remain about the relationship between injury level and changes in peripheral targets and ganglia. In this dissertation, I addressed these questions using male Wistar rats with a high thoracic transection (T3x), which eliminates the majority of supraspinal connections to sympathetic preganglionics (including those innervating the splanchnic bed and adrenal glands), or a high lumbar transection (L2x), which preserve these connections but directly damage neurons innervating the pelvic peripheral ganglia and PV.

I examined gene expression changes in DRGs and PGs one month post-T3x using RNA sequencing and found indications for unexpected neuron-target interactions, including changes in growth factor signaling and cell communication. In the PG, decreased expression of tyrosine hydroxylase (TH) after T3x was supported by atrophy of sympathetic (TH-positive) neurons. SCI results in bladder hypertrophy, and though L2x resulted in increased bladder weights compared to both T3x and naïve animals, the expression of TH in the PG decreased and TH-positive neuron hypertrophy was only transient. These results indicate a more complex relationship between target size and neurotrophism than generally accepted.

Examination of PV changes after high and low SCI revealed different patterns of bladder activity. Two days after injury, there was augmented bladder activity at low intravesical pressures in L2x compared to T3x and naïve animals. I found that disrupting signal transmission

through the PG did not change the bladder activity patterns, however, bilateral adrenalectomy concurrent to L2x resulted in bladder activity patterns that more closely resembled the T3x injury. Further to this, circulating catecholamine levels were higher in animals with intact innervation to the adrenal gland, implicating adrenal function in bladder changes after SCI.

The findings in this thesis highlight the importance of studying injury level both from the perspective of both local circuitry and systemic changes.

Lay Summary

Spinal cord injury (SCI) results in all body systems, including pelvic organ dysfunction which plays an important role in the quality of life for individuals with SCI. The peripheral sensory and autonomic neurons that directly connect to the pelvic organs, found in dorsal root ganglia (DRG) and pelvic ganglia (PG) respectively, are impacted by the injury itself and by changes in their target organs. In this work, I used male rats to model how the DRG, PG, and bladder respond differently to high and low SCI. I found gene expression and cell size changes in the ganglia that indicate a more complex relationship between target and neuron changes than previously reported. I also found different patterns of bladder activity after high and low injury that are linked to preserved adrenal function after lower injuries. These findings highlight the importance of looking at both local and systemic changes after SCI.

Preface

I wrote **Chapter 1** with editing help from Drs. L.M. and M.S. Ramer.

Experiments in **Chapter 2 and 3** were designed by myself, and Drs. L.M. and M.S. Ramer. Surgeries and animal care were performed by myself and Dr. L.M. Ramer at both ICORD, in Vancouver, Canada and at King's College London, in London UK. I performed the majority of the sample preparation and analysis of the RNA sequencing experiments, with help from Drs. L.M. and M.S. Ramer and RNA sequencing analysis advice from Drs. M. Crow and F. Denk. I performed the tissue preparation, processing, and imaging as well as data analysis and presentation for the cell size analysis and quantitative polymerase chain reaction. I prepared the text and figures for these chapters with assistance and edits from Dr. M.S. Ramer.

A version of **Chapter 4** has been accepted for publication in *Frontiers in Physiology* with the citation: Hunter DV, Holland SD and Ramer MS (2018) Preserved Adrenal Function After Lumbar Spinal Cord Transection Augments Low Pressure Bladder Activity in the Rat. *Front. Physiol.* 9:1239. doi: 10.3389/fphys.2018.01239. I performed the surgeries, animal care, data collection and analysis with minor assistance from S.D. Holland. I prepared the text and figures with edits from S.D. Holland and M.S. Ramer.

I wrote **Chapter 5** with edits from Dr. M.S. Ramer.

The work presented in this thesis was approved by the Animal Care Committee of the University of British Columbia, under certificates numbered A13-0154 and A17-0176.

Table of Contents

Abstract.....	iii
Lay Summary	v
Preface.....	vi
Table of Contents	vii
List of Tables	xiv
List of Figures.....	xv
List of Abbreviations	xvii
Acknowledgements	xix
Dedication	xx
Chapter 1: Introduction	1
1.1 Overview.....	1
1.2 Neural control of the pelvic viscera	2
1.2.1 Autonomic efferent pelvic control	3
1.2.2 Afferent pelvic input to the cord.....	7
1.2.3 Somatic innervation of sphincters and striated muscles	12
1.2.3.1 Innervation of the Lower Urinary Tract.....	13
1.3 Peripheral neuronal populations that innervate the pelvic viscera.....	14
1.3.1 Lumbosacral dorsal root ganglia.....	15
1.3.2 Pelvic ganglia.....	17
1.4 Integration of the systems for control of the pelvic viscera.....	19
1.4.1 Developmental aspects.....	19

1.4.2	Anatomical aspects	20
1.4.3	Functional aspects.....	21
1.5	The clinical importance of pelvic organ dysfunction following SCI: A function of level, severity and time	22
1.5.1	Consequences of injury level on pelvic organ dysfunction	24
1.5.2	Pelvic organ function and severity of SCI	27
1.5.3	The time course of pelvic organ (dys)function after SCI	29
1.6	Modelling SCI induced changes in the pelvic viscera	30
1.6.1	Animal models of spinal cord injury and autonomic dysfunction.....	32
1.6.2	Pelvic Visceral contributions to autonomic dysreflexia	37
1.6.3	Modelling and quantifying changes in the LUT.....	39
1.7	SCI-induced cellular changes in pelvic neuroviscera	43
1.7.1	Changes in lumbosacral spinal circuitry	43
1.7.2	Changes in lumbosacral dorsal root ganglia	45
1.7.3	Changes in pelvic ganglia	47
1.7.4	Changes in the bladder.....	48
1.8	Experimental overview and hypotheses.....	49
1.8.1	Cellular changes within the pelvic peripheral ganglia	50
1.8.2	Differential responses in bladder activity	51
 Chapter 2: Transcriptional and morphological changes in pelvic sensory and autonomic neurons following high spinal cord injury reveal unexpected neuron-target interactions...52		
2.1	Summary	52
2.2	Introduction.....	54

2.3	Materials and Methods.....	56
2.3.1	Animals procedures	56
2.3.2	Spinal cord injury surgeries	57
2.3.3	Post-operative animal care.....	58
2.3.4	RNA isolation	59
2.3.5	RNA sequencing.....	61
2.3.6	Functional annotation clustering of differentially expressed DRG genes	61
2.3.7	Ingenuity pathway analysis of differentially expressed DRG genes	62
2.3.8	Quantitative PCR	62
2.3.9	Tissue processing and immunohistochemistry	63
2.3.10	Image analysis.....	64
2.3.11	Statistical Analyses of neuronal sizes	67
2.4	Results.....	67
2.4.1	Differential gene expression in pelvic peripheral ganglia after high thoracic spinal cord injury.....	67
2.4.2	High thoracic transection results in gene expression changes in L6/S1 DRGs	70
2.4.3	Functional clustering annotation of differentially expressed DRG genes	74
2.4.4	Ingenuity pathway analysis of differentially expressed DRG genes	78
2.4.5	High thoracic transection results in modest gene expression changes in PGs.....	81
2.4.6	Examination of gene expression changes in PG using quantitative PCR.....	85
2.4.7	Recursive translation in analyzing cell size distributions of PG.....	87
2.4.7.1	High thoracic injury results in atrophy of TH-positive neurons.....	89
2.5	Discussion.....	93

2.5.1	Comparison of differential expression in the two ganglion classes.....	93
2.5.2	Functional clustering annotation for DRGs	94
2.5.3	Growth factor signaling downregulation in the DRG after T3x.....	95
2.5.4	Differential gene expression and neuronal atrophy in pelvic ganglia.....	97
2.5.5	Conclusions.....	99

Chapter 3: Pelvic autonomic neuron morphology and phenotypic changes reveal novel neuron-target interactions after lumbar spinal cord transection.....100

3.1	Summary	100
3.2	Introduction.....	101
3.3	Materials and Methods.....	103
3.3.1	Animal procedures	103
3.3.2	Wet bladder weights	104
3.3.3	RNA isolation and quantitative PCR	104
3.3.4	Tissue processing, immunohistochemistry and image analysis.....	104
3.3.5	Statistical analyses	105
3.4	Results.....	105
3.4.1	Bladder weights after chronic SCI.....	105
3.4.2	Lumbar transection results in a transient hypertrophy of TH-positive neurons .	107
3.4.3	Gene expression changes in PG.....	110
3.5	Discussion.....	112
3.5.1	Bladder hypertrophy varies with injury level	112
3.5.2	Transient hypertrophy of PG neurons following L2x.....	113
3.5.3	Changes in PG gene expression, morphology, and the neurotrophic hypothesis	114

3.5.4	Conclusions.....	116
Chapter 4: Preserved adrenal function after lumbar spinal cord transection augments low pressure bladder activity in the rat.....118		
4.1	Summary.....	118
4.2	Introduction.....	119
4.3	Materials and methods.....	121
4.3.1	Animal procedures.....	121
4.3.2	Intravesical recordings.....	121
4.3.3	Spinal cord injury surgeries and post-operative care.....	122
4.3.4	Bilateral pelvic ganglionectomy (PGx).....	122
4.3.5	Bilateral adrenalectomies and L2 transections (AdxL2x).....	123
4.3.6	Bladder pressure recordings in anaesthetized animals.....	123
4.3.7	Bladder pressure recordings in awake animals.....	124
4.3.8	L2x during bladder pressure recordings.....	125
4.3.9	HexBr and PGx during bladder pressure recordings.....	125
4.3.10	Pressure recordings analysis.....	125
4.3.11	Epinephrine and norepinephrine ELISAs.....	128
4.3.12	Statistical analyses.....	128
4.4	Results.....	128
4.4.1	Short and long-term consequences of high and low SCI on the rat bladder.....	129
4.4.2	Increased low-pressure NVC amplitude emerges in the acute period.....	132
4.4.3	Increased low-pressure NVC activity is not dependent on neural circuitry below an L2 SCI.....	134

4.4.4	Adrenal function underlies low-pressure NVCs following L2 SCI.....	138
4.5	Discussion.....	142
4.5.1	Timing of NVC changes after transection	142
4.5.2	Interrupting the peripheral signaling to the bladder.....	143
4.5.3	Adrenal medulla innervation and function after SCI.....	143
4.5.4	Adrenergic signaling in the bladder.....	145
4.5.5	Adrenal cortex and the bladder.....	146
4.5.6	Clinical Use of Norepinephrine in the Acute Management of SCI	146
4.5.7	Conclusions.....	147
Chapter 5: General discussion.....		148
5.1	Summary and conclusions	148
5.1.1	Transcriptional changes in viscerally projecting lumbosacral dorsal root ganglia after high spinal cord transection.....	148
5.1.2	Morphological and transcriptional changes within pelvic ganglia after spinal cord transection.....	149
5.1.3	Activity differences in the bladder with high thoracic and lumbar spinal cord transection.....	150
5.2	Limitations and areas of future research.....	151
5.2.1	Animal models of human disease	151
5.2.2	RNA sequencing of whole tissue samples.....	152
5.2.3	Tracking changes after injury at individual time points in neurons and targets .	154
5.3	Significance of findings with regards to the systemic consequences of SCI.....	156
5.3.1	Contrasting changes in PG and bladder after peripheral and central injuries.....	156

5.3.2	Alterations in adrenal function due to injury level has multiple systemic consequences.....	158
References.....		161
Appendix.....		216
	Complete RNA sequencing tables from Chapter 2.....	216

List of Tables

Table 2.1 Primer pairs for quantitative PCR.....	63
Table 2.2 Primary antibodies used for immunohistochemistry.....	64
Table 2.3 Annotated DRG genes upregulated one month post-T3x sorted by fold change.....	71
Table 2.4 Annotated DRG genes downregulated one month post-T3x sorted by fold change....	72
Table 2.5 Functional Clustering Annotation of upregulated DRG genes	76
Table 2.6 Functional Clustering Annotation of downregulated DRG genes	77
Table 2.7 Canonical Pathway analysis of differentially expressed DRG genes, (z-score > 2) ...	79
Table 2.8 Annotated PG genes upregulated one month post-T3x sorted by fold change	82
Table 2.9 Annotated PG genes downregulated one month post-T3x sorted by fold changes.....	83
Table 2.10 Investigator-led interrogation of genes differentially expressed in the PG one month post-T3x	84
Appendix Table 1: Complete list of annotated genes upregulated in the DRG one month post-T3x sorted by fold change.....	217
Appendix Table 2: Complete list of annotated genes downregulated in the DRG one month post-T3x sorted by fold change.....	227
Appendix Table 3: Complete list of annotated genes upregulated in the PG one month post-T3x sorted by fold change	238
Appendix Table 4: Complete list of annotated genes downregulated in the PG one month post-T3x sorted by fold change.....	240
Appendix Table 5: Complete list of canonical pathway analysis of differentially expressed DRG genes, complete table with all z-scores	243

List of Figures

Figure 1.1 The pathways of sensory and autonomic neurons innervating the pelvic viscera.....	10
Figure 1.2 Differential disruption of the pelvic neuroviscera by high-thoracic and high-lumbar spinal cord injury	36
Figure 2.1 Experimental outline for RNA sequencing of pelvic peripheral ganglia	60
Figure 2.2 Reconstructing sizes of neuronal populations using sectioned tissue and recursive translation.....	66
Figure 2.3 Analysis of RNA sequencing results of PGs and DRGs	69
Figure 2.4 Quantitative PCR of L6/S1 DRGs two weeks and one month post-T3x.....	73
Figure 2.5 Functional annotation clustering for genes differentially expressed in the DRG one month post T3x	75
Figure 2.6 Upstream analysis predicts BDNF activity as inhibited within the DRG one month post-T3x	80
Figure 2.7 Quantitative PCR of PGs two weeks and one month post-T3x.....	86
Figure 2.8 Expression of tyrosine hydroxylase (TH) and choline acetyltransferase (ChAT) in the rat pelvic ganglion.....	88
Figure 2.9 TH-positive neurons are responsible for the leftward size distribution shift one month post-T3x	90
Figure 2.10 TH-positive neuronal size change also present at two weeks post-T3x.....	92
Figure 3.1 Chronic lumbar spinal cord transections result in bladder hypertrophy.....	106
Figure 3.2 Hypertrophy of TH-positive neurons two weeks post-L2x	108
Figure 3.3 By one month post-L2x the TH-positive neuronal population size was no different from sham	109

Figure 3.4 Quantitative PCR of TH, VIP and NGFR expression in the PG after L2x	111
Figure 4.1 Pressure changes during infusions and analysis of minima and amplitude of bladder contractions	127
Figure 4.2 Amplitude of NVCs is increased at low pressures after L2x	130
Figure 4.3 Increased amplitude of low-pressure contractions persist to one month post-L2x ..	131
Figure 4.4 Larger amplitude NVCs at higher pressures are immediately reduced by L2 transection	133
Figure 4.5 Eliminating bladder innervation results in decreased large amplitude NVCs but does not eliminate the low pressure NVCs 2-days post-L2x	137
Figure 4.6 Relationship between amplitude of contractions and intravesical pressure after L2x is governed by adrenal function.....	141

List of Abbreviations

Acetylcholine (ACh)
Adenosine triphosphate (ATP)
Adrenalectomy immediately prior to L2x (AdxL2x)
American Spinal Injury Association (ASIA)
Autonomic dysreflexia (AD)
Autonomic nervous system (ANS)
Bioinformatics and Statistical genetics (BSG)
Bladder outlet obstruction (BOO)
Brain derived neurotrophic factor (BDNF)
Calcitonin gene-related peptide (CGRP)
Central nervous system (CNS)
Ciliary derived neurotrophic factor (CNTF)
Cold inducible RNA binding protein (CIRBP)
Colorectal distension (CRD)
Database for annotation, visualization and integrated discovery (DAVID)
Detrusor sphincter dyssynergia (DSD)
Dorsal root ganglia (DRG)
Fibroblast growth factor receptor 1 (FGFR1)
Functional clustering analysis (FCA)
Glial cell-line derived neurotrophic factor (GDNF)
Hexamethonium bromide (HexBr)
Hypogastric nerve (HGN)
Ingenuity pathway analysis (IPA)
Intraperitoneal (i.p.)
Kolmogorov-Smirnov (K-S)
Lower urinary tract (LUT)
Lumbo-sacral dorsal root ganglia (LS-DRG)
Nerve growth factor (NGF)
Neuropeptide Y (NPY)
Neurotrophin-3 (NT-3)
Neurotrophin-4 (NT-4)
Nitric oxide (NO)
Non-adrenergic non-cholinergic (NANC)
Non-voiding contractions (NVCs)
Norepinephrine/Noradrenaline (NE)
p75 neurotrophin receptor (P75^{NTR})
Pelvic ganglia (PG)

Pelvic Ganglionectomy (PGx)
Pelvic nerve (PN)
Pelvic viscera (PV)
Peripheral nervous system (PNS)
Pituitary adenylate cyclase-activating peptide (PACAP)
Pontine micturition centre (PMC)
Quantitative polymerase chain reaction (qPCR)
Ribonucleic acid (RNA)
RNA sequencing (RNAseq)
Spinal cord injury (SCI)
Subcutaneous (s.c.)
Substance P (SP)
Transection at the second lumbar cord segment (L2x)
Transection at the third thoracic cord segment (T3x)
Transient receptor potential (TRP)
Transient receptor potential vanilloid 1 (TRPV1)
Tropomyosin receptor kinase A (TrkA)
Tyrosine hydroxylase (TH)
Vasoactive intestinal peptide (VIP)
Vesicular acetylcholine transmitter (VAcHT)

Acknowledgements

I have been very lucky to receive an incredible amount of support during my time as a graduate student. I am thankful for the funding I received from the following agencies: Natural Science and Engineering Research Council, ICORD, and the Faculties of Graduate Studies and Medicine. In addition, there have been countless individuals who have contributed to my growth and development over the last number of years and though I cannot mention them all, I would like to especially acknowledge the following people:

- My supervisor, Dr. Matthew Ramer, for giving me the opportunity to learn more than I could have ever fathomed during my time in graduate school.
- My supervisory committee, Drs. Stacy Elliott, Tim O'Connor and Chris Maxwell, for their support, guidance, and thoughtful questions and contributions.
- Dr. Leanne Ramer, I am not certain I would have finished this thesis without you. Thank you so much for your mentorship and friendship.
- The labs of Drs. Elizabeth Bradbury and Stephen MacMahon at King's College London, who welcomed me warmly and provided a stimulating and exciting scientific environment for me to visit and to briefly call home.
- Dr. Wolfram Tetzlaff, as director of ICORD you have shown your dedication to research and training in the field of SCI, I truly appreciate that you were always willing to listen to my ideas and concerns.
- Dr. Lowell McPhail and Cheryl Niamath who give so much to ICORD - it is noticed and appreciated.
- Mark Crawford, who started this journey with me and was the best lab brother anyone could ask for.
- Mario Cruz, who was both an amazing lab manager and friend. You left us way too soon and it was just not the same without you.
- The current members of the Ramer Lab, Erin Erskine, Seth Holland and Brittney Smaila, for providing me with excellent company and so often trusting me to give good science and life advice - I hope I got it more right than wrong.
- The amazing graduate students and researchers who have enriched my time at ICORD with discussions, insights, laughs, and beers. Though I do not have room to mention them all, I want to draw special attention to: Jacquelyn Cragg, Jessica Inskip, Malihe Poormasjedi, Peggy Assinck, Freda Warner, Catherine Jutzeler, Cindy Li, and to all the other amazing women.
- My family, and especially my parents, who instilled and encouraged my love of science from a young age and provided an incalculable amount of emotional and financial support over these many, many years.
- Last but by no means least, my husband David, who has supported, encouraged, cajoled, and believed in me to a measure I do not believe I deserve (but he believes and that means the world to me).

To the little girl who 25 years ago was so curious and full of questions about the world that she was inexplicably excited by even the most mundane of elementary school science experiments. Though the realities of Science are infinitely more complicated, hopefully the curiosity and wonder persist indefinitely.

“Promise me you will not spend so much time treading water and trying to keep your head above the waves that you forget, truly forget, how much you have always loved to swim.”

— Tyler Knott Gregson

Chapter 1: Introduction

1.1 Overview

The spinal cord acts as a conduit, connecting the supraspinal and central neurons to the peripheral reaches of the body via an intricate system of tracts and nerves. The nervous system, with its many functional and anatomical components, works as an integrated whole to coordinate motor, sensory, and autonomic functions. The elaborate integration required for the proper functioning of the body's systems is exemplified in the urogenital tract, which requires careful and coordinated interplay of all parts of the nervous system. This integration becomes especially apparent when spinal cord injury (SCI) disrupts the coordination and communication of these integrated systems, resulting in bladder, bowel and sexual dysfunction. SCI-induced changes in the function of the pelvic viscera may not be visible, but they are some of the highest priority areas for individuals with any level of SCI.¹

The work presented in this dissertation focuses on the peripheral sensory and autonomic neurons that innervate the pelvic visceral organs and how they are differentially affected by spinal cord transection. These neurons reside within the lumbosacral dorsal root ganglia (LS-DRG) and the pelvic ganglia (PG) and bridge the divide between centrally located control areas and the pelvic effector organs. These are important, but perhaps under studied, information stations in the nervous system: necessary for the relay of information but also potential sites of integration.² Even when these neurons are not directly injured by SCI, they are affected by the cascade of changes that occur both centrally and peripherally.^{3,4} In this thesis I use two models of complete spinal cord transection (a high-thoracic transection, T3x, that results in the loss of supraspinal control without direct damage to the pelvic neurons and a high-lumbar transection,

L2x, that directly damages a population of pelvic neurons) to examine how the injury level impacts changes in the ganglia and the end organs.

In this first chapter I begin with an overview of the neural circuitry that controls the functioning of the pelvic viscera, focusing in on the neurons of the DRG and PG. Building on this understanding of the pelvic neurovisceral circuitry, I delve into the clinical consequences of SCI by describing how injury level, severity, and time play into autonomic dysfunction, with special attention given to bladder dysfunction and autonomic dysreflexia. I also address the use of animal models in the examination of the autonomic consequences of SCI. Finally, I give a brief review of the literature that describes SCI-induced changes to the different components of the pelvic neuroviscera (lumbosacral spinal cord, DRG, PG, bladder) in order to setup the hypotheses that I address in the subsequent data chapters.

1.2 Neural control of the pelvic viscera

Of the three main organ systems of the pelvic viscera (the lower urinary tract (LUT), the distal bowel and colon, and the reproductive organs) the first two share the same primary functions: storage and evacuation. Since it is important, to most adult humans at least, that urination, defecation, and sexual activity occur at socially acceptable and discrete times, these systems require the integration of the sensory, somatic, and autonomic nervous systems to align voluntary control with involuntary reflexes. To achieve this integration, neural circuitry at multiple levels of the nervous system is required, so local reflex loops and peripheral effectors are connected to supraspinal input. Since pelvic visceral functions depends on an expansive neural network, they are vulnerable to damage at points all along the neuraxis. To understand

how different levels of SCI differentially impact the pelvic viscera we must first appreciate the normal circuitry controlling these organs.

This thesis focuses on changes that occur below the level of SCI, in the peripheral pelvic organs and their associated ganglia, so I will focus the following review on the innervation of these targets by the autonomic, sensory, and somatic circuits within the spinal cord and periphery. I will briefly introduce the autonomic, sensory and somatic systems before addressing their role in the control of the pelvic viscera, with special attention to the innervation of the LUT. Since numerous comprehensive reviews of pelvic visceral innervation exist,⁵⁻¹² I will attempt to limit myself to the circuitry relevant to the studies in this thesis, including the basic scheme of bladder and adrenal gland innervation; though the adrenal glands are not part of the pelvic viscera, their pattern of innervation is both notable and relevant to Chapter 4.

1.2.1 Autonomic efferent pelvic control

The autonomic nervous system (ANS) controls bodily functions that normally occur below the level of conscious control. Whereas somatic motor neurons innervate the voluntarily controlled skeletal muscle, the maintenance of homeostasis of the internal milieu to changing circumstance and environment is achieved by ANS regulation of cardiac and smooth muscle activity, visceral reflexes, and glandular secretions.¹³

Though subdividing the nervous system may not accurately reflect the degree of interdependence and integration of the components, the sheer complexity of the system makes functional and/or anatomical division necessary for meaningful and practical description.¹⁴ With this caveat in mind, the ANS, itself a subdivision of the motor system, is classically divided into three parts: the sympathetic, parasympathetic, and enteric nervous systems.¹⁵ Though the enteric

nervous system, responsible for the gastrointestinal system, is itself a fascinating topic that could easily fill a whole thesis, it is beyond the scope of this thesis (for reviews see¹⁶⁻¹⁸) and as such I will focus my discussion on the other parts of the ANS. Historically (and colloquially) the sympathetic and parasympathetic systems are often characterized as doing opposite things at different times (i.e. rest/digest or fight/flight). However, the majority of internal organs function because of the coordination of both systems working in conjunction. This results in closely associated systems with distinctive features, including the location of their preganglionic neurons, their distribution in relation to their target organs, and their neurochemical properties.

Both the sympathetic and parasympathetic nervous systems innervate their targets through a relay consisting of a preganglionic neuron within the spinal cord and a ganglionic neuron in the periphery.¹³ The locations of the preganglionic neurons within the central nervous system (CNS) are historically a key defining feature of the parasympathetic and sympathetic systems and as such they are often referred to as the craniosacral and thoracolumbar systems, respectively (recent controversy surrounding this distinction is discussed below). The parasympathetic preganglionics reside in the nucleus ambiguus of the brainstem, in the dorsal motor nucleus of the vagus, or in the intermediolateral cell column and central grey matter of the sacral cord, in a region aptly named the sacral parasympathetic nucleus.^{19,20} The majority of the sympathetic preganglionics are found in clusters in the intermediolateral nuclei of the thoracic and lumbar spinal cord, though some are also found in the intercalated nuclei and central autonomic area in the same spinal cord segments.^{13,21-23}

Recently, the classical categorization of the spinal autonomic outflow has been called into question. A 2016 publication proposes that all spinal autonomic outflow should be considered sympathetic based on expression of developmental and genetic markers.²⁰ This idea

has been met with significant pushback; after all, the developmental similarities between the lumbar and sacral spinal outflow do not negate the functional differences.^{20,24–26} Perhaps this is a good reminder that the understanding of the nuance and complexity of neurophysiology must balance the generalizations and simplifications we rely on in biology: sacral autonomies can develop genetically in a manner similar to other spinal (sympathetic) systems and still assume the neurochemical and physiological properties of their parasympathetic function.²⁷

The spinal preganglionic axons of both systems exit the cord through the ventral roots and travel via the ramus communicans to synapse within peripheral autonomic ganglia. The synapses between sympathetic pre- and ganglionic neurons were the first identified example of neuroneuronal chemical transmission.²⁸ Indeed, both sympathetic and parasympathetic ganglionic transmission occurs by release of acetylcholine by preganglionic neurons onto nicotinic receptors of the ganglionic neurons.²⁹ The sympathetic ganglia run in parallel chains on either side of the vertebral column; most of the neurons within the sympathetic paravertebral ganglia are noradrenergic and innervate the peripheral vasculature, though there is a population of cholinergic sympathetic neurons that supply the sweat glands.² Parasympathetic ganglionic neurons, on the other hand, are usually cholinergic and generally reside in prevertebral ganglia that are near or within the target organs they innervate. Additionally, a subset of sympathetic preganglionic processes from the mid thoracic to upper lumbar cord bypass the paravertebral chain without synapsing and instead connect to ganglionic neurons of the prevertebral ganglia, including the celiac, superior mesenteric, inferior mesenteric and pelvic ganglia. However, in general, the axons of the sympathetic ganglionic neurons tend to be longer in order to reach their more distant targets whereas parasympathetic postganglionic axons tend to be shorter as

their targets are nearby. The ganglionic neurons send out axons in mixed nerves (often consisting of other motor and sensory axons) to directly innervate their targets.³⁰

There are, however, exceptions to these organizational rules, the most obvious being the sympathetic innervation of the adrenal medulla. A subset of preganglionic sympathetic neurons from the third thoracic (T3) to the third lumbar (L3) segment, with the majority between T5 and T12, directly innervate the chromaffin cells of the adrenal medulla, which acts like a specialized ganglion.³¹ The chromaffin cells originate from the same population of progenitors as the autonomic ganglionic neurons, but differentiate into specialized cells to make up this neuroendocrine gland that produces and releases epinephrine (adrenaline) and norepinephrine (noradrenaline) into the blood stream. The majority of circulating epinephrine, and a small percent of circulating norepinephrine (NE), is released into circulation by the adrenal medulla.³¹ The sympathetic innervation of the adrenal medulla is an important link between the ANS and the stress axis and hormonal control.^{32,33} Recent studies have further highlighted the sympathetic nervous system's role in integrating multiple body systems by linking interruption of adrenal innervation after SCI to immune system dysfunction.³³

An additional example of unusual connections in the autonomic system, one which is also central to this thesis, is the autonomic innervation of the pelvic viscera.² Pelvic ganglionic autonomic neurons reside close to their targets amongst the pelvic organs in discrete bilateral pelvic ganglia (PG, in male rodents and guinea pigs) or in more diffuse pelvic plexi (in female rodents and larger mammals). The PG is the only example of an autonomic ganglion that contains both types of ganglionic neurons, with sympathetic ganglionics receiving input from the lumbar cord via the hypogastric nerve and parasympathetics receiving input from the sacral cord via the pelvic nerve.^{2,34} The axons of the ganglionic neurons travel the short distance from the

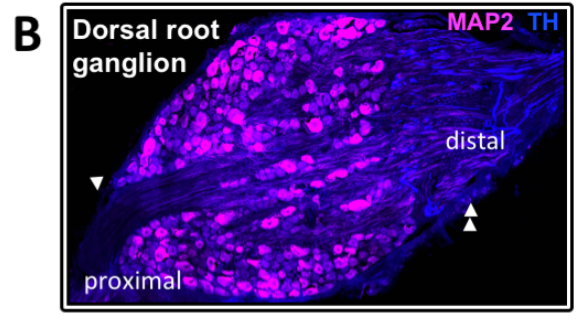
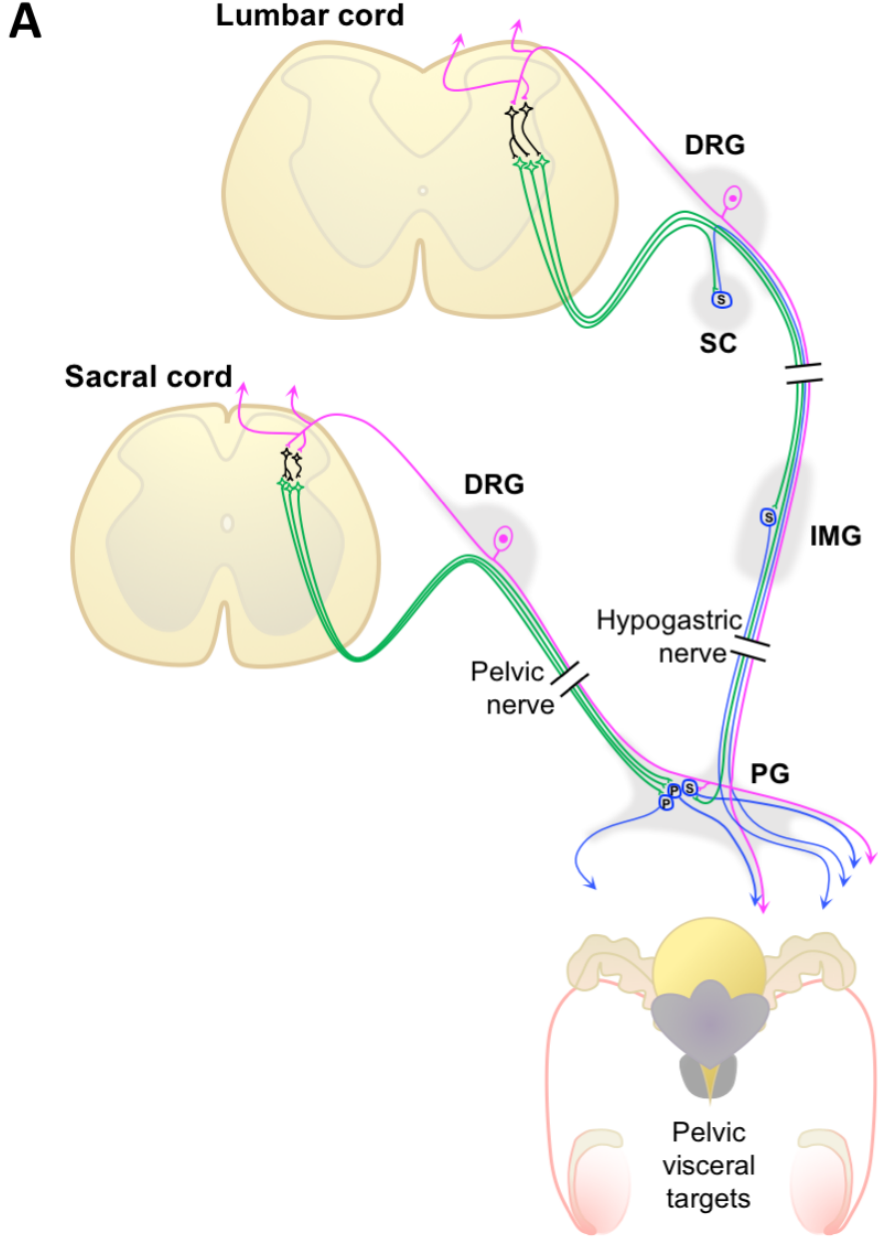
PG to the target tissue alongside sensory axons, often in mixed nerves. Within the target tissue, postganglionic axons form neuroeffector junctions where combinations of primary neurotransmitters, generally NE and adenosine triphosphate (ATP) from sympathetic axons and acetylcholine from parasympathetic axons, along with other co-transmitters, are released to control end organs.

1.2.2 Afferent pelvic input to the cord

The primary sensory neurons responsible for the transduction of pelvic sensory information to the central nervous system reside in the lumbosacral dorsal root ganglia (LS-DRG). These DRGs contain both the exteroceptive somatic neurons that innervate pelvic somatic structures, such as the muscle and skin of the abdomen, and the interoceptive visceral afferents that carry nociceptive, chemo- and mechanosensory information from the internal organs. Retrograde tracing from pelvic organs label a small portion of small-to-medium-sized neurons distributed throughout the LS-DRGs. There remains some level of debate over the exact contribution of each lumbosacral DRG to the innervation of the pelvic viscera, with conflicting reports on whether sacral or thoracolumbar afferent axons are most abundant in the pelvic organs.³⁵⁻³⁷ However, it is well established that the L6 and S1 DRGs of the rat (S2-4 in humans) contain many of the afferents that project to the pelvic viscera, including the urinary bladder, penis, clitoris, and urethra.^{36,38-40}

The first-order sensory neurons, which conduct impulses from the receptors in the skin and viscera, have cell bodies reside within the DRGs and are part of the peripheral nervous system (PNS). Their unique pseudo-unipolar structure allows them to span the PNS and CNS, with a single bifurcating axon from which emanates both a centrally- and peripherally-projecting

process (Figure 1.1). The caudal shift of the DRGs along the rostral-caudal axis of the spinal cord results in the extended lengths of both processes of the LS-DRG neurons (named for the spinal segment to which they connect) that innervate the pelvic organs.⁴¹



- Primary sensory
- Preganglionic
- Ganglionic
- Interneurons

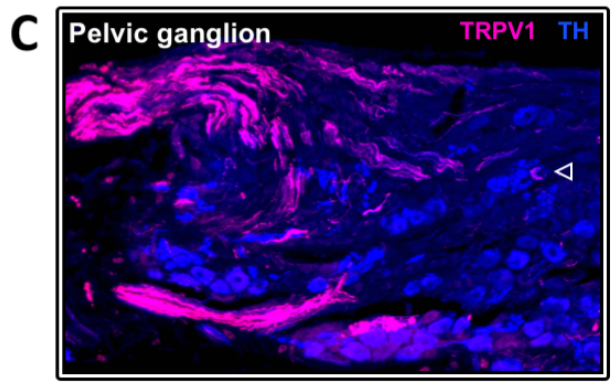


Figure 1.1 The pathways of sensory and autonomic neurons innervating the pelvic viscera

(A) Pelvic sympathetic preganglionics originate in the predominantly high-lumbar cord (L1-2 in rat) exiting via the ventral nerve to synapse on ganglionic neurons within the paravertebral ganglion of the sympathetic chain (SC), inferior mesenteric ganglion (IMG), or pelvic ganglion (PG). The PG is a mixed autonomic ganglion that also contains parasympathetic (P) neurons that receive input from the sacral (L6-S1 in rat) cord and sympathetic (S) neurons that receive input from the lumbar cord (predominantly L1-2 in rat). The nerves containing the preganglionic autonomic fibers, the hypogastric nerve and pelvic nerve, also carry the sensory axons from the lumbosacral dorsal root ganglia (DRG). Interneurons (black) connect the sensory and autonomic neurons at the cord level; supraspinal and between segment connections are also present though not shown. (B) In sections of DRG tissue, sympathetic fibres (TH, blue) are not present in the proximal root (single arrowhead) or cell layer of the DRG. (C) Within section of PG tissue, the close association of autonomic and sensory neurons can also be seen. Sensory (TRPV1, magenta) fibres and baskets (empty arrowhead) are present surrounding the sympathetic (TH, blue) and parasympathetic neurons.

The peripheral process exits the LS-DRG and joins with other peripherally projecting processes in mixed spinal nerves. Visceral sensory neurons take the same path as the preganglionic neurons to reach their target tissue, often traversing the autonomic ganglia en route (Figure 1.1). The pelvic viscera are innervated by a relatively low density, compared to somatic structures such as skin and muscle, of A δ and C fibers that form free nerve endings within the tissue to collect information on the distension of visceral smooth muscle and chemosensory signals. The diversity of receptors expressed in visceral afferents suggests that they are polymodal, and this has been confirmed physiologically: visceral afferents that respond to low mechanical thresholds can also code noxious stimuli.⁴² Certain afferent fibres in the mucosal and muscular layers of pelvic visceral organs respond to both mechanical stimulation, such as distension and blunt probing, as well as chemical stimulation.^{37,43-45}

The central process of a LS-DRG neuron travels rostrally through the long dorsal root, passing through the dorsal root entry zone into the dorsal horn of the spinal cord. Since the central process of a DRG neuron is tasked with providing sensory information to multiple levels of the CNS, it branches upon entry into the cord to synapse on interneurons or second-order sensory neurons at the same level, to connect to the surrounding cord segments via Lissauer's tract, and to ascend to carry signals to higher sensory nuclei via the dorsal funiculus. The termination pattern of the central process of sensory neurons varies with a number of factors, including the location and modality of the afferent. Matching the low afferent innervation density of viscera, only about 5-15% of afferent input to the relevant spinal cord segments originates from visceral afferents. Furthermore, the majority of second order spinal dorsal horn neurons receive multiple inputs, including inputs from multiple organs or somatic inputs alongside the

visceral organs.⁴⁶ Though the role of the primary afferents is to pass sensory information to the CNS, a significant portion of the signals received from the pelvic viscera do not elicit conscious awareness, but instead signal through local interneurons and exert their influence at the level of local reflexes and spinal circuitry.

1.2.3 Somatic innervation of sphincters and striated muscles

Of course, operation of the pelvic organs includes an aspect of voluntary control, which is enacted through the somatic motor system. Cortical and brainstem structures exert control over urination, defecation, and sexual function through the coordination of reflex timing and the activity of the external sphincters. Brainstem nuclei, such as the pontine micturition centre and the nucleus paragigantocellularis, receive inputs from higher brain centers and modulate the activity of spinal cord circuitry to inhibit or facilitate excitability and thereby influence pelvic organ function.^{8,47,48}

The peripheral portion of these somatic pathways is relatively small, consisting of the axons of the pelvic-projecting somatic motor neurons that reside in the ventral horn of the sacral spinal cord in Onuf's nucleus. The axons of these sacral plexus neurons travel via the pudendal nerve, which also contains parasympathetic motor axons and sensory neurons, to the urogenital organs. Urinary and fecal continence are maintained in part through the voluntary contraction of the striated muscles of the external urethral and anal sphincters, which act to inhibit the elimination of waste until appropriate times. Alongside the sphincters, the muscles of the pelvic floor play an important role in physically supporting the pelvic organs as well as supporting their functioning through voluntary contraction and relaxation that is coordinated with the autonomic innervation.⁴⁹

1.2.3.1 Innervation of the Lower Urinary Tract (LUT)

Since the last data chapter of this thesis focuses on changes in the bladder after SCI, I will take the time now to go through the specific innervation of the LUT both for future reference and as an example of the interconnected nature of the neural control of the pelvic organs. The LUT consists of the bladder and urethra, which are directly innervated by both peripherally- and centrally-located neurons with processes in three main nerves, the hypogastric, pelvic and pudendal nerves.

Trans-synaptic pseudorabies virus tracing from the urinary bladder has revealed the network of neurons that are involved in innervation of the rat bladder. At early time points after injection, the virus is found in neurons that directly innervate the bladder: the sensory neurons of L6 and S1 DRGs and preganglionic neurons in the lumbosacral cord. Subsequently, interneurons in the intermediate grey region and secondary sensory neurons in the superficial dorsal horn were labelled before the appearance of the tracer in supraspinal structures, including many cells in the pontine micturition centre (PMC).⁵⁰ Dye injection into the bladder also revealed that the peripheral autonomic neurons that directly innervate the bladder are distributed throughout the PG.⁵¹

Functionally there are two stages in LUT control, filling and voiding, with sympathetic and parasympathetic control dominating in each respectively. During bladder filling, continence is maintained through the action of both the sympathetic and somatic motor systems. Sympathetic ganglion neurons release noradrenaline onto the bladder neck, lower trigone, and internal urethral sphincter activating α -adrenergic excitatory receptors and resulting in contraction and continence. At the same time, noradrenaline release in the bladder wall results in

bladder wall relaxation by β -adrenergic inhibitory receptors. Somatic neurons from Onuf's nucleus (S2-S4 cord) activate the external urethral sphincter during storage to support sympathetic activity and help prevent urination until needed.⁵²

The switch from filling to voiding activity is coordinated by the spinobulbospinal pathway through the pontine micturition centre (PMC, Barrington's nucleus). In the rat, the sensory neurons responsible for relaying information to the CNS on the pressure, tension, and chemical properties of the bladder are the A δ - and C- fibres in the L6/S1 DRGs.⁵³ The urothelium when stretched releases chemical mediators, such as ATP, that act on sensory afferent receptors, such as P2X3, to signal bladder fullness.⁵⁴

Parasympathetic activation of voiding occurs by both cholinergic and non-adrenergic, non-cholinergic transmitters that cause the bladder detrusor to contract. Muscarinic and purinergic receptors are activated by acetylcholine (ACh) and ATP released from the parasympathetic ganglionic axons. Inhibition of urethral smooth muscle also occurs through nitric oxide (NO) released from parasympathetic fibres to allow for unobstructed flow of urine.⁵³ For proper voiding to occur the parasympathetic detrusor activation occurs in coordination with relaxation of the somatically controlled external urethral sphincter, allowing for efficient and timely urine flow.⁴⁹

1.3 Peripheral neuronal populations that innervate the pelvic viscera

The pelvic peripheral ganglia are home to the majority of the autonomic and sensory neurons that directly innervate pelvic viscera. They consist of neural crest derived neurons and glia alongside resident immune cells and blood vessels, and act as a critical bridge between the CNS and the effector organs. Though previously thought of as a simple relay, uncomplicated

compared to the central circuits, the composition of these peripheral ganglia is diverse and complex. As such, classification of the neurons within these ganglia has not been straightforward.

However, significant amounts of data on the morphological, neurochemical, electrophysiological and functional properties of the neurons of these ganglia are available. This understanding has led to, amongst other things, the concept of “chemical coding,” where the neuropeptides and receptors can be related to the functions of the neuron to aid in identification and classification of different subtypes of neurons.^{2,55-57}

1.3.1 Lumbosacral dorsal root ganglia

The primary sensory neurons contained within the DRG are remarkably heterogeneous, with overlapping characteristics that make attempting comprehensive categorization of DRG neurons a trying process, resulting in an impenetrable, multidimensional Venn diagram.⁵⁸ Though the complexity of the DRG has been extensively reviewed elsewhere, for the purposes of this thesis I will describe the structure and termination patterns of the three main classes of DRG neurons before focusing on the sensory neuron types predominantly innervating the pelvic viscera.^{59,60} Large myelinated $A\beta$ fibres carry innocuous mechanoreceptive and proprioceptive input to laminae II and V of the dorsal horn. These fibers generally innervate somatic tissues and often connect to specialized receptor end organs in the skin, muscles, and tendons.⁶¹ Noxious stimuli, on the other hand, are carried by two classes of nociceptors with free nerve endings: the thinly myelinated $A\delta$ fibers which terminate in laminae I and V and the unmyelinated C-fibers which terminate in laminae I and II.⁶² C-fibers are further classified based on their trophic factor sensitivity and whether they express specific neuropeptides. Early in development virtually all

small diameter neurons rely on target derived nerve growth factor (NGF) for survival; those that continue to express tropomyosin-related kinase A (TrkA), an NGF receptor, into adulthood also contain neuropeptides such as CGRP and substance P (SP; making them peptidergic). The other approximately one-half of small, unmyelinated neurons lose TrkA expression postnatally and become responsive to the glial cell-line derived neurotrophic factor (GDNF) family of neurotrophic factors, most of which are non-peptidergic though the subset of sensory neurons expressing the GFR α 3, which binds the GDNF family member artemin, are peptidergic.⁶³

Visceral afferents are important for monitoring the state of the viscera, activating reflex mechanisms, and preserving tissue homeostasis.³⁷ The role of different subtypes of DRG neurons in visceral innervation has been best-characterized for the bladder. Though exact numbers vary between studies, axonal tracing from the rat bladder has identified approximately one third of the afferents to be A δ –fibers and the other two third C-fibres, most of which are peptidergic.^{64,65} Under normal physiological conditions the majority of information about bladder tension is carried by small, thinly-myelinated, mechanosensitive A δ -fibers. The small unmyelinated C-fibers innervating the bladder are often referred to as ‘silent’ since they do not respond to passive distention during normal micturition but instead are important for nociceptive signaling.^{46,66} In cases of disease and injury, C-fibres can become responsive to bladder distension and contribute to voiding and neurogenic bladder contractions.^{42,66,67}

Additional insights into the functional subclasses of viscerally projecting LS-DRG neurons have come from the extensive expansion of information related to the expression of sensory receptors and neuropeptides. The most commonly described receptors in bladder afferent neurons are transient receptor potential (TRP) channels and purinergic receptors.⁶⁸ The majority of C-fiber bladder sensory neurons are peptidergic and express transient receptor potential

vanilloid 1 (TRPV1).^{69,70} Purinergic receptors, including numerous P2X and P2Y subunits, are also commonly expressed by bladder afferents and respond to ATP released from efferent fibres and the bladder urothelium.⁷¹⁻⁷³ Studies of both P2X₃ and TRPV1 knockout mice demonstrate detrusor underactivity indicative of bladder sensory deficits.⁷⁴⁻⁷⁶

The set of receptors expressed by afferents clearly plays a role in sensory information transduction, but expression of neuropeptides is also important for signaling within the target tissue. Neuropeptides such as such as calcitonin gene-related peptide (CGRP), SP, pituitary activating (PACAP), and vasoactive intestinal peptide (VIP) are common in bladder afferents and act as neurotransmitters in the spinal cord, but they can also be released peripherally resulting in target changes such as vasodilation and plasma extravasation.^{7,77-79} Interestingly, the bladder urothelium is also implicated in multiple aspects of bladder sensation; it both expresses receptors similar to the afferents innervating the bladder and also produces factors, such as ATP, that act on sensory fibers.^{54,80-83}

1.3.2 Pelvic ganglia

Given that the PG is a major contributor to the innervation of the sexual organs, it is perhaps no surprise that there is significant sexual dimorphism in its composition. The PGs of the male rat reside bilaterally on the dorsolateral aspect of the prostate, in amongst the connective tissue and blood vessels that are abundant in the vicinity.⁸⁴ The male PG is a cohesive collection of approximately 15,000-20,000 ganglionic neuronal cell bodies surrounded by glia and immune cells.⁸⁵ Female rats contain significantly fewer neurons, estimated to be around 6000, that are spread out in a web in amongst the lower pelvic organs.⁸⁵ This sex difference is further supported by the greater number of pelvic preganglionics in the male lumbar cord and the relatively denser

innervation of male internal reproductive organs.^{86,87} Though the structure of the ganglia may vary between animals, the functional organization of pelvic visceral innervation is maintained across species, making the simplified organization and accessibility of the male rat PG a convenient model for studying the peripheral ANS.^{51,88,89}

Like the DRG, the PG is a peripheral ganglion composed of neurons and glia derived from neural crest cells. Unlike the DRG neurons, with their direct connection to the CNS, the vast majority of synaptic input to the neurons of the PG originates from the cholinergic preganglionics in the lumbar and sacral cord. The neurons themselves, especially in rats, tend to be simple in structure, with few if any dendrites and a limited number of inputs. Historically, the neurons of the PG have been divided into two main groups defined by the level of their central input: sympathetic neurons, with lumbar input and NE as the primary transmitter and parasympathetic neurons, with sacral input and acetylcholine as the primary transmitter.^{90,91} Noradrenergic neurons tend to be larger than cholinergic neurons.^{92,93}

The heterogeneity of ganglionic neurons, which reflects the numerous and diverse targets of this ganglia, is more elaborate than a simple sympathetic and parasympathetic dichotomy. Cholinergic neurons in the PG commonly express VIP and neuropeptide Y (NPY), the latter of which is also found in noradrenergic PG neurons. Though the vast majority of neurons within the rat PG are clearly either noradrenergic or cholinergic there are a small number of non-adrenergic, non-cholinergic (NANC) neurons (potentially more common in higher mammals) and a large number of transmitters that coexist and contribute to the neural responses in the ganglia and their targets, including nitric oxide which plays an important role in sexual function.^{94,95} Extensive immunohistochemical and tracing studies have revealed more detailed neurochemical coding and viscerotopic organization of the ganglionic neurons correlating to the targets they

innervate.^{2,34,51,96,97} For example, the majority of the penis-projecting neurons cluster around the exit point of the penile nerve and express acetylcholine and VIP, which reflects their vasodilator function.^{93,98,99} The bladder, on the other hand, is innervated by neurons that are spread more evenly throughout the PG. The cholinergic parasympathetic neurons, which also express ATP, extensively innervate the detrusor muscle whereas noradrenergic sympathetic neurons from the PG are more rare in the bladder, innervating mostly the bladder base and neck.^{51,69}

1.4 Integration of the systems for control of the pelvic viscera

Though details of each system are often explained individually, it is worth taking the time to appreciate the interconnected nature of sensory and autonomic innervation, particularly with regards to the pelvic organs.¹⁴ The systems are required to work together as an integrated whole and overlap with regards to a number of developmental, anatomical and functional aspects, which I will outline here.

1.4.1 Developmental aspects

The shared developmental lineage of sensory and autonomic neurons underlies phenotypic similarities, including overlap in the expression of a number of receptors and neuropeptides. During their differentiation, neural crest cells respond to a series of growth factor signals in order to produce the various cells of the PNS. Small peptidergic sensory neurons and ganglionic sympathetic neurons rely on target derived factors for survival during development and continue to express the NGF receptors TrkA and the p75 neurotrophin receptor (P75^{NTR}) into adulthood.^{34,63,100,101} In adulthood, these target derived factors appear to be less important for neuronal survival but instead play a larger role in regulating the phenotype of the neurons.^{102,103}

Staining for neurochemical markers can identify neural subtypes in processed tissue but the shared neurochemistry of peripheral neurons requires this to be interpreted with caution. For example, tyrosine hydroxylase (TH), the rate limiting enzyme in catecholamine production, is commonly used to label sympathetic neurons in rats but in mice it is also expressed in a sizeable subpopulation of sensory neurons.⁵⁸ Though many other neuropeptides are differentially expressed in adult sensory, sympathetic and parasympathetic neurons, expression in these populations may overlap and nerve injuries are known to alter normal neuropeptide distribution.^{104–109} Overlapping gene expression between these peripheral populations also complicates efforts to develop genetic tools for specifically manipulating one of these populations. Even advillin, an actin-binding protein involved in the development of peripheral ganglion neurons (which has been used to specifically target sensory neurons for genetic manipulation) has since been found to also be expressed in sympathetic ganglionic neurons (unpublished observations from manuscript in preparation D. Hunter *et al.*, 2018).

1.4.2 Anatomical aspects

At least in part a consequence of their similar developmental origins, the neurons of the sensory and autonomic systems have significant anatomical connections. Indeed, elegant developmental studies have demonstrated sympathetic axon outgrowth's dependence on the prior fasciculation of sensory axons.¹¹⁰ Therefore the tracts leading from the lumbar and sacral cord through the PG and to the pelvic organs contain the majority of both the autonomic and sensory axons innervating these targets (Figure 1.1).^{104,111} This close association can make *in vivo* experimental manipulations targeting one particular population challenging and necessitates the consideration of damage to both neuronal types during injury studies.³⁴

Furthermore, the proximity of sensory fibers with the autonomic ganglion neurons provides opportunity for signaling between these two systems in the periphery. Evidence of branches from sensory neurons forming varicose structures around autonomic neurons of the PG support the idea that the PG may not be just a simple relay station but may also be a site of information integration (Figure 1.1).^{28,30,104} Interestingly, though the sensory axons normally travel alongside the autonomic axons and pass through autonomic ganglia, the autonomic processes are excluded from the cell layer of the DRG during development. After peripheral nerve injuries and SCI, however, sympathetic fibers can invade into the cell layer of the DRG and form baskets around the sensory neurons.¹¹²⁻¹¹⁴ The functional consequences of these connections are not fully understood, but they have been implicated in mechanisms of both neuropathic pain and autonomic dysreflexia.

1.4.3 Functional aspects

Functionally, the lines between afferent and efferent activity also blur in the pelvic viscera. Though the predominant role of the peripheral process of the sensory neuron is to transmit input received from the internal environment, peripheral release of factors such as CGRP and SP from their free endings can modulate target tissue behaviour.^{14,115,116} This appears to be particularly relevant within the bladder, where release of such factors contributes to bladder sensitivity and neurogenic inflammation.^{77,117}

Sensory input and autonomic output are connected in the cord indirectly through interneurons in the dorsal horn and spinal autonomic areas. It is suggested that there is potential for direct peripheral connections. TRPV1 and CGRP sensory fibres within the PG that are 'passing through' also form varicosities and baskets within the ganglia, though it is unclear

whether these produce functional connections (Figure 1.1).^{84,104,118} This also plays into the suggestion that autonomic ganglia may not be just simple relay stations. Anatomical studies have estimated that there is a significant convergence of signals in rat paravertebral sympathetic pathways, as well as in prevertebral ganglia of higher mammals.¹¹⁹ However, it is less clear whether this extends to the prevertebral ganglia, particularly in the rat where the neurons are simpler and tend to receive fewer inputs.¹²⁰ However, some PG neurons may receive multiple inputs, including from both lumbar and sacral preganglionics as well as sensory fibers.^{34,104,121,122} Additionally, a small number of viserofugal projections to the PG via the rectal nerves from the distal colon further hints at this ganglion being more than just a simple relay.^{123,124} In retrograde labelling studies where multiple pelvic organs are labeled, a small number of PG neurons contain multiple tracers.⁵¹ This is also true in the DRG, where single DRG neurons potentially innervate multiple pelvic visceral structures, suggesting another potential layer of signal integration and a substrate for cross-sensitization.¹²⁵⁻¹²⁹ These facts emphasize that peripheral ganglia may play a role in the integration and amplification of signals from the CNS to targets.^{28,41}

1.5 The clinical importance of pelvic organ dysfunction following SCI: A function of level, severity and time

Since the spinal cord is the main connection between the brain and body, damage to it has ramifications for all organ systems. Deficits in movement are the most apparent; historically, this has led to a research bias, with the great majority of restorative work focused on overcoming paralysis.⁵² However, loss of volitional motor control is not necessarily the most important change that occurs with a SCI. The bodily functions that directly determine our survival,

including respiratory, cardiovascular, digestive, and urogenital function, are governed and coordinated by the ANS. In able-bodied individuals, these (largely) autonomic functions usually demand little conscious attention. However, disruption of autonomic pathways due to SCI can radically expand the time, effort and interventions required to perform these basic functions, dramatically impacting quality of life.^{130–133} Though cardiovascular and respiratory changes, especially after high SCI, are areas of intense interest and research, the work in this thesis focuses on the changes to pelvic neurovisceral networks after different levels of SCI since bladder, bowel and sexual functions are high priorities for persons with SCI.

From a clinical perspective, the urogenital tract and bowel deserve special attention, since they are a major source of life-threatening secondary complications after SCI. Urinary tract infections are a common reason individuals with SCI seek medical attention, resulting in significant costs to both individual quality of life and the health care system.^{132,134–136} Only 21% of individuals with SCI reported normal bladder voiding without additional management interventions, including timed voiding, manual pressure-induced voiding (i.e., Credé's maneuver), intermittent catheterization or use of indwelling catheters.^{137–140} Bowel management is similarly complicated after injury, with 37% of all patients with SCI requiring assistance with routine bowel care.¹⁴¹ An individual's bowel program often requires medications, as well as dietary and behavioral changes including scheduling a bowel regimen that can last between 15 minutes to more than 120 minutes per episode, with complications including incontinence, rectal damage and autonomic dysreflexia (pathologically high blood pressure triggered by sensory stimulation below the level of SCI).^{131,142}

Changes to sexual response after SCI is also complex and multifaceted, with components of the response being affected by direct damage to signaling pathways as well as impacted by the

dysfunction of the neighboring pelvic organs; bladder and bowel dysfunction affect sexual activity and satisfaction. In a survey of individuals with SCI, 35.3% reported that concerns about bladder and bowel incontinence interfered with or prevented them from seeking sexual activity; subsequent studies found decreased sexual satisfaction was predicted by bowel and bladder incontinence.^{143,144} The hassle and indignity of incontinence, combined with altered physical capability, sexual dysfunction, and loss of sensation, profoundly affect sexuality: 83.2% of individuals with SCI report having an altered sexual sense of self, and that improving sexual satisfaction would improve their quality of life.¹⁴⁵

Given the diverse and intimate effects of autonomic dysfunction, it is hardly surprising that when individuals with SCI were asked to prioritize areas that impact quality of life, autonomic functions such as bowel, bladder, sexual function, and the elimination of autonomic dysreflexia are a high priority for individuals with both quadriplegia and paraplegia.^{1,133,143} The heterogeneous nature of human SCI makes understanding the mechanisms underlying functional changes within the pelvic organs challenging. Due to numerous complexities, including incomplete injuries, multi-system trauma, and imprecise neurological assessment in the acute stages, there is an incomplete and imprecise understanding of the relationship between visceral organ dysfunction and spinal cord injury level, severity, and time post-injury.¹⁴⁶ This thesis seeks to shed light on these issues.

1.5.1 Consequences of injury level on pelvic organ dysfunction

The level of SCI has both local and systemic consequences: it directly damages cells at the site of injury, it disrupts supraspinal input to the cord, it impedes the rostral flow of sensory information, and it induces systemic changes upon denervation of organ systems. Akin to the

pervasive research bias toward paralysis, there is a tendency to focus on loss of supraspinal input to the cord as the key consequence of SCI. However, all of these effects of injury noted above need to be taken into account when considering pelvic organ dysfunction after SCI.

Stratification of SCI by level in the clinical population reveals that acute traumatic injuries are primarily cervical (55%), while thoracic, thoracolumbar and lumbosacral injuries occurring less frequently (15% each).^{147,148} This is not the case with regards to non-traumatic injuries (caused by developmental, neoplastic, degenerative, ischemic, or other such processes). For example, the majority of cases of myelomeningocele (85%), the most severe form of spina bifida, occur in the lumbosacral spinal cord.^{149,150} Of clinical importance, the incidence of myelomeningocele far exceeds that of traumatic spinal cord injury; the current incidence remains at approximately 1 in 1000 births in both Canada and the US.¹⁵⁰

Injury to the lumbosacral cord is of particular interest with respect to pelvic organ function since the spinal centers that govern the reflex activity of the pelvic organs reside within the lumbosacral spinal cord. The loss of parasympathetic control of smooth muscle of the bladder and bowel results in atonia and areflexia: the clinical picture is flaccid bladder and bowel paralysis, with little reflexive emptying.^{10,131} Similarly, parasympathetic neurons within the sacral cord control erection and tumescence, such that destruction of these centers result in the loss of sexual reflexes, although psychogenic tumescence (“psychogenic erections”) mediated by more rostral autonomic circuitry that travel through the hypogastric nerves may be preserved.^{131,151,152}

Complete injuries (defined below) above the level of the sacral cord result in the disconnection of parasympathetic spinal centers from the supraspinal centers that modulate their function. For the pelvic organs, reflexes that are spontaneously re-established after SCI are no

longer under conscious regulation and the baseline excitability within the cord is disrupted. Unlike the bladder areflexia that follows sacral injuries, suprasacral injuries typically result in pathological ‘gain of function’ outcomes, including loss of coordination of the bladder smooth muscle (detrusor) and sphincters (known as detrusor-sphincter dyssynergia), and detrusor hyperreflexia.¹³¹ The bowel, sluggish in the acute stages of SCI, also recovers reflexive function, resulting in spontaneous, albeit inefficient emptying, and fecal incontinence due to loss of sphincter control. The spinal sexual reflexes, which are under tonic inhibitory control of supraspinal centers, may be disconnected from affective sexual arousal.^{152,153} This means that complete injuries allow for disinhibited reflex erection centers in the cord such that non-sexual touch can trigger reflex erections (e.g. by clothes rubbing or catheterization) without voluntary control.¹⁵² However, sexual touch does not necessarily lead to the satisfactory maintenance of sexual reflex erections, since both psychogenic and reflexogenic components are usually required.^{154,155}

Not all suprasacral injuries are created equal. The lumbar spinal cord is home to sympathetic efferents, as well as somatic motor and sensory neurons that innervate the pelvic organs. Therefore, lumbar injuries cut off both supraspinal control to the sacral parasympathetics and directly damage spinal neurons. As a result, the nature and extent of pelvic organ dysfunction varies with the level and extent of local damage in the lumbar cord. While these details are often overlooked clinically as simply complicating the outcome of SCI, they are informative in studying the mechanistic details of pelvic organ dysfunction.

Pelvic organ function is also reliant on visceral sensation, and sparing of sensory function varies dramatically among individuals with lumbosacral injuries. For example, the majority of individuals with complete SCI below T10 retain bladder sensation, most likely mediated by

intact afferent fibers that travel through the hypogastric nerve to the thoracolumbar cord.¹⁵⁶

Despite these important distinctions, the overall pattern of dysfunction is predictable: in higher SCI, more spinal segments and targets are cut off from supraspinal control, resulting in more substantial complications in pelvic organ function, either directly (due to loss of supraspinal input) or indirectly (due to loss of hand function rendering self-care challenging or impossible).¹⁵⁷

In addition to disrupting descending pathways to the pelvic organs, cervical and high thoracic injuries can also result in systemic dysfunction, such as autonomic dysreflexia. AD develops after severe SCI at T6 and above, and manifests as hypertension triggered by noxious and innocuous sensory stimulation below the level of injury. Interestingly, pelvic viscera afferent activity is a key trigger for AD events, the details of which will be addressed later. Other key autonomically-regulated players in homeostasis such as hormone regulation, circadian rhythms, metabolism and immune system function, are also disrupted after high SCI.^{32,158–160} These systemic changes also impact secondary complications of SCI, including pelvic organ (dys)function, and questions remain as to whether these changes are the result of changes in previously present circuitry or the formation of new connections.

1.5.2 Pelvic organ function and severity of SCI

The clinical classification of SCI is based on residual function and describes the loss of function simply in terms of complete or incomplete. Originally (and still commonly), severity of SCI is based on motor and sensory function, using the American Spinal Injury Association Impairment Scale (AIS, modified from the Frankel classification).^{161,162} More recently, autonomic function has been considered as a component of SCI classification, and the terms

‘autonomically complete/incomplete’ have entered the vernacular in the field.^{163,164} While motor and sensory dysfunction do not reliably predict residual autonomic outcome on an individual basis, pelvic organ dysfunction in general is more severe among people with motor and sensory complete SCI.^{146,165–168}

Anatomically complete SCI is relatively rare in the clinical setting; when it does occur, it leaves the caudal portions of the cord isolated from descending input and solely responsible for the reflex control of the pelvic viscera. The profile of pelvic organ dysfunction is more complex in instances of incomplete SCI. With recent changes in etiology and acute management, including early surgical decompression, the incidence of complete SCI is decreasing.^{147,148} Common injury mechanisms such as contusion and compression of the spinal cord spare tissue within the injury site and preserve white matter that can act as a substrate for neurological recovery, for better or worse altering long term functional outcomes (discussed below).¹⁶⁹ Diverse supraspinal centres govern the pelvic organs; as a result, autonomic preganglionic neurons in the distal spinal cord are innervated by diffuse collections of fibers that are not anatomically circumscribed or well characterized.^{170,171} As a result, autonomic functions are more difficult to predict based on the spinal cord tracts that are damaged, compared to motor and sensory functions with well-defined pathways. Studies comparing bladder function after complete and incomplete SCI (based on motor and sensory scores) find that these measures are insufficient for predicting the complexities of bladder outcomes, and that urodynamic or other detailed functional assays, are required to assess bladder function and design appropriate management plans.¹⁷²

1.5.3 The time course of pelvic organ (dys)function after SCI

Though the terms ‘acute’ and ‘chronic’ are often used in the SCI field, a clear delineation of the post-injury time range in each of these categories is unclear, especially when comparing animal models of SCI to human counterparts. Immediately following SCI there is a period of spinal shock, presenting as depressed spinal reflexes caudal to the injury site.¹⁷³ Though the concept of spinal shock is an old one, dating back to the mid-1700s, there is limited consensus over the extent and time course to which it takes place.¹⁷⁴ As such, the clinical definition of spinal shock resolution varies widely, from within days, when the bulbocavernosus reflex reappears, to months, when reflexive detrusor activity returns. A more recent model of spinal shock proposes a gradual resolution of the initial areflexia that corresponds to physiological changes that occur within the isolated cord below the injury.¹⁷⁴

Over time, changes in the excitability of spinal neurons below the injury, result in the reemergence of tone and reflexes, both normal and, in the case of high severe SCI, hyperreflexic (as in AD described above).¹⁷⁵ Assessments of pelvic organ function, including full urodynamic assessment alongside the recently developed Autonomic Standards Committee guidelines, are usually performed after the period of spinal shock has resolved to better define residual function and potential development of dyssynergias, which are common after SCI.^{176,177} Though the timing varies for each individual, bladder areflexia typically resolves (if it is going to) approximately three months after the injury, whereas detrusor overactivity or dyssynergias can develop and change in both acute and chronic periods following SCI.^{131,178}

The question of cause and effect can arise: functional changes that result from the loss of supraspinal coordination have the potential to feed back to produce further changes over time. For example, changes in the neural control of the bladder that result in detrusor-sphincter

dyssynergia-induced detrusor hypertrophy and concomitant release of increased neurotrophic factors can, in turn, affect the properties of the neurons innervating the bladder.^{179,180} This phenomenon also appears to play a role in the development of AD: while the complete picture of the mechanisms underlying the development of AD is still being investigated, it is clear that injury-induced changes that occur in the weeks and months after the disconnection of supraspinal centres from spinal and peripheral networks contribute to its development and severity. In animal models, spontaneous AD is present from acute time points after SCI and after an early dip in frequency and severity (between 6 and 10 days post injury) continues to show signs of increasing intensity over time.¹⁸¹ Similarly, in humans, AD events at acute time periods are documented, though it is generally thought of as a chronic condition with the negative consequences (such as elevated blood pressure) potentially increasing with the time post-injury.¹⁸²⁻¹⁸⁴ Therefore, though an acute traumatic SCI may appear to be a single event, the complexity and adaptability of the circuitry involved means that it needs to be looked at as an evolving and progressing condition.

1.6 Modelling SCI induced changes in the pelvic viscera

Characterizing the progression of clinical SCI is instrumental for determining research priorities, identifying appropriate models, and understanding the complexity of the human condition. However, small participant numbers, the mixed profile of injury level and anatomical damage, and the inherently variable nature of human research limit our ability to elucidate mechanisms underlying the functional changes that occur following SCI. Despite technological advances in imaging and improved instruments for clinical assessment, we rely on simple models (and often, self-reporting) to study many fundamental aspects of this complex injury.¹⁸⁵ Examining SCI in animal models allows for control over injury level, severity, and mechanism,

as well as countless other variables that cannot be manipulated in clinical populations. Each model has its advantages and drawbacks and choosing an appropriate model is fundamental to scientific investigation.

Experimental models in SCI research encompass a wide range of species and approaches. For example, classical locomotion and electrophysiological studies were largely performed in cats, following complete transection of the spinal cord.^{186,187} More recently, advances in manipulating the murine genome have rendered the mouse a species of choice for examining the roles of specific genes and proteins in SCI. In parallel, larger animal models such as primates, and more recently yucatan pigs, have been developed to test candidate therapies at an anatomical scale closer to humans.^{188,189} But for more than a century, the rat has been the species of choice for physiological and behavioural studies in neuroscience, creating a wealth of phenotypic and comparative information on the naïve animal and on the consequences of SCI.¹⁹⁰ Rats and humans undergo many of the same dysfunctional changes after SCI, including spasticity and neuropathic pain.⁵² Rat SCI is also pathologically similar to human SCI, in that a fluid filled cyst forms at the lesion epicenter, and is bordered by astrocytic scar.¹⁹¹ Central to my work, rats and humans also exhibit similar changes in autonomic function after SCI, including cardiovascular abnormalities, bladder dysfunctions, slowed gastrointestinal transit time, and sexual dysfunctions such as retrograde ejaculation.^{192,193} There are also anatomical advantages to studying SCI-induced changes in the pelvic neural circuitry in male rats, not to mention the clinical prevalence of SCI among males. The pelvic ganglia in male rats are cohesive, rather than the diffuse collection of cell bodies that form the pelvic “ganglia” in female rats, and the autonomic innervation of the pelvic sexual organs has been well-characterized.^{2,194}

When examining changes in structure and function of the pelvic viscera after SCI it is important to obtain quantifiable measurements that can be interpreted and compared. Though the organs of the pelvic viscera in different species share many anatomical and physiological commonalities, including the basic arrangement of autonomic innervation and the functions of storage and elimination, examining certain properties in animal models is not always straightforward. For example, studying sexual dysfunction in animal models is complicated by the fact that so much of the sexual experience is subjective.¹⁵³ In contrast, the bladder provides an excellent opportunity to examine changes in research models and relate them to phenomena assessed via analogous techniques in the clinical setting.⁵² Here I will describe the techniques used to assess LUT function after SCI and illustrate how complete spinal cord transection at different levels in the rat permit the examination of changes in the pelvic viscera and their relation to other complications after SCI, such as AD.

1.6.1 Animal models of spinal cord injury and autonomic dysfunction

When the focus of the research model is the injury mechanism, rats present an immediate challenge for studying functional (and particularly motor) outcomes. Rats are a robust species with a surprising capacity for recovery; within hours of a severe SCI, rats are alert, moving and active.^{195,196} A rat injury designed to replicate the extent of anatomical damage commonly seen in human SCI (e.g., contusion injury with a spared rim of spinal cord tissue) results in very different outcomes: while people are often paralyzed below the level of contusion SCI, rats regain substantial motor function spontaneously over days and weeks.¹⁹⁰ Recent data from my colleagues at ICORD elaborate on the differences between rats and humans with SCI. While people with high contusion SCI often develop AD in the absence of anatomical transection, rats

do not: an impact force of 400kdyn with dwell time of 5 seconds, which resulted in near blunt transection of the cord with little to no white matter sparing or neuronal cell bodies at the epicenter, was required to reliably induce AD in rats.^{197–200}

Therefore, the scientific questions being addressed are key to selecting appropriate model systems. Studies that look to understand and examine injury mechanism, or to test translatable therapies for SCI, aim to replicate the types of injuries seen in clinical settings (contusions, dislocations, etc.). Unfortunately (though perhaps faithful to the clinical scenario), the pathological and functional variability in these injury models is notoriously high: the same settings for force and dwell time on computer-controlled impactors produce a wide range of injuries across individual animals.^{201,202} In contrast, when the aim is to study complications and functional changes after SCI, reproducibility is crucial. The most reliable and reproducible injury model suitable for studying autonomic dysfunction is complete transection of the spinal cord. In addition to the consistency across animals, complete transections address specific and interesting scientific questions about what happens when neurons and circuits below the injury are completely isolated from supraspinal control, and how the level of isolation affects the outcomes and the neurons below the injury.

Complete transection of the spinal cord in the rat induces chronic dysfunction of the LUT that is reminiscent of the human condition. As in people with SCI, the first manifestation of bladder dysfunction is urinary retention that requires catheterization or manual expression of the bladder. When the spinal micturition centre (in the lower lumbar and sacral cord) is spared, reflex micturition is reestablished within one to two weeks of SCI in rats, but remains dysfunctional: rats with suprasacral SCI tend to urinate larger volumes less frequently and with greater residual volumes.²⁰³ This same pattern follows incomplete injuries that bilaterally

damage the cord, such as a midline compression or contusion of sufficient force, although reflexive micturition recovers more quickly and persistent deficits are less severe.^{202,204}

Autonomic dysfunction in people with SCI generally increases with ascending level of injury, and the same appears to be true in rats; however, T3 approaches the upper limit for sustaining animals with severe SCI over chronic time points in the laboratory setting. Rats with severe cervical SCI tend to develop infections and respiratory problems (personal communication, colleagues at ICORD); in contrast, studying rats with a T3 transection allows for the examination of many of the complications seen in humans after high SCI including bladder, bowel, and sexual dysfunction, and AD development (discussed in the next section) while preserving the animal's ability to move around the cage in good health.^{33,158,196}

While the advantages of using a T3 transection model to study autonomic function are well established, a more challenging question is the most appropriate level of SCI to use as a comparison group. Many studies examining cardiovascular function after SCI use a T8-10 transection in their control group, because SCI below the level of splanchnic sympathetic innervation does not result in AD. However, recent work at ICORD has revealed that animals with low-thoracic SCI develop significant cardiovascular dysfunction, and thus are not autonomic "normal" (C. West, personal communication June 2017). This is predictable, given systemic consequences of SCI; for example, the sympathetic preganglionics that innervate the rat adrenal glands mainly reside within the thoracic spinal cord and injuries to this mid- or low-thoracic region may continue to disrupt circulating hormones.³¹ More caudal injuries may preserve cardiac and adrenal innervation, but damage spinal circuitry innervating the pelvic organs. Lumbar transections damage the most caudal sympathetic preganglionic neurons within the cord, resulting in direct damage to a portion of the sensory and sympathetic neurons that

innervate the pelvic organs and preserving a portion of supraspinal connections to the pelvic organs. This produces an interesting contrast to the T3 transection: whereas a T3 transection cuts off the majority of input to sympathetic preganglionics, a L2 transection preserves the majority of them; a T3 transection preserves the bladder spinal circuitry whereas with a L2 transection there is direct damage to these circuits; a T3 transection results in autonomic dysreflexia and immune suppression whereas a L2 transection does not (Figure 1.2).²⁰⁵ Using these two transection models we can compare the changes that occur in the pelvic viscera and peripheral neurons that innervate these structures when there is a distant injury that removes all supraspinal input and a more proximal injury that damages neurons at the spinal levels responsible for these organs innervation.

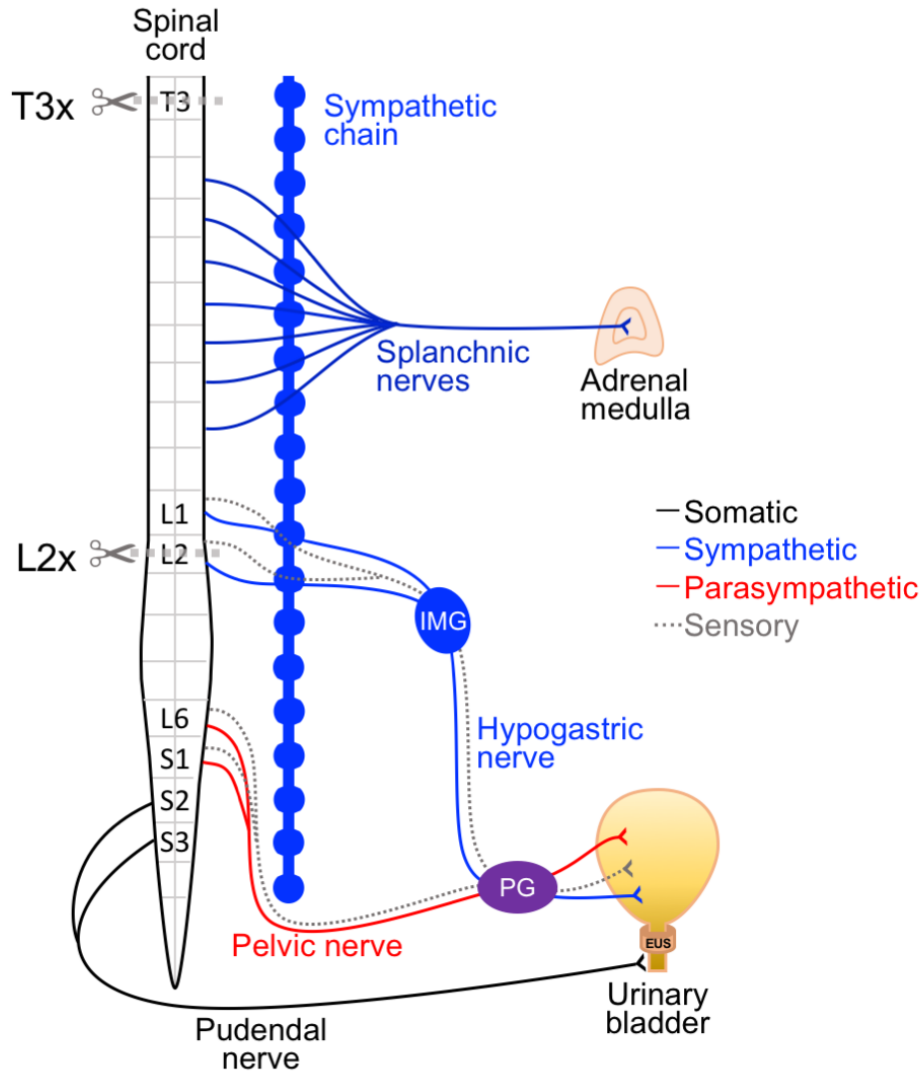


Figure 1.2 Differential disruption of the pelvic neuroviscera by high-thoracic and high-lumbar spinal cord injury in the rat

Sympathetic innervation of the adrenal gland bypasses the sympathetic chain, so preganglionics directly connect to the adrenal medulla, making it a form of specialized sympathetic ganglion. Autonomic preganglionic neurons that control the bladder originate in the L1-2 (sympathetic) and L6-S1 (parasympathetic) rat spinal cord. The primary sensory neurons innervating the bladder reside within the L1-2 and L6-S1 dorsal root ganglia (not shown, see Figure 1.1). Somatic innervation of the lower urinary tract arises predominantly from the sacral cord via the pudendal nerve to the rhabdosphincter. High-thoracic spinal cord transection eliminates supraspinal control of the preganglionics that connect to the adrenal medulla (T5-T11) and pelvic neuroviscera (L1-2, L6-S3). High-lumbar transection leaves the vast majority of the adrenal innervation intact, but directly damages some sympathetic and sensory pathways to the bladder and isolates the parasympathetic and somatic pathways. IMG: interior mesenteric ganglion, PG: pelvic ganglion, T3x: transection at the third thoracic spinal segment, L2x: transection at the second lumbar spinal segment.

A final consideration is the time points to examine after SCI. Due to the variability in the timeline for reflex return and recovery after SCI, direct comparisons between individuals are difficult and this is compounded many-fold when comparing humans to animal models. For example, late phase H-reflex changes that occur in humans at 12-16 weeks are seen at 3-4 weeks in the rat, and the return of detrusor voiding activity after spinal shock which occurs around 3 months in humans is present at 1-2 weeks in the rat.^{131,174,178} Though this complicates the direct comparison of processes occurring after SCI in humans and rats, it also provides an opportunity to look at similar physiological changes in a smaller, expedited model.

Most functional research studies on pelvic organ function are performed after the emergence of spinally mediated reflexes, such as reflexive bladder voiding, but it is clear that changes occur within the cord and the end organs starting much sooner after injury.^{206,207} Changes to the bladder urothelium occur within the first few hours after injury, and though the bladder lacks the reflexive voiding that occurs after spinal shock, there is still smooth muscle activity in the LUT early after injury.^{207,208} Additionally, AD events occur very early, subside and then return and increase in severity within a couple weeks after injury in rat models.¹⁸¹ Therefore, it is of interest to study both early time points, when immediate changes caused by the injury itself are driving changes, at the later time points, when adaptations to the injury have developed, and at time points during the transition between these stages.

1.6.2 Pelvic Visceral contributions to autonomic dysreflexia

AD occurs after SCIs that result in autonomically complete injuries at or above the level of innervation to the splanchnic vascular bed (around T6 in both rats and humans).²⁰⁹ AD is elicited by a sensory stimulus below the level of injury that results in sympathetic activation

causing significant ($> 20\text{mmHg}$ above baseline) increase in systolic blood pressure.¹⁷⁶ Without input from the brainstem there is dysregulated activity in sympathetic preganglionic neurons resulting in high sympathetic tone. Additionally, changes in the peripheral and spinal pathways below the level of the injury result in aberrant sensory-sympathetic cross-talk that leads to sensory stimulation resulting in uncontrolled sympathetic outflow. This means that a visceral or somatic sensory stimulus, either innocuous or noxious, below the level of injury can trigger a sympathetic surge that increases vascular resistance and results in a dramatic rise in blood pressure.^{210,211}

The event that stimulates AD can be an external event, such as a tight belt or sitting on a sharp object, but more often it is an internal event stemming from the activity of the pelvic organs. The majority of AD episodes that require clinical treatment result from bladder-related events, such as an overfull bladder, catheter dysfunction, or urinary tract infections.²¹² But the other pelvic organs also play a role, with numerous documented cases of both bowel routine and sexual stimulation resulting in pronounced hypertension, with or without symptoms.^{213–215} When symptoms are present they can be debilitating – a severe pounding headache, sweating, nausea – though the severity of the symptoms do not necessarily match the severity of the hypertension. This means that for individuals with high SCI, their daily systolic blood pressure can vary significantly: for example, ranging from 80 mmHg at rest to ≥ 170 mmHg during a bowel routine.²¹³ And there are more extreme examples: one case study reported an individual whose systolic blood pressure exceeded 300mmHg during sexual activity²¹⁶. Therefore, everyday occurrences, such as a full bladder, full bowel, or sexual arousal can result in significant spikes in blood pressure into clinically dangerous ranges. These dramatic daily fluctuations in blood pressure have both acute and chronic consequences. Severe AD episodes have the potential to

lead to immediate adverse events, such as stroke, and long term blood pressure instability may cause vascular injury, increasing the risk of cardiovascular disease, which is elevated in persons with SCI.^{217–220}

The pelvic viscera's role in the occurrence of AD is also apparent in rat models of cervical or high-thoracic SCI. Recent work with telemetric blood pressure monitoring showed that like in humans AD is also a common feature in the awake lives of rats with T3 complete transections.¹⁸¹ Additionally, a number of experimental procedures involving the pelvic viscera are documented to elicit AD including colo-rectal, bladder, and vagino-cervical distension.^{221,222} Experimental AD is most often elicited via colo-rectal distension, a reliable and straight-forward technique that induces AD in SCI rats and mice.^{211,221,223,224}

1.6.3 Modelling and quantifying changes in the LUT

LUT function involves the coordination of the bladder, urethral and external sphincters through integration of the somatic, sensory and autonomic nervous systems. Proper timing and location of urination in humans is a learned behavior that relies on cortical, spinal and peripheral circuitry and is therefore sensitive to damage along any part of the signaling pathway. The suite of functional and structural LUT assessments available for both human and animal studies has provided insight into how the different components work together, or fail to do so, after disruption to the central nervous system. Specifically, rat *in vivo* bladder studies have shed light on the neural circuitry that signals and controls bladder filling and emptying as well as the course of changes that occurs after SCI.

Structural changes occur in both the uroepithelium, which forms the cell layers on the inner mucosal surface of the bladder, and the detrusor smooth muscle layer of the bladder after

SCI. The uroepithelium was once considered a simple passive barrier, however, it is now clear that in addition to regulating the bladder permeability, the uroepithelium is also involved with both immune responses and cell-to-cell communication, which includes interactions with closely associated efferent and afferent fibers.⁸⁰ Furthermore, it was found that the cells of the uroepithelium have neuron-like properties, including expressing sensory receptors such as TRPV1 and P2X₂, and responding to chemical and stretch stimuli with the release of factors such as ATP, ACh, and NO.^{76,80,83,225} Changes to the uroepithelium occur quickly upon SCI; in rats, disruption to the mucosal lining occurs within two hours of injury and includes morphological changes as well as decreased transepithelial resistance.²⁰⁷ Hematuria also commonly occurs in the days following injury, indicating breakdown of the bladder's protective barrier.^{204,207} Though some of the initial disruptions to uroepithelial structure recover within a few weeks of injury, signs of long term changes persist, including decreased cellular volumes, increased cellular disorganization, and changes in expression of sensory receptors and neurotrophic factor mRNA.^{72,207,226}

A clinical study of bladder wall biopsies from 94 individuals with SCI, ranging from 4 months to 528 months post injury, found that 91.5% had alterations in the bladder wall, including signs of inflammation and fibrosis.²²⁷ Additionally, bladder wall thickening has been examined by ultrasound and has been identified as an issue in cases of SCI, bladder outlet obstruction and myelodysplasia.²²⁸⁻²³⁰ A study with access to full thickness bladder biopsies from patients undergoing augmentation cystoplasty for bladder dysfunction, including from SCI, found that the bladder walls had increased connective tissue and a higher ratio of type III to type I collagen.²³¹ These changes are consistent with tissue remodeling seen in rats three weeks after SCI which

include decreased collagen and increased elastin content that may affect bladder compliance and contractility.²³²

The driving forces behind these bladder changes are multi-fold and feedback on each other. In addition to affecting the mechanical properties of the bladder, changes to the bladder cellular structure influences the neural circuitry innervating the bladder.^{72,233} Numerous factors play into the changes that occur within the bladder acutely and chronically after SCI: the initial loss of neural control and potential increased pressures and volumes in the bladder, followed by uncoordinated reflexes, dyssynergias and muscle hypertrophy can feedback into increased neurotrophic production and neuronal change which may reinforce and modify functional changes. However, much of how each of these factors relate to each other and play out over time needs clarifying.

To complement the examination of bladder structural changes there are multiple functional assessments available to record and quantify LUT changes in rat models that are essentially similar to their human equivalents.⁵² Cystometric urodynamic analysis is the most common method used for assessing LUT function and consists recording of bladder pressure during physiological filling or controlled filling achieved with a catheter placed into the lumen of the bladder. This provides information on the relationship between intravesical pressure and volume, bladder capacity, residual void volumes, as well as allows for the identification of urodynamic patterns indicative of detrusor overactivity and dyssynergias.

In humans, this procedure can be performed in the urologist's office while the patient is alert, with feedback collected on bladder sensation, if present, during filling. The basic urodynamic procedure can be performed in a very similar manner in animal models, such as the rat, with a few modifications to account for challenges such as the difficulty with animal

movement and their inability to report on any potential sensory feedback. Natural behaviours, such as walking and grooming, will affect the abdominal pressure and therefore bladder pressure, so urodynamics are frequently performed in anesthetized animals.²³⁴ Caution, however, must be applied since anesthetics are known to affect the micturition reflex.²³⁵ Urethane is commonly used for bladder studies because it produces a long term and stable anesthesia, however it is known to affect the LUT, particularly with regards to the urethral function.²³⁶⁻²³⁸ However, using lower doses of urethane helps address undesirable anesthetic effects while still allowing urodynamic measurements to be performed in anesthetized animals.²³⁹

Urodynamic studies in rat models of SCI demonstrate similar phenomena seen after SCI in humans and provide quantifiable measures of LUT function that can be compared across injury types and time points to piece together how the neural control of different LUT components is affected by SCI. Different patterns of urodynamic findings indicate different types of dysfunction in the neural circuitry of the LUT. Like in humans, detrusor-sphincter dyssynergia (DSD) can be recognized after SCI by the presence of bladder detrusor contractions, and therefore bladder pressure increases, alongside activation of the external urethral sphincter, indicating a dyscoordination of the sympathetic and parasympathetic pathways controlling these components. An overactive detrusor can also be identified on urodynamic traces by the presence of increases in intravesical pressure that do not result in voiding, known as non-voiding contractions (NVCs). These types of urodynamic findings can reveal changes in aspects of the neural control as well as intrinsic properties of the bladder. In order to understand the implications and the relevance of SCI induced changes occurring within the bladder, and other pelvic organs, an understanding of normal pelvic neurovisceral circuitry is necessary.

1.7 SCI-induced cellular changes in pelvic neuroviscera

SCI results in significant functional changes within the pelvic neuroviscera, that are also reflected in cellular changes within the lumbosacral spinal cord, LS-DRG, PG, and pelvic organs. Numerous studies have extensively examined and reviewed the changes in the cord at the site of the injury and in the spinal circuitry below the injury.²⁴⁰ Likewise, functional and structural changes in the bladder have been described with both suprasacral and sacral injuries. Changes in the pelvic peripheral ganglia after SCI are also garnering more attention of late, especially with regards to the DRG and the circuitry involved in AD and neuropathic pain development.^{3,193,241-243} However, the literature surrounding injury induced changes in the DRG and PG is significantly more abundant for peripheral nerve injuries. Here I will briefly review cellular changes that occur within the pelvic neuroviscera after SCI.

1.7.1 Changes in lumbosacral spinal circuitry

The level of the SCI will determine which spinal neurons are most affected. Clearly, damage to the central portions of the sensory and motor neurons controlling the pelvic viscera occurs most overtly with lumbosacral SCI. Significant cell death and axonal damage occurs at the site of injury as a progression of well-studied inflammatory and fibrotic responses occur.^{240,244-246} The combination of cytokines and chemokines released from astroglia and the interruption to descending inhibitory pathways can result in significant activation of neurons within the regions caudal to the injury.²⁴⁷⁻²⁴⁹ However, when the injury occurs at the level of the lumbosacral cord, central components of the pelvic neuroviscera (the sympathetic preganglionics and central processes of DRG neurons) are damaged. Permanent loss of relevant autonomic preganglionic neurons, interneurons, and sensory terminals at the site of the injury likely underlie

a significant portion of the permanent functional loss that occurs and is described in previous sections.

Cervical and thoracic injuries, far rostral to the lumbosacral cord, also result in cellular changes within the caudal regions of the cord. For example, after complete high-thoracic SCI the dendritic arbors of the mid-thoracic spinal sympathetic preganglionic neurons (SPNs) initially retract, seemingly due to the loss of descending synapses.^{250,251} However, within two weeks of the injury sprouting of interneurons, primary afferents, or spared axons replace degenerated synapses, resulting in the regrowth of the dendritic arbors, but also perhaps in the formation of potentially aberrant connections.^{252,253} The reliance of SPNs within the lumbar cord on descending input is less clear; lumbar preganglionics undergo fewer changes after high transection, indicating that local connections may be more important for lumbar and sacral preganglionics.²⁵⁴ Though disruptions to descending tracts is an integral part of the changes within the lumbosacral circuitry, it is important to note that changes in peripheral signaling also play a role.

Work over the last twenty years has highlighted how changes in local circuitry contribute to systemic changes, especially with regards to the development of AD. Krassioukov and Weaver *et al.* first described in 1995 changes in the central termination patterns of nociceptors after SCI, linking this change to the development of AD.²²¹ Since then numerous studies have demonstrated that high-thoracic spinal transection results in lumbosacral peptidergic nociceptors extending into deeper laminae, traditionally non-nociceptive, regions of the cord.^{255–259} In 2006, Rabchevsky and colleagues added support for the causal link between sensory sprouting in the dorsal horn and AD via genetic manipulation of sensory sprouting at different levels of the spinal cord. Inhibition of the growth of peptidergic (CGRP-positive) afferent fibers in the lumbosacral

cord resulted in reduced responses to colorectal distension (CRD); the extent of CGRP-positive fiber sprouting and the severity of AD was also positively correlated.²⁶⁰

Spinal sensory plasticity is linked to other pelvic dysfunctions; both peptidergic and non-peptidergic afferents in the lumbosacral cord sprout into deeper laminae at time points relevant to the emergence of dysfunctional bladder patterns.^{261,262} Selective elimination of the IB4+ non-peptidergic afferents in the lumbar cord resulted in more efficient voiding in spinal cord transected animals.²⁶² Furthermore, intrathecal administration of a neurokinin-1 receptor agonist (binds SP and other tachykinins produced by peptidergic sensory neurons) antagonist at L6-S1 blocked the spinal micturition reflex in animals two weeks post-T10 spinal cord transection but did not affect voiding in intact rats.²⁶³ These studies indicate that sensory plasticity in the lumbosacral may also play a significant role in the changes in bladder function after SCI. More recent work has also identified a population of dopaminergic interneurons in the lumbosacral cord that expand after SCI along coincident to the partial recovery of the micturition reflex.²⁶⁴ After complete thoracic SCI, the depletion of these dopaminergic neurons or the blockade of spinal dopaminergic receptors reduced bladder activity, indicating that these neurons may also be involved in spinal micturition circuits after SCI.²⁶⁴

1.7.2 Changes in lumbosacral dorsal root ganglia

Direct injury of LS-DRG neurons occurs when the central projections are damaged by SCIs. This is most common when the injury is within a few segments of the central projection insertion into the dorsal horn of the cord, though there are a population of long-distance sensory projections. Regardless, it is clear that the greatest changes occur in DRGs close to injury; the greatest inflammatory response is found within the DRG near the injury. Like in the case of the

spinal cord these responses can be prolonged and can extend far from the site of injury. Inflammatory responses, including increased immune cell density, develop many segments caudal in the LS-DRG early after transection of the spinal cord and, in certain cases, earlier than in the corresponding segments of the cord.²⁶⁵ Changes within the ganglion environment and in circulatory factors (the DRG has a relatively permeable vascular barrier) can significantly impact neuronal function; many non-neuronal cells contribute cytokines, growth factors, and signaling molecules that can sensitize and change the response properties of neurons.^{246,266,267}

Like with intraspinal neural plasticity, changes within the LS-DRG neurons go hand-in-hand with changes in other functional systems, notably both autonomic and LUT dysfunction. In rats one month after T3 transection, when there is a strong AD response to CRD, there is a small but significant increase in the somal size of TRPV1-positive nociceptors in LS-DRGs.³ Hypertrophy of neurons is linked to changes in activity and target derived factors. Indeed, even with lower transection models, increases in TRPV1 expression in lumbar DRGs occurred alongside increased responses of dissociated DRG neurons to capsaicin.²⁴² These changes are often studied in regard to neuropathic pain, however there is overlap between nociceptor hypersensitivity, spontaneous activity, and AD development. Reduction of TRPV1-positive central projections in the lumbar dorsal horn by intrathecal capsaicin treatment results in decreased AD response to CRD.³ In line with these findings, *in vitro* and *in vivo* recordings from small nociceptive DRG neurons from animals with SCI show increased responsiveness to capsaicin and spontaneous activity.^{241–243}

Many of the studies examining LS-DRGs after SCI have also focused on bladder projecting neurons. Indeed, when bladder traced DRG neurons were specifically examined after T9 SCI, both increases in soma cross-sectional area and upregulation of a number of

neuropeptides including PACAP, galanin and VIP were found.^{4,268-270} Changes in the activation and excitability of bladder projecting afferents have also been identified.²⁶⁸ After thoracic SCI increases in the excitability of C-fibres innervating the bladder, linked to Na⁺ and K⁺ channel expression changes, are believed to contribute to the development of overactive bladder.^{268,271,272} These results indicate that there are complex changes occurring within the DRG with different levels of neurotrauma and that both direct effects and response to these changes within the circuitry overtime may be playing a role in the outcomes of these injuries.

1.7.3 Changes in pelvic ganglia

Compared to the DRG, the PGs are further removed from the spinal cord, residing closer to their targets than to the cord, and unlike DRG neurons the neuronal constituents of the PG are not directly damaged by SCI. However, based on studies of lumbar DRGs after high-thoracic transection, it is clear that SCI can result in changes to neurons far caudal to the injury.³ Furthermore, considering that changes within target organs are known to significantly impact the character of their innervating neurons and that significant structural and functional changes occur within the pelvic viscera after SCI, one might expect there to be concomitant changes within the PG. However, SCI-induced changes to the PG are not well understood.

Indeed, very few studies have directly examined changes in the PG after SCI. Both published studies examining changes in the PG of the male rat used a model of complete transection at T9, which severs the cord immediately rostral to the sympathetic preganglionics that innervate the PG.^{4,273} Kruse *et al.* examined morphological changes of PG neurons and found no significant differences in soma size with transection alone. However, decentralization of the PG alongside spinal cord transection resulted in a significant increase in the cross-

sectional area of PG neurons, indicating that preganglionic input may have a role in regulating cell size changes in the PG.⁴ The only other study examined changes in cholinergic terminals in the PG using vesicular acetylcholine transmitter (VAcHT) immunoreactivity. After T9 transection the number of neurons with VAcHT-positive terminals decreased, with the lowest levels at 7 days post injury, and partial recovery after 28 days.²⁷³ As both of these studies used T9 transections, how the level of SCI impacts these and other potential changes within the PG remains to be shown.

1.7.4 Changes in the bladder

Both SCI and peripheral nerve injuries are known to cause significant structural and functional changes within the urogenital tract. Though a number of studies have highlighted how neurotrauma impacts the sexual organs and colon, the bladder has been most extensively studied in this context.²⁷⁴ As I previously discussed modelling LUT changes after SCI, I will confine this discussion to key changes that occur in the structural and functional components of the bladder after SCI.

Injury level and severity impact the extent of changes seen within the bladder after neurotrauma.^{172,275} Central injuries that result in the destruction of the spinal parasympathetic nucleus in the sacral cord result in lasting bladder areflexia similar to pelvic nerve injury. SCIs that spare the sacral micturition centre, have a complicated outcome trajectory with significant functional and structural changes that develop and change over time, as discussed above. When spinal mediated reflex voiding occurs after SCI it is often accompanied by DSD and NVCs, which are linked to bladder hypertrophy, fibrosis, and changes in compliance.²⁷⁶⁻²⁷⁹ Muscle fiber orientation and connective tissue within the bladder wall also change dynamically after SCI, with

initial increases in elastin and decreases in collagen, which may be linked to the changing compliance.^{280,281} Analysis of early changes in bladder gene expression after SCI found that many related to inflammation, infection, and tissue remodeling.²⁸² Changes to the factors secreted by the bladder after SCI can also influence the neural circuitry. NGF, and possibly brain derived neurotrophic factor (BDNF), from hypertrophied bladders are linked to development of detrusor overactivity and increases in the somal size of bladder projecting sensory and motor neurons.^{100,270,283–285} It is also important to note that hypertrophy of the bladder wall is not dependent on innervation; bladder outlet obstruction (BOO) still results in muscle hypertrophy even when both PGs are removed,²⁸⁶ and non-neurogenic causes of bladder hypertrophy, such as BOO, are also linked to increased neuronal cell sizes.²⁸⁷ The feedback loop between neurotrauma-induced end organ changes and plasticity of the governing circuitry has garnered considerable interest as mechanisms for pelvic organ dysfunction after SCI.

1.8 Experimental overview and hypotheses

This thesis centres on changes within the pelvic peripheral ganglia and their targets after different levels of spinal cord injury. Throughout this thesis I use two main injury models in adult male Wistar rats, a complete transection at the third thoracic (T3x) or second lumbar (L2x) level. These two injury models are of particular interest because the high thoracic transection results in interesting systemic outcomes including the development of AD and the isolation of the circuitry innervating the adrenal glands. The lumbar injury, preserves (at least mostly) innervation to the splanchnic bed and adrenal gland, but causes direct damage to the neurons that innervate the pelvic viscera, potentially resulting in significantly different outcomes. Therefore,

it is of interest to examine changes within the pelvic viscera, and for the purposes of this thesis specifically the bladder, and the peripheral neurons that innervate them.

1.8.1 Cellular changes within the pelvic peripheral ganglia

There are clear differences in the (dys)functional outcomes of high thoracic and lumbar spinal cord transection. Furthermore, numerous studies have looked at morphological changes in the sensory neurons of the DRGs with regards to AD, neuropathic pain, and LUT dysfunction after high thoracic SCI.^{3,243} The other pelvic peripheral neurons innervating the LUT, the autonomic neurons of the pelvic ganglion/plexus, are relatively understudied after SCI. Starting in Chapter 2 with the commonly used model of T3 complete transection, I examined the differential gene expression in both the LS-DRGs and PGs one month after injury to better understand the longer term cellular changes in these ganglia. This tested the hypothesis that even distant SCI, both in time and space, which results in significant changes to the pelvic viscera, also causes lasting gene expression changes in the pelvic peripheral ganglia.

Furthermore, based on known changes within the LS-DRGs and pelvic viscera after SCI and the results of the RNA sequencing experiments, I hypothesized that the PG neurons would also undergo morphological changes upon spinal cord transection. Because of the differences seen functionally with T3x and L2x, I also hypothesized that these injury levels would result in disparate cellular responses. I addressed these questions in Chapters 2 and 3, where I analyzed cell morphological changes of both the sympathetic (TH-positive) and parasympathetic (TH-negative) populations in the PG after both injury levels and at two different time points. Interestingly, the results in both Chapters 2 and 3, demonstrate complex relationships between

target and neuron changes, indicating that previously described relationships, such as the neurotrophic hypothesis, may not sufficiently explain pelvic neuroviscera changes after SCI.

1.8.2 Differential responses in bladder activity

Based on gross differences observed in the bladders of chronic T3x and L2x rats, with L2x animals having significantly heavier wet weights, I hypothesized that there may also be differences in bladder activity after injury. I examined this hypothesis in Chapter 4 where I observed increased low amplitude non-voiding activity in the bladder of rats acutely after L2x but not T3x. Due to the differences in the damage to the sympathetic and sensory neurons that are involved in bladder innervation with these two injuries, I hypothesized that the direct damage to neurons innervating the bladder after a L2x injury was responsible for the differences in early bladder activity. However, transection of the hypogastric and pelvic nerves, blocking signal transmission through the PG with drugs, and complete denervation of the bladder, did not affect the presence or development of the acutely presenting non-voiding contractions. This lead me to investigate alternative pathways that are differentially influenced by these injuries. Since others have shown that high SCI may result in decreased adrenal function,^{33,158} I hypothesized that preserved adrenal function in the L2x model contributed to the small-amplitude contractions at low pressures acutely after injury. To test this, I removed adrenal gland surgically immediately prior to SCI in the L2x model, resulting in a low injury without preserved adrenal gland function and compared the bladder activity between the different injury groups.

Chapter 2: Transcriptional and morphological changes in pelvic sensory and autonomic neurons following high spinal cord injury reveal unexpected neuron-target interactions

2.1 Summary

Spinal cord injury (SCI) interrupts communication between the brain and spinal cord, and has profound and long-lasting effects on peripheral organ function. Among the most important of these to people with SCI is pelvic visceral (bladder, bowel, sexual) function. Since neurons rely on target-derived trophic support for phenotypic maintenance, SCI-induced changes (such as bladder hypertrophy) can be expected to alter peripheral sensory and autonomic gene expression. Here we used RNA sequencing to ask how a high-thoracic (T3) complete SCI affects whole-ganglionic transcriptomes of pelvic dorsal root ganglia (L6/S1 DRG) and pelvic autonomic ganglia one month later. Comparison of sham and T3-injured L6/S1 DRGs identified 525 differentially expressed genes. Functional Clustering Annotation (FCA) revealed that nucleotide and RNA-binding genes were enriched in both the up- and downregulated gene sets. Downregulated genes with annotations relating to synapses and cell junctions were also enriched. Canonical Pathway Analysis indicated reduced signaling in multiple growth factor and cytokine pathways, the majority of which with high z-scores ($>|2|$) involved reduced FGFR1 expression. Ingenuity Pathway (upstream) Analysis identified changes in gene expression consistent with reduced BDNF signaling. Fewer differentially expressed genes (108) were identified in the pelvic ganglia (PG), precluding robust FCA. Nevertheless, expression of genes related to neurotransmitter and co-transmitter synthesis, expression, and processing was reduced, and nerve growth factor receptor expression was increased. These transcriptomic changes in the

PG were only partly consistent with increased neurotrophic support from the hypertrophic bladder after T3 SCI, and atrophy of PG neurons at the same time points to a more complex relationship between target size and neurotrophism than generally accepted.

2.2 Introduction

The pelvic peripheral sensory and autonomic ganglia serve respectively as the first input to, and the final output from, central nervous system control of visceral targets such as the bowel, bladder and sexual organs. The lumbosacral dorsal root ganglia (LS-DRG, conveying the input), contain pseudounipolar sensory neurons that have both peripherally and centrally projecting processes. The peripheral process of all DRG neurons extend through the spinal nerves to their targets, while their central processes project *via* the dorsal root into the cord, usually synapsing on spinal neurons within a few spinal segments of their entry.⁴¹ Unlike primary sensory neurons, PG autonomic neurons (relaying output from the CNS) only project to peripheral targets. These receive synaptic inputs from preganglionic neurons in the thoraco-lumbar and sacral cord *via* the hypogastric and pelvic nerves, respectively.^{11,28} SCI above the sacral cord interrupts both afferent and efferent arms of central pelvic visceral control, and results in trophic changes in pelvic organs, the most dramatic of which is bladder hypertrophy.^{206,288}

The neurotrophic hypothesis, a major tenet in neurobiology initially formulated by Levi-Montalcini and Hamburger,²⁸⁹ highlights the importance of target-derived neurotrophic support during the developmental period of naturally occurring cell death, but the influence of target-derived factors extends far beyond this period.²⁹⁰ Adult peripheral neurons rely on target-derived factors for phenotypic maintenance, which has been demonstrated by isolation of peripheral sensory and autonomic neurons from their targets.^{103,291} For instance, axotomy results in a cell body reaction that includes changes in the expression of a number of neuropeptides. Sympathetic neurons of the superior cervical ganglion when axotomized upregulate galanin, vasoactive intestinal peptide (VIP), and substance P, which are normally not expressed by these neurons, and downregulate neuropeptide Y (NPY). Likewise, axotomized lumbar DRG neurons increase

expression of galanin and VIP, while substance P and calcitonin gene related peptide (CGRP) are downregulated. These cell body responses result both from injury-induced signalling as well as loss of target-derived factors, such as NGF.^{292,293} This is evident from studies demonstrating that antagonizing NGF signalling recapitulates many changes seen after axotomy, and from studies in which application of exogenous NGF after an injury partially rescues neuronal phenotype.^{292,294–296}

SCI-induced disruption to the pathways innervating the pelvic viscera result in significant changes within target organs that evolve over the course of days, months and even years after injury. Numerous studies have examined changes in both the LS-DRGs and pelvic viscera, most notably the LUT, after SCI. Dyssynergia of the urinary bladder detrusor and sphincter are believed to result in hypertrophy of the detrusor muscle and increased neurotrophic factor production by the bladder wall,^{72,140,226,275,297} including NGF, BDNF, GDNF, CNTF, NT-3, and NT-4, all of which remain elevated (at the mRNA level) for at least 4-6 weeks following SCI.²²⁶

The production of NGF in particular has been associated with hypertrophy of bladder-projecting primary afferents.⁷ Results from our laboratory and others have identified TRPV1-positive LS-DRG neurons (potential contributors to AD, bladder dysfunction, and neuropathic pain^{3,7,42,242}) as particularly susceptible to hypertrophy following T3 SCI.³ These findings align with independent studies that show increased spontaneous activity in capsaicin-sensitive neurons after SCI.^{242,243} The absence of hypertrophy of peptidergic nociceptors (those which express the NGF receptor TrkA) is intriguing given the hypothesized association between bladder-derived NGF and neuronal hypertrophy.

Less is known about changes that occur within the PG after SCI. Two studies have examined cellular changes within PG neurons after SCI; one identified a reduction in the density

of cholinergic terminals (i.e. either preganglionic or intrinsic parasympathetic ganglionic neurons) that partially recovered over time, and the other found no significant changes in cell sizes one month after a T9 spinal cord transection injury.^{4,273} As with cell-size changes in L6/S1 DRG neurons after SCI, this finding is at odds with the hypothesis that NGF produced in excess by the hypertrophic bladder is functionally significant (at least at this post-operative time point), since exposure of intact PG neurons to exogenous NGF results in somal hypertrophy.²⁹⁸ Thus, the relationship between SCI-induced trophic changes in pelvic viscera and their connecting neurons requires further clarification.

In the present study, I examine transcriptomic changes in the rat pelvic sensory and autonomic ganglia after high thoracic (T3x) spinal cord transection. Using RNA sequencing, I identify a set of small but significant changes within the L6/S1 DRGs and PGs one month after injury. Using functional annotation, I examine patterns of gene expression changes in the ganglia to gain insight into affected signaling pathways. By combining transcriptomics with morphological analysis of PG neurons, I provide evidence for a more complex relationship between target size and neurotrophic support than that originally posited by the neurotrophic hypothesis.

2.3 Materials and Methods

2.3.1 Animals procedures

I performed the animal experiments for the RNA sequencing experiments (n=6 T3 SCI and 6 sham) at King's College London, Guy's Campus in the laboratories of Profs. Stephen MacMahon and Elizabeth Bradbury, with ethics approval from the UK Home Office Animals (Scientific Procedures) Act, 1986. Confirmation of changes in selected genes (n=14 T3 SCI and

10 sham) and morphological experiments (n=11 T3 SCI and 10 sham) were carried out using separate material and at two postoperative time points (two weeks and one month) at the University of British Columbia with approval of the institutional Animal Care Committee in accordance with the guidelines established by the Canadian Council on Animal Care.

2.3.2 Spinal cord injury surgeries

Complete transection of the spinal cord was performed at the third thoracic (T3) spinal segment in adult male Wistar rats (300-400g, from Harlan, UK, or Envigo, Mississauga, Canada). Sham surgeries were also performed concurrently, and in the same manner as the transection surgeries, up to and including the durotomy. Rats were housed in groups of 2-4 at a secure conventional facility with a standard 12-hour light-dark cycle. Details of the surgical procedure and post-operative care have been previously detailed and published¹⁹⁶, but major procedures will be detailed here.

Prophylactic enrofloxacin (Baytril; 10 mg/kg, subcutaneous (s.c.), Associated Veterinary Purchasing (AVP), Langley, Canada) was administered to all surgical animals for three days prior to as well as on the day of SCI surgery. In preparation for surgery the animals were initially anesthetized with isoflurane followed by an intraperitoneal injection of combined ketamine hydrochloride (Vetalar®; 70mg/kg, i.p., University of McGill Animal Resources Centre, Montreal, Canada) and dexmedetomidine hydrochloride (Dexdomitor®; 0.5 mg/kg, i.p., AVP). Buprenorphine (Temgesic®; 0.02 mg/kg, s.c., University of McGill) and ketoprofen (Anafen®, 5 mg/kg, s.c., AVP) were administered just prior to surgery for analgesic purposes. The skin at the surgical site was shaved, cleaned three times with alternating hibitane and alcohol, and treated with iodine. The anesthetized animal was placed prone on a water circulating heating pad for the

duration of the procedure.

For T3 transections and shams a 5ml syringe was placed behind the elbows and under the rib cage to obtain the appropriate curvature of the spine. The spinal column was exposed *via* a midline incision in the skin, approximately 3cm long above C8-T3 vertebrae. The T2-T3 intervertebral space was then exposed by blunt dissection of the overlying muscle and connective tissue. The sham operations were completed with the opening of the dura and wound closure. For the complete transections, the cord was cut completely with surgical scissors. Completeness was verified under the surgical microscope by visualization of clear separation and retraction of the two cut stumps of the cord. After cessation of bleeding, the muscle and skin were closed with continuous, 4-0 Vicryl sutures, and interrupted, 4-0 Prolene sutures, respectively.

2.3.3 Post-operative animal care

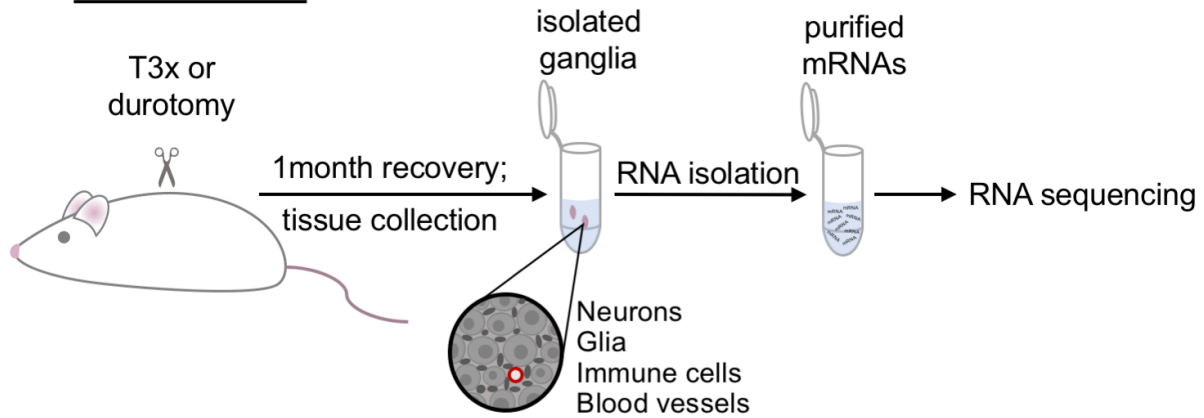
Upon completion of surgery, fluids were replaced with warmed Lactated Ringer's solution (5 ml, s.c.). Anesthesia was reversed with atipamezole hydrochloride (Antisedan; 1 mg/kg, s.c., Novartis, Mississauga, Canada) and the animals were allowed to regain consciousness in a warm, temperature-controlled environment (Animal Intensive Care Unit, HotSpot for Birds, Los Angeles, CA). Enrofloxacin (10 mg/kg, s.c.), buprenorphine (0.02 mg/kg, s.c.), ketoprofen (5 mg/kg, s.c.) and warmed lactated ringers (5ml, s.c.) were administered once per day for three days following surgery and thereafter only as needed. Rubber matting was placed under the woodchips in the cages of rats with SCI, to assist with traction when moving. To aid in recovery and encourage foraging, water bottles were equipped with long spouts and food was scattered around the cage.¹⁹⁶ Animals were supported with an enriched diet, including Rodent Liquid Diet (Bioserv, Flemington, NJ, USA), flavoured jelly, cereals and commercially

available rat treats. The bladder was manually expressed 3-4 times daily until spontaneous bladder function returned (7-10 days post-injury). Monitoring of body weight, activity level, social behaviour, healing at the surgery site and clinical signs of morbidity was completed daily for the first two weeks after surgery and every two days thereafter.

2.3.4 RNA isolation

Figure 2.1 outlines the RNA sequencing workflow. Rats were euthanized (6 animals per group) and perfused through the heart with approximately 100ml of cold PBS. The L6/S1 DRGs and PGs were immediately dissected, frozen with liquid nitrogen, and stored at -80° until RNA extraction. The standard procedure for RNA isolation outlined in the Trizol Reagent manual was followed using 1-Bromo-3-chloropropane and Phase Lock Gel (5 PRIME Phase Lock Gel, Heavy, Quantabio, Beverly, MA, USA cat# 2302810) to isolate the RNA. The RNeasy MinElute kit (Qiagen Inc., Toronto, Ontario, Canada cat#74204) was subsequently used according to manufacturer's instructions to purify RNA using RNase-Free DNase set (Qiagen Inc., Toronto, Ontario, Canada cat#79254) as per the instructions. Isolated RNA was analyzed by Nanodrop and Bioanalyzer 2100 (Agilent Technologies, Santa Clara, CA, USA) to ensure quality of sample prior to RNA sequencing.

A RNA isolation



B RNA sequencing

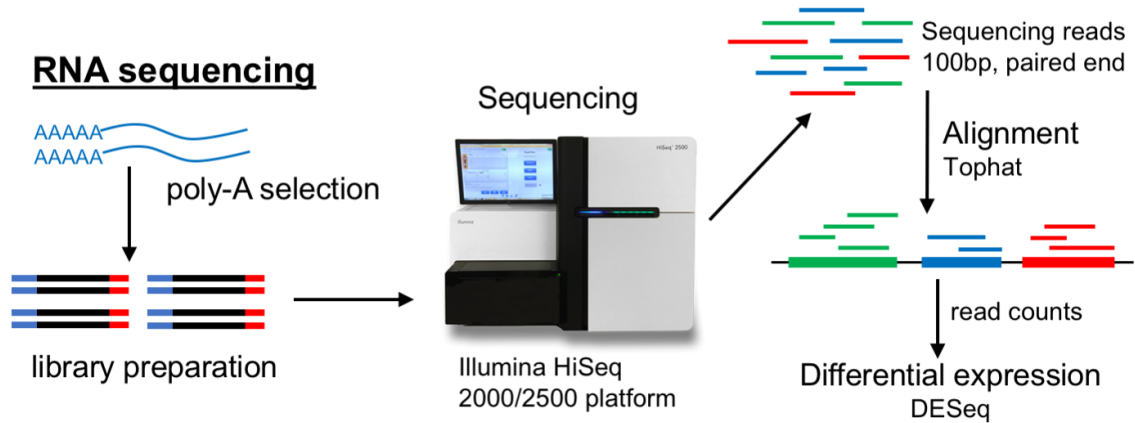


Figure 2.1 Experimental outline for RNA sequencing of pelvic peripheral ganglia
(A) Ganglia (PGs and pooled L6/S1 DRGs) were isolated from PBS perfused rats one month post-T3x or sham surgery. mRNA was isolated from whole ganglia and sent for RNA sequencing at the Oxford Genomics Centre. (B) Sequencing reads were aligned using TopHat and differential expression was performed using DESeq.

2.3.5 RNA sequencing

1µg of RNA was sent to the Oxford Genomics Centre, Bioinformatics and Statistical Genetics (BSG) core facility. Samples were tested for sufficient quality prior to polyA selection (using oligodT magnetic beads) and libraries were prepared using the NEBNext Ultra directional RNA Library Prep Kit (E7420L). Illumina universal paired end adaptors (5' PGA TCG GAA GAG CGG TTC AGC AGG AAT GCC GAG and 5' ACA CTC TTT CCC TAC ACG ACG CTC TTC CGA TCT) were used along with custom BSG barcoding sequences for multiplexing which are incorporated during the amplification rounds (12 cycles for the libraries). Samples were sequenced on the Illumina HiSeq 2000/2500 platform (100bp read length, paired end) using reagent kits v3. Sequenced reads were aligned to the reference sequence (Ensembl version Rnor_5.0.77) using TopHat.²⁹⁹ Principle component analysis was performed as part of the initial quality control analysis from the BSG core. Heat maps were produced using normalized counts and the Broad Institute Morpheus software (<https://software.broadinstitute.org/morpheus>) with hierarchical clustering performed using one minus pearson correlation and average linkage method. Differential gene expression was determined for both the L6/S1 DRGs and the PGs by comparing animals one month post T3-durotomy (sham) to animals one month post-complete T3 transection using DESeq.³⁰⁰ The adjusted p-values (using Benjamini-Hochberg method to control for false discovery rate) were considered significant for values less than 0.05.

2.3.6 Functional annotation clustering of differentially expressed DRG genes

The lists of significantly up- and downregulated DRG genes were analyzed separately using the Functional annotation clustering tool of the online DAVID software.^{301,302} Within each cluster are annotation terms that contain p-values (Fisher's exact test) as well as group

enrichment scores (the geometric mean (in -log scale) of the p-values of the cluster's members), which help identify clusters with potential biological significance.

2.3.7 Ingenuity pathway analysis of differentially expressed DRG genes

The canonical pathway analysis and upstream activator network were generated through the use of IPA (QIAGEN Inc., <https://www.qiagenbioinformatics.com/products/ingenuity-pathway-analysis>).³⁰³ The differential gene expression data for the DRG analysis (including log₂ fold change and adjusted p-values) were inputted for the core analysis using default settings.

2.3.8 Quantitative PCR

The RNA extraction of samples was performed as described for the RNA sequencing experiments. Targets identified by RNA sequencing for both the DRG and PG were selected for further analysis with quantitative PCR (qPCR). Primers were designed for each of the targets using Primer-BLAST NCBI. Primers used in this study are listed in Table 2.1. Extracted RNA (1ug) was reverse transcribed using RT² First Strand Kit (Qiagen Inc., Toronto, Ontario, Canada cat#330404) and cDNA was stored at -20 ° until quantitative PCR (qPCR) was performed. qPCR was performed on Applied Biosystems Vii7 (Life Technologies) using PerfeCTa SYBR Green FastMix, Low ROX (Quantabio, Beverly, MA, USA cat#95074) and analyzed using the Quant Studio Real-Time PCR Software v1.2. Initial experiments were performed to validate primers within the PGs or DRGs tissue using normal adult male rat tissue, prior to the use of the primers to examine relative expression in experimental samples. After an initial denaturation at 95°C for 20 seconds, the fast 2-step cycling protocol was for 40 cycles: 95°C for 1 second and 60°C for 20

seconds. The comparative C_t method was used to determine the relative gene expression levels between sham and SCI groups (U6 used as reference gene).³⁰⁴

Table 2.1 Primer pairs for quantitative PCR

Gene	Forward Primer	Reverse Primer
VIP	AGA CCC AAG GAG GCA CCG A	GAA CTG CAG CCT GTC ATC CA
TH	TGA AGG AGC GGA CTG GCT T	CGG TCA GCC AAC ATG GGT A
NGFR	GGC TCG GGA CTC GTG TTC T	TCG ACC AGG GAT CTC TTC G
CIRBP	CCG ACT CAG CGA AAG GCT A	CGA AGC TGA GAC CTC CCA C
FGFR1	CAA ACC AAA CCG TAG GCC TGT	CCC ACT CGA CGG GCA TTT
U6	CTC GCT TCG GCA GCA CA	AAC GCT TCA CGA ATT TGC GT

2.3.9 Tissue processing and immunohistochemistry

Rats were euthanized with an overdose of chloral hydrate (1g/kg, i.p.) and perfused through the heart with room temperature phosphate-buffered saline (PBS, approximately 100ml) followed by cold 4% paraformaldehyde (PF, approximately 400ml). Pelvic ganglia were removed, post-fixed in 4% PF overnight and cryoprotected in 20% sucrose in 0.1M phosphate buffer for at least 24 hours. Tissue was embedded in Cyromatrix (Fisher Scientific, Ottawa, Canada), and frozen on a liquid nitrogen-cooled copper block. The tissue was sectioned on a cryostat at 16 μ m and thaw-mounted and dried onto glass slides. Slides were stored at -80°C until needed.

For immunohistochemistry, slides were thawed and blocked with 10% normal donkey serum in PBS with Triton X-100 (0.1%) and sodium azide (1g/l; PBS-Tx-NaAz) for 30min-1h at room temperature. Primary antibodies (see Table 2.2) were diluted in PBS-Tx-NaAz and

incubated on the slides overnight. After three 10-min washes in PBS, secondary antibodies raised in donkey and conjugated to Cy3 (Jackson ImmunoResearch, West Grove, USA) or Alexa 488 (Invitrogen, Eugene, USA) were applied at 1:500, in PBS-Tx-SdAz for 2 h. A final three 10-minute washes with PBS were performed prior to coverslipping with ProLong® Gold antifade reagent (Life Technologies Corporation, Eugene, Oregon, USA). Images of the ganglia were captured with a Zeiss Axio Imager.Z2 laser scanning confocal microscope and all images for each set of quantitative analyses were captured using identical imaging settings.

Table 2.2 Primary antibodies used for immunohistochemistry

Antibody	Immunogen	Source	Species	Concentration
anti-TH	Denatured tyrosine hydroxylase from rat pheochromocytoma	Millipore (AB152)	Rabbit, polyclonal	1:200
anti-MAP2	Full length native protein (purified) corresponding to Cow MAP2	Abcam (ab5392)	Chicken, polyclonal	1:1000
anti-ChAT	Human placental enzyme	Millipore (AB144P)	Goat, polyclonal	1:500

2.3.10 Image analysis

All images were analyzed using the image processing package Fiji (<https://fiji.sc/>, RRID:SCR_002285).³⁰⁵ The neuronal population size-frequency distributions for the peripheral ganglia were determined using recursive translation (Fig. 2.2),³⁰⁶ which uses the diameters from neuronal profiles in section to mathematically reconstruct the cell population from which the profiles were traced (as described previously; Ramer et al., 2001).³⁰⁷ The perimeters of the profiles were manually traced in FIJI and the feret diameter and mean intensity of the soma for each traced profile was calculated automatically by the program. A histogram of the cell

diameters was produced for each ganglion by separating them into 4 μ m bins. Recursive translation was performed on these binned measurements using a Microsoft Excel program constructed from the corrected Rose and Rohrlach (1988) algorithm.³⁰⁶ For analysis of for the subpopulations of TH-positive and TH-negative neurons, thresholding within FIJI was used to distinguish the two subpopulations; the two populations have different cell size distributions as previously described.³⁰

A Measurement of neuronal diameters



trace cell perimeters
determine feret diameters

Diameters
38.15
41.12
38.74
37.55
25.67
40.84
51.53
26.34
24.44
37.43
16.84
⋮
33.12

sort diameters
into bins

B Recursive translation

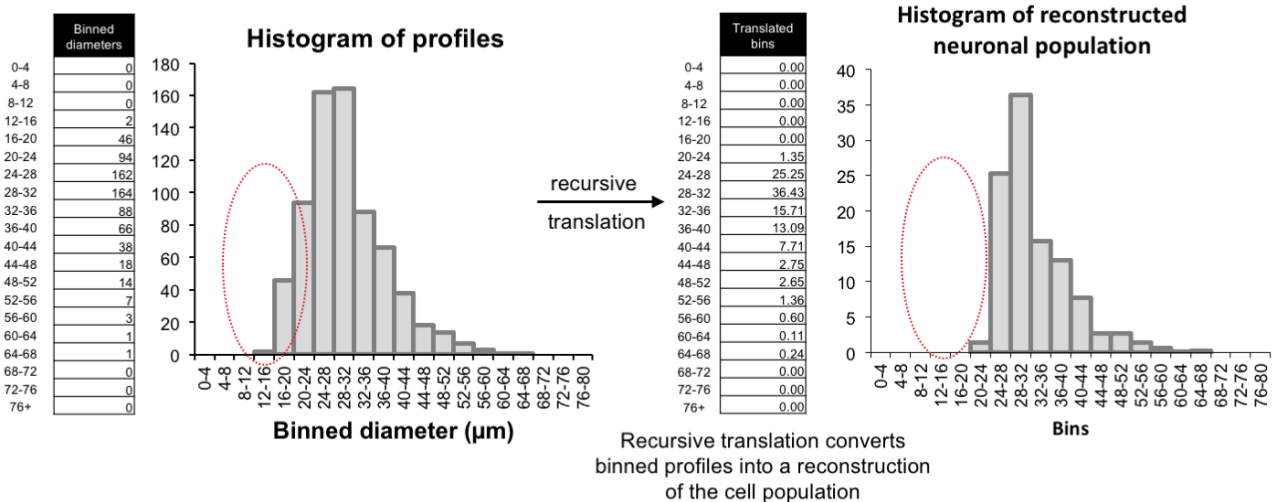


Figure 2.2 Reconstructing sizes of neuronal populations using sectioned tissue and recursive translation

(A) Neuronal diameters are obtained by tracing the outlines of the neuronal cell bodies (A, only select outlines shown) in sections of stained PG tissue. All profiles are traced regardless of nuclear position, presence or absence. FIJI software is used to measure the feret diameters of the traced profiles. (B) The diameters are sorted into bins to produce a histogram of the neuronal profile diameters. Recursive translation is performed on the binned data to correct for the over-representation of small profiles when larger neurons are sectioned at their smaller ends (red oval). The proportions of reconstructed neuronal populations can be compared between experimental groups using the Kolmogorov-Smirnov goodness-of-fit test.

2.3.11 Statistical Analyses of neuronal sizes

Kolmogorov–Smirnov (K–S) goodness-of-fit tests were performed on PG size distribution data to determine whether the neuronal cumulative size-frequency distributions differed between groups (sham versus spinal cord-injured at each time point). To determine statistical significance, the maximum difference between cumulative size-frequency distributions (the D-statistic) was compared to a critical value given by $1.36/\sqrt{N}$, where N is the combined number of cells for groups being compared. When $D >$ the critical value, $p < 0.05$. Proportions of neurons labeled with each antigen were compared using Student's *t*-test, significance at $p < 0.05$.

2.4 Results

2.4.1 Differential gene expression in pelvic peripheral ganglia after high thoracic spinal cord injury

Transection of the spinal cord in the high thoracic region results in significant central and peripheral changes that are relevant to the development of autonomic and sensory dysfunction.⁵² The pelvic peripheral ganglia bridge the central nervous system and the pelvic effector organs. Though numerous studies have linked changes in the lumbosacral DRGs to the development of autonomic dysreflexia and neuropathic pain, a full examination of gene changes in the LS-DRGs or the PGs after SCI has not been performed.^{3,242,243} Here I use RNA sequencing on ganglia from sham and T3x animals 1-month post-surgery to determine whether peripheral changes after SCI are reflected in transcriptomic and morphological changes in pelvic organ-projecting neurons (Fig. 2.1).

RNA sequencing was performed on 6 animals per group. PCA identified one sham PG as an outlier and therefore it was not included in further analysis (Fig. 2.3A). Differential gene expression was performed using the R-package DESeq. Differences identified by DESeq were considered significant if the adjusted p-value (using the Benjamini-Hochberg method) was less than 0.05.³⁰⁰ Only annotated genes were used for further analysis. Comparison of sham and T3x L6/S1 DRGs resulted in the identification of 525 differentially expressed genes 1 month post-T3x (Supplementary Tables 1 and 2 in Appendix). The same analysis comparing PGs 1 month post-sham or T3x surgery identified fewer differentially expressed genes, 108 genes in total (Supplementary Tables 3 and 4 in Appendix). A small, but significant, overlap (one-tailed Fisher's exact test, $p < 6.756E-4$) of differentially expressed genes were identified between two ganglia, with nine genes undergoing the same direction of change in both ganglia after injury (Fig. 2.3).

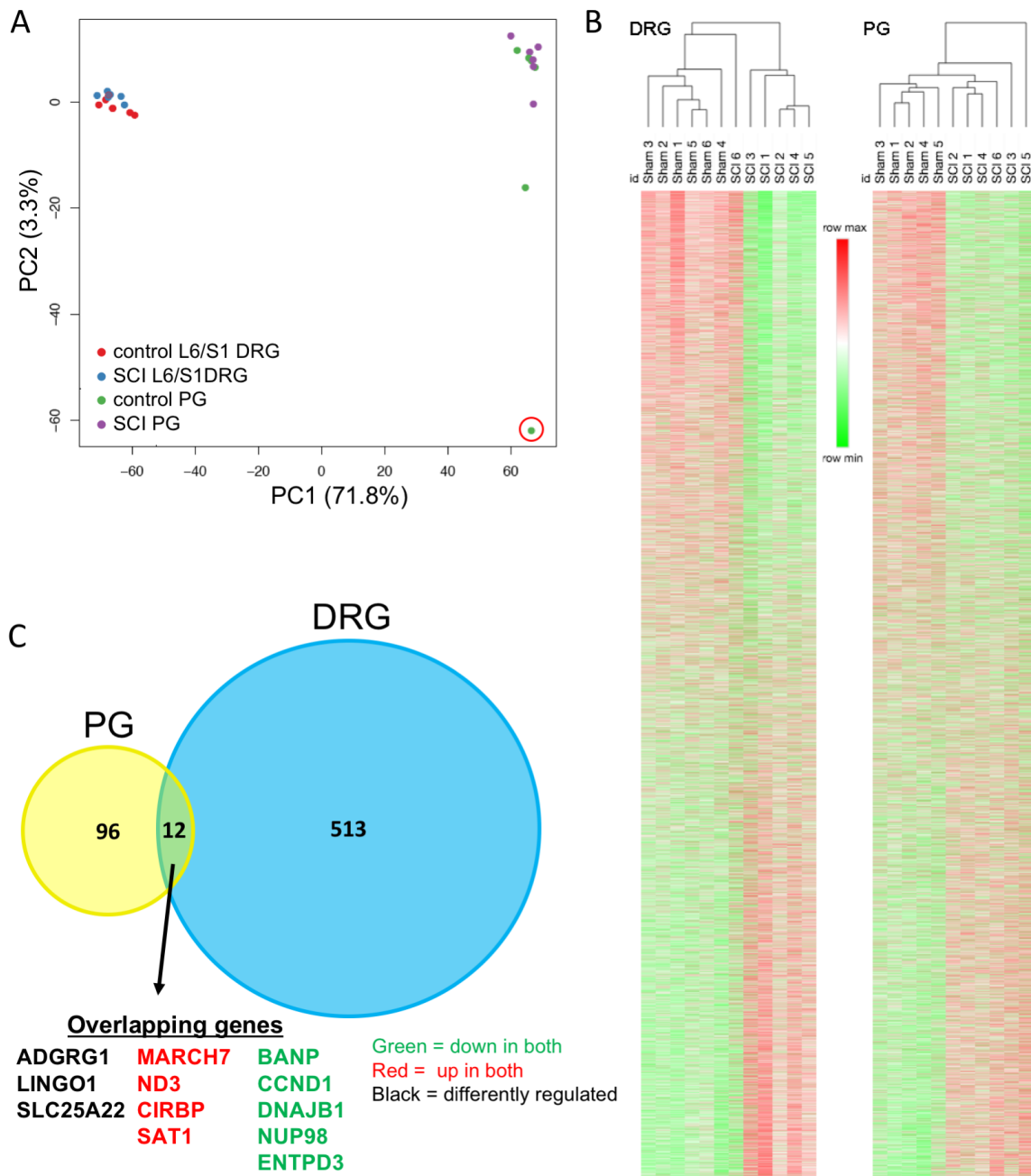


Figure 2.3 Analysis of RNA sequencing results of PGs and DRGs

(A) PCA of RNA sequencing results of all samples showed clear separation of the ganglia types (PC1). One control PG sample (red circle) was identified as an outlier and not used for subsequent differential gene expression analysis. (B) Heat map of genes identified by RNA sequencing, sorted based on expression differences and hierarchical clustering of samples. (C) Twelve genes were differentially expressed in both the L6/S1 DRG and the PG one month post-T3x. Four of the genes were commonly upregulated (red), five commonly downregulated (green) and three differentially affected in the ganglia (all upregulated in PG and downregulated in DRG). The overlap between these two sets of differentially expressed genes is significant (one-tailed Fisher's exact test; $p < 4.825E-6$).

2.4.2 High thoracic transection results in gene expression changes in L6/S1 DRGs

DESeq analysis identified 525 differentially expressed genes in the L6/S1 DRGs 1 month post-T3x. Of those, 287 genes were downregulated with the range of fold changes between 0.6290 and 0.9154, and 238 genes were upregulated with a range of fold changes between 1.115 and 1.540. The top twenty-five up- and downregulated genes, sorted by fold change, are presented in Table 2.3 and 2.4, with the full list of significant ($p < 0.05$) DESeq results in Appendix Tables 1 and 2. Follow-up on the differential gene expression analysis using quantitative PCR was performed for two genes of interest in the DRG. Consistent with the RNA sequencing results, the expression of FGFR1 mRNA was decreased at one month post-T3x, but was unchanged at an earlier (two week) time point (Fig. 2.4A). For CIRBP, which was identified in both the DRG and PG as being upregulated after T3x, there was a significant increase in its mRNA levels in the L6/S1 DRGs at two weeks after T3x but this was not significant in the qPCR analysis at one month post-injury (Fig. 2.4B).

Table 2.3 Annotated DRG genes upregulated one month post-T3x sorted by fold change

Gene ID	Gene description	Fold change	Adj. p-value
ENSRNOG00000003809	spermidine/spermine N1-acetyl transferase 1 (Sat1)	1.540	7.61E-12
ENSRNOG00000005387	RNA binding motif (RNP1, RRM) protein 3 (Rbm3)	1.519	8.58E-11
ENSRNOG000000047194	ADP-ribosylation factor like GTPase 13B (Arl13b)	1.376	0.000348
ENSRNOG000000033697	caspase 4 (Casp4)	1.374	0.00108
ENSRNOG000000022871	similar to zinc finger protein 84 (HPF2) (LOC691170)	1.370	0.00701
ENSRNOG000000018069	Neuroguidin (Ngdn)	1.368	0.000220
ENSRNOG000000008075	intraflagellar transport 74 (Ift74)	1.359	0.00360
ENSRNOG000000013078	zinc finger CCHC-type containing 7 (Zcchc7)	1.350	4.56E-05
ENSRNOG000000014463	URI1, prefoldin-like chaperone (Uri1)	1.350	5.70E-05
ENSRNOG000000036592	zinc finger protein 518A (Zfp518a)	1.342	0.000231
ENSRNOG000000020464	mitochondrial ribosomal protein L54 (Mrpl54)	1.339	0.00180
ENSRNOG000000002835	LUC7-like 3 pre-mRNA splicing factor (Luc7l3)	1.335	1.49E-05
ENSRNOG000000016581	serpin family B member 1A (Serpinb1a)	1.332	0.000220
ENSRNOG000000014380	zinc finger protein 850-like (LOC102555672)	1.327	0.00119
ENSRNOG000000012929	WD repeat and SOCS box-containing 1 (Wsb1)	1.322	4.56E-05
ENSRNOG000000010050	StAR-related lipid transfer domain containing 9 (Stard9)	1.319	0.0123
ENSRNOG000000013738	glutaredoxin-like protein (LOC100174910)	1.318	0.0167
ENSRNOG000000019659	Aspartoacylase (Aspa)	1.317	0.0257
ENSRNOG000000020264	dehydrogenase/reductase 1 (Dhrs1)	1.316	1.19E-05
ENSRNOG000000007159	C-C motif chemokine ligand 2 (Ccl2)	1.313	0.0188
ENSRNOG000000010248	serpin family I member 1 (Serpin1)	1.312	6.18E-06
ENSRNOG000000029841	cadherin 19 (Cdh19)	1.306	0.00844
ENSRNOG000000017959	cilia and flagella associated protein 100 (Cfap100)	1.306	0.0290
ENSRNOG000000004268	zinc finger protein 386 (Kruppel-like) (Zfp386)	1.303	0.0127
ENSRNOG000000036802	small nucleolar RNA host gene 11 (Snhg11)	1.296	1.49E-05

Table 2.4 Annotated DRG genes downregulated one month post-T3x sorted by fold change

Gene ID	Gene description	Fold change	Adj. p-value
ENSRNOG00000020369	insulin-like growth factor 2 (Igf2)	0.6290	3.09E-05
ENSRNOG00000006548	mannose receptor, C type 2 (Mrc2)	0.6965	0.00244
ENSRNOG000000031801	Eph receptor B3 (Ephb3)	0.7207	0.00225
ENSRNOG000000013954	alkaline phosphatase, liver/bone/kidney (Alpl)	0.7325	0.000615
ENSRNOG000000020263	ATPase Na ⁺ /K ⁺ transporting subunit alpha 3 (Atp1a3)	0.7334	0.00154
ENSRNOG000000019955	oxoglutarate dehydrogenase-like (Ogdhl)	0.7363	0.00225
ENSRNOG000000005148	scratch family transcriptional repressor 2 (Scrt2)	0.7494	0.000452
ENSRNOG000000025612	seizure related 6 homolog like (Sez6l)	0.7532	0.0149
ENSRNOG000000009446	retinoid X receptor alpha (Rxra)	0.7603	0.0181
ENSRNOG000000049944	solute carrier family 25 member 22 (Slc25a22)	0.7616	0.000275
ENSRNOG000000020918	cyclin D1 (Ccnd1)	0.7617	0.000739
ENSRNOG000000017154	ATPase phospholipid transporting 11A (Atp11a)	0.7697	0.00340
ENSRNOG000000008471	kinesin family member 21B (Kif21b)	0.7733	0.0353
ENSRNOG000000001621	C2 calcium-dependent domain containing 2 (C2cd2)	0.7746	0.00874
ENSRNOG000000009967	Otoferrin (Otof)	0.7755	0.0299
ENSRNOG000000005076	BCL6 co-repressor-like 1 (Bcorl1)	0.7772	0.0103
ENSRNOG000000016050	Fibroblast growth factor receptor 1 (Fgfr1)	0.7787	2.62E-06
ENSRNOG000000012546	FERM and PDZ domain containing 1 (Frmpd1)	0.7795	0.000673
ENSRNOG000000048043	coagulation factor II (thrombin) receptor (F2r)	0.7799	0.0172
ENSRNOG000000028580	pecanex homolog 2 (Drosophila) (Pcnx2)	0.7821	0.00859
ENSRNOG000000042855	AT hook, DNA binding motif, containing 1 (Ahdc1)	0.7826	0.00958
ENSRNOG000000009629	carbonic anhydrase 2 (Car2)	0.7832	0.00995
ENSRNOG000000018251	mannose receptor, C type 1 (Mrc1)	0.7858	0.0255
ENSRNOG000000020339	neutralized E3 ubiquitin protein ligase 1 (Neurl1)	0.7870	0.00883
ENSRNOG000000000955	ligand of numb-protein X 2 (Lnx2)	0.7873	0.0151

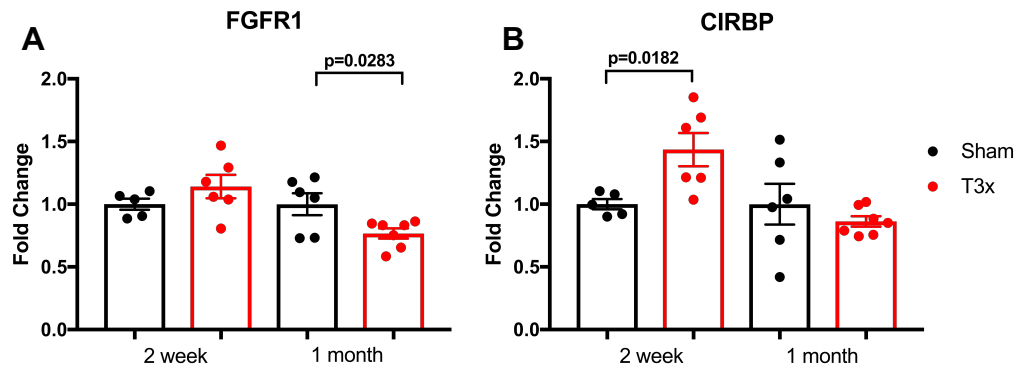


Figure 2.4 Quantitative PCR of L6/S1 DRGs two weeks and one month post-T3x
 (A) Consistent with the RNA sequencing findings there is a decrease in FGFR1 mRNA expression one month after T3x, but no significant difference between sham and T3x at two weeks after injury. (B) CIRBP mRNA was only significantly increased at two weeks post injury when compared to sham. Mean±S.E.M., unpaired t-test, exact p-values shown.

2.4.3 Functional clustering annotation of differentially expressed DRG genes

Isolation of RNA from whole ganglia results in samples from mix of cell types including neurons, glia, and blood vessels. Therefore, transcriptomic changes within both the neurons and the supporting cells would be reflected in this analysis. To identify if specific types of genes were over-represented in the differentially expressed L6/S1 DRG genes we performed functional clustering annotation (FCA) on the up and down regulated genes independently (Fig. 2.5; Tables 2.5 and 2.6).^{301,302} Numerous annotation types are used to categorize genes based on a number of different biological aspects (such as gene ontology, molecular functions, protein interactions, etc.); DAVID's (database for annotation, visualization and integrated discovery) FCA brings together over forty annotation systems to allow for the identification of common enriched functions across multiple annotation types.^{301,302} The group enrichment scores, which are the geometric mean of the p-values of the cluster's members (in negative log scale), are highest for groups that contain members with low p-values, therefore helping to identify biologically significant clusters. Nucleotide and RNA binding genes were enriched in both the up- and downregulated DRG genes. For the set of downregulated genes, annotations relating to synapses and cell junctions were also enriched (Fig. 2.5A, Table 2.5).

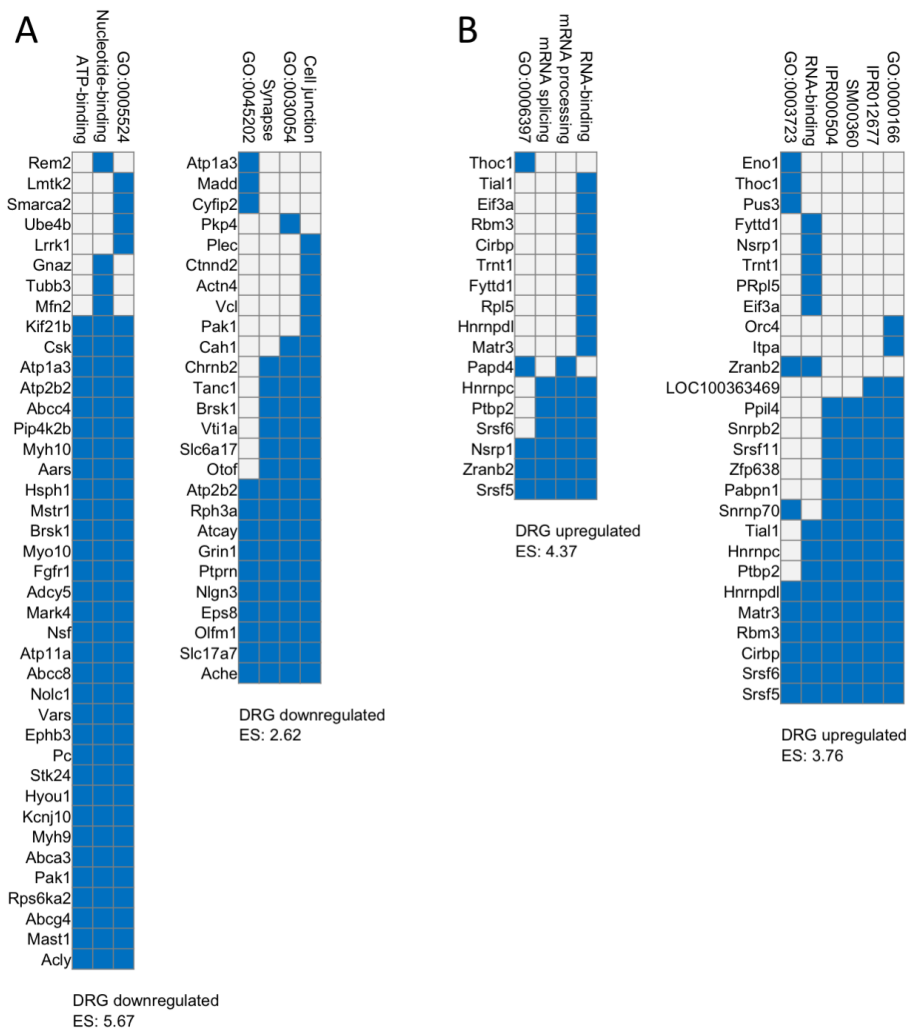


Figure 2.5 Functional annotation clustering for genes differentially expressed in the DRG one month post T3x

Functional annotation clusters were identified using DAVID 6.8. The clusters with the two highest enrichment scores for the (A) downregulated genes and (B) upregulated genes in the DRG one month post-T3x. Filled blue squares correspond to gene-terms that have a positive association reported with the given annotation, empty square represents no reported association. Enrichment scores (ES) are given for each of the categories. Titles represent keywords, gene ontology (GO:0005524: ATP-binding; GO:0030054: cell junction; GO:0045202: synapse; GO:0006397: mRNA processing; GO:0003723: RNA binding; GO:0000166: nucleotide binding), INTERPRO (IPR000504: RNA recognition motif domain; IPR012677: nucleotide-binding alpha-beta plait domain superfamily) and SMART (SM00360: RNA recognition motif). Clusters of genes associated with nucleotide and RNA binding appear to be enriched both set of differentially expressed genes, however downregulated genes appear to be specifically enriched in cell junction and synapse genes.

Table 2.5 Functional Clustering Annotation of upregulated DRG genes

Annotation Cluster 1 - Enrichment Score: 5.669					
Category	Term	%	p-value	Gene symbols	Benjamini
SMART	SM00360: RRM	6.410	3.07E-8	Zfp638, MATR3, TIAL1, SRSF5, SNRNP70, SRSF6, PTBP2, RBM3, SRSF11, CIRBP, PPIL4, PABPN1, SNRPB2, HNRNPC, HNRNPDL	2.49E-6
INTERPRO	IPR000504: RNA recognition motif domain	6.410	1.66E-7	Zfp638, MATR3, TIAL1, SRSF5, SNRNP70, SRSF6, PTBP2, RBM3, SRSF11, CIRBP, PPIL4, PABPN1, SNRPB2, HNRNPC, HNRNPDL	6.65E-5
GOTERM_MF_DIRECT	GO:0000166~ nucleotide binding	7.692	1.74E-7	ITPA, Zfp638, MATR3, TIAL1, SRSF5, SNRNP70, ORC4, SRSF6, PTBP2, RBM3, SRSF11, CIRBP, PPIL4, PABPN1, SNRPB2, LOC100363469, HNRNPC, HNRNPDL	2.38E-5
INTERPRO	IPR012677: Nucleotide-binding, alpha-beta plait	6.838	2.40E-7	Zfp638, MATR3, TIAL1, SRSF5, SNRNP70, SRSF6, PTBP2, RBM3, SRSF11, CIRBP, PPIL4, PABPN1, SNRPB2, LOC100363469, HNRNPC, HNRNPDL	4.81E-5
UP_KEYWORDS	RNA-binding	6.410	1.11E-5	MATR3, TIAL1, SRSF5, NSRP1, SRSF6, PTBP2, TRNT1, RBM3, CIRBP, RPL5, EIF3A, FYTTD1, HNRNPC, ZRANB2, HNRNPDL	1.01E-3
GOTERM_MF_DIRECT	GO:0003723~ RNA binding	4.701	4.10E-3	ENO1, MATR3, SRSF5, SNRNP70, SRSF6, RBM3, ZRANB2, THOC1, CIRBP, HNRNPDL, PUS3	7.61E-1
Annotation Cluster 2 - Enrichment Score: 2.615					
Category	Term	%	p-value	Gene symbols	Benjamini
UP_KEYWORDS	RNA-binding	6.410	1.11E-5	MATR3, TIAL1, SRSF5, NSRP1, SRSF6, PTBP2, TRNT1, RBM3, CIRBP, RPL5, EIF3A, FYTTD1, HNRNPC, ZRANB2, HNRNPDL	1.01E-3
UP_KEYWORDS	mRNA processing	2.991	5.74E-3	SRSF5, NSRP1, HNRNPC, SRSF6, PTBP2, ZRANB2, PAPD4	1.39E-1
UP_KEYWORDS	mRNA splicing	2.564	8.93E-3	SRSF5, NSRP1, PTBP2, HNRNPC, SRSF6, ZRANB2	1.66E-1
GOTERM_BP_DIRECT	GO:0006397~ mRNA processing	2.1367	6.07E-2	SRSF5, NSRP1, ZRANB2, PAPD4, THOC1	9.90E-1

Table 2.6 Functional Clustering Annotation of downregulated DRG genes

Annotation Cluster 1 - Enrichment Score: 4.371					
Category	Term	%	p-value	Genes	Benjamini
UP_KEYWORDS	Cell junction	7.774	1.86E-6	CHRNA2, GRIN1, VTI1A, ATP2B2, OLFM1, VCL, TANC1, CDH1, BRSK1, OTOF, SLC6A17, RPH3A, NLGN3, ATCAY, PLEC, ACTN4, EPS8, SLC17A7, ACHE, PAK1, CTNND2, PTPRN	1.02E-4
UP_KEYWORDS	Synapse	5.654	1.33E-5	CHRNA2, GRIN1, VTI1A, ATP2B2, OLFM1, TANC1, BRSK1, OTOF, SLC6A17, RPH3A, NLGN3, ATCAY, EPS8, SLC17A7, ACHE, PTPRN	5.83E-4
GOTERM_CC_DIRECT	GO:0030054~cell junction	6.360	1.06E-4	CHRNA2, GRIN1, PKP4, VTI1A, ATP2B2, OLFM1, TANC1, CDH1, BRSK1, OTOF, SLC6A17, RPH3A, NLGN3, ATCAY, EPS8, SLC17A7, ACHE, PTPRN	5.82E-3
GOTERM_CC_DIRECT	GO:0045202~synapse	4.593	1.25E-3	GRIN1, ATP1A3, ATP2B2, OLFM1, MADD, RPH3A, NLGN3, ATCAY, EPS8, SLC17A7, ACHE, PTPRN, CYFIP2	3.13E-2
Annotation Cluster 2 - Enrichment Score: 3.756					
Category	Term	%	p-value	Genes	Benjamini
UP_KEYWORDS	ATP-binding	11.31	2.82E-5	ABCA3, MYH10, PIP4K2B, ADCY5, ACLY, PC, CSK, EPHB3, ABCC4, MYO10, FGFR1, ATP11A, KCNJ10, VARS, STK24, MST1R, AARS, ATP1A3, ABCC8, NOLC1, ATP2B2, NSF, MARK4, RPS6KA2, HYOU1, ABCG4, BRSK1, MAST1, HSPH1, PAK1, MYH9, KIF21B	1.03E-3
UP_KEYWORDS	Nucleotide-binding	12.72	1.26E-4	ABCA3, MYH10, PIP4K2B, ADCY5, ACLY, PC, EPHB3, CSK, ABCC4, MYO10, FGFR1, ATP11A, KCNJ10, VARS, STK24, AARS, MST1R, ATP1A3, ABCC8, NOLC1, GNAZ, ATP2B2, NSF, MARK4, MFN2, RPS6KA2, HYOU1, ABCG4, BRSK1, MAST1, HSPH1, REM2, PAK1, TUBB3, MYH9, KIF21B	3.43E-3
GOTERM_MF_DIRECT	GO:0005524~ATP binding	12.72	1.52E-3	ABCA3, MYH10, LRRK1, PIP4K2B, ADCY5, ACLY, PC, EPHB3, CSK, ABCC4, MYO10, SMARCA2, FGFR1, ATP11A, KCNJ10, VARS, STK24, AARS, MST1R, ATP1A3, LMTK2, ABCC8, NOLC1, ATP2B2, UBE4B, NSF, MARK4, RPS6KA2, HYOU1, ABCG4, BRSK1, MAST1, HSPH1, PAK1, MYH9, KIF21B	2.21E-1

% = percentage of involved genes from list/total genes in category; p-value adjustment performed using Benjamini-Hochberg

2.4.4 Ingenuity pathway analysis of differentially expressed DRG genes

Ingenuity pathway analysis (IPA) allows for the identification of predicated biological functions, pathways and upstream effectors by taking into account the direction of differential expression, which is not considered in functional clustering analysis.³⁰³ Canonical pathway analysis (CPA) identifies potentially activated or inhibited pathways based on the differential gene expression data by calculating a z-score. A positive z-score indicates that the differential gene expression is consistent with an activation of a given pathway or biological function, with a negative z-score indicating the opposite. The results from the differentially expressed DRG genes one month post-T3x with significant z-scores ($>|2|$) are presented in Table 2.7, with a complete list of CPA results in Appendix Table 5. A number of the canonical pathways identified are involved in the regulation of growth signaling (including CNTF, mTOR, and growth factor signaling) as well as immune cell regulation (GM-CSF, FLT3, and IL-3 signaling). Notably, the only canonical pathway identified as being significantly activated is the oxidative phosphorylation pathway, suggesting there may be an increased energy demand in the DRG after injury (Table 2.7).³⁰⁸ Additionally, IPA upstream analysis, which identifies potential upstream effectors that may explain patterns in the differential gene expression, identified BDNF signalling as probably inhibited with a z-score of -3.014 ($p=0.00109$). Of the 525 differentially expressed genes in the DRG, 17 were downstream of BDNF and of those 14 were differentially regulated in the direction consistent with decreased BDNF activity (Fig 2.6).

Table 2.7 Canonical Pathway analysis of differentially expressed DRG genes, (z-score >|2|)

Canonical pathway	p-value	Ratio	z-score	Gene symbols
Actin cytoskeleton signaling	0.000248	0.066 (15/227)	-2.324	ACTN4, ARPC3, BRK1, CSK, F2R, <u>FGFR1</u> , GRB2, MYH9, MYH10, PAK1, PIK3CD, PIP4K2B, SLC9A1, TMSB10, VCL
Phosphatidylglycerol biosynthesis II (non-plastidic)	0.000271	0.192 (5/26)	-2.236	AGPAT1, CDS1, LPCAT1, LPCAT4, PGS1
CNTF signaling	0.0034	0.094 (6/64)	-2.449	CNTFR, <u>FGFR1</u> , GRB2, PIK3CD, RPS6KA2, STAT3
Aldosterone signaling in epithelial cells	0.00543	0.06 (10/168)	-2.236	DNAJB1, DNAJC7, DNAJC11, <u>FGFR1</u> , GRB2, HSPB8, HSPH1, PIK3CD, PIP4K2B, SLC9A1,
mTOR signaling	0.00677	0.055 (11/201)	-2.121	EIF3A, EIF3K, EIF3M, <u>FGFR1</u> , GRB2, PIK3CD, PPM1J, PRKAB1, RPS6KA2, RPTOR, TSC2
Growth hormone signaling	0.0133	0.071 (6/85)	-2.236	<u>FGFR1</u> , GRB2, IGF2, PIK3CD, RPS6KA2, STAT3
Amyotrophic lateral sclerosis signaling	0.0139	0.063 (7/111)	-2.236	<u>FGFR1</u> , GRB2, GRIN1, NEFH, NEFL, PAK1, PIK3CD
Pancreatic adenocarcinoma signaling	0.0205	0.058 (7/120)	-2.646	CCND1, <u>FGFR1</u> , GRB2, NOTCH1, PIK3CD, RALGDS, STAT3
ErbB2-ErbB3 signaling	0.0208	0.072 (5/69)	-2.236	CCND1, <u>FGFR1</u> , GRB2, PIK3CD, STAT3
GM-CSF signaling	0.0259	0.068 (5/73)	-2.236	CCND1, <u>FGFR1</u> , GRB2, PIK3CD, STAT3
Oxidative phosphorylation	0.0393	0.055 (6/109)	2.449	ATP5MF, MT-CO2, MT-ND3, NDUFB9, NDUFS4, UQCRC2
IL-3 signaling	0.0417	0.06 (5/83)	-2.236	<u>FGFR1</u> , GRB2, PAK1, PIK3CD, STAT3
HGF signaling	0.0488	0.052 (6/115)	-2.449	CCND1, <u>FGFR1</u> , GRB2, PAK1, PIK3CD, STAT3
FLT3 signaling in hematopoietic progenitor cells	0.0493	0.057 (5/87)	-2.236	<u>FGFR1</u> , GRB2, PIK3CD, RPS6KA2, STAT3

Full table included as Appendix Table 5. FGFR1 underlined to show prevalence in pathways

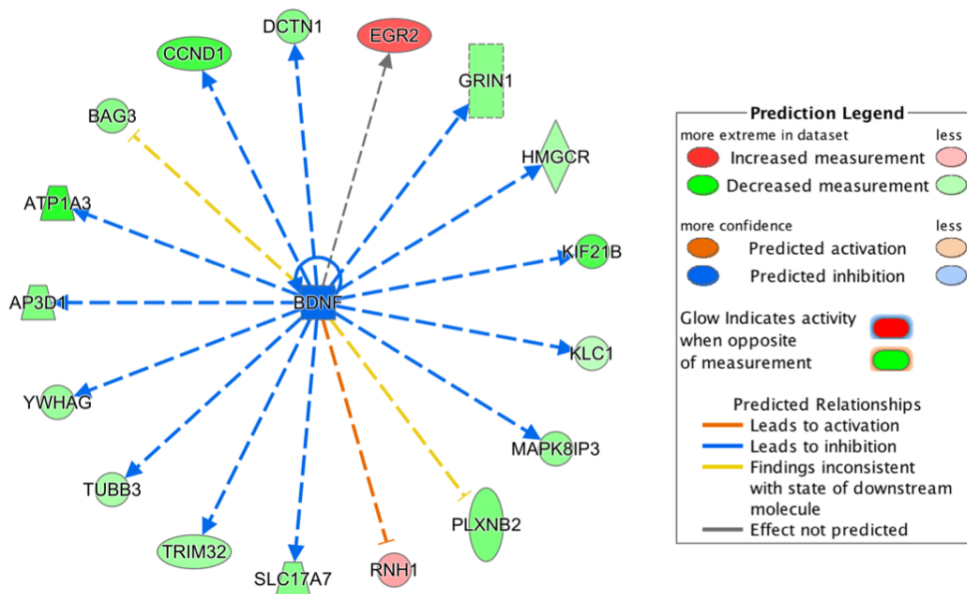


Figure 2.6 Upstream analysis predicts BDNF activity as inhibited within the DRG one month post-T3x

17 genes within the list of differentially expressed genes are downstream of the growth factor BDNF. Of those 17 genes, 14 are found to change in the direction consistent with inhibition of BDNF. For the differentially expressed genes, red and green represent up- and down-regulation, respectively and the intensity of colour relates to the extent of differences in the dataset. Connecting lines are coloured based on whether results are consistent with predicted activation (orange), predicted inhibition (blue), or inconsistent relationship between BDNF inhibition and change in the downstream gene expression. The shape of the arrowhead represents the expected activation (pointy) or inhibition (blunt) of the downstream molecule.

2.4.5 High thoracic transection results in modest gene expression changes in PGs

Compared to the DRG, fewer differentially expressed genes were identified in the PGs one month post-T3 transection, though the range of fold changes, between 0.6880 - 0.8884 (Appendix Table 4) and 1.093 – 1.316 (Appendix Table 3) were comparable between the ganglia. The twenty-five genes identified with the greatest differential expression are presented in Tables 2.8 (upregulated) and Table 2.9 (downregulated). Small lists of differentially expressed genes are often not conducive to workflows involving conventional functional annotation analysis. Despite this, interesting changes in gene expression are identified in the PG after SCI (Table 2.10).

Table 2.8 Annotated PG genes upregulated one month post-T3x sorted by fold change

Gene ID	Gene description	Fold change	Adj. p-value
ENSRNOG00000015999	cold inducible RNA binding protein (Cirbp)	1.316	3.71E-05
ENSRNOG00000015685	major facilitator superfamily domain containing 3 (Mfsd3)	1.310	0.00683
ENSRNOG00000014350	cysteine-rich, angiogenic inducer, 61 (Cyr61)	1.308	0.0352
ENSRNOG00000026447	dispatched RND transporter family member 3 (Disp3)	1.308	0.00701
ENSRNOG00000005392	nerve growth factor receptor (Ngfr)	1.283	2.73E-06
ENSRNOG00000033402	similar to Glutathione S-transferase A1 (GTH1) (HA subunit 1) (GST-epsilon) (GSTA1-1) (GST class-alpha) (LOC501110)	1.246	0.0248
ENSRNOG00000017752	methylcrotonoyl-CoA carboxylase 2 (Mccc2)	1.241	0.0164
ENSRNOG00000000967	acetoacetyl-CoA synthetase (Aacs)	1.238	0.00299
ENSRNOG00000003809	spermidine/spermine N1-acetyl transferase 1 (Sat1)	1.232	0.00235
ENSRNOG00000003217	galectin 3 binding protein (Lgals3bp)	1.224	0.00431
ENSRNOG00000042691	armadillo repeat containing 7 (Armc7)	1.223	0.0416
ENSRNOG00000000974	zinc finger protein 358 (Zfp358)	1.221	0.0367
ENSRNOG00000052880	Peripherin (Prph)	1.220	1.59E-05
ENSRNOG00000012439	BH3 interacting domain death agonist (Bid)	1.219	0.0365
ENSRNOG00000049944	solute carrier family 25 member 22 (Slc25a22)	1.217	0.00487
ENSRNOG00000020881	FERM domain containing 8 (Frmd8)	1.211	2.07E-05
ENSRNOG00000032902	Y box protein 1 related, pseudogene 3 (Ybx1-ps3)	1.210	0.0378
ENSRNOG00000012260	DEAD-box helicase 25 (Ddx25)	1.202	0.0409
ENSRNOG00000019869	leucine rich repeat and fibronectin type III domain containing 1 (Lrfn1)	1.199	0.0409
ENSRNOG00000010535	cadherin 18 (Cdh18)	1.199	0.0380
ENSRNOG00000021150	phospholipase C beta 3 (Plcb3)	1.192	0.00683
ENSRNOG00000004377	lipin 1 (Lpin1)	1.190	0.0221
ENSRNOG00000009872	potassium voltage-gated channel subfamily H member 2 (Kcnh2)	1.185	0.0164
ENSRNOG00000005905	phosphodiesterase 4B(Pde4b)	1.181	0.0175
ENSRNOG00000000476	zinc finger and BTB domain containing 22(Zbtb22)	1.181	0.0328

Top 25 differentially expressed genes, for complete list see Appendix Table 3

Table 2.9 Annotated PG genes downregulated one month post-T3x sorted by fold changes

Gene ID	Gene description	Fold change	Adj. p-value
ENSRNOG00000015957	coagulation factor XIII A1 chain (F13a1)	0.6880	1.19E-05
ENSRNOG00000049882	adenylate cyclase activating polypeptide 1 (Adcyap1)	0.7406	0.00121
ENSRNOG00000011992	solute carrier family 18 member A1 (Slc18a1)	0.7453	0.00287
ENSRNOG00000003221	Myocilin (Myoc)	0.7539	0.0223
ENSRNOG00000019140	Btg3 associated nuclear protein (Banp)	0.7569	0.00487
ENSRNOG00000002810	glutamine-fructose-6-phosphate transaminase 2 (Gfpt2)	0.7589	0.00806
ENSRNOG00000018808	vasoactive intestinal peptide (Vip)	0.7764	0.000324
ENSRNOG00000020410	tyrosine hydroxylase (Th)	0.7780	0.00121
ENSRNOG00000016437	transmembrane 4 L six family member 4 (Tm4sf4)	0.7861	0.000299
ENSRNOG00000019622	atypical chemokine receptor 3 (Acr3)	0.7933	0.0363
ENSRNOG00000008415	Ngfi-A binding protein 2 (Nab2)	0.7949	3.71E-05
ENSRNOG00000001607	ADAM metallopeptidase with thrombospondin type 1 motif, 1 (Adams1)	0.7989	0.00205
ENSRNOG00000000924	solute carrier family 7 member 1 (Slc7a1)	0.8034	0.0332
ENSRNOG00000011823	transcription factor AP-2 beta(Tfap2b)	0.8041	0.00287
ENSRNOG00000007597	rhopilin, Rho GTPase binding protein 1 (Rhpn1)	0.8066	0.0382
ENSRNOG00000012959	Ngfi-A binding protein 1(Nab1)	0.8069	0.00115
ENSRNOG00000038784	piezo-type mechanosensitive ion channel component 2 (Piezo2)	0.8082	0.0150
ENSRNOG00000021198	histone cluster 1, H2bh(Hist1h2bh)	0.8119	0.0181
ENSRNOG00000023778	glucosaminyl (N-acetyl) transferase 2, I-branching enzyme (Gcnt2)	0.8120	0.00784
ENSRNOG00000050655	prolyl 4-hydroxylase subunit alpha 1 (P4ha1)	0.8163	0.0468
ENSRNOG00000027016	cordon-bleu WH2 repeat protein-like 1 (Cobll1)	0.8167	0.00758
ENSRNOG00000015232	phosphatidylinositol-4-phosphate 5-kinase type 1 beta (Pip5k1b)	0.8174	0.0391
ENSRNOG00000004048	leucine-rich repeat kinase 2 (Lrrk2)	0.8192	0.000863
ENSRNOG00000002580	tRNA methyltransferase 1-like (Trmt11)	0.8196	0.0297
ENSRNOG00000021824	DnaJ heat shock protein family (Hsp40) member B1 (Dnajb1)	0.8246	0.0294

Top 25 differentially expressed genes, for complete list see Appendix Table 4

Table 2.10 Investigator-led interrogation of genes differentially expressed in the PG one month post-T3x

Gene	Encodes	Fold Change	Padj	(Probable) function in autonomic neurons	NGF-regulated in mature sympathetic neurons?	Ref
Ngfr	nerve growth factor receptor (TNFR superfamily, member 16) (p75 ^{NTR})	1.283	2.73E-06	Neurotrophin receptor	yes (up)	298
Prph	peripherin	1.220	1.59E-05	Cytoskeleton (intermediate filament)	unknown (up in NGF-differentiated PC12 cells)	309
Ntrk1	neurotrophic tyrosine kinase, receptor, type 1 (TrkA)	1.178	0.0297	NGF receptor	yes (up)	310
Ndn	neccin homolog (mouse)	1.152	0.0219	Required for NGF signaling	unknown	311,312
Lingo1	leucine rich repeat and Ig domain containing 1	1.151	0.0493	Ngfr-binding and Ntrk1 lysosomal degradation	unknown (up in DRG neurons)	313-315
Grina	glutamate receptor, ionotropic, N-methyl D-aspartate-associated protein 1	1.128	0.0297	Neurotransmission (post-synaptic)	unknown (up in inflammation)	316
Thy1	Thy-1 cell surface antigen	0.8809	0.0409	Neurite outgrowth	unknown (up in NGF-differentiated PC12 cells)	317
Snap25	synaptosomal-associated protein 25	0.8773	0.0108	Neurotransmission (pre-synaptic)	unknown	318,319
Ina	internexin neuronal intermediate filament protein, alpha	0.8671	0.0165	Cytoskeleton (intermediate filament)	unknown	320
Pdlim5	PDZ and LIM domain 5	0.8286	0.0409	Neurite stability	unknown	321,322
Piezo2	piezo-type mechanosensitive ion channel component 2	0.8082	0.0150	Mechano-transduction	unknown	323
Scn1a	sodium channel, voltage-gated, type I, alpha	0.7876	0.0431	Action potential	unknown	324
Th	tyrosine hydroxylase	0.7780	0.0012	Neurotransmission (adrenergic)	yes (up)	325,326
Vip	vasoactive intestinal peptide	0.7764	0.0003	Neurotransmission (cholinergic)	yes (down)	292
Slc18a1	solute carrier family 18 (vesicular monoamine), member 1	0.7453	0.0029	Neurotransmission (monoaminergic)	unknown	327,328
Adcyap1	pituitary adenylate cyclase activating polypeptide	0.7407	0.0012	Neurotransmission (cholinergic)	unknown	329

2.4.6 Examination of gene expression changes in PG using quantitative PCR

To validate the RNA sequencing based differential gene expression findings in the PG and to examine how the expression of genes of interest differ with time since injury I performed qPCR for three genes: TH, VIP and NGFR (Fig. 2.7). I found that, consistent with the RNA sequencing results, the expression of both TH and VIP was decreased one month post-T3x. For TH, one month post-T3x was the only time point and injury with a significant difference in expression levels between sham and injured animals. However, VIP expression was decreased at both two weeks and one month post-T3x. NGFR was elevated at two weeks post-T3x, but by QPCR, there was no longer a difference at one month.

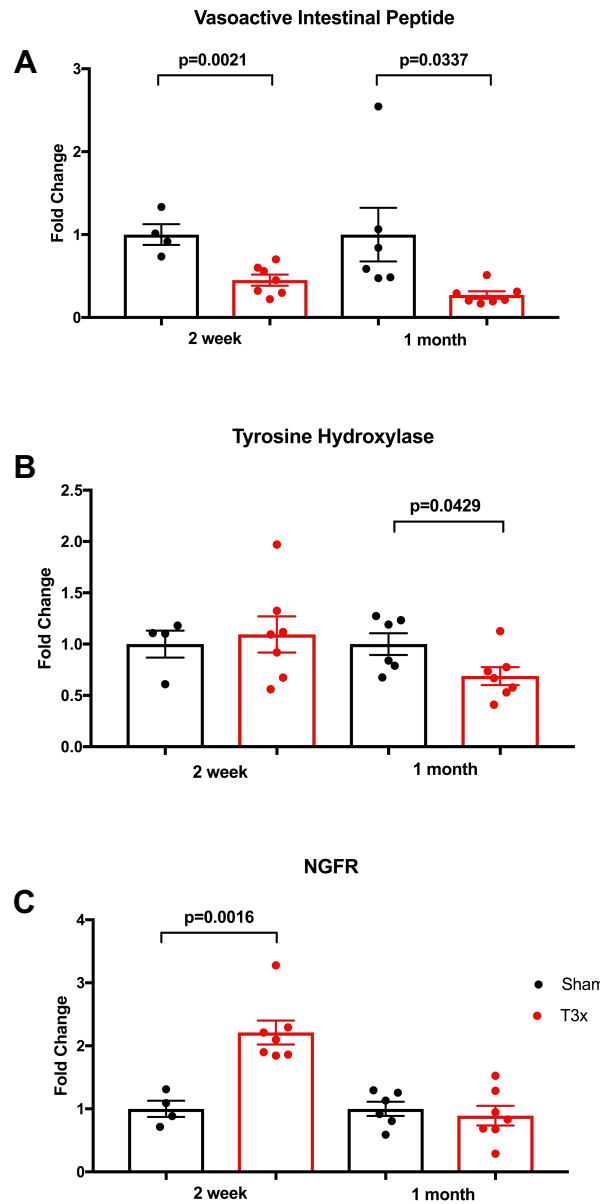


Figure 2.7 Quantitative PCR of PGs two weeks and one month post-T3x

(A) VIP mRNA expression is decreased at both two weeks and one month-post T3x. (B) TH mRNA was decreased at one month, but not two weeks, post-T3x. (C) Increased expression of NGFR mRNA was only significant at two weeks post-T3x when measured by qPCR. Mean±S.E.M., unpaired t-test, exact p-values shown.

2.4.7 Recursive translation in analyzing cell size distributions of PG

Due to the challenges of comparing cell sizes in populations of peripheral neurons using nucleus-based stereological techniques, including the large variation in cell body size and the relatively large neuronal nuclei, we quantified changes within the neuronal population using the technique of recursive translation. Recursive translation reconstructs mathematically the distribution of cell sizes from information obtained by tracing the profiles of sectioned neurons. The technique was published in 1988 with algorithm for running the recursive translation; I translated the program into an easy-to-follow procedure using FIJI³⁰⁵ and an excel workbook I designed (Fig. 2.2). Using this technique, I examined the distribution of cell sizes of the entire neuronal population of the PG using pan-neuronal markers such as MAP2 (Fig. 2.8), as well as specific PG subpopulations, such as tyrosine hydroxylase (TH) positive neurons. Though peripheral autonomic neurons are classically-defined based on the spinal level from which their preganglionic input arises (with sympathetic neurons receiving thoracic or lumbar input and parasympathetic neurons receiving cranial or sacral input), enzymes involved in neurotransmitter production are often used as surrogates to identify these different populations in the PG.² Immunohistochemistry for tyrosine hydroxylase (TH), the rate-limiting enzyme in catecholamine biosynthesis, allows for the separation of different population of PG neurons: generally speaking, sympathetic (TH-positive) and parasympathetic (TH-negative) (Fig. 2.8).

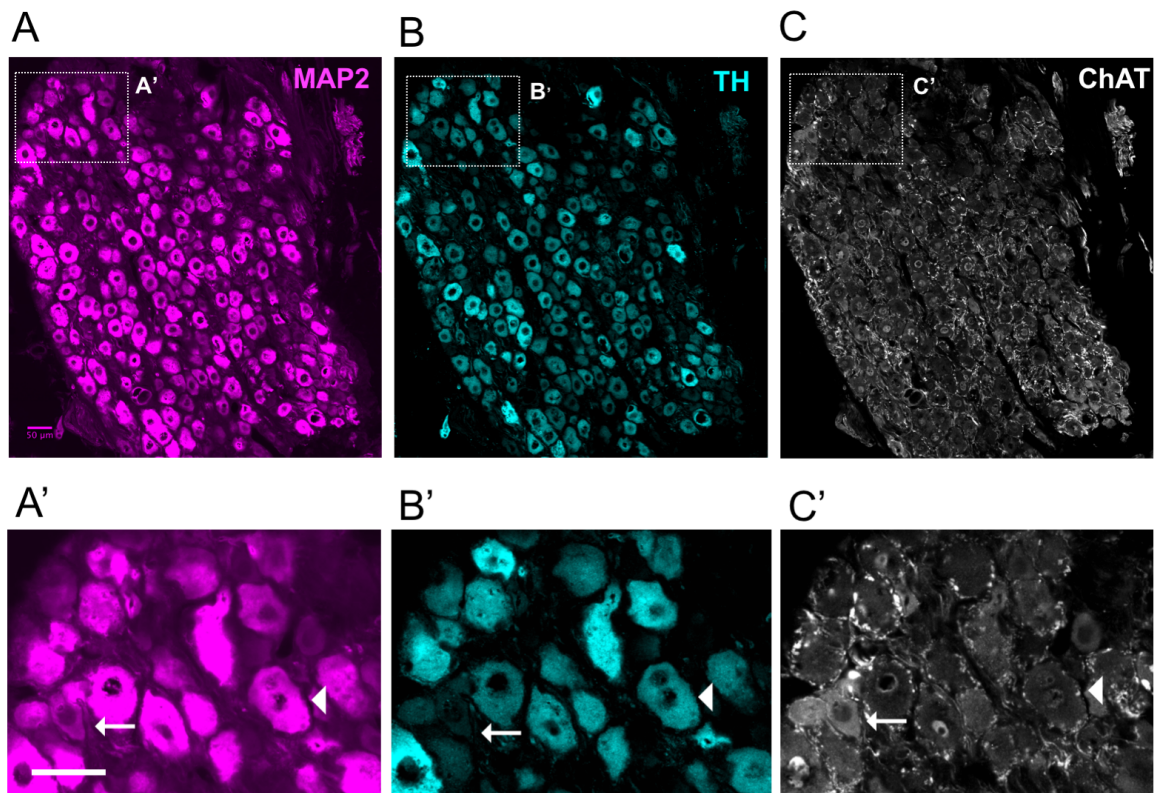


Figure 2.8 Expression of tyrosine hydroxylase (TH) and choline acetyltransferase (ChAT) in the rat pelvic ganglion

(A) MAP2 fills the cell bodies of both sympathetic and parasympathetic neurons in the PG. (B) PG neuronal phenotypes can be distinguished based on their expression of TH. (C) TH negative neurons (arrows) are ChAT positive; ChAT expression is also found in the preganglionic fibres surrounding the PG neuron cell bodies. Binucleate neurons are present within the PG. Error bars are 50µm.

2.4.7.1 High thoracic injury results in atrophy of TH-positive neurons

Examination of the distribution of cell sizes for the entire neuronal population of PG neurons one month post-T3x using the pan-neuronal marker MAP2 identified a small leftward shift in cell sizes, indicating either neuronal atrophy or loss of large neurons (Fig. 2.9). Since differential gene expression of RNA sequencing data found that TH was decreased in the PG one month post-T3x (Table 2.9), I hypothesized that the leftward shift of the neuronal population may be specific to TH-positive neurons. Examination of TH-positive and TH-negative populations separately identified that the TH-positive neurons were responsible for the leftward shift (Fig. 2.9A-C), with no significant changes in cell population size identified in the TH-negative population (Fig. 2.9D).

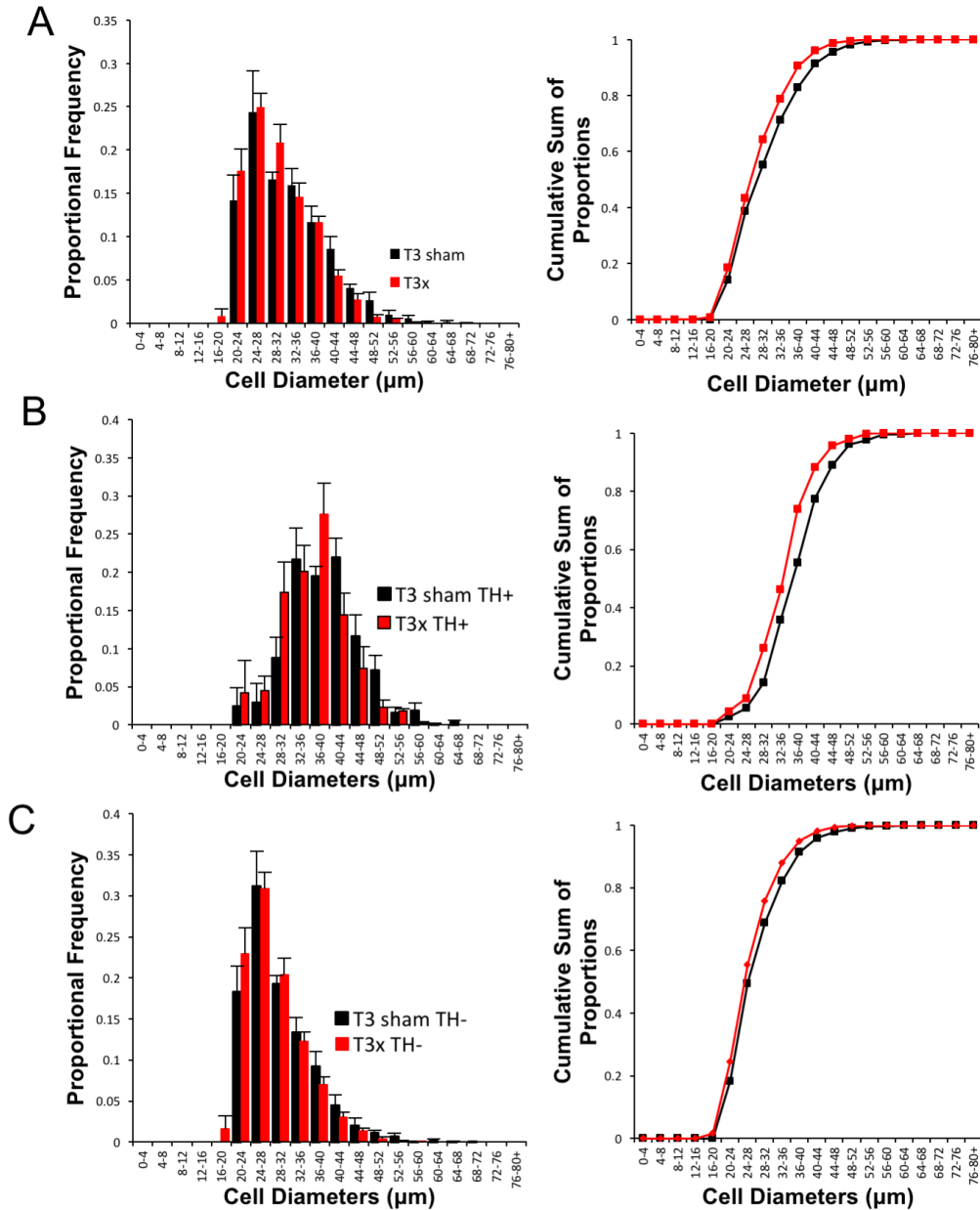


Figure 2.9 TH-positive neurons are responsible for the leftward size distribution shift one month post-T3x

(A-C) Size frequency distributions and plots of the cumulative sum of the proportions for the neuronal populations of the PG in T3x (n=6, red) and T3 sham (n=5, black) animals one month post-injury. (A) The leftward shift in the entire neuronal population (A) was due to changes within the TH-positive neuronal population (B). The TH-negative neurons were not significantly different between injured and sham animals. Kolmogorov-Smirnov goodness-of-fit tests were performed using the cumulative sum of the proportions to determine if there is a statistical difference between the groups. The proportion of the TH+ neurons after injury was unchanged compared to sham animals (mean±S.E.M. of T3x: 0.2105 ± 0.04463 vs. T3 sham: 0.2484 ± 0.04464 ; unpaired t-test, p-value=0.903)

Functional and morphological changes after SCI are known to be dynamic. Therefore, I next asked if the shift in TH-positive neurons was already present at an earlier time point. Unlike the expression data, which did not identify a significant difference in mRNA levels at two weeks post-T3x (Fig. 2.7), the cell size distribution data showed a leftward shift in the TH-positive neuron population (Fig. 2.10A) by two weeks post-injury. There was once again no difference in the TH-negative population of neurons or a change in the proportion of TH-positive and -negative neurons (Fig. 2.10 B,C)

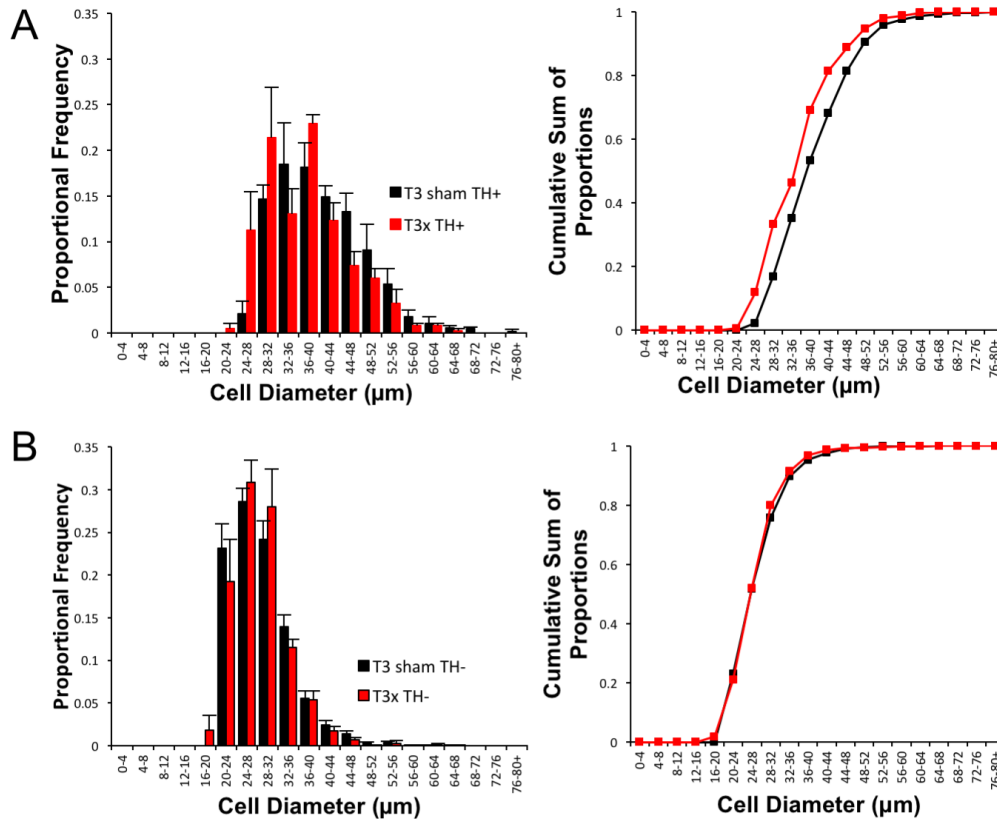


Figure 2.10 TH-positive neuronal size change also present at two weeks post-T3x (A,B) Size frequency distributions and plots of the cumulative sum of the proportions for neuronal populations of the PG from T3x (n=5, red) and T3 sham (n=5, black) animals two weeks post-injury. (A) The leftward shift in the population was accounted for by changes in the TH-positive neurons (A) and the TH-negative population was unchanged compared to sham (B). Kolmogorov-Smirnov goodness-of-fit tests were performed using the cumulative sum of the proportions to determine if there is a statistical difference between the groups, D-statistic calculated for $p < 0.05$. The proportion of the TH+ neurons after injury was unchanged compared to sham animals (mean \pm S.E.M. of T3x: 0.2985 ± 0.007109 vs. T3 sham: 0.3216 ± 0.02099 ; unpaired t-test, p -value=0.346)

2.5 Discussion

In this chapter, I describe the differential gene expression changes in the pelvic sensory and autonomic ganglia of the male rat one month post-T3 transection, with a view to assessing potential relationships between pelvic organ dysfunction and neurotrophic effects on their innervating neurons. Examination of the L6/S1 DRGs identified a pattern of changes consistent with alterations in both cell communication and growth factor signaling. Canonical Pathway Analysis revealed a decrease in growth factor signaling pathways within these DRGs one month after injury. Notably, upstream effector analysis also identified BDNF signaling as being decreased in sensory ganglia. In PGs, a smaller number of genes were differentially expressed, however patterns implicating altered neurotransmission and growth factor signaling were also identified. Decreased expression of genes related to sympathetic and parasympathetic neurotransmission, alongside atrophy of TH-positive neurons, suggests a non-canonical relationship between bladder hypertrophy and trophic effects on PG neurons.

2.5.1 Comparison of differential expression in the two ganglion classes

High thoracic spinal cord transection is far removed from the neurons of the pelvic peripheral ganglia. DRGs have central projections that enter the cord and are thus vulnerable to SCI. Most of these central projections synapse within a few segments of their entry point, save for a relatively small number of cutaneous mechanosensitive neurons having brainstem-projecting processes that may be directly injured by T3 SCI (lumbar proprioceptive DRG neurons terminate in Clarke's column in the thoracic cord and do not ascend as far as T3).³³⁰ Therefore, it is expected that the majority of neurons in both L6/S1 DRGs (and most certainly PGs) are not directly damaged by T3x.

The differences between these ganglia are worth noting, but so are the similarities in their response to SCI. One of the interesting commonalities is the upregulation in both populations of cold responsive proteins. Cold inducible RNA binding protein (*Cirbp*) mRNA was upregulated in both ganglia after injury, and the RNA binding motif protein 3 (*Rbm3*) was also significantly increased in the DRGs (Fig. 2.2 and Table 2.1). Thermoregulation is known to be disrupted by SCI and studies have shown decreases in core body temperature in the acute periods with this injury model.¹⁸¹ Notably, *Rbm3* is activated in astrocytes and neurons cultured at 36°C, indicating that even a small drop in temperature could contribute to the activation of these genes.³³¹ The cause of the upregulation of these mRNAs, whether due to core body temperature changes or other stress mechanisms, requires further investigation. Follow-up on this class of proteins may be particularly worthwhile because they are linked to both neuroprotection and inflammation with different injury types and models.^{332–334}

2.5.2 Functional clustering annotation for DRGs

A useful way to identify patterns of gene expression changes takes advantage of Functional Annotation Clustering, which relies on concept that functionally similar genes will also have similar annotation profiles which helps identify affected biological modules.³³⁵ The lists of genes down-regulated after SCI were enriched for genes related to nucleotide binding. This large class of genes that include those that bind to molecules, such as ATP, GTP and cAMP, that are involved in energy and signaling. Within the DRG itself, purinergic signaling is known to be important for communication between the neurons and the surrounding satellite glia.³³⁶ Additionally, genes related to cell junctions and synapses were also enriched in the list of downregulated genes. Axotomy of sensory neurons results in a dramatic shift in cell junction and

synaptic proteins that aligns with the loss of connection with the targets, however, it is interesting that the largely indirect insult to the neurons of LS-DRG by SCI also results in changes to this category of genes. One of the cell communication genes decreased after injury is SLC17A7 (also known as vesicular glutamate transporter 1, VGLUT1), expressed in medium to large DRG neurons with long central processes that may be injured by T3 transection.³³⁷ Since DRG neuron axotomy is known to reduce the expression of glutamate transporters, this decrease expression of VGLUT1 could relate to the direct injury of these neurons.³³⁸ It is also important to consider that changes in cell junctions and synapses may also be the result of communication and signaling changes within the ganglion itself, between the neurons and their surrounding support cells.³³⁶ A reduction in the expression of structurally-stabilizing cell junctional and synaptic genes sits well with the notion that there is a disruption in the balance between the normal function of adult neurons (signal transmission), and the reactive plasticity emerging in the wake of direct or indirect trauma.

2.5.3 Growth factor signaling downregulation in the DRG after T3x

Despite the indirect nature of injury to the pelvic peripheral ganglia, studies of lumbosacral DRGs have identified significant changes that occur within specific subpopulations of neurons. After high thoracic spinal cord transection, there is a specific hypertrophy and increased spontaneous activity of TRPV1-positive lumbosacral DRG neurons, indicating that this subpopulation of neurons may respond to changes in peripheral trophic support.^{3,243} TRPV1-positive DRG neurons express GFR α 3 receptors, conferring upon them sensitivity to artemin, a member of the GDNF family of neurotrophic factors.³³⁹ Interestingly, RNA sequencing results did not identify changes in either TRPV1 or artemin signaling, which could be for a number of

reasons, including the heterogeneous nature of DRG diluting out effects occurring within small subpopulations of cells. However, gene expression pattern changes identified by Ingenuity Pathway Analysis highlighted the importance of growth factor signaling after injury (Fig. 2.4; Table 2.7). The majority of growth factor signaling pathways were identified as potentially downregulated in the lumbosacral-DRGs one month post-T3x. Considering the literature surrounding increased growth factor expression by the pelvic organs, this finding was unexpected.

One of the more strongly-downregulated genes was FGFR1, which participates in multiple pathways identified in the functional clustering analysis. FGFR1 is known to be expressed by sensory neurons, but it is not regulated by peripheral nerve injury.^{340,341} While FGFR1 is required for the development of small-diameter DRG neurons, and stimulation of FGFR1 overexpression enhances neurite outgrowth, little is known about its normal function in the adult DRG.³⁴²⁻³⁴⁶ The downregulation of FGFR1 after SCI, and its centrality to numerous signaling pathways identified by canonical pathway analysis, especially considered alongside evidence that FGFR1 ligands have been used to promote sensory axon growth after experimental SCI, give reason to speculate that it should prove a useful target for further study.³⁴⁷

Upstream effector analysis drew attention to the downregulation of BDNF signaling in the DRG (Fig. 2.4). Previous studies have identified increases in BDNF mRNA after injury, but it is unclear whether this translated into increased expression of the BDNF protein.²²⁶ The timing of BDNF signaling is also important for pelvic viscera function after SCI, especially with regard to bladder outcomes; blocking BDNF signaling in the acute time points after SCI resulted in the early development of neurogenic bladder symptoms, but late sequestration of BDNF resulted in better bladder outcomes.³⁴⁸ The decrease in BDNF signaling we identified may be specific to this

injury level and time point, with drops in peripheral and/or central BDNF signaling. It may also reflect changes in expression of TrkB splice variants: the BDNF-sequestering truncated isoform is upregulated in the injured spinal cord at the lesion site and in glial cells in degenerating tracts well below the lesion.^{349–351}

2.5.4 Differential gene expression and neuronal atrophy in pelvic ganglia

Individual interrogation of differentially-expressed genes within the PG identified several genes with relevance to neuronal morphology, neurotransmission, and NGF signaling (Table 2.8). Upregulation of the ionotropic NMDA glutamate receptor subunit 1 (*Grina*) may subserve pathological interactions between glutamate-releasing sensory axons and autonomic neurons potentially influencing pelvic organ cross-sensitization.¹²⁸ The significance of downregulation of two other ion channels, *Nav1.1* (*Scn1a*) and the mechanotransducer *Piezo2* is unknown, as these channels have not been previously identified in autonomic neurons outside of microarray datasets.³⁵²

Decreased expression of tyrosine hydroxylase (TH) draws special attention as it is the rate-limiting enzyme in catecholamine production, which includes norepinephrine, the defining neurotransmitter of sympathetic PG neurons. Since the level of TH activity is a major factor in the control of norepinephrine levels, its decreased expression may indicate a disruption to peripheral sympathetic control, at least for pelvic viscera.³⁵³ Similarly, vasoactive intestinal peptide (VIP), which is a common co-transmitter in PG cholinergic neurons,³⁵⁴ is also decreased one month post-T3x. Interestingly, *Adcyap1* (encoding pituitary adenylate cyclase activating peptide, PACAP) is not normally expressed by PG neurons,³⁵⁵ and so its downregulation after SCI was surprising. However, PACAP (and its mRNA) is transported in sensory axons³⁵⁶ and

preganglionic cholinergic neurons,³⁵⁷ both of which are plentiful in the PG. Furthermore, an absence of PACAP is correlated with bladder dysfunction (including hypertrophy).³⁵⁸ Transgenic overexpression of NGF in the urothelium downregulates sensory axonal PACAP,³⁵⁹ but the effect of NGF on PACAP expression by PG neurons is unknown. SLC18A1 (vesicular monoamine transporter 1, VMAT1) transfers cytosolic monoamines to large dense-core vesicles in chromaffin cells of the sympathoadrenal lineage;^{327,360,361} in sympathetic ganglia, VMAT1 is expressed by small intensely fluorescent (SIF) cells,³²⁹ which are generally considered to have a neuroendocrine function or possibly to act as ganglionic interneurons.³⁶² Thus, SCI effects changes in gene expression underlying transmitter or co-transmitter function in all types of neuronal (and neuron-like SIF cells) in the PG.

In contrast, four genes important in nerve growth factor signalling increased after injury. The gene for the high affinity NGF receptor, TrkA, and nerve growth factor receptor, p75^{NTR}, were both increased one month post-T3x in the PG, as were mRNAs for necln – an intracellular NGFR and TrkA-binding protein required for NGF signaling,^{311,312} and LINGO1 – which also interacts with both NGFR and TrkA, negatively regulating signaling through the latter.^{313–315} Sympathetic neurons are one of the few populations that retain relatively high levels of NGFR expression into adulthood, though this dynamically regulated receptor may play a role in both neural and immune cells in response to injury and stress.^{113,363–367} The increase in NGF receptor mRNA expression is consistent with an increase in target-derived NGF signaling since NGF upregulates both its TrkA receptor and p75^{NTR} in neurons.^{368,369} It is also supported by a decrease in VIP expression, known to be negatively-regulated by NGF, and induced by axotomy or NGF antiserum.^{292,370} However, tyrosine hydroxylase mRNA, which is downstream of NGF signaling in NGF-sensitive sympathetic neurons,³⁷¹ decreases after injury. This result is opposite

of what is expected based on the increased expression of *Ntrk1* and *Ngfr*, but may indicate more complicated signaling changes occurring at this time point.

Expression changes in genes likely related to somal morphology included intermediate filaments peripherin (upregulated) and internexin-alpha (down-regulated to a similar extent), and PDZ and LIM domain 5, which binds to alpha-actinin and regulates dendritic spine morphology.^{321,322} Somal hypertrophy of sensory and sympathetic neurons is a well-documented response to exogenous neurotrophic factor treatment or transgenic overexpression,^{298,307,326,372–375} and studies from our lab have previously shown hypertrophy of artemin-sensitive lumbosacral DRG neurons following T3 SCI.³ It was therefore surprising to find atrophy of neuronal somata of sympathetic ganglion neurons following T3 SCI. The reduction in size of TH-positive neurons following SCI (both two weeks and one month after), argues against (particularly NGF-mediated) increased trophic support of sympathetic neurons. Also, one must consider that the heterogeneous population of PG neurons innervates all the organs of the pelvic viscera, and not just the bladder. Therefore, differential responses within the pelvic organs may be resulting in distinct target-driven changes within different neuronal populations.

2.5.5 Conclusions

SCI results in significant changes in gene expression and morphology of neurons even at levels far below the region where the injury occurred. Examination of the pelvic peripheral ganglia, identify alterations in growth factor and cellular signaling which give cause to reevaluate the classical neurotrophic hypothesis, at least with regard to bladder-neuron interactions following SCI. The results presented here have implications for formulating treatments which target SCI-induced pelvic organ dysfunction.

Chapter 3: Pelvic autonomic neuron morphology and phenotypic changes reveal novel neuron-target interactions after lumbar spinal cord transection

3.1 Summary

Pelvic ganglia (PG) provide autonomic input to the bladder and other pelvic visceral organs. These, like all neurons of the adult peripheral nervous system, require target-derived neurotrophic support for phenotypic maintenance, and augmented neurotrophic factor availability due to increased amount of target tissue has predictable effects on neuronal gene expression and morphology. Bladder outlet obstruction, for example, induces both bladder and neuronal hypertrophy, increased production of nerve growth factor (NGF), and increased neuronal sensitivity to NGF. Spinal cord injury (SCI) also results in enlarged bladders, and yet in chapter 2, I showed atrophy of TH-positive PG neurons at two weeks and one month after high thoracic spinal cord transection. This led me to ask whether a lower transection, which in humans results in greater bladder deficits, might unmask a more canonical neuron-target relationship. Lumbar spinal cord transection in the male rat (L2x) resulted in bladders that were, by three months post-injury, five times larger than after upper thoracic transection (T3x), and by two weeks post-injury, NGF-sensitive PG neurons from L2x animals were indeed increased in size. However, two weeks later there was no longer a difference between animals with L2x or sham surgeries, indicating that an increased amount of bladder tissue following L2x is not associated with sustained neuronal hypertrophy. A concomitant decrease in tyrosine hydroxylase mRNA expression following L2x, and the absence of increased NGF receptor expression, also argue against increased NGF availability. Vasoactive intestinal polypeptide mRNA, expressed by

NGF-insensitive penis-innervating cholinergic neurons, was also decreased following L2x (but with no change in neuronal diameter) suggesting previously undescribed neuron-target interactions in this subpopulation following SCI.

3.2 Introduction

Pelvic ganglia (PG) link lumbar and sacral spinal autonomic centres to pelvic visceral organs. PG neurons are synaptically driven by spinal preganglionic autonomic neurons in both the lumbar intermediolateral cell column and dorsal commissural nuclei (sympathetic), or the sacral preganglionic nuclei (parasympathetic). PG are unique in that they contain both sympathetic and parasympathetic neurons in bilateral collections that lie against the prostate (in the case of the male rat) or in a plexus amongst the pelvic organs (in female rats and larger mammals).³⁰ The axons of these neurons exit the ganglia and innervate their nearby targets including the urogenital tract, lower bowel, and sexual organs.

During development and into adulthood, autonomic neurons (among others) rely on target-derived neurotrophic support for survival and phenotypic maintenance, respectively.^{289,290} Following SCI, the bladder, a major autonomic target, undergoes significant structural and functional changes. Initial disruption to the uroepithelium resolves in the acute phases of injury,²⁰⁷ but over time the detrusor often undergoes hypertrophy, which is thought to develop subsequent to a loss of coordinated control of the bladder wall and sphincters (see Chapter 4 for further discussion).^{72,376} A number of studies link bladder hypertrophy to increased growth factor production; non-SCI models of hypertrophic bladder, such as bladder outlet obstruction, demonstrate higher levels of nerve growth factor (NGF), increased NGF-sensitivity of bladder-innervating neurons, and neuronal hypertrophy,^{283,377–379} which are consistent and predictable

responses to excess NGF and other neurotrophic factors.^{298,307,326,372-375} By this reasoning, bladder hypertrophy following SCI ought to be followed by somal hypertrophy of PG neurons, but evidence from the previous chapter argues otherwise: two weeks after T3 complete transection TH-positive neurons undergo atrophy, and remain smaller than those of sham-operated controls for at least one month post-injury.

Expression of genes associated with both neuronal and paraneuronal (SIF) cells of the PG are also altered one month following SCI, and again these are not altogether supportive of an increased NGF-dependent trophic influence of the hypertrophic bladder. While expression of nerve growth factor receptors NGFR and Ntrk1 mRNAs were increased (agreeing with known effects of NGF),^{292,368-370} tyrosine hydroxylase (TH), the rate-limiting enzyme in norepinephrine production, was decreased in the PG over the first month after injury. Like atrophy of TH-positive neurons, this is inconsistent with the idea of increased trophic influences of bladder-derived NGF on autonomic neurons.^{325,326,371}

In the present study, I ask how SCI level influences bladder size, and whether injuries that augment bladder hypertrophy are reflected in morphological changes and alterations in gene expression consistent with the neurotrophic hypothesis. In humans, lower spinal cord injury (low thoracic or high lumbar) results in a greater incidence of vesicoureteral reflex over the first several months of injury,^{146,380} suggesting enhanced detrusor-sphincter dyssynergia (DSD), and pressures high enough to force urine into the upper urinary tract. DSD is generally considered to underlie bladder hypertrophy,⁵² and so we hypothesized that rats with lumbar SCI (at L2) would have larger bladders, and that morphological and molecular changes in PG neurons would better agree with what is known about neuron-target interactions. Three months post SCI, bladders were significantly heavier in rats with L2x than high thoracic (T3x) or age-matched naïve rats.

There was a transient hypertrophy of TH-positive PG neurons two weeks after L2x that waned by one month post-lesion. mRNA for TH and VIP were decreased between two weeks and one month following L2x, whereas NGFR mRNA was unchanged. Thus, while bladder hypertrophy was associated with temporary somal size increases consistent with increased NGF signalling by the bladder, such a mechanism is not bolstered by concomitant changes in NGF-dependent gene expression.

3.3 Materials and Methods

3.3.1 Animal procedures

All animal procedures were approved by the University of British Columbia Animal Care Committee in accordance with the guidelines established by the Canadian Animal Care Committee. All experiments in this chapter were performed on male Wistar rats (200-300g) from Envigo, Mississauga, Canada at the ICORD facility in Vancouver, BC. The complete transection spinal cord injury surgeries and post-operative care of the animals was performed as described in Chapter 2 Material and Methods Sections 2.3.2 and 2.3.3 with the following adjustments for the lumbar (L2) spinal segment transections. The midline incision was made above the T11-L1 vertebrae and muscle was removed surrounding the T13 vertebra. A laminectomy at T13 was performed to expose the underlying L2 cord where the transection (for L2x) or durotomy alone (L2 sham) was performed. All other procedures were consistent with T3x as described in Chapter, sections 2.3.2 and 2.3.3.

3.3.2 Wet bladder weights

The weights of bladders from rats three month post-T3x or L2x were compared to age matched naïve controls. The wet bladder weights were measured as previously described.³⁸¹ Briefly, after completion of cardiac perfusion fixation with 4% paraformaldehyde, the bladders were carefully dissected free from the surrounding tissue and isolated above the neck at the level of the trigone, just superior to the ureter insertion points. The bladders were voided upon dissection, as needed, suspended until almost dry and weighed on a precision electronic Sartorius milligram balance (CP423S-OCE, Bohemia, NY, USA).

3.3.3 RNA isolation and quantitative PCR

RNA was isolated from PGs dissected and quantitative PCR (qPCR) was performed as described in Chapter 2. qPCR results were pooled from animals two weeks and one month post-L2x or sham surgery. Pooling was performed because of high variability and low numbers, particularly at the one-month time point (data from each time point are clearly identified in the analysis). Primer sequences and protocols for the qPCR can be found in Chapter 2 Materials and Methods Section 2.3.8 and Table 2.1.

3.3.4 Tissue processing, immunohistochemistry and image analysis

Tissue collection, processing, staining, imaging, and analysis were described in Chapter 2 Materials and Methods Sections 2.3.9 and 2.3.10. The same procedures were performed on PGs from animals two weeks and one month post L2x or sham surgery.

3.3.5 Statistical analyses

Differences in bladder weight were analyzed by Welch's ANOVA for unequal variances followed by Games Howell post-test for unequal variances of bladder weights using Real Statistics Using Excel (Excel add-in available at www.real-statistics.com). Kolmogorov–Smirnov (K–S) goodness-of-fit tests were performed on PG size distribution data as described in Chapter 2, Materials and Methods Section 2.3.11. Statistics for the quantitative PCR results were analyzed in Prism 7: first, the ROUT method (robust regression and outlier removal)³⁸² with aggressiveness (Q) =1% was used to identify outliers (this is the recommended aggressiveness: Q=0.1% identifies definite outliers, while Q=10% identifies likely outliers). This method identified one outlier each in the following groups: L2x TH, L2x VIP and sham NGFR. The cleaned data were then compared using unpaired t-tests, with p-values <0.05 considered significant.

3.4 Results

3.4.1 Bladder weights after chronic SCI

Bladder hypertrophy was marked at chronic (3 month) time points after both complete thoracic (T3x) or lumbar (L2x) injuries (Fig. 3.1). The wet weights of bladders from rats with chronic T3x were approximately double the weight of age matched controls (T3x: 0.211 ± 0.0145 g vs. naïve: 0.0907 ± 0.00695 g; mean \pm S.E.M.). Bladders of animals post-L2x weighed significantly more than both T3x and naïve animals (L2x: 0.984 ± 0.199 g; mean \pm S.E.M.). There was also a statistically significant difference in variability between groups (Levene's test, $p=3.33E-05$).

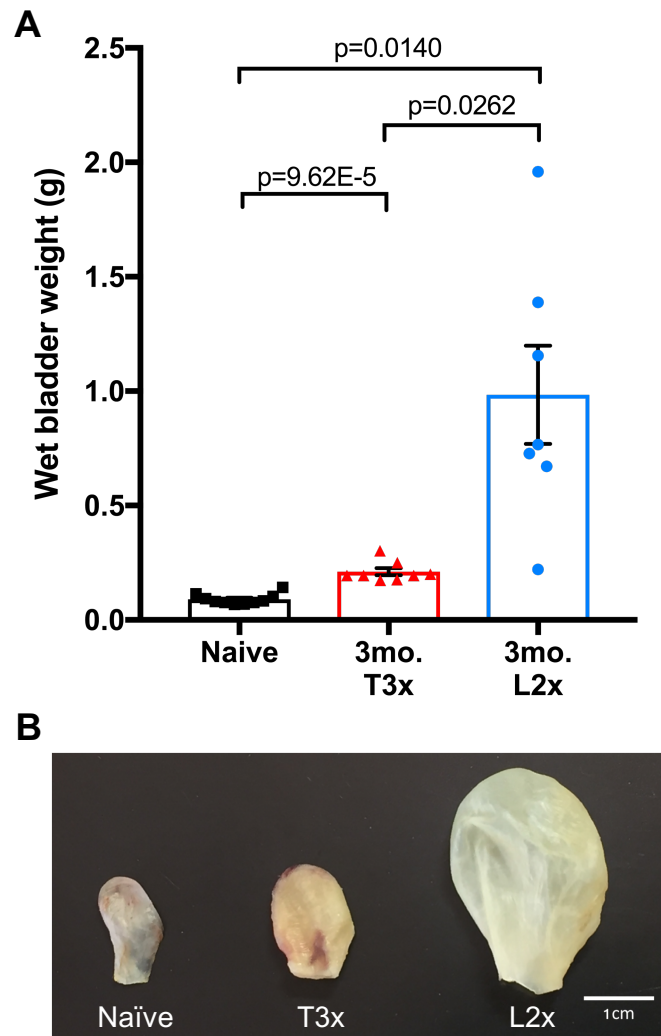


Figure 3.1 Chronic lumbar spinal cord transections result in bladder hypertrophy

(A) Three months after complete transection at T3x or L2x, the wet weights of the bladder were significantly greater than in age-matched naïve controls. L2x injury also resulted in heavier bladders than T3x injury. One-way Welch’s ANOVA ($p < 0.0001$) followed by Games Howell post-test for unequally distributed data, mean \pm S.E.M. and exact p-values shown. (B) Representative images of bladders from (left to right) naïve age-matched animals, and three months-post T3x or chronic L2x injury. Weights of representative bladders: naïve: 0.080g; T3x: 0.302g; L2x: 1.156g.

3.4.2 Lumbar transection results in a transient hypertrophy of TH-positive neurons

Despite the clear increase in bladder size after T3x (Fig. 3.1), analysis from Chapter 2 found that TH-positive neurons of the PG were atrophic at both two weeks and one month post-injury (Chapter 2, Figs. 2.9 and 2.10). To determine whether the greater increase in bladder sizes after L2x were reflected in neuronal PG size changes, I examined the cell size distributions of TH-positive and TH-negative PG neurons after spinal cord transection at L2x at both two weeks (Fig. 3.2) and one month (Fig. 3.3) time points. Two weeks after L2x, shortly after the establishment of a spinal cord-mediated micturition reflex, there was a transient rightward shift in the TH-positive neuron size-frequency distribution (Fig. 3.2A), while the TH-negative neurons were not significantly different from shams (Fig. 3.3B). By one-month post-L2x there were no longer any differences in the cell size-frequency distributions of either population of PG neurons (Fig. 3.4A,B). The proportion of TH-positive and TH-negative neurons were unchanged compared to sham animals in both comparison groups (two week L2x: 0.3316 ± 0.0425 vs. L2 sham: 0.4162 ± 0.05593 , $p\text{-value}=0.654$ and one month L2x: 0.4299 ± 0.05667 vs. L2 sham: 0.3312 ± 0.01855 , $p\text{-value}=0.160$; unpaired t-test, $\text{mean} \pm \text{S.E.M.}$).

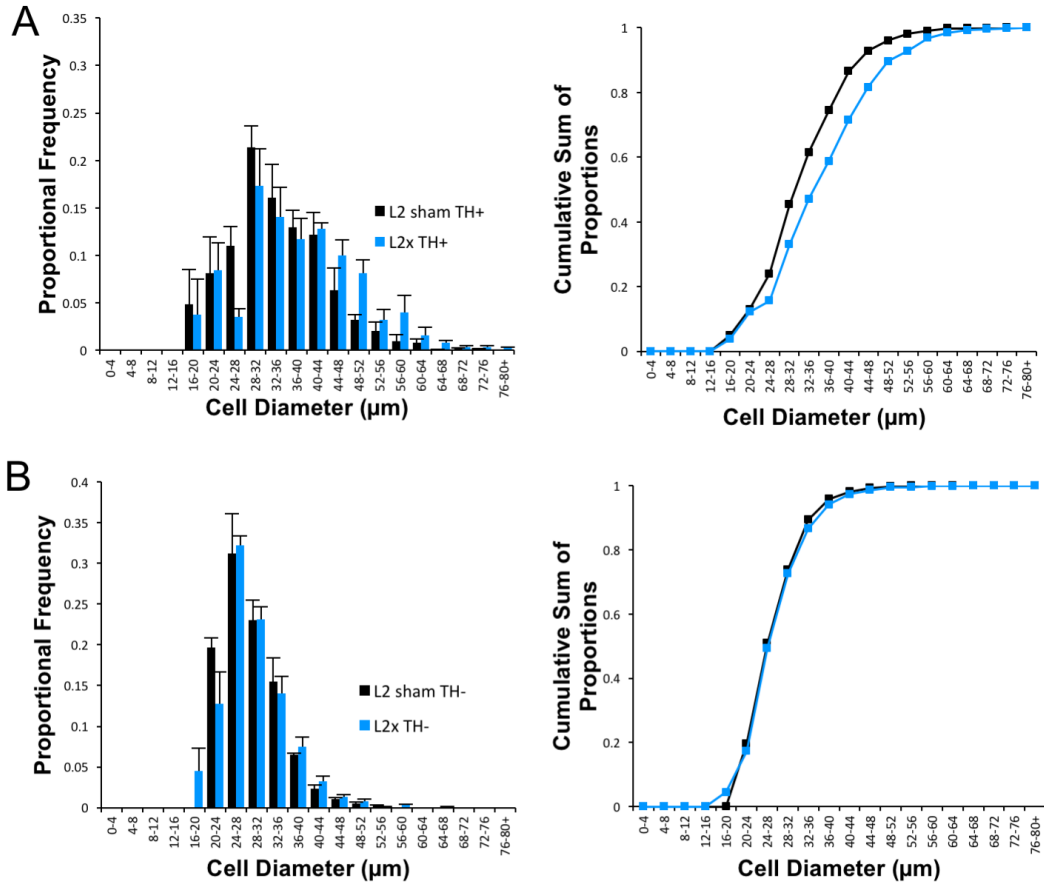


Figure 3.2 Hypertrophy of TH-positive neurons two weeks post-L2x

(A-B) Size-frequency distributions and plots of the cumulative sums of the proportions for the TH-positive and TH-negative neurons of the PG from L2x (n=5, blue) and L2 sham (n=5, black) animals two weeks post-injury. (A) The TH-positive neurons undergo a rightward shift in the cell size distribution(B). The TH-negative neurons were not significantly different between injured and sham animals. K-S goodness-of-fit tests were performed using the cumulative sum of the proportions to determine if there is a statistical difference between the groups, D-statistic calculated for $p < 0.05$.

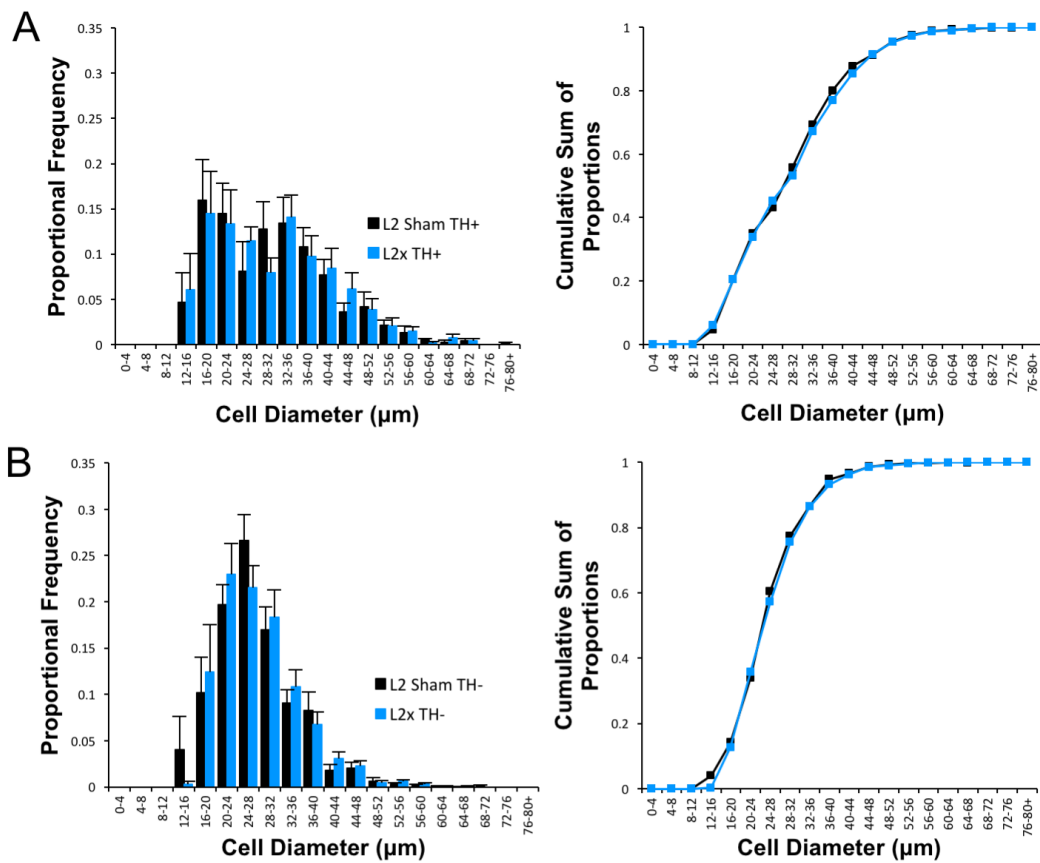


Figure 3.3 By one month post-L2x the TH-positive neuronal population size was no different from sham

(A-B) Size frequency distributions and plots of the cumulative sum of the proportions for the TH-positive and TH-negative neurons of the PG from L2x (n=5, blue) and L2 sham (n=5, black) animals one month post-injury. (A) Unlike at two weeks, there is no difference in the cell size distributions the TH-positive or TH-negative neurons between injured and sham animals at one month post-injury. K-S goodness-of-fit tests were calculated using D-statistic for $p < 0.05$.

3.4.3 Gene expression changes in PG

From the RNA sequencing data performed on PGs one month after T3x, there were clear alterations in gene expression patterns related to neurotransmission and growth factor signaling. To determine whether a lower SCI results in different patterns of gene expression changes, I examined the mRNA expression levels of TH, VIP and NGFR following L2x (pooled two weeks and one month) and (pooled) L2 shams (Fig. 3.4). Both TH and VIP mRNAs were downregulated between two weeks and one month after L2x. NGFR expression was unchanged compared to sham controls at both time points.

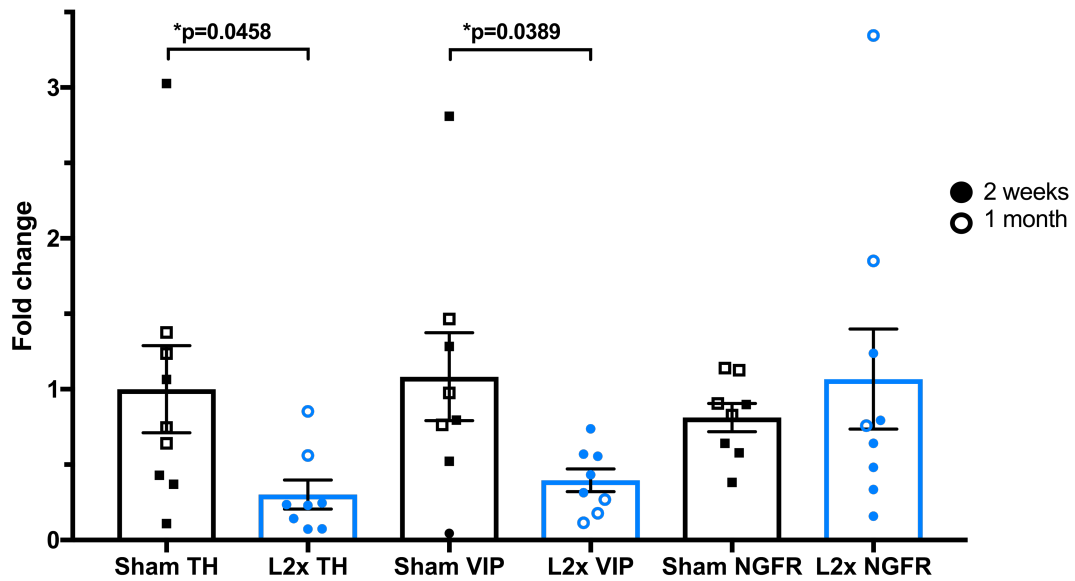


Figure 3.4 Quantitative PCR of TH, VIP and NGFR expression in the PG after L2x

There is a significant decrease in the expression of both TH and VIP after L2x when the data from two weeks (filled in symbols) and one month (open symbols) post-L2x are pooled. NGFR mRNA expression was unaffected ($p=0.4940$). Unpaired t-tests, mean \pm S.E.M. and exact p-values as shown.

3.5 Discussion

While previous studies have highlighted the importance of the level of SCI on changes within sensory neurons innervating the pelvic viscera, these have generally not been extended to peripheral autonomic neurons.³ The pelvic viscera are differentially affected by the level of spinal cord transection,³⁸³ and here I show that L2x increases bladder hypertrophy well beyond that of T3x. In the previous chapter, I identified gene expression changes in the PG one month after T3x that are important to growth factor signaling and neurotransmission in both sympathetic and parasympathetic neurons. I also found that PG neurons (specifically TH-positive neurons) underwent significant atrophy. Since some of these results were inconsistent with the idea that the hypertrophic bladder should effect NGF-dependent changes in neuronal morphology and gene expression, I reassessed such a potential relationship using an injury which significantly augmented bladder size (L2x).

3.5.1 Bladder hypertrophy varies with injury level

The increase in bladder weight following L2x is consistent with previous findings that bladder dysfunction is dependent on (suprasacral) injury level and severity.^{381,383} A study by Ozsoy *et al.*, which examined compression SCIs in the thoracic cord, found that the most severe compression injury resulted in the greatest bladder dysfunction and size. Importantly, the histological analysis also demonstrated that the most severe compression also resulted in the greatest spread of injury, including damaging the upper lumbar segments.³⁸¹ This supports that notion that injury level, as well as severity, plays a role in bladder dysfunction. Increased bladder size after lower injuries may depend on a loss of preganglionic input to the pelvic ganglion since complete transection of the upper lumbar cord should result in the loss of some sympathetic

preganglionic neurons,³⁸⁴ or it may be a consequence of other systemic SCI level-dependent effects (see below, and Chapter 4).

3.5.2 Transient hypertrophy of PG neurons following L2x

Previous studies have found that an increase in the cross-sectional area of bladder-innervating PG neurons correlates with bladder hypertrophy following bladder outlet obstruction.^{283,378} Only one prior study has investigated changes in somal size of bladder-projecting PG neurons 4-6 weeks after complete spinal transection (at T9).⁴ In this case there was no demonstrable hypertrophy of PG neurons (in agreement with one-month data presented here), unless the PG was also concomitantly deafferented by transection of the hypogastric (sympathetic) and pelvic (parasympathetic) nerves. The hypothesized explanation is that preganglionic input to the PG mitigates some unknown process that would otherwise cause PG neurons to increase in size. Viewed in this light, and based on the spinal distribution of preganglionic axons in the rat hypogastric nerve (L1/2 intermediate grey),³⁸⁴ it is relevant that L2x is expected to destroy (an unknown amount of) sympathetic input to the PG. The regression of cell sizes following L2x toward those of sham-operated animals by one month post-injury may represent compensation (sprouting) by spared sympathetic preganglionic axons, an effect which has previously been demonstrated following PG deafferentation by either lumbar or sacral spinal nerve injury.³⁸⁵

This leads to the question as to why T3x, but not transection at T9,⁴ causes neuronal atrophy in the PG (Chapter 2), since both injuries spare PG preganglionic input. The answer may lie in differences between the two injuries in terms of more systemic effects: the spinal segment with the greatest number of preganglionic neurons projecting to the rat adrenal medulla, for

example, is T9, although T7-T12 contribute as well.³⁸⁶ Indeed, the differences between T3x (somal atrophy), T9x (no change), and L2x (transient somal hypertrophy) correlate with the amount of descending adrenal medullary control following each injury type: none (T3), partial (T9), and full (L2). In Chapter 4 I explore the role of adrenal function in physiological bladder activity following low (L2) and high (T3) spinal transections.

3.5.3 Changes in PG gene expression, morphology, and the neurotrophic hypothesis

TH and VIP mRNAs were downregulated, and NGFR remained unchanged following L2x. A potential caveat is that it was necessary to pool material from two weeks and 1 month post-lesion and remove outliers given the small number of samples and large variability. It should be pointed out that the high single fold-change data points for sham-TH and sham-VIP are (a) not statistical outliers given the relatively conservative method used to define them and (b) do not overly influence the results since their removal by more aggressive outlier identification (Q=10%) does not change the outcome.

Since they tend to be oppositely regulated in sympathetic neurons, downregulation of both TH and VIP indicates that changes within the PG after injury are probably driven by multiple processes and multiple target organs.^{93,293,325,326,387-390} TH-positive and VIP-positive neurons are differentially distributed within the PG, and project to different tissues: TH-positive neurons are concentrated toward the rostral and medial parts of the ganglion, whereas VIP-positive neurons are most abundant ventrolaterally, near the penile nerve; the majority of penis-projecting neurons contain VIP immunoreactivity and relatively few VIP-positive neurons project to the bladder.^{93,98,391} Compared to the bladder, little is known about changes in the sexual organs after SCI. However, one study of erectile dysfunction in men after SCI identified

changes in penile structure, including increased apoptosis of cavernous endothelial and smooth muscle cells.³⁹² Whether and how this relates to loss of VIP mRNA expression in the PG after SCI remains to be determined.

NGF receptor expression also differs between TH- and VIP-expressing PG neurons. Approximately 90% of TH-positive adrenergic neurons in the PG express TrkA (Ntrk1) and NGFR1, whereas only 10-20% of VIP-expressing cholinergics do.³⁹³ Expression of both TH and NGFR are dependent on endogenous NGF and are increased by exogenous NGF.^{325,369,394-397} The most parsimonious explanation for decreased TH and unchanged NGFR shown here would be decreased NGF production by the bladder following L2x. Indeed, while the mRNA expression of several growth factors (including NGF, BDNF, and CNTF) increased in the bladder after mid-thoracic spinal cord transection, NGF protein expression was decreased at both four days and four weeks.²²⁶ A more recent study of changes in bladder protein levels after T9x also found significantly decreased NGF at four and twelve weeks post-injury.³⁹⁸ These results are in contrast to what is known about bladder outlet obstruction, in which the hypertrophic bladder expresses more NGF.^{283,377,378} Thus, even though bladder outlet obstruction and SCI-induced detrusor-sphincter dyssnergia both produce a hypertrophic bladder, the catalogue of growth factors they produce is probably quite different.

The decrease in TH expression may be attributable to decreased NGF signaling, or to other processes. By four weeks post T9 spinal transection, for example, expression of multiple proinflammatory interleukins, CXC chemokines, CX3CL1, and CCL2 were significantly increased in detrusor muscles.³⁹⁸ However, there is not yet evidence that any of these regulate TH expression in sympathetic neurons. Injury-induced gp130 receptor-binding cytokines such as leukaemia inhibitory factor (LIF) decrease TH expression in sympathetic neurons both *in vitro*

and *in vivo* (e.g. following cardiac injury),³⁹⁹⁻⁴⁰² and although there are no data on injury-induced cytokine expression in the bladder, bladder stretch increases LIF expression in both rats and humans.⁴⁰³ It is reasonable to speculate that the massively enlarged bladders in L2x was produced at least in part by persistent stretch.

What can be said about the relationship between changes in gene expression and cell size is also a matter of speculation. Interestingly, exogenous LIF causes dendritic retraction of sympathetic neurons *in vitro*,⁴⁰⁴ a finding that may be related to regression of TH-positive somal diameters between the second and fourth weeks post-injury shown here, and perhaps even neuronal atrophy following T3 complete transection (Chapter 2). Furthermore, in medial septal cholinergic neurons, LIF prevents loss of NGFR immunoreactivity and reduces somal size after axotomy,⁴⁰⁵ potentially explaining the absence of any change in NGFR expression by PG neurons shown here, and possibly also the upregulation of NGFR after T3 transection (Chapter 2).

3.5.4 Conclusions

In summary, transection of the rat spinal cord at the second lumbar segment results in significant increases in bladder size at three months compared to both naïve and T3x animals. The chronically hypertrophied bladders of the L2x animals do not result in a sustained hypertrophy of TH-positive neurons within the PG, but only a significant rightward shift in cell size distribution at two weeks. Furthermore, the mRNA levels of TH decrease after L2x, further supporting previous studies that indicate hypertrophied SCI bladders may produce less NGF after injury.^{226,398} Finally, decreased mRNA expression of VIP, which predominates in cholinergic

neurons innervating the penis, highlights the need for further study into SCI-induced changes to other organs of the pelvic viscera.

Chapter 4: Preserved adrenal function after lumbar spinal cord transection augments low pressure bladder activity in the rat

4.1 Summary

Spinal cord injury (SCI) disconnects supraspinal micturition centres from the lower urinary tract resulting in immediate and long-term changes in bladder structure and function. While cervical and high thoracic SCI have a greater range of systemic effects, clinical data suggest that those with lower (but supraconal) injuries develop poorer bladder outcomes. Here we assess the impact of SCI level on acute changes in bladder activity. We used two SCI models, T3 and L2 complete transections in male Wistar rats and compared bladder pressure fluctuations to those of naïve and bladder-denervated animals. By two days after L2x, but not T3x or bladder denervation, small amplitude rhythmic contractions (1mmHg, 0.06Hz) were present at low intravesical pressures (<6mmHg); these were still present one month following injury, and at three months, bladders from L2x animals were significantly larger than those from T3 SCI or naïve animals. Low-pressure contractions were unaffected by blocking ganglionic signaling or bladder denervation at the time of measurements. L2x but not T3x preserves supraspinal adrenal control, and by ELISA we show higher plasma adrenal catecholamine concentration in the former. When an adrenalectomy preceded the L2x, the aberrant low-pressure contractions more closely resembled those after T3x, indicating that the increased bladder activity after lumbar SCI is mediated by preserved adrenal function. Since ongoing low-pressure contractions may condition the detrusor and exacerbate detrusor-sphincter dyssynergia, moderating bladder catecholamine signaling may be a clinically viable intervention strategy.

4.2 Introduction

Voluntary control of the urinary bladder relies on the coordination of autonomic, sensory and somatic nervous systems.⁵ When supraspinal input to these systems is interrupted by spinal cord injury (SCI) there are immediate and long-term consequences to bladder function. The loss of coordination between the cord-mediated reflex centers that control contraction of the detrusor and the external urethral sphincter often leads to the development of detrusor-sphincter-dyssynergias (DSD), where the bladder and sphincter contract together, resulting in high intravesical pressures and inefficient voiding.²³³ Without intervention, these complications can lead to vesicoureteral reflux, urinary tract infections, and upper urinary tract damage, all of which impact health care costs and quality of life for individuals with SCI.⁴⁰⁶ It is no surprise, then, that advances in bladder management and care are top priorities of both researchers and individuals with SCI.¹

During normal urinary bladder filling, low-amplitude rhythmic increases of intravesical pressure occur without inducing micturition. These non-voiding contractions (NVCs) have been documented in many animal species, dating back to the time of Sherrington's experiments in cats, where during bladder filling NVCs preceded higher amplitude voiding contractions.^{234,407,408} Recently, the presence of NVCs during normal bladder filling has been linked to activation of sensory afferents and may be important for signaling bladder fullness.^{409,410} However, both denervated and *ex vivo* bladders also exhibit a pattern of increased contractions with filling, indicating that NVCs are likely an intrinsic property of the bladder muscle.^{409,411,412} Importantly, aberrant NVC patterns after SCI are linked to overactivity in the detrusor muscle and changes to primary afferent signaling, which contribute to bladder dysfunction.^{239,413}

After SCI in both humans and rats, there is an initial loss of voiding reflex that is followed by variable recovery dependent on the level and severity of injury.^{381,383,414} Loss of coordination afforded by descending control combined with reorganization of micturition circuits after SCI results in the development of what is termed the neurogenic bladder. DSDs and bladder overactivity tend to emerge over time and are widely considered to underlie the hypertrophy of the bladder detrusor muscle. However, during the earliest time points post-injury, while the bladder is still considered areflexic, significant changes occur to the bladder wall.^{207,277} In rat spinal cord transection models, the urothelium of the bladder is disrupted within hours of the injury and wet bladder weights and intravesical volumes increase significantly during the first week.^{207,277} These findings suggest that dyssynergias, which are prevalent at higher intravesical pressures, may not be the sole cause of structural and functional changes within the bladder wall. Clinically, bladder outcomes vary with the level of SCI; one study identified patients with acute low-thoracic or high-lumbar SCI as having a greater incidence of vesicoureteral reflex.^{146,380} In rats however, most studies investigating bladder activity are performed using a mid to low thoracic injury, and after reflex voiding reemerges.^{410,415-417} This leaves questions with regards to bladder activity in the acute time periods after SCI and the role that the level of SCI plays in their manifestation.

Here we assess bladder activity in the acute time period after SCI by measuring and quantifying changes in the intravesical pressure of rats with either high thoracic (T3x) or lumbar (L2x) spinal cord transection. We find that within two days of L2x there is increased bladder activity at low pressures that is absent two days after T3x, and by three months post SCI, bladders from L2x animals are substantially larger than those of T3x rats. We also show that this differential bladder activity is not due to aberrant neural activity, but is dependent on preserved

adrenal function after L2x. We suggest that increased adrenal-endocrine mediated activity in the bladder at low-pressures contribute to poorer bladder outcomes when descending control of adrenal function is preserved.

4.3 Materials and methods

4.3.1 Animal procedures

The experiment was conducted on 89 adult male Wistar rats (300-400g, Envigo, Mississauga, Canada). Animals were acclimatized for at least one week before surgical procedures and testing in temperature and light-controlled (12 h light–dark reversed cycle) rooms. All surgical and euthanasia procedures were performed in accordance with ethical guidelines of the according to the Canadian Council for Animal Care, with ethical approval obtained from the University of British Columbia. From an additional 28 rats we harvested and weighed bladders three months following complete T3 SCI (n=8), L2 SCI (n=9) and sham operated rats (n=11), which were surplus to another experiment in our centre.

4.3.2 Intravesical recordings

Initial recordings at low intravesical pressures were recorded in naïve rats (n=4) and rats two days post-transection (T3x n=5; L2x n=5) and one month post-sham or transection (L2 sham n=6; L2x n=6). Bladder pressure recordings in awake animals were performed 2 days post-L2x (n=3) and in age matched naïve (n=4) animals. For animals that received a treatment or injury at the time of recordings four animals were used in each group (L2x at time n=4; Hexamethonium bromide, HexBr n=4; pelvic ganglionectomy, PGx n=4). Plasma epinephrine and norepinephrine measurements were performed in animals two days post-injury that did not have any other

experimental manipulations (T3x n=5; L2x n=5). To assess the response of the bladder to filling, infusions were performed in naïve animals and two days after each injury type (naïve n=8; PGx n=5; T3x n=7; L2x n=7; adrenalectomy, AdxL2x n=7).

4.3.3 Spinal cord injury surgeries and post-operative care

Complete transection of the spinal cord was performed at either the third thoracic (T3) or second lumbar (L2) spinal cord segment in adult male Wistar rats. Sham surgeries were performed concurrently, and in the same manner as the transection surgeries, up to and including the durotomy. Rats were housed in groups of 2-4 at a secure conventional facility with a standard 12-hour light-dark cycle. The details of the surgical procedure and post-operative care have been previously published,¹⁹⁶ and the major procedures involved in the SCI surgeries were described in sections 2.2.2 and 3.3.1 and post-operative care procedures were also described in section 2.3.3 of this thesis.

4.3.4 Bilateral pelvic ganglionectomy (PGx)

A 2cm midline abdominal incision through the skin and muscle layer was made just rostral to the pubis. The major pelvic ganglia were exposed on the ventrolateral surface of the prostate by blunt dissection using sterile cotton swabs. Using microscissors and forceps the body of the pelvic ganglion was detached from the connective tissue on the surface of the prostate and carefully cut from the connecting nerves, avoiding large blood vessels. Any small bleeds were treated with pressure applied by a cotton swab. When both pelvic ganglia were removed, the muscle was sutured with continuous 4-0 Vicryl suture and the skin was closed using 5-0 Vicryl subcuticular suture.

4.3.5 Bilateral adrenalectomies and L2 transections (AdxL2x)

Bilateral removal of the adrenal glands was performed immediately prior to L2 transections in the AdxL2x animal group. Prior to the surgery 5ml of hypotonic saline (0.45% sodium chloride solution) was given subcutaneously (s.c.) to help maintain blood volume and pressure. The surgical site was prepared as described above and the same analgesics and antibiotics were given. Upon reaching surgical plane with Isoflurane anesthetic, a midline incision was made above the T10-L2 vertebrae and the adrenal glands were accessed through two small incisions in the muscle layer on either side of the spinal column immediately caudal to the rib cage. The adrenal glands were identified in the retroperitoneal fat pad above the kidneys and carefully excised, minimizing blood loss and tissue damage. The muscle wall was closed with 4-0 vicryl suture. Upon completion of the adrenalectomy, the L2 complete transection was performed as described above prior to suturing the single skin incision.

4.3.6 Bladder pressure recordings in anaesthetized animals

Rats were given 1.2g/kg urethane (0.5g/ml in saline, intraperitoneally (i.p.); U2500, SIGMA, St. Louis, USA) to anesthetize to surgical plane, upon which they were placed supine on a water circulating heating pad. A midline abdominal incision was made to expose the detrusor. A purse-string suture (6-0 silk) in the dome of the bladder was made to secure both the pressure transducer end of a Millar Rat Pressure Telemeter (model: TRM54P, Millar, Houston, USA) and an infusion line attached to a syringe infusion pump 22 (Harvard Apparatus, South Natick, MA, USA). The pressure transducer of the telemetry device was calibrated using a sphygmomanometer prior to each set of measurements. After confirming the patency of the

infusion line, the bladder was emptied via urine withdrawal through the infusion line. To measure changes in pressure within the bladder during filling, room temperature saline was infused into the bladder at a physiologically relevant rate of 100 μ l/min.⁴¹⁸ Intravesical bladder pressure data were transmitted from the telemeter to a SmartPad (model: TR181, Millar, Houston, USA) connected to a PowerLab 16/30 (model: ML880, ADInstruments, Colorado Springs, USA) and recorded in LabChart v.7 (ADInstruments, Colorado Springs, USA) at 1000Hz.

4.3.7 Bladder pressure recordings in awake animals

Animals (n=4 naïve, n=3 L2x) were anesthetized to surgical plane with 2% Isoflurane in oxygen. The pressure transducer was inserted into the bladder and secured with a purse string suture as above. The abdominal muscle wall was then sutured and a pocket for the body of the telemetry device was made by separating the skin from the underlying muscle. Once the telemetry device was tucked under the skin of the abdomen, the skin incision was closed (4-0 prolene, discontinuous sutures). The animal was then allowed to awaken and was placed in an observation cage and continuously monitored for 4 hours, when they subsequently reached the experimental endpoint. Measurements were recorded using the same pressure transducer system as in the anesthetized rats while natural filling of the bladder occurred. Since behavioral movements result in changes to the abdominal pressures which can mask changes in bladder pressure, only recordings from resting periods were used for analysis.²³⁴

4.3.8 L2x during bladder pressure recordings

Naïve rats were prepared as above for the anesthetized bladder measurements. Upon completing two infusion cycles, the rats were carefully placed on their stomach and an L2 transection was performed as described above. Upon completion of the transection the animals were returned to the supine position and bladder measurements continued for at least two hours post-L2x.

4.3.9 HexBr and PGx during bladder pressure recordings

A subset of rats two days post-L2x had pressure recordings taken before and after either hexamethonium bromide (HexBr) injection (n=4) at 20mg/kg via tail vein injection, or bilateral pelvic ganglionectomy (n=4, performed as described above). The NVC amplitudes were recorded before and one hour after the intervention at comparable low pressures.

4.3.10 Pressure recordings analysis

Identification and analysis of NVCs was performed using the Peak Analysis Add-On for Labchart v.7. as described by Heppner *et al.*, 2016. Collected pressure data was initially smoothed (2s) and then analyzed under the general unstimulated section in Peak Analysis, using the parameters of 20 second normalization and a minimum two standard deviations between peaks and minimum baseline values.⁴⁰⁹ For the comparison of NVC amplitude with increasing intravesical pressure, the NVC heights were sorted into 1mmHg bins based on the minimum starting pressure before each recorded peak (Fig. 4.1). A minimum of two infusion cycles were used for each animal in the analysis. Bins with fewer than three NVC amplitudes were not included in the analysis. The intravesical pressure at which the NVC amplitudes reached 1mmHg

were recorded during the bladder infusions and the values were averaged for at least two infusions per animal.

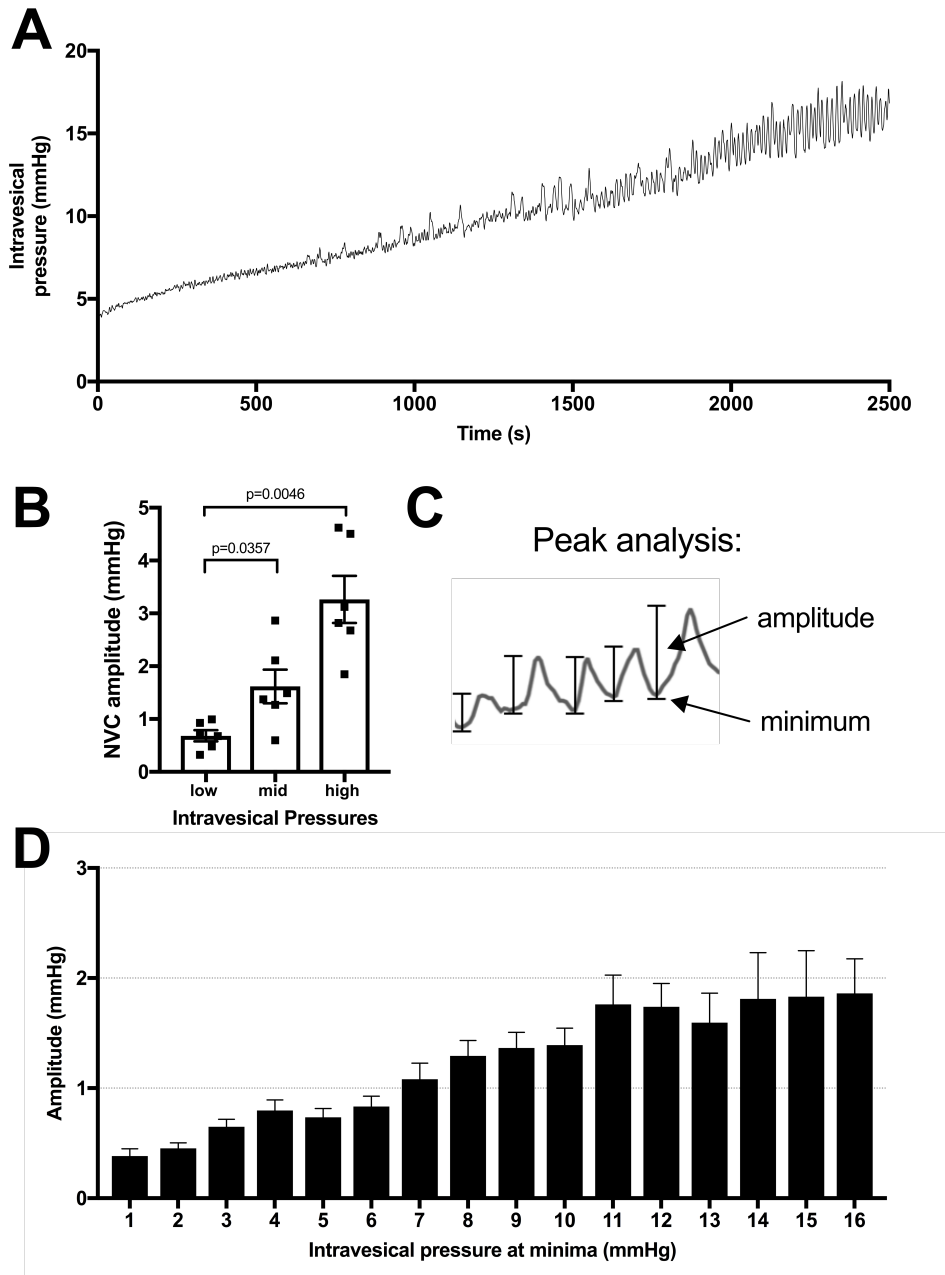


Figure 4.1 Pressure changes during infusions and analysis of minima and amplitude of bladder contractions

(A) Representative pressure recording from a urethane anesthetized rat during bladder filling at a rate of 50 μ l/min. (B) Amplitude of NVCs are significantly higher at mid (7-10mmHg) and high (14-18mmHg) vs low (1-4mmHg) intravesical pressure, mean \pm SEM, repeated measures one-way ANOVA, p-values as shown. (C) Peak analysis is used to analyze the relationship between intravesical pressure and NVC amplitude. (D) The measured amplitudes are binned based on the intravesical pressure at their minima, the resulting bar graph for naïve animals is presented as an example.

4.3.11 Epinephrine and norepinephrine ELISAs

Rats with either an L2 sham, T3x, or L2x transection (n=5 per group) were deeply anesthetized two days after injury with 5% inhalant isoflurane and blood was collected via cardiac puncture into K2 EDTA blood collection tubes (BD Vacutainer®, Becton, Dickinson and Company, Franklin Lakes, NJ, USA). Blood samples were spun at 4°C for 10min at 1000 xg and plasma was collected and stored at -80°C. ELISAs were performed to measure plasma concentrations of epinephrine (BA E-6100, LDN® immunoassays and services, Nordhorn, Germany) and norepinephrine (CEA907DGe, Cloud-Clone Corp., Katy, Texas, USA), following manufacturer's instructions. For the norepinephrine measurements, the ELISA was performed on only four T3x and L2x animals due to limited plasma volumes.

4.3.12 Statistical analyses

All statistical analyses were performed using Graph Pad Prism 7, except in one case (Welch's ANOVA for unequal variances followed by Games Howell post-test for unequal variances of bladder weights) where we used Real Statistics Using Excel (Excel add-in available at www.real-statistics.com). Statistical tests and exact p-values are given in the results and figure legends. Statistical significance was set at $p < 0.05$. Data are displayed as means \pm SEM.

4.4 Results

Patients with acute SCI between T10 and L2 have a greater incidence of vesicoureteral reflux than those with higher-level injuries, suggesting increased bladder hyperactivity after low injury.³⁸⁰ Furthermore, the wet weights of rat bladders after chronic L2x were significantly

heavier than after T3x (Chapter 3, Fig. 2.1). Bladder hyperreactivity and DSD probably both contribute to hypertrophy. The facts that bladder hypertrophy is a gradual process, and that the higher incidence of vesicoureteral reflux in patients with acute low SCI was not correlated with differences in bladder cystometric or biomechanical findings, prompted us to ask whether acute changes in bladder activity differed between high and low SCI.³⁸⁰

4.4.1 Short and long-term consequences of high and low SCI on the rat bladder

Consistent with previous studies, infusion of saline into the naïve bladder results in a steady increase in intravesical pressure and the appearance of increasingly greater NVC amplitudes as the pressure within the bladder increases (Fig. 4.1A,B).²³⁴ When we assessed bladder activity at low pressures (<6mmHg) in rats two days post-L2x we found that the amplitude of NVCs was significantly greater than those in naïve rats or those transected at T3 and occurred at a frequency of $0.061 \pm 0.0043\text{Hz}$ (n=12) (Fig. 4.2A-D). Since anaesthesia is known to impact the micturition response in both naïve and SCI injured rats we wanted to confirm that the presence of these low-pressure, small amplitude NVCs were not due to urethane.^{235,236,238} The amplitude of NVCs in awake L2x animals (Fig. 4.2E) was significantly higher than in naïve animals (Fig. 4.2F, G) at the same low intravesical pressures (Fig. 4.2H).

To ask whether this phenomenon was restricted to acute time points after L2x, we compared bladder activity in animals 1 month after L2x or sham injury (Fig. 4.3). The larger amplitude low-pressure NVCs persisted for at least one month following injury (Fig. 4.2A-C), and did not depend on differences in baseline intravesical pressures (Fig. 4.3D).

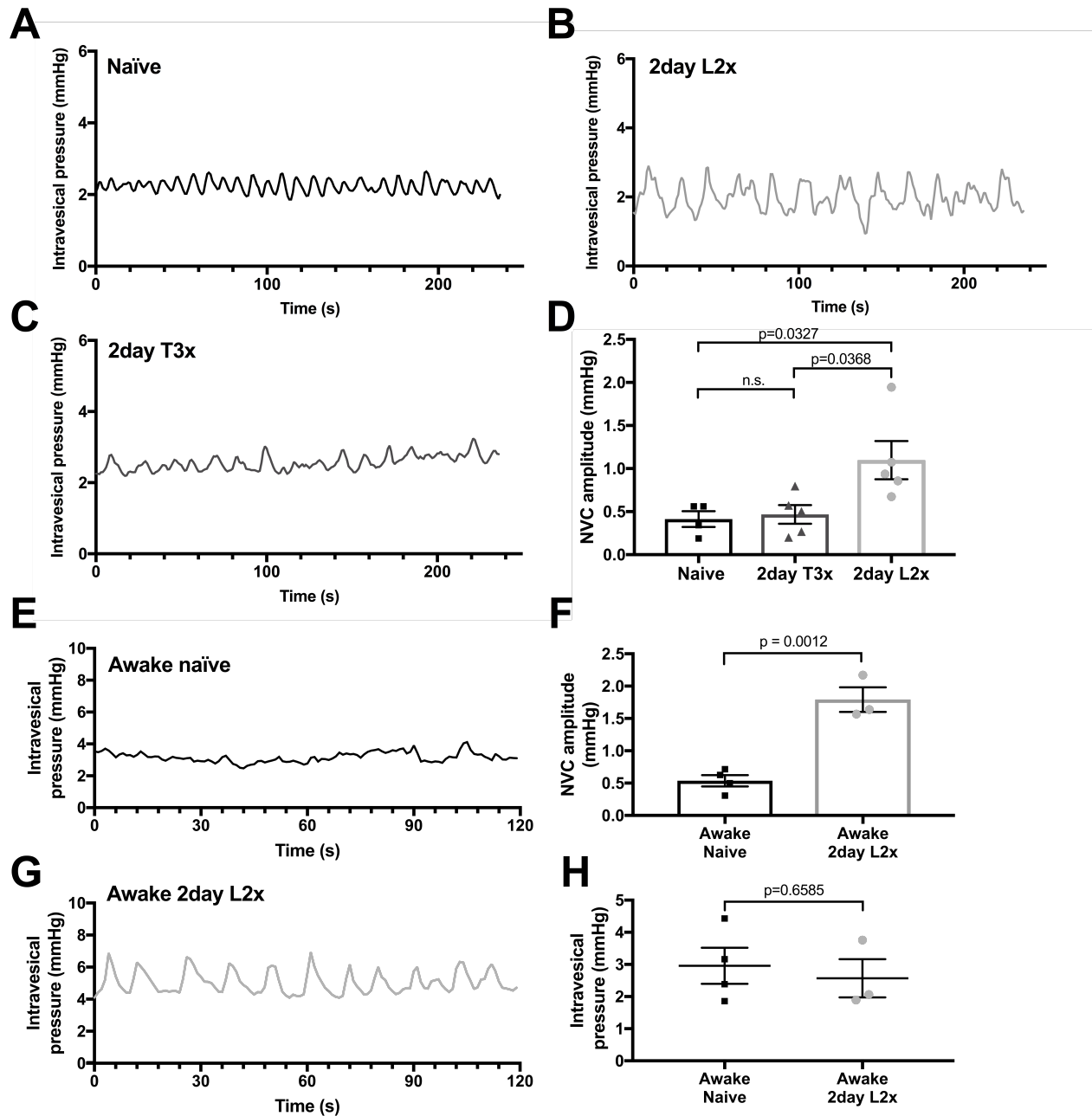


Figure 4.2 Amplitude of NVCs is increased at low pressures after L2x

(A-C) Representative traces of intravesical bladder pressures after different injury levels in urethane anesthetized rats. (D) Amplitude of NVCs is significantly higher two days post-L2 transection (L2x) compared to two days post-T3 transection (T3x) and naïve controls; one-way ANOVA, mean \pm SEM. (E, G) Representative traces of low intravesical bladder pressures of awake rats that are naïve or two days post-L2x. (F) The amplitude of NVCs in awake L2x animals is significantly higher than that in naïve animals, (H) with no difference in baseline intravesical pressures, t-tests, mean \pm SEM. Exact p-values shown.

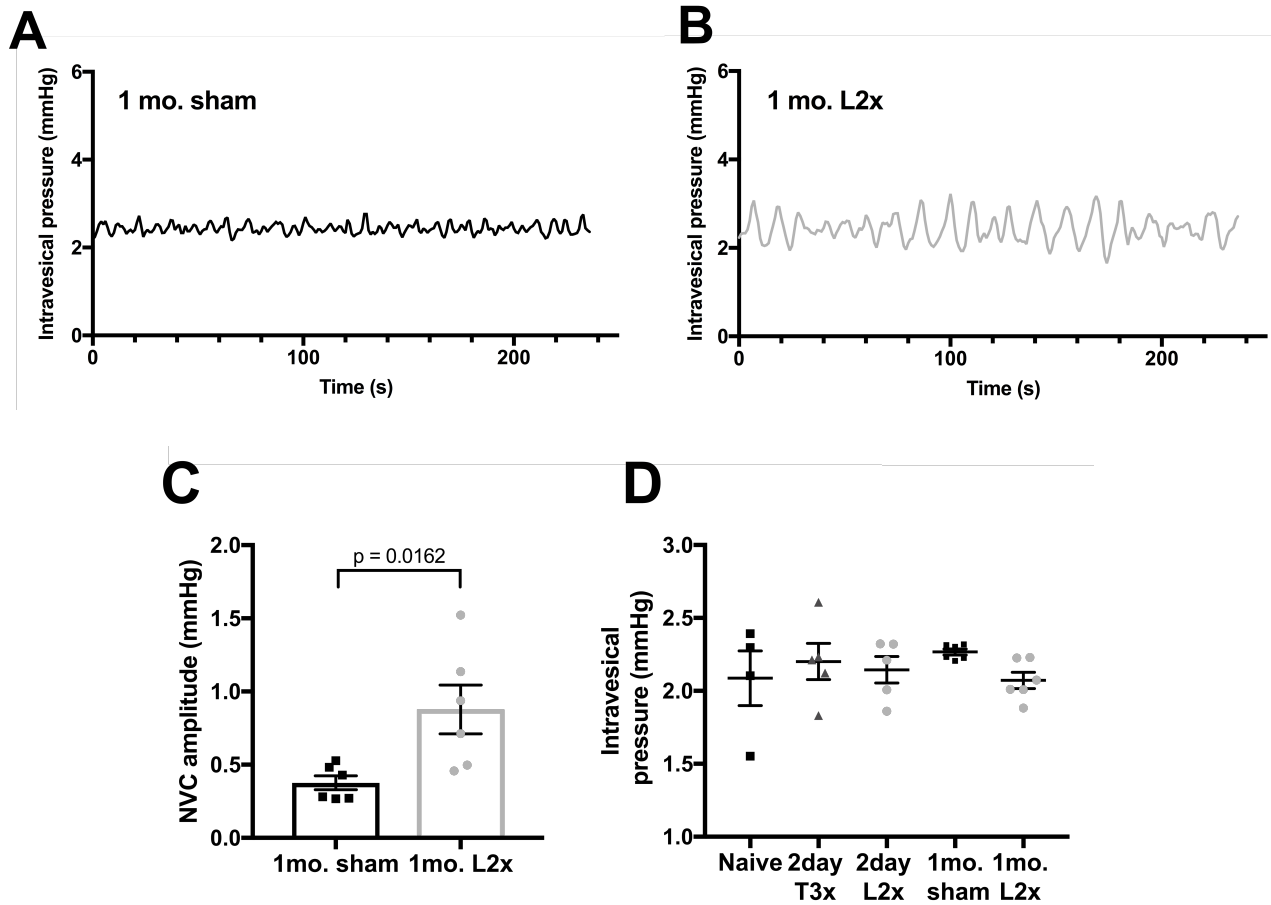


Figure 4.3 Increased amplitude of low-pressure contractions persist to one month post-L2x (A-C) Increased NVC amplitude after L2x is still elevated at least 1 month post-injury compared to sham operated animals; unpaired t-test, mean \pm SEM. (D) The baseline intravesical pressure at which the NVCs were measured at was not different between groups, one-way ANOVA ($p=0.5602$).

4.4.2 Increased low-pressure NVC amplitude emerges in the acute period

Detrusor hyperactivity following SCI has been mainly attributed to loss of descending modulation from supraspinal storage and micturition centres.⁴¹⁹ Therefore, we asked whether hyperacute SCI (up to 2h following transection) led to the emergence of NVCs by interrupting descending control. In these experiments we examined NVC-pressure relationship during bladder filling; amplitudes of NVCs increase and drive afferent activity which is important for sensation of bladder fullness.⁴⁰⁹ Similar to previous reports, we found that NVC amplitudes increase during physiologically relevant filling of *in vivo* naïve rat bladders under urethane anesthesia (Fig. 4.1A, Fig. 4.4A). Following L2x, NVC amplitude at low pressures remained statistically unchanged for at least two hours post-injury (Fig. 4.4B) indicating that simple loss of descending modulation is not responsible for suppressing ongoing NVC activity. However, immediately following spinal cord transection there is significant decline in the maximum amplitude of NVCs reached at high pressures, which is consistent with these animals' failure to void (Fig. 4.4D).

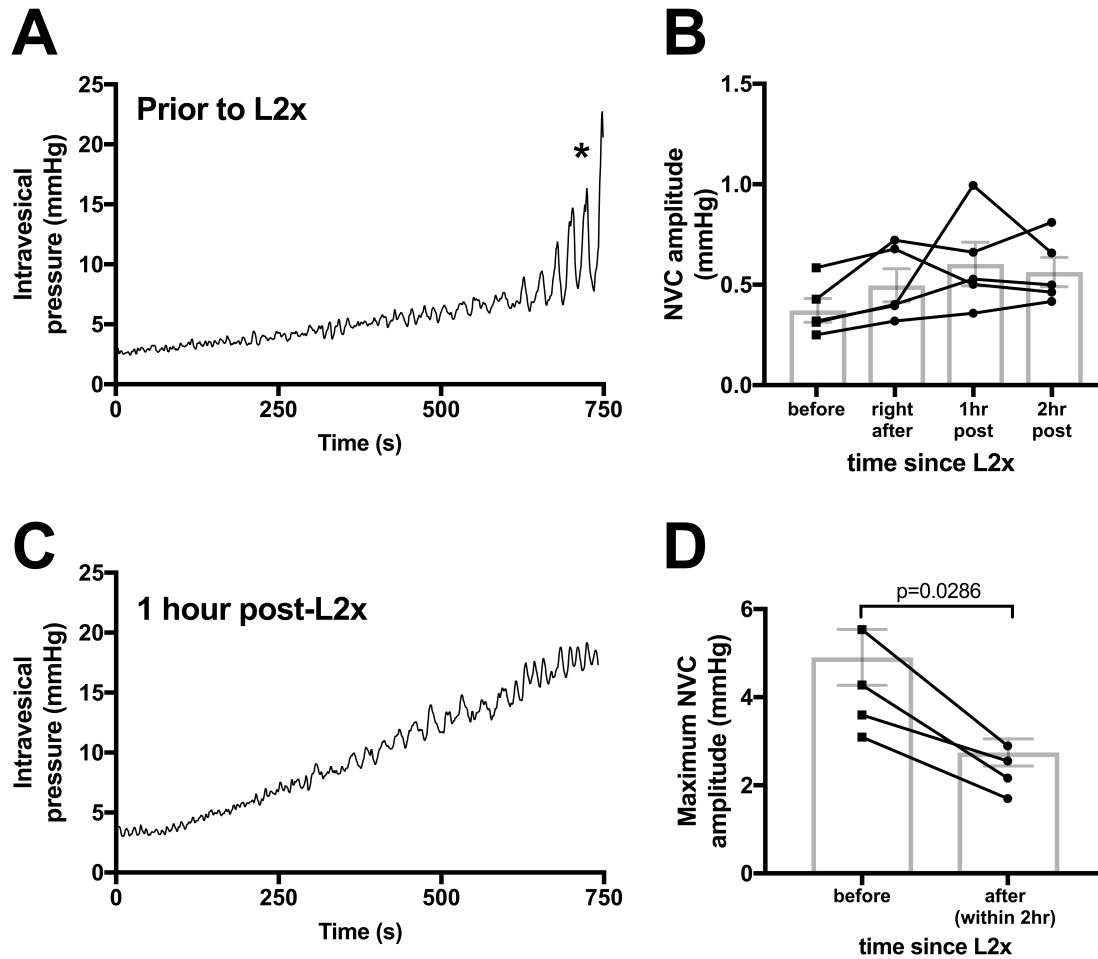


Figure 4.4 Larger amplitude NVCs at higher pressures are immediately reduced by L2 transection

(A,C) Example bladder pressures traces from one animal during 100ul/min saline infusion either before (C) or 1 hour after (D) L2 transection, *indicates start of bladder voiding in naïve animal. (B) There is no difference in low pressure NVC amplitudes immediately following and up to two hours after L2x, repeated measures ANOVA, $p=0.1939$. Lines connect individual animals over the 2-hour timeline. (D) Maximum amplitude of NVCs during infusions decreased upon transection of the L2 cord, Mann-Whitney two tailed test. Exact p-values shown.

4.4.3 Increased low-pressure NVC activity is not dependent on neural circuitry below an L2 SCI

Larger NVCs at lower pressures could indicate enhanced sacral parasympathetic output from the cord, possibly driven by amplified bladder-afferent input. To test this hypothesis, we used hexamethonium bromide (HexBr), a ganglionic transmission blocker, to eliminate signals from the cord to the pelvic ganglia in rats two days following L2x. HexBr administration at the time of recordings did not reduce low-pressure NVC amplitude (Fig. 4.5A), arguing against reflexive neurogenic hyperreflexia either at the level of sacral parasympathetic output, or at the level of thoraco-lumbar sympathetic output (which is partially preserved following L2x). Primary afferent axons also have efferent functions (such as neurogenic vasodilation), and so we asked whether low-pressure NVCs could be mediated by sensory axons directly.⁷⁸ To this end we acutely removed pelvic ganglia (through which bladder afferents travel) bilaterally (PGx) in rats with L2x performed two days earlier. Acute PGx did not reduce low-pressure NVC amplitude, arguing against an ongoing efferent role for sensory axons (Fig. 4.5B).

We also explored the possibility that the loss of autonomic or efferent-type sensory activity in the detrusor underpinned the emergence of low-pressure NVCs over the first few days following injury. We therefore performed a bilateral PGx two days prior to measuring NVC-pressure relationships and compared them to naïve rats (Fig. 4.5C-H). By sorting the NVC amplitudes into bins based on the intravesical pressure at the NVC minima (see Fig. 4.1) we were able to compare the relationship between increasing intravesical pressure and NVC amplitude (Fig. 4.5E, F). The denervation of the bladder resulted in a decrease of maximum

NVC amplitude (Fig. 4.5H) similar to that of L2x (Fig. 4.4D) but did not result in higher NVC amplitudes at low pressures (Fig. 4.5F). Therefore, increased NVC amplitude at low pressures following L2x is not due to hypoactivity in de-centralized (parasympathetic), partially preserved (sympathetic), or primary afferent bladder circuitry. NVC frequency did not differ between any of the anesthetized L2x groups ($p=0.2916$, one-way ANOVA).

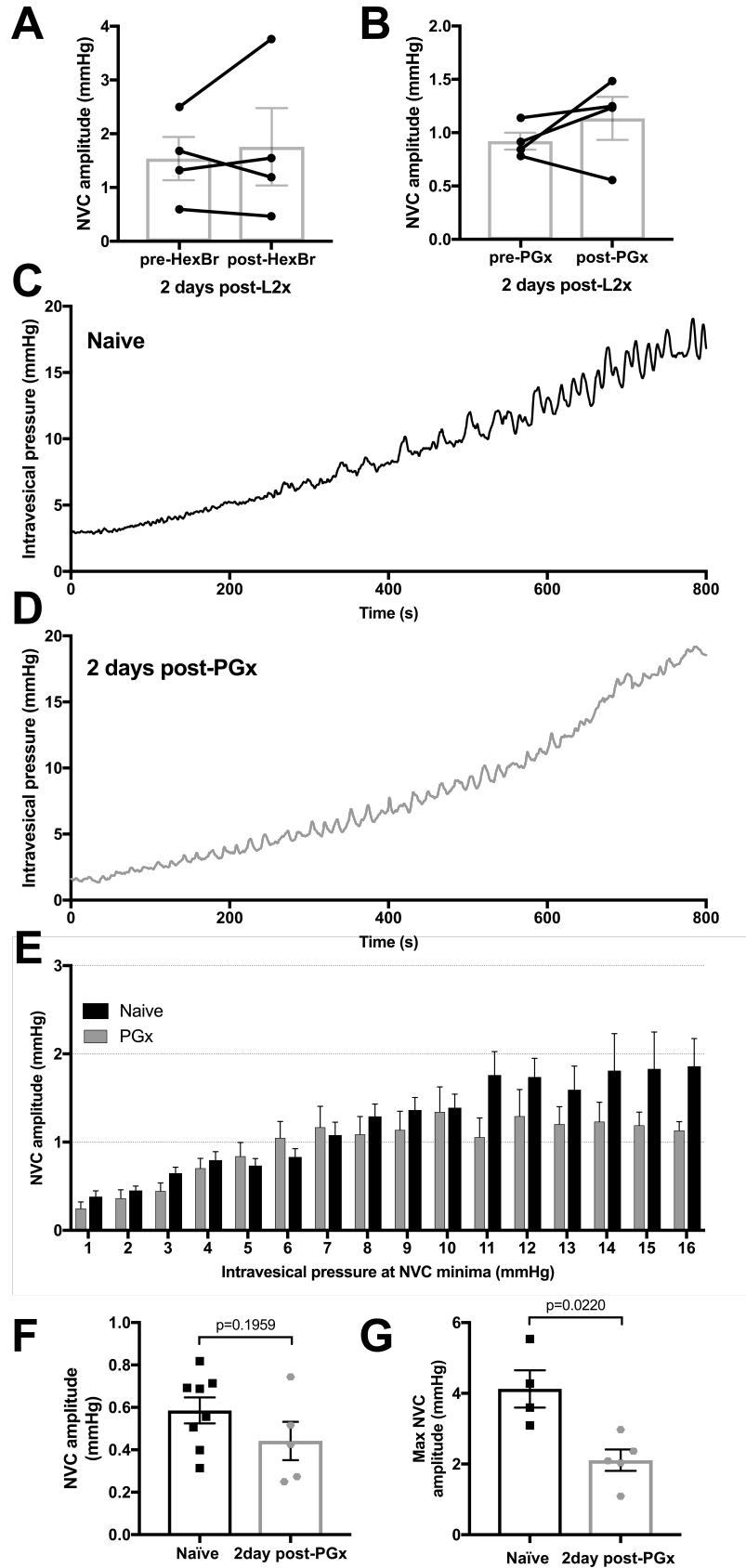


Figure 4.5 Eliminating bladder innervation results in decreased large amplitude NVCs but does not eliminate the low pressure NVCs 2-days post-L2x

(A, B) NVCs from animals two days post-L2x were recorded before and after treatment with hexamethonium bromide (HexBr, A) or bilateral removal of the pelvic ganglia (B). Neither treatment affected the NVC amplitude at low pressures, paired t tests, (A) $p=0.6042$; (B) $p=0.3285$. (C, D) Representative traces of intravesical pressures during bladder filling, 100 μ l/min of saline in naïve animals (C) and two days post-bilateral pelvic ganglionectomy (PGx, D). (E) NVC amplitudes sorted into 1mmHg bins based on intravesical pressure at NVC minima (see Fig. 4.1). As pressure increases, NVC amplitude increases in naïve animals (C, E, $n=8$) but higher amplitude NVCs are lost when bladder is denervated (D, E, $n=5$). (F, G) NVC amplitudes at low pressures are not increased two days post-PGx (F) but the maximum NVC amplitude reached was significantly lower two days post-PGx (G), unpaired t-tests, exact p-values shown.

4.4.4 Adrenal function underlies low-pressure NVCs following L2 SCI

Previous studies in humans found that individuals with injuries below T5 had significantly higher plasma epinephrine levels compared to individuals with higher injuries.^{420,421} A recently published study using similar models of high and low SCI in mice identified significant differences in adrenal function between injury groups, which impacted immune function. Mice with high thoracic transections had decreased expression of circulating norepinephrine acutely after injury compared to low injuries and controls.³³ Since higher injuries remove descending input to spinal neurons innervating the adrenal medulla, we hypothesized that animals with a T3x would have lower plasma levels of epinephrine and/or norepinephrine compared to those with either a L2x or sham injury and sham.

The concentrations of individual adrenal catecholamines were highly variable, although both our findings and previous studies indicate that there are lower levels in the T3x animals compared to (Fig. 4.6A).³³ Capturing accurate and representative measurements of individual catecholamines in plasma is notoriously difficult due to their sensitivity to stressors and fast turnover.⁴²² However, when we considered adrenal catecholamines on the whole (by normalizing concentrations of each to those of sham-operated rats and then averaging the relative concentrations for each animal), there was indeed a significant difference between T3x and animals with intact adrenal gland innervation ($p=0.0283$, Welch's t-test).

To determine whether adrenal function contributed to NVC development two days after L2x injury we surgically removed the adrenal glands immediately prior to L2x (AdxL2x). The raw low-pressure bladder traces two days post-AdxL2x (Fig. 4.6D) more closely resembled those occurring after T3x (Fig. 4.6C) than those following L2x alone (Fig. 4.6B). NVCs in animals with the L2x alone reached an amplitude of 1mmHg at lower pressures than they did in naïve,

T3x or AdxL2x animals (Fig. 4.6E). The distribution of NVC amplitudes at low pressures (0-6 mmHg) in the AdxL2x animals also more closely resembled that of T3x rats than that of L2x animals (Fig. 4.6F).

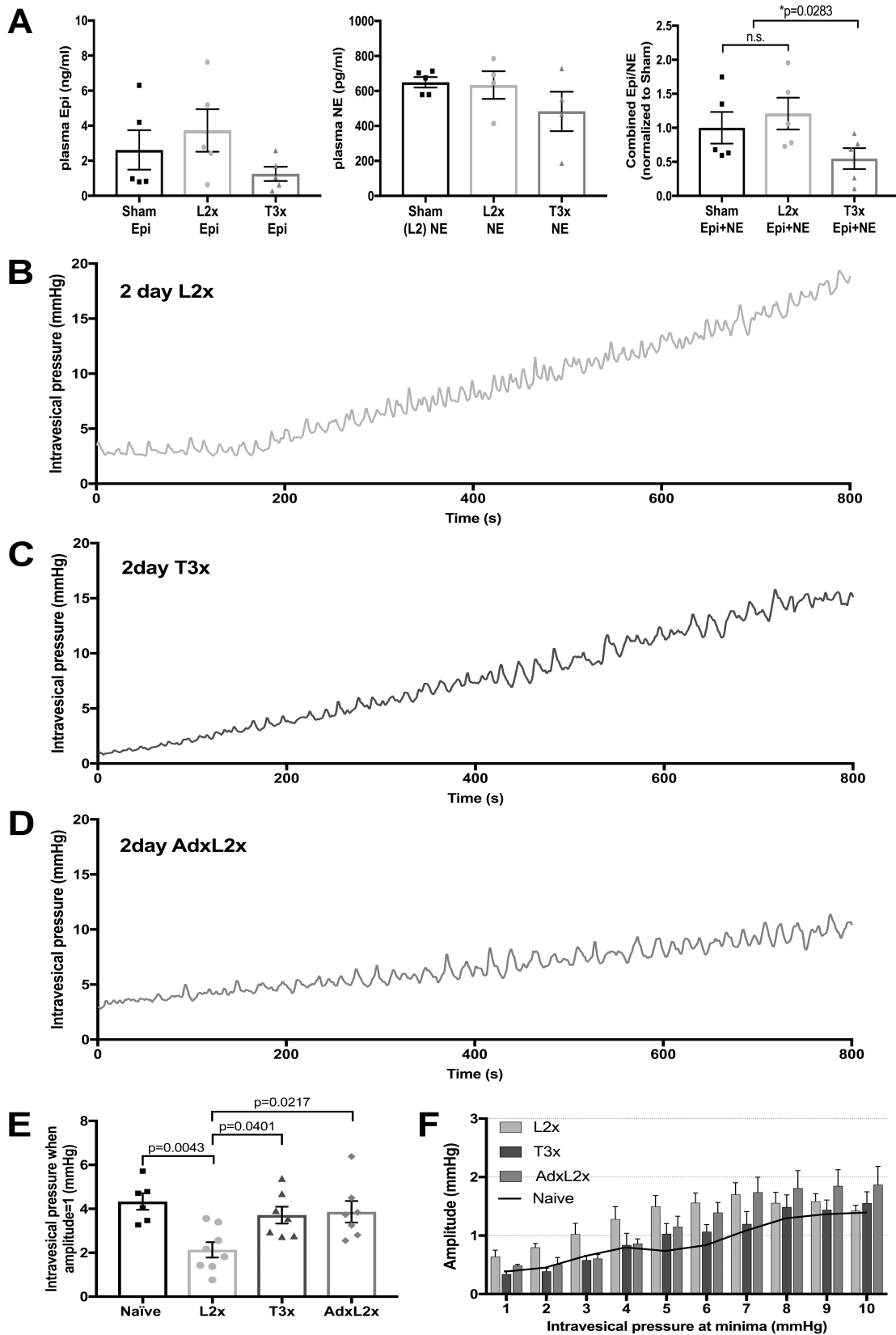


Figure 4.6 Relationship between amplitude of contractions and intravesical pressure after L2x is influenced by adrenal function

(A) Plasma concentrations of individual adrenal catecholamines were not significantly different between groups 2 days after L2x or T3x. There was no difference in overall catecholamine concentration between the two groups with intact adrenal innervation (sham and L2x), however levels of catecholamines were significantly lower in T3x animals compared to animals with intact adrenal innervation (mean \pm SEM, Welch's t-tests). (B-D) Representative traces of intravesical pressures during 100 μ l/min of saline bladder filling 2-days after (B) L2x, (C) T3x and (D) AdxL2x. (E) The intravesical pressures at which the NVC amplitudes reach 1mmHg for each injury group are plotted, amplitudes reach 1mmHg at lower pressures 2 days post-L2x compared to naïve, T3x or AdxL2x; one-way ANOVA, Tukey's multiple comparisons test, mean \pm SEM, exact p-values shown. (F) NVC amplitudes sorted into 1mmHg bins based on intravesical pressure at contraction minima (see Fig. 4.1C) show elevated amplitudes at low pressures after L2x, but not after T3x or when an adrenalectomy is performed immediately prior to the L2x (AdxL2x). Black line in (F) shows mean naïve values from Fig. 4.5E for reference.

4.5 Discussion

The development of neurogenic bladder hyperactivity that occurs in the weeks following SCI in the rat is expected and well documented.^{5,233,413} However, after L2x we saw an unexpected phenomenon of increased bladder activity, presenting as small amplitude NVCs at low pressures, in the acute time period (within two days) that was not present after T3x. Examination of both direct and indirect neural pathways led us to link this phenomenon to adrenal gland function, which is likely to be better preserved after L2x than T3x.

4.5.1 Timing of NVC changes after transection

Acutely after SCI, during the period of spinal shock when the bladder is areflexic, lower urinary tract activity is present, which is also true of acutely decentralized bladders.^{208,409} Therefore, even though the spinal cord-mediated micturition reflex is not present, bladder properties can change in a hyperacute timeframe after injury.²⁰⁷ Changes in the structure of the bladder wall occur within hours after SCI. In rats two hours after thoracic transection, uroepithelial barrier function is compromised and it shows signs of cellular breakdown that lasts up to two weeks after injury.²⁰⁷ Blocking efferent activity at the time of transection was also shown to prevent bladder epithelial disruptions, implicating efferent signaling from the cord in acute bladder dysfunction. However, the delay we see in the development of the increased bladder activity after lumbar SCI is consistent with a slower-acting mechanism, such as might be produced *via* hormonal changes.

4.5.2 Interrupting the peripheral signaling to the bladder

Rat pelvic ganglia contain both sympathetic and parasympathetic ganglionic cell bodies as well as primary afferent fibres that innervate the pelvic organs. It has been suggested that the PG could be involved in the integration of pelvic organ signaling, particularly after SCI.² We initially hypothesized that the differences seen in the L2x group was caused by changes that occur within the PG when the thoraco-lumbar preganglionics and central projections of L1/2 DRG neurons that course through the ganglia are directly damaged. This seemed to be supported by previous studies where bladder epithelial breakdown was prevented by blocking ganglionic transmission.²⁰⁷ Additionally, a recent study by Persyn *et al.* found that the at-time removal of the PG resulted in increased baseline bladder pressure and NVC amplitude. This effect did not occur with transection of the hypogastric and pelvic nerves indicating that there may be changes within the PG itself.⁴²³ However, in our experiments two days after L2x, blocking signals through the PG, either by HexBr treatment or by bilateral pelvic ganglionectomy, did not change the amplitude of the low pressure NVCs. Furthermore, two days after the bilateral removal of the PG there was no increase in NVC amplitude at low pressures. Taken together these results led us to look for an alternative signaling pathway, outside of direct neural connections, that differs between thoracic and lumbar transections.

4.5.3 Adrenal medulla innervation and function after SCI

Studies that investigate how the level of SCI affects hormone production have shown a difference in adrenal medullary production of epinephrine with high and low SCI: individuals with lower SCIs have higher levels of circulating epinephrine and norepinephrine compared to individuals with higher level injuries.^{420,421,424,425} The adrenal gland is innervated by cholinergic

preganglionic sympathetics arising from the intermediolateral column of the T1 to L1 segments in the rat spinal cord, with the majority of the preganglionics residing in T9 and the adjacent segments.³¹ Therefore, T3x eliminates the majority of the circuitry innervating the adrenal preganglionics, whereas L2 transections preserve these connections. This is supported by a recent publication by Pruss *et al.* that examined the role of adrenal function in sympathetic and immune system function after different levels of spinal cord transection. They found that mice with a high thoracic spinal cord transection had lower norepinephrine levels and poorer immune function compared to those with lumbar transections.³³ We also found higher plasma adrenal catecholamine concentrations in sham animals or those with low spinal transections, which appeared to be driven primarily by the epinephrine component. Plasma norepinephrine concentration is a function of both sympathetic nerve activity and adrenal function, and so it makes sense that the difference between low and high transection is not as evident. However, when both adrenal catecholamines are considered together, there is a clear decrease in plasma concentration in animals in which descending input to adrenal preganglionic neurons is interrupted.

A potential caveat is that capturing changes to the baseline levels of circulating catecholamines is challenging; for example, epinephrine is produced very rapidly in response to stress (two seconds) and the half-life in the blood is very short (less than 70 seconds); similarly, it is tightly regulated.^{426,427} Therefore, experimental manipulations are likely to cause rapid changes in levels of these catecholamines, increasing the inherent variability; the lower variability in T3x animals supports the idea a loss of descending adrenal control.

Notwithstanding the known difficulties in measuring plasma catecholamines, results from the

surgical removal of the adrenal gland alongside L2x clearly support the influence of adrenal signaling on bladder function after SCI.

4.5.4 Adrenergic signaling in the bladder

There is evidence for the expression of two α -adrenergic and three β -adrenergic receptor isoforms in parts of the lower urinary tract and there is ample evidence that small contractions of the bladder wall are sensitive to adrenergic signaling.^{428–430} Indeed, catecholaminergic therapies for overactive bladder generally involve antagonizing alpha receptors ($1\alpha/D$) or activating beta receptors ($\beta3$).⁴³¹ What effect circulating catecholamines have on the bladder are unknown, but it has previously been speculated that circulating epinephrine may play a role in the activation of adrenergic receptors in the bladder.⁴³⁰ Although still a matter of conjecture, at least two scenarios could account for adrenergically-mediated large low-pressure NVCs after SCI. One is that circulating adrenal epinephrine and norepinephrine act on alpha-1 receptors to stimulate contractions, or that these catecholamines stimulate beta receptors, effecting (over)relaxation and hence stretch-induced contractions *via* e.g. the urothelial mechanosensory ion channel Piezo1.^{432,433} In either case, it can be argued that it is probably not a change in plasma catecholamine concentration which underlies aberrant bladder activity following L2x (there is no evidence that relative concentration differs from sham controls, Fig. 4.6A). Rather, it is the effects of preserved adrenal control on the bladder after SCI. That is, reduced plasma catecholamines after high thoracic injuries is protective. The very large differences in bladder weights between T3x and L2x groups, and the smaller differences between sham and T3x groups supports this notion.

4.5.5 Adrenal cortex and the bladder

Stress related hormones have previously been linked to overactive bladder symptoms. Numerous studies have linked stress, anxiety and depression to lower urinary tract dysfunctions including overactive bladder.⁴³⁴ However, it is unclear whether the bladder symptoms are contributing to the stress or the other way around.⁴³⁵ Corticotropin-releasing factor (and ultimately cortisol) has been implicated in social-stress induced bladder dysfunction, including an increase in the number of neurons immunoreactive for CRF in Barrington's nucleus, an area of the brainstem involved in controlling micturition.⁴³⁶ In this study of male rats subjected to daily social stress for one week, there were distinct urodynamic functional changes including the presence of NVCs in stressed animals. However, since SCI at any level should preserve hypothalamic-pituitary function, our results argue in favour of circulating catecholamines as underlying increased low-pressure NVC activity, rather than products of the adrenal cortex.

4.5.6 Clinical Use of Norepinephrine in the Acute Management of SCI

Clinical guidelines currently recommend the augmentation of mean arterial pressure to 85-90mmHg for the first seven days after an acute spinal cord injury.⁴³⁷ This is done to maintain adequate spinal cord perfusion pressure, and is accomplished with the administration of vasopressors.⁴³⁸ No single vasopressor is universally used in the management of SCI but recent evidence suggests that norepinephrine may emerge as the optimal choice.⁴³⁹ The results presented here suggest that this systemic administration of catecholamines to thoracic or cervical spinal cord injuries could adversely impact bladder outcomes. The research presented in this chapter further highlights the importance of understanding the interdependence of individual physiological systems that are often studied independently after SCI. It is clear that blood

pressure regulation is vital in the acute time points after SCI, when individuals can be dangerously hypotensive, therefore strategies may need to be developed to block catecholamine signaling locally within the bladder.

4.5.7 Conclusions

In summary, neurogenic bladder is a significant detriment to quality of life after SCI, and those with lower injuries have poorer bladder outcomes due to vesicoureteral reflux and consequent higher chance of kidney dysfunction. In this work, we show that after lumbar transection, even at very low pressures and at acute time points, the bladder undergoes small rhythmic contractions that develop when supraspinal control of the adrenal gland remains intact. This activity develops early, and is persistent. Such ongoing activity is likely to strengthen the detrusor and thus exacerbate detrusor-sphincter dyssynergia at higher pressures and at more chronic stages. Our data suggest that targeting differences in adrenal function after SCI may impact bladder outcomes. An injury level-dependent influence on the development of dysfunction *via* peripheral mechanisms is not a new concept: the development of autonomic dysreflexia after high injuries that interrupt neural control of mesenteric arterial bed vascular tone has been linked to a number of changes in the periphery.³ The findings of this research continue to reinforce that the consequences of SCI do not arise merely from direct damage to neural circuits, but also from subsequent and systemic neurogenic and endocrine effects.

Chapter 5: General discussion

5.1 Summary and conclusions

In this dissertation, I examined transcriptional, morphological, and functional changes in the pelvic neuroviscera that occur as a consequence of complete high thoracic and lumbar spinal cord transection. My work focused on injury level dependent changes in the pelvic peripheral sensory and autonomic neurons, residing within the L6/S1 dorsal root ganglia (DRG) and pelvic ganglia (PG) respectively, and the differential effects of high and low SCI.

5.1.1 Transcriptional changes in viscerally projecting lumbosacral dorsal root ganglia after high spinal cord transection

In Chapter 2, I focused on high thoracic spinal cord injury-induced changes in the peripheral sensory and autonomic ganglia that innervate the pelvic visceral organs. Functional and morphological studies of DRG neurons have identified changes to specific subpopulation in relation to sensory subtype and target organ.^{3,4,242,243} Given that specific subpopulations of DRG neurons are affected by high thoracic transection, notably hypertrophy of TRPV1-positive nociceptors and bladder projecting neurons,^{3,4} I hypothesized that changes in gene expression would reflect growth factor signaling changes driven by pelvic peripheral target changes in accordance with the neurotrophic hypothesis. Consistent with this hypothesis, differential gene expression analysis of RNA sequencing results from L6/S1 DRGs identified cell communication and growth factor signaling pathways as differentially affected by injury. However, the majority of growth factor signaling pathways identified in the analysis were downregulated with injury. This is in contrast to the neurotrophic hypothesis, which posits that increased target tissue,

exemplified by the hypertrophy of the bladder after SCI, results in increased production of neurotrophic factors that influence adult neuron phenotype.^{289,290} This analysis gives cause to re-examine the classical interpretation of the neurotrophic hypothesis with regards to the response to SCI of sensory neurons that innervate the pelvic viscera.

5.1.2 Morphological and transcriptional changes within pelvic ganglia after spinal cord transection

The pelvic ganglia contain the sympathetic and parasympathetic neurons responsible for the autonomic innervation of the pelvic viscera.^{2,99} Yet, despite the numerous functional and morphological changes that occur within the pelvic viscera and DRG neurons upon spinal cord transection,^{3,4,9} few studies have examined the impact of SCI on PG neurons.^{4,273} A major aim of both Chapters 2 and 3 was to examine the transcriptional and morphological responses of PG neurons to different levels of SCI. Based on hypertrophy of bladder projecting sensory neurons after SCI and the classical interpretations of the neurotrophic hypothesis,^{4,289,290} I hypothesized that the PG neurons would hypertrophy after SCI. However, in Chapter 2, I found that after T3-transection the TH-positive, sympathetic neuron population of the PG atrophied. This unexpected result led me to ask whether a lower injury model, which in humans results in greater bladder deficits,^{146,380} might reveal more standard neuron-target interactions resulting from target hypertrophy. Despite a significant increase in bladder weights chronically, lumbar transection did not result in sustained neuronal hypertrophy of PG neurons. Furthermore, decreased TH and VIP mRNA expression in the PG after L2x was consistent with decreases seen after T3x. Though there is clear bladder hypertrophy after SCI, like in BOO, the autonomic neurons of the PG do not hypertrophy as expected through the simple application of the neurotrophic hypothesis,

revealing a non-standard relationship between target and neurons after SCI. Further investigation is required to determine the signaling between target and neuron that underlies these unexpected changes within the pelvic ganglia with different levels of spinal cord transection.

5.1.3 Activity differences in the bladder with high thoracic and lumbar spinal cord transection

When examining bladder activity after high thoracic and lumbar spinal cord transection, it became readily apparent that there was augmented bladder activity at low pressures after lumbar transection. Lumbar transection directly injures a subpopulation of sensory and sympathetic neurons that innervate the pelvic viscera, which includes the bladder.^{53,440} Therefore, I hypothesized that differential damage to these neurons was responsible for increased bladder activity at low pressures. To test this hypothesis, I examined how blocking signaling through the PG, which contains both autonomic neurons as well as the majority of bladder projecting sensory fibres, affects the manifestation of increased low-pressure activity. Contrary to my original hypothesis, I found no difference in the low-amplitude contractions in the lumbar transected rats when signalling was blocked via drugs or removal of the PG.

This prompted me to look for mechanisms outside of the direct neural pathway to the bladder that could be driving injury level differences. Recent work has identified decreased adrenal function after high spinal cord transections compared to low transections in mice.³³ This led me to hypothesize that differences in adrenal function after lumbar and high thoracic spinal cord transection contribute to augmented bladder activity. I examined this hypothesis in two ways, first by measuring the circulating levels of catecholamines and second, by performing an adrenalectomy at the time of L2-transection. Examination of the combined catecholamine load at

two days post-injury revealed lower levels after T3x compared to L2x. However, since circulating catecholamine levels are difficult to measure reliably, I performed a follow-up experiment by removing the adrenal glands from the rats immediately prior to the lumbar transection. In these animals, the pattern of low pressure bladder activity more closely matched the pattern seen in T3x animals. Therefore, preserved adrenal function after lumbar transection results in augmented bladder activity at low intravesical pressures, which may contribute to longer term negative outcomes in bladder function. These results indicate that circulating catecholamines may have a detrimental effect on the bladder after SCI.

5.2 Limitations and areas of future research

5.2.1 Animal models of human disease

The physiology of the rat is strikingly similar to humans and many of the classic dysfunctions present in humans after SCI are recapitulated in the rat model, including both the development of autonomic dysreflexia and lower urinary tract dysfunction.^{52,441} However, by their nature, models are a simplified and imperfect representations. This is exemplified in the pelvic ganglion of the male rat; the properties that make this ganglion convenient for study and manipulation also sets it apart from humans.² The anatomical arrangement of rat PG neurons into bilateral ganglia may provide greater opportunity for interactions between these neurons compared to humans where clusters of neurons are spread out in amongst the pelvic viscera, potentially impacting the response of the neurons to denervation of themselves or their neighbors. After injury of the hypogastric or pelvic nerves, which respectively contain the preganglionic sympathetic and parasympathetic fibres, sprouts form from intact preganglionic fibres and ganglionic neurons form around denervated neurons.^{385,442} Further research is

required to determine whether this also takes place in mammals with less discrete pelvic ganglia. However, the connectivity between the neurons and their peripheral targets is similar in mammals and, as demonstrated in this thesis, this model system can provide novel insights into the interactions between the pelvic peripheral neurons and their targets. Therefore, though caution is required before directly applying the findings from rats to the humans, the convenient and unique anatomy of the rat pelvic neuroviscera provides opportunities to identify interactions that might be hard to ascertain in mammals with more complex and diffuse innervation of the pelvic organs.

5.2.2 RNA sequencing of whole tissue samples

RNA sequencing is a powerful tool for identifying patterns of gene expression changes after disease and injury. In this thesis, I chose to extract RNA from whole ganglia, which has both its benefits and drawbacks. In isolating mRNA from a whole tissue, one can potentially identify changes occurring across multiple cell types, but meaningful changes occurring in small subpopulations of cells may be lost in the heterogeneity of the sample. At steady state, when protein and mRNA levels are remaining stable over time, the amount of protein is predominantly controlled by the amount of mRNA.^{443,444} Though the condition of a rat at one month post-SCI is often considered stable, it is important to keep in mind that ongoing changes after SCI may alter mRNA stability, translational efficiency, and protein turnover, and thus impact the relationship between mRNA and protein level. Furthermore, whole tissue RNA-sequencing does not provide any information on the expression in specific cell types. To follow up on the mRNA levels the conventional approach would use western blot or ELISA to quantify protein levels, however,

immunohistochemical analysis, though only semi-quantitative, would also provide information about the localization of the proteins, which would be particularly valuable in this case.

An interesting and complementary follow-up to the tissue-based RNA sequencing performed for this thesis is the now more commonly used technique of RNA sequencing sorted or single cells. Sorting of subpopulations of DRG or PG neurons, based on neuropeptide or receptor expression profiles or on the presence of tracers from specific targets, may uncover targeted changes that may be disguised in the whole tissue analysis. This technique seems particularly attractive with the PG, where the sympathetic and parasympathetic neurons could be isolated and compared separately to identify different patterns of changing gene expression.

Parasympathetic and sympathetic neurons of the pelvic ganglion are often classified based on TH-expression (as I did in this thesis) and this could be used to sort PG neurons prior to RNA sequencing.² Gene expression changes identified in sorted neuron populations could be compared between injury groups to decrease sample heterogeneity and increase the ability to identify differential expression within these neuron subtypes. However, using TH expression to sort PG neurons potentially over simplifies the heterogeneity of the autonomic neuron population; there are subclasses within these broad categories based on neuropeptide expression and target innervation as well as neurons that do not fit this definition, the smaller population of non-adrenergic non-cholinergic neurons.^{2,445} Previous studies using single cell RNA sequencing of mouse DRG neurons identified eleven classes of sensory neurons through an method of unbiased classification, employing the same approach to individual neurons from the PG would shed light into the yet undetermined extent of complexity present in this neuron population.^{58,446} However, cell sorting and single cell RNA sequencing are not without their own drawbacks. In addition to the added cost and technical challenges of the sequencing, manipulation of tissues

outside the body has the potential to change mRNA levels as transcriptional changes can occur rapidly, requiring additional consideration during data analysis and interpretation.^{444,447} Rapid advances in methods of analysis and interpretation of RNA sequencing data, including new published alignments and updates to differential gene expression approaches, lends power to the data collected in this thesis, since the raw data can be reanalyzed and combined with new data sets as updates and additional information become available.

5.2.3 Tracking changes after injury at individual time points in neurons and targets

It is apparent in both animal and human studies that changes occurring after SCI are dynamic and ongoing and debate continues on when conditions stabilize and can be considered chronic.¹⁷⁵ The experiments in this thesis look at individual snapshots in time with different groups of animals examined at different endpoints after injury. Even though I examined multiple time points, it is not possible to construct a complete picture of the events responsible for development of differences over time without further studies. In Chapter 2, I identify a transient hypertrophy of TH-positive neurons in the PG after L2x, which is present at two weeks but no longer different from sham at one month, which demonstrates that these changes are dynamic but leaves questions about the timeline in which this effect develops and then reverts. Though it would be impractical, and potentially only minimally more informative, to perform cell size analysis, such as recursive translation, on an extensive series of time points to exactly determine the development of these changes, it would be valuable to look at relevant time points to identify potential changes in target and neuron interactions over time. At the time of tissue collection for RNA sequencing and PG cell size analysis I was unaware of the unexpected neuron-target relationships that my analyses would reveal. Therefore, the ‘target half’ of the story remains to

be investigated. Ideally, peripheral ganglia and pelvic viscera would be collected from the same animals at the different time points after high and low SCI in order to compare and correlate changes within the one population with the responses in the other. For thoroughness, full gene expression and morphological analysis could be completed, but a more practical and targeted approach would be to start by examining the specific growth factor signalling pathways identified in the analysis I performed on the PGs and DRGs after T3x, most notably NGF and BDNF.

The timeline of changes after an injury also play an important role in my final data chapter, where I focus on the early changes in bladder activity at early time points that are not often considered with regards to bladder function after SCI. The acute period after injury, while the bladder is areflexic, is not commonly studied, though my results in Chapter 4 clearly show that changes in activity are present in this acute period before the spinal mediated micturition reflex is established after SCI.^{175,208} The augmented bladder activity present at two days, but not immediately upon injury, supports the notion that the causative agent comes from outside of the direct neural pathway, however, the precise developmental timeline remains to be determined. Additionally, from the studies presented here it is unclear how the long-term bladder outcomes, including cystometric and morphological measurements, are affected in T3x, L2x, and L2xAdx animals. To address these issues, I suggest the use of telemetric bladder pressure measurements to allow for the comparison of bladder activity before and at multiple time points after injury.⁴⁴⁸ This relatively new approach may prove challenging after SCI, where there is significant remodelling of the bladder and increased chance of infection, however it would provide the opportunity to determine the timeline of the development of augmented activity as well as track its progress overtime.^{207,448,449}

The bladder is an important model for autonomic dysfunction after SCI due to the ample techniques available for measuring and quantifying function, but it by no means the only pelvic organ of significance. Based on my findings of decreased expression of VIP in PG tissue, which is associated with parasympathetic (potentially penis-projecting) neurons, it will be important to examine not just SCI-induced changes in the bladder, but also in other pelvic organs. Both sexual and bowel function are also key priorities for individuals with SCI and exploring ways to quantify changes within these organs and the neurons that innervate them are equally as important going forward.^{1,52}

5.3 Significance of findings with regards to the systemic consequences of SCI

The observation that numerous systemic consequences occur as a result of SCI is not novel and studies into the development of autonomic dysreflexia and immune suppression after high SCI have highlighted this finding over the last number of years.^{32,199,205,441,450} To focus what could be a whole body of discussion on areas relevant to the work presented in this thesis, I will limit my discussion of this broad topic to two points of interest: 1) that the patterns of changes in the pelvic neuroviscera after central injuries do not necessarily match peripheral injuries and 2) that variations in adrenal medulla signaling as a result of different levels of spinal cord transection impacts multiple body systems, including the bladder.

5.3.1 Contrasting changes in PG and bladder after peripheral and central injuries

The work presented in Chapters 2 and 3 identify interactions after SCI between peripheral neurons and their pelvic targets that differ from what is observed after peripheral

injuries. One of the most common forms of peripherally mediated lower urinary tract dysfunction is caused by bladder outlet obstruction, which occurs commonly in older men with enlarged prostates. The increased force required to empty the bladder with increased resistance results in increased bladder sizes, increased NGF production, and hypertrophy of bladder projecting autonomic and sensory neurons.^{283,377,378} Hypertrophied target tissue resulting in increased production of growth factors and subsequent neuron hypertrophy fits in nicely with the neurotrophic hypothesis. It is attractive to assume that this relationship also occurs after SCI. However, whether growth factors, and in particular NGF, increase in the bladder after SCI is unclear.^{226,270,451-453} The work presented in this thesis and in a number of previous studies support a potential decrease in NGF in the bladder after SCI.^{226,398,451} This is not necessarily in contrast to evidence from NGF immunoneutralization studies, which found that NGF is involved in the plasticity of the micturition pathway at the level of the spinal cord, but suggests that NGF's role may not extend to the peripheral organs.^{180,454}

These findings lead to the question of why peripheral injuries leading to bladder hypertrophy, such as bladder outlet obstruction and peripheral nerve injury, result in increased bladder NGF production but spinal cord transection, which also results in bladder hypertrophy, does not. One potentially interesting difference between the BOO and SCI is in regard to bladder denervation after injury. Inflammation and stretch induced hypoxia injury caused by BOO results in decreased nerve density in the bladder of humans.^{455,456} However, it is unclear whether this occurs in the bladders of rats and there are conflicting results on whether the density of nerves in the bladder also change after SCI.^{381,457} Therefore, an important follow-up experiment would include the characterization of changes in the distribution and density of both sensory and autonomic nerve fibers in the bladder after both high and low SCI. Changes in the fibres within

the bladder and other pelvic organs could underlie some of the differences in the cell body responses seen with different injuries.

5.3.2 Alterations in adrenal function due to injury level has multiple systemic consequences

Dysfunction of the sympathetic nervous system after high SCI has drawn significant attention over the years for its role in both the development of autonomic dysreflexia and immune suppression.^{199,441,458} Autonomic dysreflexia develops in the days and weeks following SCIs that eliminate autonomic supply to the splanchnic bed (typically considered to be autonomically complete injuries at T6 and above). Though there are a number of factors identified as contributing to the development and severity of AD, the manifestation is a surge of sympathetic signaling induced by sensory stimulation from below the level of the injury that triggers a pressor response, elevating the blood pressure of the individual to sometimes life-threatening levels.²¹⁹ This sympathetic surge has recently been linked to immune dysfunction present after high SCI. The majority of the attention with regards to immune suppression has centred around disruption to the hypothalamic-pituitary axis and increased activity of sympathetic neurons releasing norepinephrine directly into lymphoid tissue, both of which contribute to lymphocyte apoptosis.^{32,205,450}

However, this research has very recently been extended to include a role for circulating catecholamines and the adrenal gland, which were previously discounted due to the transient nature of catecholamines in the blood.^{32,33,450,459} A study contrasting immune function after different levels of spinal cord transection in mice found a graded decline in catecholamine production by the adrenal medulla and concurrent overproduction of glucocorticoids by the

adrenal cortex, mediated by an aberrant sympathetic-neuroendocrine adrenal reflex.³³ Consistent with these findings, I identified a decline in circulating catecholamine expression after T3x compared to L2x. Adding an additional experimental group of T9x injured animals to the findings in this thesis could determine whether there was a similar graded response by the bladder to injury level and adrenal function.

In contrast to findings in the immune system, where alterations in adrenal function after high thoracic transection result in functional decline, the combination of preserved sympathetic drive to the adrenal gland alongside disruption to the central micturition pathways after lumbar transection promotes aberrant activity in the bladder. This finding may be relevant in the clinical setting, since catecholamines are commonly used to treat hypotension acutely after SCI.^{437,438} An important and clinically relevant follow-up study to the ones presented in Chapter 4 would be to administer catecholamines after high thoracic transection and measure the effect on bladder activity at acute and chronic time points.

The mechanisms underlying adrenal mediated bladder activity after lumbar transection require further elucidation. Both alpha- and beta-adrenergic receptors (α -ARs, β -ARs) are expressed throughout the micturition pathway and respond differently to ligand binding, with norepinephrine having a higher affinity for α -ARs than β -ARs. In the bladder α -ARs are predominantly expressed in the trigone and urethra and result in smooth muscle contraction and β -ARs are expressed in the dome and result in relaxation.⁴⁶⁰ In this way sympathetic innervation of the bladder promotes urine storage.⁵³ The role circulating catecholamines play in bladder function and how those roles might change with spinal cord injury are unknown, but based on the results from Chapter 4 it appears that, *via* some unknown mechanism, lower plasma catecholamine levels have protective effects.

With the differential effects of injury level on the TH-positive, sympathetic PG neurons after SCI, it would also be interesting to investigate whether catecholamine levels influence PG neuron character. The expression of adrenergic receptors in PG neurons has not been established, however, previous studies have demonstrated the expression of adrenergic receptors in sympathetic and sensory ganglia.⁴⁶¹⁻⁴⁶³ Furthermore, RNA sequencing data collected for this thesis showed expression of both α ARs and β ARs in PG tissue. However, since the RNA-sequencing was performed on whole tissue, additional experiments are required to determine whether the ganglionic neurons themselves express ARs. Immunohistochemical analysis of the localization of AR subtypes is challenging due to specificity issues with available antibodies, however, previously mentioned single cell RNA sequencing experiments could also shed light on this issue. The expression of adrenergic receptors by PG neurons would open up an avenue of exploration with regards to the role of circulating catecholamines on peripheral sympathetic neurons' response to SCI.

Changes in the levels of norepinephrine and epinephrine are known to shift immune cell phenotype based on differences in the affinities of different adrenergic receptor subtypes to catecholamines.⁴⁶⁴ There is also the possibility that the subtypes of receptors change with injury. Analysis of receptor subtype in the bladder could be performed with different injury levels to determine if this occurs. Even if the subtype balance does not change, the different receptor subtypes have different affinities for the different catecholamines and an imbalance caused by dysregulated adrenal function may impact the receptors that are activated.

References

1. Anderson, K.D. (2004). Targeting recovery: priorities of the spinal cord-injured population. *J. Neurotrauma* 21, 1371–1383.
2. Keast, J.R. (1999). Unusual autonomic ganglia: connections, chemistry, and plasticity of pelvic ganglia. *Int. Rev. Cytol.* 193, 1–69.
3. Ramer, L.M., van Stolk, A.P., Inskip, J.A., Ramer, M.S., and Krassioukov, A. V. (2012). Plasticity of TRPV1-Expressing Sensory Neurons Mediating Autonomic Dysreflexia Following Spinal Cord Injury. *Front. Physiol.* 3.
4. Kruse, M.N., Bray, L.A., and de Groat, W.C. (1995). Influence of spinal cord injury on the morphology of bladder afferent and efferent neurons. *J. Auton. Nerv. Syst.* 54, 215–224.
5. Yoshimura, N., and de Groat, W.C. (1997). Neural control of the lower urinary tract. *Int. J. Urol.* 4, 111–25.
6. Chai, T.C., and Steers, W.D. (1996). Neurophysiology of micturition and continence. *Urol. Clin. North Am.* 23, 221–236.
7. Yoshimura, N. (1999). Bladder afferent pathway and spinal cord injury: Possible mechanisms inducing hyperreflexia of the urinary bladder. *Prog. Neurobiol.* 57, 583–606.
8. de Groat, W.C. (2006). Integrative control of the lower urinary tract: preclinical perspective. *Br. J. Pharmacol.* 147, S25–S40.
9. Craggs, M.D., Balasubramaniam, A.V., Chung, E.A.L., and Emmanuel, A. V. (2006). Aberrant reflexes and function of the pelvic organs following spinal cord injury in man. *Auton. Neurosci.* 126–127, 355–370.
10. Stiens, S.A., Bergman, S.B., and Goetz, L.L. (1997). Neurogenic bowel dysfunction after

- spinal cord injury: clinical evaluation and rehabilitative management. *Arch. Phys. Med. Rehabil.* 78, S86-102.
11. Jänig, W., and McLachlan, E.M. (1987). Organization of lumbar spinal outflow to distal colon and pelvic organs. *Physiol. Rev.* 67, 1332–404.
 12. McKenna, K.E. (2001). Neural circuitry involved in sexual function. *J. Spinal Cord Med.* 24, 148–54.
 13. Jänig, W. (2006). *The integrative action of the autonomic nervous system : neurobiology of homeostasis.* Cambridge University Press, 610 p.
 14. Gibbins, I. (2013). Functional organization of autonomic neural pathways. *Organogenesis* 9, 169–175.
 15. Langley, J.N. (1921). *The autonomic nervous system.* Cambridge, England: W. Heffer & Sons.
 16. Goyal, R.K., and Hirano, I. (1996). The enteric nervous system. *N. Engl. J. Med.* 334, 1106–15.
 17. Boeckxstaens, G.E. (2002). Understanding and controlling the enteric nervous system. *Best Pract. Res. Clin. Gastroenterol.* 16, 1013–23.
 18. Furness, J.B., Callaghan, B.P., Rivera, L.R., and Cho, H.-J. (2014). The enteric nervous system and gastrointestinal innervation: integrated local and central control. *Adv. Exp. Med. Biol.* 817, 39–71.
 19. Banrezes, B., Andrey, P., Maschino, E., Schirar, A., Peytevin, J., Rampin, O., and Maurin, Y. (2002). Spatial segregation within the sacral parasympathetic nucleus of neurons innervating the bladder or the penis of the rat as revealed by three-dimensional reconstruction. *Neuroscience* 115, 97–109.

20. Epinosa-Medina, I., Saha, O., Boismoreau, F., Chettouh, Z., Rossi, F., Richardson, W.D., and Brunet, J.-F. (2016). The sacral autonomic outflow is sympathetic. *Science* (80-). 354, 893–897.
21. Henry, J.L., and Calaresu, F.R. (1972). Topography and numerical distribution of neurons of the thoraco-lumbar intermediolateral nucleus in the cat. *J. Comp. Neurol.* 144, 205–14.
22. Pyner, S., and Coote, J.H. (1994). Evidence that sympathetic preganglionic neurones are arranged in target-specific columns in the thoracic spinal cord of the rat. *J. Comp. Neurol.* 342, 15–22.
23. Amendt, K., Czachurski, J., Dembowski, K., and Seller, H. (1979). Bulbospinal projections to the intermediolateral cell column: a neuroanatomical study. *J. Auton. Nerv. Syst.* 1, 103–7.
24. Adameyko, I. (2016). Neural circuitry gets rewired. *Science* (80-). 354, 833–834.
25. Hoehmann, C.L., and Cuoco, J.A. (2017). Landmark Article Transforms Traditional View of the Autonomic Nervous System. *J. Am. Osteopath. Assoc.* 117, 72.
26. Jänig, W., Keast, J.R., McLachlan, E.M., Neuhuber, W.L., and Southard-Smith, M. (2017). Renaming all spinal autonomic outflows as sympathetic is a mistake. *Auton. Neurosci.* 206, 60–62.
27. Neuhuber, W., Mclachlan, E., and Jänig, W. (2017). The Sacral Autonomic Outflow Is Spinal, but Not “Sympathetic.” *Anat. Rec.* 300, 1369–1370.
28. McLachlan, E.M. (2003). Transmission of signals through sympathetic ganglia-- modulation, integration or simply distribution? *Acta Physiol. Scand.* 177, 227–35.
29. Kimura, H., and Tooyama, I. (1998). [Chemical neuroanatomy of cholinergic neurons]. *Rinsho Shinkeigaku* 38, 1005–8.

30. Keast, J.R. (1999). Unusual autonomic ganglia: connections, chemistry, and plasticity of pelvic ganglia. *Int. Rev. Cytol.* 193, 1–69.
31. Parker, T.L., Kesse, W.K., Mohamed, A.A., and Afework, M. (1993). The innervation of the mammalian adrenal gland. *J. Anat.* 183 (Pt 2), 265–76.
32. Lucin, K.M., Sanders, V.M., and Popovich, P.G. (2009). Stress hormones collaborate to induce lymphocyte apoptosis after high level spinal cord injury. *J. Neurochem.* 110, 1409–1421.
33. Prüss, H., Tedeschi, A., Thiriot, A., Lynch, L., Loughhead, S.M., Stutte, S., Mazo, I.B., Kopp, M.A., Brommer, B., Blex, C., Geurtz, L.-C., Liebscher, T., Niedeggen, A., Dirnagl, U., Bradke, F., Volz, M.S., DeVivo, M.J., Chen, Y., von Andrian, U.H., and Schwab, J.M. (2017). Spinal cord injury-induced immunodeficiency is mediated by a sympathetic-neuroendocrine adrenal reflex. *Nat. Neurosci.* 20, 1549–1559.
34. Keast, J.R. (2006). Plasticity of Pelvic Autonomic Ganglia and Urogenital Innervation., in: *International Review of Cytology*. pps. 141–208.
35. Baron, R., and Jänig, W. (1991). Afferent and sympathetic neurons projecting into lumbar visceral nerves of the male rat. *J. Comp. Neurol.* 314, 429–36.
36. Keast, J.R., and De Groat, W.C. (1992). Segmental distribution and peptide content of primary afferent neurons innervating the urogenital organs and colon of male rats. *J. Comp. Neurol.* 319, 615–23.
37. Christianson, J.A., Bielefeldt, K., Altier, C., Cenac, N., Davis, B.M., Gebhart, G.F., High, K.W., Kollarik, M., Randich, A., Udem, B., and Vergnolle, N. (2009). Development, plasticity and modulation of visceral afferents. *Brain Res. Rev.* 60, 171–186.
38. Vera, P.L., and Nadelhaft, I. (1992). Afferent and sympathetic innervation of the dome

- and the base of the urinary bladder of the female rat. *Brain Res. Bull.* 29, 651–8.
39. Yoshimura, N., Seki, S., Erickson, K.A., Erickson, V.L., Hancellor, M.B., and de Groat, W.C. (2003). Histological and electrical properties of rat dorsal root ganglion neurons innervating the lower urinary tract. *J. Neurosci.* 23, 4355–61.
 40. Cruz, Y., Zempoalteca, R., Angelica Lucio, R., Pacheco, P., Hudson, R., and Martínez-Gómez, M. (2004). Pattern of sensory innervation of the perineal skin in the female rat. *Brain Res.* 1024, 97–103.
 41. Devor, M. (1999). Unexplained peculiarities of the dorsal root ganglion. *Pain Suppl* 6, S27-35.
 42. de Groat, W.C., and Yoshimura, N. (2010). Changes in afferent activity after spinal cord injury. *Neurourol Urodyn* 29, 63–76.
 43. Lynn, P.A., and Blackshaw, L.A. (1999). In vitro recordings of afferent fibres with receptive fields in the serosa, muscle and mucosa of rat colon. *J. Physiol.* 518, 271–82.
 44. Sengupta, J.N., and Gebhart, G.F. (1994). Characterization of mechanosensitive pelvic nerve afferent fibers innervating the colon of the rat. *J. Neurophysiol.* 71, 2046–60.
 45. Sengupta, J.N., and Gebhart, G.F. (1994). Mechanosensitive properties of pelvic nerve afferent fibers innervating the urinary bladder of the rat. *J. Neurophysiol.* 72, 2420–30.
 46. Gebhart, G.F., Bielefeldt, K., Gebhart, G.F., and Bielefeldt, K. (2016). Physiology of Visceral Pain., in: *Comprehensive Physiology*. Hoboken, NJ, USA: John Wiley & Sons, Inc., pps. 1609–1633.
 47. Drake, M.J., Fowler, C.J., Griffiths, D., Mayer, E., Paton, J.F.R., and Birdier, L. (2010). Neural control of the lower urinary and gastrointestinal tracts: Supraspinal CNS mechanisms. *Neurourol. Urodyn.* 29, 119–127.

48. Meston, C.M., and Frohlich, P.F. (2000). The neurobiology of sexual function. *Arch. Gen. Psychiatry* 57, 1012–30.
49. Shah, A.P., Mevcha, A., Wilby, D., Alatsatianos, A., Hardman, J.C., Jacques, S., and Wilton, J.C. (2014). Continence and micturition: An anatomical basis. *Clin. Anat.* 27, 1275–1283.
50. Nadelhaft, I., Vera, P.L., Card, J.P., and Miselis, R.R. (1992). Central nervous system neurons labelled following the injection of pseudorabies virus into the rat urinary bladder. *Neurosci. Lett.* 143, 271–4.
51. Keast, J.R., Booth, A.M., and de Groat, W.C. (1989). Distribution of neurons in the major pelvic ganglion of the rat which supply the bladder, colon or penis. *Cell Tissue Res.* 256, 105–112.
52. Inskip, J.A., Ramer, L.M., Ramer, M.S., and Krassioukov, A. V. (2008). Autonomic assessment of animals with spinal cord injury: tools, techniques and translation. *Spinal Cord* 47, 2–35.
53. Fowler, C.J., Griffiths, D., and de Groat, W.C. (2008). The neural control of micturition. *Nat. Rev. Neurosci.* 9, 453–66.
54. Fry, C.H., Ikeda, Y., Harvey, R., Wu, C., and Sui, G.P. (2004). Control of bladder function by peripheral nerves: Avenues for novel drug targets., in: *Urology*. pps. 24–31.
55. Gibbins, I.L., Morris, J.L., Furness, J.B., and Costa, M. (1987). Chemical coding of autonomic neurons. *Exp Brain Res Ser.* 16, 23–27.
56. Costa, M., Furness, J.B., and Gibbins, I.L. (1986). Chemical coding of enteric neurons. *Prog. Brain Res.* 68, 217–239.
57. Furness, J.B., Morris, J.L., Gibbins, I.L., and Costa, M. (1989). Chemical coding of

- neurons and plurichemical transmission. *Annu. Rev. Pharmacol. Toxicol.* 29, 289–306.
58. Usoskin, D., Furlan, A., Islam, S., Abdo, H., Lönnnerberg, P., Lou, D., Hjerling-Leffler, J., Haeggström, J., Kharchenko, O., Kharchenko, P. V, Linnarsson, S., and Ernfors, P. (2015). Unbiased classification of sensory neuron types by large-scale single-cell RNA sequencing. *Nat. Neurosci.* 18, 145–153.
59. Marmigère, F., and Ernfors, P. (2007). Specification and connectivity of neuronal subtypes in the sensory lineage. *Nat. Rev. Neurosci.* 8, 114–127.
60. de Moraes, E.R., Kushmerick, C., and Naves, L.A. (2017). Morphological and functional diversity of first-order somatosensory neurons. *Biophys. Rev.* 9, 847–856.
61. Delmas, P., Hao, J., and Rodat-Despoix, L. (2011). Molecular mechanisms of mechanotransduction in mammalian sensory neurons. *Nat. Rev. Neurosci.* 12, 139–153.
62. Dubin, A.E., and Patapoutian, A. (2010). Nociceptors: the sensors of the pain pathway. *J. Clin. Invest.* 120, 3760–3772.
63. Snider, W.D., and McMahon, S.B. (1998). Tackling pain at the source: new ideas about nociceptors. *Neuron* 20, 629–32.
64. Yoshimura, N., Erdman, S.L., Snider, M.W., and de Groat, W.C. (1998). Effects of spinal cord injury on neurofilament immunoreactivity and capsaicin sensitivity in rat dorsal root ganglion neurons innervating the urinary bladder. *Neuroscience* 83, 633–43.
65. Hayashi, T., Kondo, T., Ishimatsu, M., Yamada, S., Nakamura, K., Matsuoka, K., and Akasu, T. (2009). Expression of the TRPM8-immunoreactivity in dorsal root ganglion neurons innervating the rat urinary bladder. *Neurosci. Res.* 65, 245–251.
66. Michaelis, M., Häbler, H.J., and Jäenig, W. (1996). Silent afferents: a separate class of primary afferents? *Clin. Exp. Pharmacol. Physiol.* 23, 99–105.

67. Mitsui, T., Kakizaki, H., Matsuura, S., Ameda, K., Yoshioka, M., and Koyanagi, T. (2001). Afferent Fibers of the Hypogastric Nerves Are Involved in the Facilitating Effects of Chemical Bladder Irritation in Rats. *J. Neurophysiol.* 86, 2276–2284.
68. Bennett, H.L., Gustafsson, J.A., and Keast, J.R. (2003). Estrogen receptor expression in lumbosacral dorsal root ganglion cells innervating the female rat urinary bladder. *Auton. Neurosci.* 105, 90–100.
69. Keast, J.R., Smith-Anttila, C.J.A., and Osborne, P.B. (2015). Developing a functional urinary bladder: a neuronal context. *Front. Cell Dev. Biol.* 3, 53.
70. Forrest, S.L., Osborne, P.B., and Keast, J.R. (2013). Characterization of bladder sensory neurons in the context of myelination, receptors for pain modulators, and acute responses to bladder inflammation. *Front. Neurosci.* 7, 206.
71. Zhong, Y., Banning, A.S., Cockayne, D.A., Ford, A.P.D.W., Burnstock, G., and McMahon, S.B. (2003). Bladder and cutaneous sensory neurons of the rat express different functional P2X receptors. *Neuroscience* 120, 667–75.
72. Cruz, C.D., and Cruz, F. (2011). Spinal Cord Injury and Bladder Dysfunction: New Ideas about an Old Problem. *Sci. World J.* 11, 214–234.
73. Andersson, K.-E. (2015). Purinergic signalling in the urinary bladder. *Auton. Neurosci.* 191, 78–81.
74. Birder, L.A., Nakamura, Y., Kiss, S., Nealen, M.L., Barrick, S., Kanai, A.J., Wang, E., Ruiz, G., de Groat, W.C., Apodaca, G., Watkins, S., and Caterina, M.J. (2002). Altered urinary bladder function in mice lacking the vanilloid receptor TRPV1. *Nat. Neurosci.* 5, 856–860.
75. Cockayne, D.A., Hamilton, S.G., Zhu, Q.-M., Dunn, P.M., Zhong, Y., Novakovic, S.,

- Malmberg, A.B., Cain, G., Berson, A., Kassotakis, L., Hedley, L., Lachnit, W.G., Burnstock, G., McMahon, S.B., and Ford, A.P.D.W. (2000). Urinary bladder hyporeflexia and reduced pain-related behaviour in P2X₃-deficient mice. *Nature* 407, 1011–1015.
76. Apostolidis, A., Popat, R., Yiangou, Y., Cockayne, D., Ford, A.P.D.W., Davis, J.B., Dasgupta, P., Fowler, C.J., and Anand, P. (2005). Decreased sensory receptors P2X₃ and TRPV1 in suburothelial nerve fibers following intradetrusor injections of botulinum toxin for human detrusor overactivity. *J. Urol.* 174, 977–983.
77. Holzer, P., and Maggi, C.A. (1998). Dissociation of dorsal root ganglion neurons into afferent and efferent-like neurons. *Neuroscience* 86, 389–98.
78. Maggi, C.A. (1990). The dual function of capsaicin-sensitive sensory nerves in the bladder and urethra., in: *Neurobiology of Incontinence*. pps. 77–90.
79. Cuello, A.C. (1987). Peptides as neuromodulators in primary sensory neurons. *Neuropharmacology* 26, 971–9.
80. Lazzeri, M. (2006). The Physiological Function of the Urothelium – More than a Simple Barrier. *Urol. Int.* 76, 289–295.
81. de Groat, W.C. (2013). Highlights in basic autonomic neuroscience: Contribution of the urothelium to sensory mechanisms in the urinary bladder. *Auton. Neurosci.* 177, 67–71.
82. Merrill, L., Gonzalez, E.J., Girard, B.M., and Vizzard, M.A. (2016). Receptors, channels, and signalling in the urothelial sensory system in the bladder. *Nat. Rev. Urol.* 13, 193–204.
83. Birder, L.A., Wolf-Johnston, A.S., Chib, M.K., Buffington, C.A., Roppolo, J.R., and Hanna-Mitchell, A.T. (2010). Beyond neurons: Involvement of urothelial and glial cells in bladder function. *Neurourol. Urodyn.* 29, 88–96.

84. Purinton, P.T., Fletcher, T.F., and Bradley, W.E. (1973). Gross and light microscopic features of the pelvic plexus in the rat. *Anat. Rec.* 175, 697–705.
85. Greenwood, D., Coggeshall, R.E., and Hulsebosch, C.E. (1985). Sexual dimorphism in the numbers of neurons in the pelvic ganglia of adult rats. *Brain Res.* 340, 160–2.
86. Dail, W.G. (1993). Autonomic innervation of male reproductive genitalia. *Nerv. Control Urogenit. Syst.* Harwood Acad. Publ. , 69–101.
87. Nadelhaft, I., and McKenna, K.E. (1987). Sexual dimorphism in sympathetic preganglionic neurons of the rat hypogastric nerve. *J. Comp. Neurol.* 256, 308–15.
88. Langley, J.N., and Anderson, H.K. (1896). The Innervation of the Pelvic and adjoining Viscera. *J. Physiol.* 20, 372–406.
89. Woźniak, W., and Skowrońska, U. (1967). Comparative anatomy of pelvic plexus in cat, dog, rabbit, macaque and man. *Anat. Anz.* 120, 457–73.
90. Perry, W.L.M., and Talesnik, J. (1953). The role of acetylcholine in synaptic transmission at parasympathetic ganglia. *J. Physiol.* 119, 455–69.
91. von Euler, U.S. (1951). Hormones of the sympathetic nervous system and the adrenal medulla. *Br. Med. J.* 1, 105–8.
92. Dail Jr, W.G., Evan Jr, A.P., and Eason, H.R. (1975). The major ganglion in the pelvic plexus of the male rat. *Cell Tissue Res.* 159, 49–62.
93. Keast, J.R., and de Groat, W.C. (1989). Immunohistochemical characterization of pelvic neurons which project to the bladder, colon, or penis in rats. *J. Comp. Neurol.* 288, 387–400.
94. Keast, J.R., Luckensmeyer, G.B., and Schemann, M. (1995). All pelvic neurons in male rats contain immunoreactivity for the synthetic enzymes of either noradrenaline or

- acetylcholine. *Neurosci. Lett.* 196, 209–12.
95. Burnstock, G. (2013). Cotransmission in the autonomic nervous system., in: *Handbook of Clinical Neurology*. pps. 23–35.
 96. Nadelhaft, I. (2003). Cholinergic axons in the rat prostate and neurons in the pelvic ganglion. *Brain Res.* 989, 52–57.
 97. Rauchenwald, M., Steers, W.D., and Desjardins, C. (1995). Efferent innervation of the rat testis. *Biol. Reprod.* 52, 1136–1143.
 98. Dail, W.G., Moll, M.A., and Weber, K. (1983). Localization of vasoactive intestinal polypeptide in penile erectile tissue and in the major pelvic ganglion of the rat. *Neuroscience* 10, 1379–86.
 99. Dail, W.G. (1996). The pelvic plexus: innervation of pelvic and extrapelvic visceral tissues. *Microsc. Res. Tech.* 35, 95–106.
 100. Cruz, C.D. (2014). Neurotrophins in bladder function: What do we know and where do we go from here? *Neurourol. Urodyn.* 33, 39–45.
 101. Klinger, M.B., and Vizzard, M.A. (2008). Role of p75NTR in female rat urinary bladder with cyclophosphamide-induced cystitis. *AJP Ren. Physiol.* 295, F1778–F1789.
 102. Anderson, C.R., Penkethman, S.L., Bergner, A.J., McAllen, R.M., and Murphy, S.M. (2002). Control of postganglionic neurone phenotype by the rat pineal gland. *Neuroscience* 109, 329–337.
 103. Murphy, S.M., McAllen, R., Campbell, G.D., Howe, P.R., and Anderson, C.R. (2003). Re-establishment of neurochemical coding of preganglionic neurons innervating transplanted targets. *Neuroscience* 117, 347–60.
 104. Dail, W.G., and Dziurzynski, R. (1985). Substance P immunoreactivity in the major pelvic

- ganglion of the rat. *Anat. Rec.* 212, 103–109.
105. Tompkins, J.D., Girard, B.M., Vizzard, M.A., and Parsons, R.L. (2010). VIP and PACAP Effects on Mouse Major Pelvic Ganglia Neurons. *J. Mol. Neurosci.* 42, 390–396.
 106. Anand, P., Ghatei, M.A., Christofides, N.D., Blank, M.A., McGregor, G.P., Morrison, J.F., Scaravilli, F., and Bloom, S.R. (1991). Differential neuropeptide expression after visceral and somatic nerve injury in the cat and rat. *Neurosci. Lett.* 128, 57–60.
 107. Benarroch, E.E. (1994). Neuropeptides in the sympathetic system: presence, plasticity, modulation, and implications. *Ann. Neurol.* 36, 6–13.
 108. Rao, M.S., Sun, Y., Vaidyanathan, U., Landis, S.C., and Zigmond, R.E. (1993). Regulation of substance P is similar to that of vasoactive intestinal peptide after axotomy or explantation of the rat superior cervical ganglion. *J. Neurobiol.* 24, 571–580.
 109. Boeshore, K.L., Schreiber, R.C., Vaccariello, S.A., Sachs, H.H., Salazar, R., Lee, J., Ratan, R.R., Leahy, P., and Zigmond, R.E. (2004). Novel changes in gene expression following axotomy of a sympathetic ganglion: A microarray analysis. *J. Neurobiol.* 59, 216–235.
 110. Wang, L., Mongera, A., Bonanomi, D., Cyganek, L., Pfaff, S.L., Nüsslein-Volhard, C., and Marquardt, T. (2014). A conserved axon type hierarchy governing peripheral nerve assembly. *Development* 141, 1875–83.
 111. Papka, R.E. (1990). Some nerve endings in the rat pelvic paracervical autonomic ganglia and varicosities in the uterus contain calcitonin gene-related peptide and originate from dorsal root ganglia. *Neuroscience* 39, 459–70.
 112. McLachlan, E.M., Jänig, W., Devor, M., and Michaelis, M. (1993). Peripheral nerve injury triggers noradrenergic sprouting within dorsal root ganglia. *Nature* 363, 543–546.

113. Ramer, M.S., and Bisby, M.A. (1997). Rapid sprouting of sympathetic axons in dorsal root ganglia of rats with a chronic constriction injury. *Pain* 70, 237–44.
114. Ramer, M.S., and Bisby, M.A. (1998). Normal and injury-induced sympathetic innervation of rat dorsal root ganglia increases with age. *J. Comp. Neurol.* 394, 38–47.
115. Saper, C.B. (2002). The Central Autonomic Nervous System: Conscious Visceral Perception and Autonomic Pattern Generation. *Annu. Rev. Neurosci.* 25, 433–469.
116. Craig, A.D. (2003). Interoception: the sense of the physiological condition of the body. *Curr. Opin. Neurobiol.* 13, 500–5.
117. Basbaum, A.I., Bautista, D.M., Scherrer, G., and Julius, D. (2009). Cellular and Molecular Mechanisms of Pain. *Cell* 139, 267–284.
118. Papka, R.E., and McNeill, D.L. (1992). Is there a synaptic innervation of pelvic neurons by CGRP-immunoreactive sensory nerves? *Ann. N. Y. Acad. Sci.* 657, 477–80.
119. Purves, D., Rubin, E., Snider, W.D., and Lichtman, J. (1986). Relation of animal size to convergence, divergence, and neuronal number in peripheral sympathetic pathways. *J. Neurosci.* 6, 158–63.
120. Tabatabai, M., Booth, A.M., and De Groat, W.C. (1986). Morphological and electrophysiological properties of pelvic ganglion cells in the rat. *Brain Res.* 382, 61–70.
121. de Groat, W.C., and Booth, A.M. (1980). Inhibition and facilitation in parasympathetic ganglia of the urinary bladder. *Fed. Proc.* 39, 2990–6.
122. Keast, J.R., Kawatani, M., and De Groat, W.C. (1990). Sympathetic modulation of cholinergic transmission in cat vesical ganglia is mediated by alpha 1- and alpha 2-adrenoceptors. *Am. J. Physiol.* 258, R44-50.
123. Luckensmeyer, G.B., and Keast, J.R. (1995). Distribution and morphological

- characterization of viscerofugal projections from the large intestine to the inferior mesenteric and pelvic ganglia of the male rat. *Neuroscience* 66, 663–671.
124. Luckensmeyer, G.B., and Keast, J.R. (1996). Immunohistochemical characterisation of viscerofugal neurons projecting to the inferior mesenteric and major pelvic ganglia in the male rat. *J. Auton. Nerv. Syst.* 61, 6–16.
 125. Christianson, J.A., Liang, R., Ustinova, E.E., Davis, B.M., Fraser, M.O., and Pezzone, M.A. (2007). Convergence of bladder and colon sensory innervation occurs at the primary afferent level. *Pain* 128, 235–43.
 126. Chen, Y., Wu, X., Liu, J., Tang, W., Zhao, T., and Zhang, J. (2010). Distribution of Convergent Afferents Innervating Bladder and Prostate at Dorsal Root Ganglia in Rats. *Urology* 76, 764.e1-764.e6.
 127. Chaban, V., Christensen, A., Wakamatsu, M., McDonald, M., Rapkin, A., McDonald, J., and Micevych, P. (2007). The same dorsal root ganglion neurons innervate uterus and colon in the rat. *Neuroreport* 18, 209–212.
 128. Malykhina, A.P. (2007). Neural mechanisms of pelvic organ cross-sensitization. *Neuroscience* 149, 660–672.
 129. Malykhina, A.P., Qin, C., Greenwood-van Meerveld, B., Foreman, R.D., Lupu, F., and Akbarali, H.I. (2006). Hyperexcitability of convergent colon and bladder dorsal root ganglion neurons after colonic inflammation: mechanism for pelvic organ cross-talk. *Neurogastroenterol. Motil.* 18, 936–48.
 130. Glickman, S., and Kamm, M.A. (1996). Bowel dysfunction in spinal-cord-injury patients. *Lancet* (London, England) 347, 1651–3.
 131. Benevento, B.T., and Sipski, M.L. (2002). Neurogenic bladder, neurogenic bowel, and

- sexual dysfunction in people with spinal cord injury. *Phys. Ther.* 82, 601–12.
132. Wyndaele, J.-J. (2016). The management of neurogenic lower urinary tract dysfunction after spinal cord injury. *Nat. Rev. Urol.* 13, 705–714.
 133. van Loo, M.A., Post, M.W.M., Bloemen, J.H.A., and van Asbeck, F.W.A. (2010). Care needs of persons with long-term spinal cord injury living at home in the Netherlands. *Spinal Cord* 48, 423–8.
 134. Krueger, H., Noonan, V.K., Trenaman, L.M., Joshi, P., and Rivers, C.S. (2013). The economic burden of traumatic spinal cord injury in Canada. *Chronic Dis. Inj. Can.* 33, 113–22.
 135. Fonte, N. (2008). Urological care of the spinal cord-injured patient. *J. wound, ostomy, Cont. Nurs. Off. Publ. Wound, Ostomy Cont. Nurses Soc.* 35, 323-31; quiz 332–3.
 136. Cardenas, D.D., Hoffman, J.M., Kirshblum, S., and McKinley, W. (2004). Etiology and incidence of rehospitalization after traumatic spinal cord injury: a multicenter analysis. *Arch. Phys. Med. Rehabil.* 85, 1757–63.
 137. Liu, C.-W., Attar, K.H., Gall, A., Shah, J., and Craggs, M. (2010). The relationship between bladder management and health-related quality of life in patients with spinal cord injury in the UK. *Spinal Cord* 48, 319–324.
 138. Yoshiyama, M., deGroat, W.C., and Fraser, M.O. (2000). Influences of external urethral sphincter relaxation induced by alpha-bungarotoxin, a neuromuscular junction blocking agent, on voiding dysfunction in the rat with spinal cord injury. *Urology* 55, 956–60.
 139. Rabadi, M.H., and Aston, C. (2014). Complications and urologic risks of neurogenic bladder in veterans with traumatic spinal cord injury. *Spinal Cord* 53, 200–203.
 140. Al Taweel, W., and Seyam, R. (2015). Neurogenic bladder in spinal cord injury patients.

- Res. Reports Urol. 7, 85.
141. Berkowitz, M. (1992). The Economic consequences of traumatic spinal cord injury. Demos, 202 p.
 142. Lynch, A.C., and Frizelle, F.A. (2006). Colorectal motility and defecation after spinal cord injury in humans. *Prog. Brain Res.* 152, 335–43.
 143. Anderson, K.D., Borisoff, J.F., Johnson, R.D., Stiens, S.A., and Elliott, S.L. (2007). Long-term effects of spinal cord injury on sexual function in men: implications for neuroplasticity. *Spinal Cord* 45, 338–48.
 144. Sale, P., Mazzarella, F., Pagliacci, M.C., Agosti, M., Felzani, G., and Franceschini, M. (2012). Predictors of Changes in Sentimental and Sexual Life After Traumatic Spinal Cord Injury. *Arch. Phys. Med. Rehabil.* 93, 1944–1949.
 145. Anderson, K.D., Borisoff, J.F., Johnson, R.D., Stiens, S.A., and Elliott, S.L. (2006). The impact of spinal cord injury on sexual function: concerns of the general population. *Spinal Cord* 45, 328–37.
 146. Kaplan, S.A., Chancellor, M.B., and Blaivas, J.G. (1991). Bladder and sphincter behavior in patients with spinal cord lesions. *J. Urol.* 146, 113–7.
 147. Sekhon, L.H., and Fehlings, M.G. (2001). Epidemiology, demographics, and pathophysiology of acute spinal cord injury. *Spine (Phila. Pa. 1976)*. 26, S2-12.
 148. DeVivo, M.J. (2012). Epidemiology of traumatic spinal cord injury: trends and future implications. *Spinal Cord* 50, 365–372.
 149. McDonald, J.W., and Sadowsky, C. (2002). Spinal-cord injury. *Lancet* 359, 417–425.
 150. Shaer, C.M., Chescheir, N., and Schulkin, J. (2007). Myelomeningocele: a review of the epidemiology, genetics, risk factors for conception, prenatal diagnosis, and prognosis for

- affected individuals. *Obstet. Gynecol. Surv.* 62, 471–9.
151. Courtois, F.J., Goulet, M.C., Charvier, K.F., and Leriche, A. (1999). Posttraumatic erectile potential of spinal cord injured men: how physiologic recordings supplement subjective reports. *Arch. Phys. Med. Rehabil.* 80, 1268–72.
 152. Chuang, A.T., and Steers, W.D. (1999). Neurophysiology of penile erection., in: Carson, C., Kirby, R., and Goldstein, I. (eds). *Textbook of Erection Dysfunction*. Oxford, UK: ISIS Medical Media Inc., pps. 59–72.
 153. Elliott, S.L. (2006). Problems of sexual function after spinal cord injury. *Prog. Brain Res.* 152, 387–399.
 154. Elliott, S.L. (2006). Problems of sexual function after spinal cord injury. *Prog. Brain Res.* 152, 387–399.
 155. Geiger, R.C. (1979). Neurophysiology of sexual response in spinal cord injury. *Sex. Disabil.* 2, 257–266.
 156. Ersoz, M., and Akyuz, M. (2004). Bladder-filling sensation in patients with spinal cord injury and the potential for sensation-dependent bladder emptying. *Spinal Cord* 42, 110–116.
 157. Marino, R.J., Rider-Foster, D., Maissel, G., and Ditunno, J.F. (1995). Superiority of motor level over single neurological level in categorizing tetraplegia. *Paraplegia* 33, 510–3.
 158. Brommer, B., Engel, O., Kopp, M.A., Watzlawick, R., Müller, S., Prüss, H., Chen, Y., DeVivo, M.J., Finkenstaedt, F.W., Dirnagl, U., Liebscher, T., Meisel, A., and Schwab, J.M. (2016). Spinal cord injury-induced immune deficiency syndrome enhances infection susceptibility dependent on lesion level. *Brain* 139, 692–707.
 159. Munakata, M., Kameyama, J., Kanazawa, M., Nunokawa, T., Moriai, N., and Yoshinaga,

- K. (1997). Circadian blood pressure rhythm in patients with higher and lower spinal cord injury: simultaneous evaluation of autonomic nervous activity and physical activity. *J. Hypertens.* 15, 1745–9.
160. Inskip, J., Plunet, W., Ramer, L., Ramsey, J.B., Yung, A., Kozlowski, P., Ramer, M., and Krassioukov, A. (2010). Cardiometabolic risk factors in experimental spinal cord injury. *J. Neurotrauma* 27, 275–85.
161. Roberts, T.T., Leonard, G.R., and Cepela, D.J. (2017). Classifications In Brief: American Spinal Injury Association (ASIA) Impairment Scale. *Clin. Orthop. Relat. Res.* 475, 1499–1504.
162. American Spinal Injury Association. (1984). Standards for neurological classification of spinal injury patients. Chicago Am. Spinal Inj. Assoc. .
163. Krassioukov, A., Biering-Sorensen, F., Donovan, W., Kennelly, M., Kirshblum, S., Krogh, K., Alexander, M.S., Vogel, L., Wecht, J., and Autonomic Standards Committee of the American Spinal Injury Association/International Spinal Cord Society. (2012). International standards to document remaining autonomic function after spinal cord injury. *J. Spinal Cord Med.* 35, 201–210.
164. Alexander, M.S., Biering-Sorensen, F., Bodner, D., Brackett, N.L., Cardenas, D., Charlifue, S., Creasey, G., Dietz, V., Ditunno, J., Donovan, W., Elliott, S.L., Estores, I., Graves, D.E., Green, B., Gousse, A., Jackson, A.B., Kennelly, M., Karlsson, A.-K., Krassioukov, A., Krogh, K., Linsenmeyer, T., Marino, R., Mathias, C.J., Perakash, I., Sheel, A.W., Schilero, G., Shilero, G., Schurch, B., Sonksen, J., Stiens, S., Wecht, J., Wuermsler, L.A., and Wyndaele, J.-J. (2009). International standards to document remaining autonomic function after spinal cord injury. *Spinal Cord* 47, 36–43.

165. Afsar, S.I., Sarifakioglu, B., Yalbuздаğ, Ş.A., and Saraçgil Coşar, S.N. (2016). An unresolved relationship: the relationship between lesion severity and neurogenic bladder in patients with spinal cord injury. *J. Spinal Cord Med.* 39, 93–98.
166. Weld, K.J., Graney, M.J., and Dmochowski, R.R. (2000). Differences in bladder compliance with time and associations of bladder management with compliance in spinal cord injured patients. *J. Urol.* 163, 1228–33.
167. Weld, K.J., and Dmochowski, R.R. (2000). Effect of bladder management on urological complications in spinal cord injured patients. *J. Urol.* 163, 768–72.
168. Chancellor, M.B., Rivas, D.A., Huang, B., Kelly, G., Salzman, S.K., Thor, K., Steers, W., Roppolo, J.R., Beckman, A.C., and Bunnell, W.P. (1994). Micturition Patterns After Spinal Trauma As A Measure Of Autonomic Functional Recovery. *J. Urol.* 151, 250–254.
169. Basso, D.M. (2000). Neuroanatomical substrates of functional recovery after experimental spinal cord injury: implications of basic science research for human spinal cord injury. *Phys. Ther.* 80, 808–17.
170. Diaz, E., and Morales, H. (2016). Spinal Cord Anatomy and Clinical Syndromes. *Semin. Ultrasound, CT MRI* 37, 360–371.
171. Deuchars, S.A., K. Lall, V., Deuchars, S.A., and K. Lall, V. (2015). Sympathetic Preganglionic Neurons: Properties and Inputs., in: *Comprehensive Physiology*. Hoboken, NJ, USA: John Wiley & Sons, Inc., pps. 829–869.
172. Wrathall, J.R., and Emch, G.S. (2006). Effect of injury severity on lower urinary tract function after experimental spinal cord injury., in: *Progress in Brain Research*. pps. 117–134.
173. Ko, H.Y., Ditunno, J.F., Graziani, V., and Little, J.W. (1999). The pattern of reflex

- recovery during spinal shock. *Spinal Cord* 37, 402–9.
174. Ditunno, J.F., Little, J.W., Tessler, A., and Burns, A.S. (2004). Spinal shock revisited: a four-phase model. *Spinal Cord* 42, 383–95.
 175. Dietz, V., and Colombo, G. (2004). Recovery from spinal cord injury -underlying mechanisms and efficacy of rehabilitation. *Acta Neurochir* 89, 95–100.
 176. Krassioukov, A., Biering-Sørensen, F., Donovan, W., Kennelly, M., Kirshblum, S., Krogh, K., Alexander, M.S., Vogel, L., and Wecht, J. (2012). International standards to document remaining autonomic function after spinal cord injury. *J. Spinal Cord Med.* 35, 201–210.
 177. Biering-Sørensen, F., Craggs, M., Kennelly, M., Schick, E., and Wyndaele, J.-J. (2008). International urodynamic basic spinal cord injury data set. *Spinal Cord* 46, 513–6.
 178. Rudy, D.C., Awad, S.A., and Downie, J.W. (1988). External sphincter dyssynergia: an abnormal continence reflex. *J. Urol.* 140, 105–10.
 179. Tuttle, J.B., Steers, W.D., Albo, M., and Nataluk, E. (1994). Neural input regulates tissue NGF and growth of the adult rat urinary bladder. *J. Auton. Nerv. Syst.* 49, 147–158.
 180. Seki, S., Sasaki, K., Igawa, Y., Nishizawa, O., Chancellor, M.B., De Groat, W.C., and Yoshimura, N. (2004). Suppression of detrusor-sphincter dyssynergia by immunoneutralization of nerve growth factor in lumbosacral spinal cord in spinal cord injured rats. *J. Urol.* 171, 478–82.
 181. West, C.R., Popok, D., Crawford, M.A., and Krassioukov, A. V. (2015). Characterizing the Temporal Development of Cardiovascular Dysfunction in Response to Spinal Cord Injury. *J. Neurotrauma* 32, 922–930.
 182. Teasell, R.W., Arnold, J.M.O., Krassioukov, A., and Delaney, G.A. (2000).

- Cardiovascular consequences of loss of supraspinal control of the sympathetic nervous system after spinal cord injury. *Arch. Phys. Med. Rehabil.* 81, 506–516.
183. Mathias, C.J., and Frankel, H.L. (1988). Cardiovascular Control in Spinal Man. *Annu. Rev. Physiol.* 50, 577–592.
184. Silver, J.R. (2000). Early autonomic dysreflexia. *Spinal Cord* 38, 229–33.
185. Wheeler-Kingshott, C.A., Stroman, P.W., Schwab, J.M., Bacon, M., Bosma, R., Brooks, J., Cadotte, D.W., Carlstedt, T., Ciccarelli, O., Cohen-Adad, J., Curt, A., Evangelou, N., Fehlings, M.G., Filippi, M., Kelley, B.J., Kollias, S., Mackay, A., Porro, C.A., Smith, S., Strittmatter, S.M., Summers, P., Thompson, A.J., and Tracey, I. (2014). The current state-of-the-art of spinal cord imaging: Applications. *Neuroimage* 84, 1082–1093.
186. Edgerton, V.R., Roy, R.R., Hodgson, J.A., Prober, R.J., de Guzman, C.P., and de Leon, R. (1992). Potential of adult mammalian lumbosacral spinal cord to execute and acquire improved locomotion in the absence of supraspinal input. *J. Neurotrauma* 9 Suppl 1, S119-28.
187. Whelan, P.J. (1996). Control of locomotion in the decerebrate cat. *Prog. Neurobiol.* 49, 481–515.
188. Cheriyan, T., Ryan, D.J., Weinreb, J.H., Cheriyan, J., Paul, J.C., Lafage, V., Kirsch, T., and Errico, T.J. (2014). Spinal cord injury models: a review. *Spinal Cord* 52, 588–595.
189. Kwon, B.K., Streijger, F., Hill, C.E., Anderson, A.J., Bacon, M., Beattie, M.S., Blesch, A., Bradbury, E.J., Brown, A., Bresnahan, J.C., Case, C.C., Colburn, R.W., David, S., Fawcett, J.W., Ferguson, A.R., Fischer, I., Floyd, C.L., Gensel, J.C., Houle, J.D., Jakeman, L.B., Jeffery, N.D., Jones, L.A.T., Kleitman, N., Kocsis, J., Lu, P., Magnuson, D.S.K., Marsala, M., Moore, S.W., Mothe, A.J., Oudega, M., Plant, G.W., Rabchevsky,

- A.S., Schwab, J.M., Silver, J., Steward, O., Xu, X.-M., Guest, J.D., and Tetzlaff, W. (2015). Large animal and primate models of spinal cord injury for the testing of novel therapies. *Exp. Neurol.* 269, 154–168.
190. Kjell, J., and Olson, L. (2016). Rat models of spinal cord injury: from pathology to potential therapies. *Dis. Model. Mech.* 9.
191. Metz, G.A.S., Curt, A., van de Meent, H., Klusman, I., Schwab, M.E., and Dietz, V. (2000). Validation of the Weight-Drop Contusion Model in Rats: A Comparative Study of Human Spinal Cord Injury. *J. Neurotrauma* 17, 1–17.
192. Soler, J.M., and Previnaire, J.G. (2011). Ejaculatory dysfunction in spinal cord injury men is suggestive of dyssynergic ejaculation. *Eur. J. Phys. Rehabil. Med.* 47, 677–81.
193. Hou, S., and Rabchevsky, A.G. (2014). Autonomic Consequences of Spinal Cord Injury., in: *Comprehensive Physiology*. Hoboken, NJ, USA: John Wiley & Sons, Inc., pps. 1419–1453.
194. Jackson, A.B., Dijkers, M., Devivo, M.J., and Poczatek, R.B. (2004). A demographic profile of new traumatic spinal cord injuries: change and stability over 30 years. *Arch. Phys. Med. Rehabil.* 85, 1740–8.
195. Reier, P.J., Lane, M.A., Hall, E.D., Teng, Y.D., and Howland, D.R. (2012). Translational spinal cord injury research., in: *Handbook of Clinical Neurology*. pps. 411–433.
196. Ramsey, J.B.G., Ramer, L.M., Inskip, J.A., Alan, N., Ramer, M.S., and Krassioukov, A. V. (2010). Care of rats with complete high-thoracic spinal cord injury. *J. Neurotrauma* 27, 1709–1722.
197. Squair, J.W., West, C.R., Popok, D., Assinck, P., Liu, J., Tetzlaff, W., and Krassioukov, A. V. (2017). High Thoracic Contusion Model for the Investigation of Cardiovascular

- Function after Spinal Cord Injury. *J. Neurotrauma* 34, 671–684.
198. West, C., Bellantoni, A., and Krassioukov, A. (2013). Cardiovascular Function in Individuals with Incomplete Spinal Cord Injury: A Systematic Review. *Top. Spinal Cord Inj. Rehabil.* 19, 267–278.
 199. Krassioukov, A. (2009). Autonomic function following cervical spinal cord injury. *Respir. Physiol. Neurobiol.* 169, 157–164.
 200. Groah, S., Weitzenkamp, D., Sett, P., Soni, B., and Savic, G. (2001). The relationship between neurological level of injury and symptomatic cardiovascular disease risk in the aging spinal injured. *Spinal Cord* 39, 310–317.
 201. Mattucci, S., Liu, J., Fijal, P., Tetzlaff, W., and Oxland, T.R. (2017). Repeatability of a Dislocation Spinal Cord Injury Model in a Rat—A High-Speed Biomechanical Analysis. *J. Biomech. Eng.* 139, 104501.
 202. Munoz, A. (2017). Neurogenic bladder dysfunction does not correlate with astrocyte and microglia activation produced by graded force in a contusion-induced spinal cord injury. *Brain Res. Bull.* 131, 18–24.
 203. Yoshiyama, M., Nezu, F.M., Yokoyama, O., de Groat, W.C., and Chancellor, M.B. (1999). Changes in micturition after spinal cord injury in conscious rats. *Urology* 54, 929–33.
 204. Ferrero, S.L., Brady, T.D., Dugan, V.P., Armstrong, J.E., Hubscher, C.H., and Johnson, R.D. (2015). Effects of lateral funiculus sparing, spinal lesion level, and gender on recovery of bladder voiding reflexes and hematuria in rats. *J. Neurotrauma* 32, 200–8.
 205. Zhang, Y., Guan, Z., Reader, B., Shawler, T., Mandrekar-Colucci, S., Huang, K., Weil, Z., Bratasz, A., Wells, J., Powell, N.D., Sheridan, J.F., Whitacre, C.C., Rabchevsky, A.G.,

- Nash, M.S., and Popovich, P.G. (2013). Autonomic dysreflexia causes chronic immune suppression after spinal cord injury. *J. Neurosci.* 33, 12970–81.
206. Llewellyn-Smith, I.J., and Keast, J.R. (2006). Effects of spinal cord injury on synaptic inputs to sympathetic preganglionic neurons. *Prog. Brain Res.* 152, 11–26.
207. Apodaca, G., Kiss, S., Ruiz, W., Meyers, S., Zeidel, M., and Birder, L. (2003). Disruption of bladder epithelium barrier function after spinal cord injury. *Am. J. Physiol. Renal Physiol.* 284, F966-76.
208. Rossier, A.B., Fam, B.A., Dibenedetto, M., and Sarkarati, M. (1979). Urodynamics in spinal shock patients. *J. Urol.* 122, 783–7.
209. Krassioukov, A. (2009). Autonomic function following cervical spinal cord injury. *Respir. Physiol. Neurobiol.* 169, 157–164.
210. Krassioukov, A., and Claydon, V.E. (2006). The clinical problems in cardiovascular control following spinal cord injury: an overview. *Prog. Brain Res.* 152, 223–9.
211. Maiorov, D.N., Weaver, L.C., and Krassioukov, A. V. (1997). Relationship between sympathetic activity and arterial pressure in conscious spinal rats. *Am. J. Physiol.* 272, H625-31.
212. Shergill, I.S.S., Arya, M., Hamid, R., Khastgir, J., Patel, H.R.H.R.H., and Shah, P.J.R.J.R. (2004). The importance of autonomic dysreflexia to the urologist. *BJU Int.* 93, 923–926.
213. Kirshblum, S.C., House, J.G., and O'Connor, K.C. (2002). Silent autonomic dysreflexia during a routine bowel program in persons with traumatic spinal cord injury: A preliminary study. *Arch. Phys. Med. Rehabil.* 83, 1774–1776.
214. Anderson, K.D., Borisoff, J.F., Johnson, R.D., Stiens, S.A., and Elliott, S.L. (2007). Spinal cord injury influences psychogenic as well as physical components of female

- sexual ability. *Spinal Cord* 45, 349–59.
215. Forsythe, E., and Horsewell, J.E. (2006). Sexual rehabilitation of women with a spinal cord injury. *Spinal Cord* 44, 234–41.
216. McBride, F., Quah, S.P., Scott, M.E., and Dinsmore, W.W. (2003). Tripling of blood pressure by sexual stimulation in a man with spinal cord injury. *J. R. Soc. Med.* 96, 349–50.
217. Elliott, S., and Krassioukov, A. (2006). Malignant autonomic dysreflexia in spinal cord injured men. *Spinal Cord* 44, 386–392.
218. Stiens, S.A., Johnson, M.C., and Lyman, P.J. (1990). *Physical medicine and rehabilitation clinics of North America*. W.B. Saunders, 263-296 p.
219. Wan, D., and Krassioukov, A. V. (2014). Life-threatening outcomes associated with autonomic dysreflexia: a clinical review. *J. Spinal Cord Med.* 37, 2–10.
220. Cragg, J.J., Noonan, V.K., Krassioukov, A., and Borisoff, J. (2013). Cardiovascular disease and spinal cord injury: Results from a national population health survey. *Neurology* 81, 723–728.
221. Krassioukov, A. V., and Weaver, L.C. (1995). Episodic hypertension due to autonomic dysreflexia in acute and chronic spinal cord-injured rats. *Am. J. Physiol.* 268, H2077-83.
222. Krassioukov, A. V., Johns, D.G., and Schramm, L.P. (2002). Sensitivity of Sympathetically Correlated Spinal Interneurons, Renal Sympathetic Nerve Activity, and Arterial Pressure to Somatic and Visceral Stimuli after Chronic Spinal Injury. *J. Neurotrauma* 19, 1521–1529.
223. Mayorov, D.N., Adams, M.A., and Krassioukov, A. V. (2001). Telemetric Blood Pressure Monitoring in Conscious Rats Before and After Compression Injury of Spinal Cord. *J.*

- Neurotrauma 18, 727–736.
224. Jacob, J.E., Gris, P., Fehlings, M.G., Weaver, L.C., and Brown, A. (2003). Autonomic dysreflexia after spinal cord transection or compression in 129Sv, C57BL, and Wallerian degeneration slow mutant mice. *Exp. Neurol.* 183, 136–46.
225. Fry, C.H., Young, J.S., Jabr, R.I., McCarthy, C., Ikeda, Y., and Kanai, A.J. (2012). Modulation of spontaneous activity in the overactive bladder: the role of P2Y agonists. *AJP Ren. Physiol.* 302, F1447–F1454.
226. Vizzard, M.A. (2000). Changes in Urinary Bladder Neurotrophic Factor mRNA and NGF Protein Following Urinary Bladder Dysfunction. *Exp. Neurol.* 161, 273–284.
227. Janzen, J., Bersch, U., Pietsch-Breitfeld, B., Pressler, H., Michel, D., and Bültmann, B. (2001). Urinary bladder biopsies in spinal cord injured patients. *Spinal Cord* 39, 568–70.
228. Şekerci, Ç.A., İşbilen, B., İşman, F., Akbal, C., Şimşek, F., and Tarcan, T. (2014). Urinary NGF, TGF- β 1, TIMP-2 and Bladder Wall Thickness Predict Neurourological Findings in Children with Myelodysplasia. *J. Urol.* 191, 199–205.
229. Komninos, C., and Mitsogiannis, I. (2014). Obstruction-induced alterations within the urinary bladder and their role in the pathophysiology of lower urinary tract symptomatology. *Can. Urol. Assoc. J.* 8, 524.
230. Silva, J.A.F., Gonsalves, M. de C.D., de Melo, R.T., Carrerette, F.B., and Damião, R. (2015). Association between the bladder wall thickness and urodynamic findings in patients with spinal cord injury. *World J. Urol.* 33, 131–135.
231. Landau, E.H., Jayanthi, V.R., Churchill, B.M., Shapiro, E., Gilmour, R.F., Khoury, A.E., Macarak, E.J., McLorie, G.A., Steckler, R.E., and Kogan, B.A. (1994). Loss of elasticity in dysfunctional bladders: urodynamic and histochemical correlation. *J. Urol.* 152, 702–5.

232. Nagatomi, J., Gloeckner, D.C., Chancellor, M.B., DeGroat, W.C., and Sacks, M.S. (2004). Changes in the biaxial viscoelastic response of the urinary bladder following spinal cord injury. *Ann. Biomed. Eng.* 32, 1409–19.
233. de Groat, W.C., and Yoshimura, N. (2006). Mechanisms underlying the recovery of lower urinary tract function following spinal cord injury. *Prog. Brain Res.* 152, 59–84.
234. Streng, T., Hedlund, P., Talo, A., Andersson, K.E., and Gillespie, J.I. (2006). Phasic non-micturition contractions in the bladder of the anaesthetized and awake rat. *BJU Int.* 97, 1094–1101.
235. Yoshiyama, M., Roppolo, J.R., and De Groat, W.C. (1994). Alteration by urethane of glutamatergic control of micturition. *Eur. J. Pharmacol.* 264, 417–25.
236. Matsuura, S., and Downie, J.W. (2000). Effect of anesthetics on reflex micturition in the chronic cannula- implanted rat. *Neurourol. Urodyn.* 19, 87–99.
237. Chang, H.-Y., and Havton, L.A. (2008). Differential Effects of Urethane and Isoflurane on External Urethral Sphincter Electromyography and Cystometry in Rats. *Am. J. Physiol. - Ren. Physiol.* 295, F1248–F1253.
238. Yoshiyama, M., Roppolo, J.R., Takeda, M., and de Groat, W.C. (2013). Effects of urethane on reflex activity of lower urinary tract in decerebrate unanesthetized rats. *Am. J. Physiol. - Ren. Physiol.* 304, F390-6.
239. Cheng, C.L., Ma, C.P., and de Groat, W.C. (1995). Effect of capsaicin on micturition and associated reflexes in chronic spinal rats. *Brain Res.* 678, 40–8.
240. Schwab, M.E., and Bartholdi, D. (1996). Degeneration and regeneration of axons in the lesioned spinal cord. *Physiol. Rev.* 76, 319–70.
241. Walters, E.T. (2018). How is chronic pain related to sympathetic dysfunction and

- autonomic dysreflexia following spinal cord injury? *Auton. Neurosci.* 209, 79–89.
242. Wu, Z., Yang, Q., Crook, R.J., O’Neil, R.G., and Walters, E.T. (2013). TRPV1 channels make major contributions to behavioral hypersensitivity and spontaneous activity in nociceptors after spinal cord injury. *Pain* 154, 2130–2141.
243. Bedi, S.S., Yang, Q., Crook, R.J., Du, J., Wu, Z., Fishman, H.M., Grill, R.J., Carlton, S.M., and Walters, E.T. (2010). Chronic Spontaneous Activity Generated in the Somata of Primary Nociceptors Is Associated with Pain-Related Behavior after Spinal Cord Injury. *J. Neurosci.* 30, 14870–14882.
244. Popovich, P.G., Wei, P., and Stokes, B.T. (1997). Cellular inflammatory response after spinal cord injury in Sprague-Dawley and Lewis rats. *J. Comp. Neurol.* 377, 443–64.
245. Dusart, I., and Schwab, M.E. (1994). Secondary cell death and the inflammatory reaction after dorsal hemisection of the rat spinal cord. *Eur. J. Neurosci.* 6, 712–24.
246. Alexander, J.K., and Popovich, P.G. (2009). Neuroinflammation in spinal cord injury: therapeutic targets for neuroprotection and regeneration., in: *Progress in Brain Research*. pps. 125–137.
247. Gwak, Y.S., Kang, J., Unabia, G.C., and Hulsebosch, C.E. (2012). Spatial and temporal activation of spinal glial cells: Role of gliopathy in central neuropathic pain following spinal cord injury in rats. *Exp. Neurol.* 234, 362–372.
248. Hulsebosch, C.E., Hains, B.C., Crown, E.D., and Carlton, S.M. (2009). Mechanisms of chronic central neuropathic pain after spinal cord injury. *Brain Res. Rev.* 60, 202–213.
249. Hains, B.C., and Waxman, S.G. (2006). Activated Microglia Contribute to the Maintenance of Chronic Pain after Spinal Cord Injury. *J. Neurosci.* 26, 4308–4317.
250. Krassioukov, A. V, Bunge, R.P., Pucket, W.R., and Bygrave, M.A. (1999). The changes in

- human spinal sympathetic preganglionic neurons after spinal cord injury. *Spinal Cord* 37, 6–13.
251. Krassioukov, A. V, and Weaver, L.C. (1996). Morphological changes in sympathetic preganglionic neurons after spinal cord injury in rats. *Neuroscience* 70, 211–225.
 252. Llewellyn-Smith, I.J., and Weaver, L.C. (2001). Changes in synaptic inputs to sympathetic preganglionic neurons after spinal cord injury. *J. Comp. Neurol.* 435, 226–240.
 253. Christensen, M.D., and Hulsebosch, C.E. (1997). Spinal Cord Injury and Anti-NGF Treatment Results in Changes in CGRP Density and Distribution in the Dorsal Horn in the Rat. *Exp. Neurol.* 147, 463–475.
 254. Llewellyn-Smith, I.J., Weaver, L.C., and Keast, J.R. (2006). Effects of spinal cord injury on synaptic inputs to sympathetic preganglionic neurons. *Prog. Brain Res.* 152, 11–26.
 255. Maiorov, D.N., Krenz, N.R., Krassioukov, A. V, and Weaver, L.C. (1997). Role of spinal NMDA and AMPA receptors in episodic hypertension in conscious spinal rats. *Am. J. Physiol.* 273, H1266-74.
 256. Krenz, N.R., and Weaver, L.C. (1998). Sprouting of primary afferent fibers after spinal cord transection in the rat. *Neuroscience* 85, 443–58.
 257. Weaver, L.C., Verghese, P., Bruce, J.C., Fehlings, M.G., Krenz, N.R., and Marsh, D.R. (2001). Autonomic dysreflexia and primary afferent sprouting after clip-compression injury of the rat spinal cord. *J. Neurotrauma* 18, 1107–19.
 258. Wong, S.T., Atkinson, B.A., and Weaver, L.C. (2000). Confocal microscopic analysis reveals sprouting of primary afferent fibres in rat dorsal horn after spinal cord injury. *Neurosci. Lett.* 296, 65–8.
 259. Krenz, N.R., Meakin, S.O., Krassioukov, A. V, and Weaver, L.C. (1999). Neutralizing

- intraspinal nerve growth factor blocks autonomic dysreflexia caused by spinal cord injury. *J. Neurosci.* 19, 7405–14.
260. Cameron, A.A., Smith, G.M., Randall, D.C., Brown, D.R., and Rabchevsky, A.G. (2006). Genetic Manipulation of Intraspinal Plasticity after Spinal Cord Injury Alters the Severity of Autonomic Dysreflexia. *J. Neurosci.* 26, 2923–2932.
261. Zinck, N.D.T., Rafuse, V.F., and Downie, J.W. (2007). Sprouting of CGRP primary afferents in lumbosacral spinal cord precedes emergence of bladder activity after spinal injury. *Exp. Neurol.* 204, 777–90.
262. Zinck, N.D.T., and Downie, J.W. (2008). IB4 afferent sprouting contributes to bladder dysfunction in spinal rats. *Exp. Neurol.* 213, 293–302.
263. Zhang, X., Douglas, K.L., Jin, H., Eldaif, B.M., Nassar, R., Fraser, M.O., and Dolber, P.C. (2008). Sprouting of substance P-expressing primary afferent central terminals and spinal micturition reflex NK1 receptor dependence after spinal cord injury. *Am. J. Physiol. Integr. Comp. Physiol.* 295, R2084–R2096.
264. Hou, S., Carson, D.M., Wu, D., Klaw, M.C., Houlé, J.D., and Tom, V.J. (2016). Dopamine is produced in the rat spinal cord and regulates micturition reflex after spinal cord injury. *Exp. Neurol.* 285, 136–146.
265. McKay, S.M., and McLachlan, E.M. (2004). Inflammation of rat dorsal root ganglia below a mid-thoracic spinal transection. *Neuroreport* 15, 1783–6.
266. Abram, S.E., Yi, J., Fuchs, A., and Hogan, Q.H. (2006). Permeability of injured and intact peripheral nerves and dorsal root ganglia. *Anesthesiology* 105, 146–53.
267. Jimenez-Andrade, J.M., Herrera, M.B., Ghilardi, J.R., Vardanyan, M., Melemedjian, O.K., and Mantyh, P.W. (2008). Vascularization of the Dorsal Root Ganglia and Peripheral

- Nerve of the Mouse: Implications for Chemical-Induced Peripheral Sensory Neuropathies. Mol. Pain 4, 1744-8069-4-10.
268. Yoshimura, N., and de Groat, W.C. (1997). Plasticity of Na⁺ channels in afferent neurones innervating rat urinary bladder following spinal cord injury. J. Physiol. 503 (Pt 2), 269-76.
269. Zvarova, K., Dunleavy, J.D., and Vizzard, M.A. (2005). Changes in pituitary adenylate cyclase activating polypeptide expression in urinary bladder pathways after spinal cord injury. Exp. Neurol. 192, 46-59.
270. Vizzard, M.A. (2006). Neurochemical plasticity and the role of neurotrophic factors in bladder reflex pathways after spinal cord injury., in: *Progress in Brain Research*. pps. 97-115.
271. Takahashi, R., Yoshizawa, T., Yunoki, T., Tyagi, P., Naito, S., de Groat, W.C., and Yoshimura, N. (2013). Hyperexcitability of Bladder Afferent Neurons Associated with Reduction of Kv1.4 α -Subunit in Rats with Spinal Cord Injury. J. Urol. 190, 2296-2304.
272. Miyazato, M., Kadekawa, K., Kitta, T., Wada, N., Shimizu, N., de Groat, W.C., Birder, L.A., Kanai, A.J., Saito, S., and Yoshimura, N. (2017). New Frontiers of Basic Science Research in Neurogenic Lower Urinary Tract Dysfunction. Urol. Clin. North Am. 44, 491-505.
273. Takahara, Y., Maeda, M., Nakatani, T., and Kiyama, H. (2007). Transient suppression of the vesicular acetylcholine transporter in urinary bladder pathways following spinal cord injury. Brain Res. 1137, 20-28.
274. Kempinas, W.D.G., Suarez, J.D., Roberts, N.L., Strader, L.F., Ferrell, J., Goldman, J.M., Narotsky, M.G., Perreault, S.D., Evenson, D.P., and Ricker, D.D. (1998). Fertility of rat

- epididymal sperm after chemically and surgically induced sympathectomy. *Biol. Reprod.* 59, 897–904.
275. Píkov, V., and Wrathall, J.R. (2001). Coordination of the bladder detrusor and the external urethral sphincter in a rat model of spinal cord injury: effect of injury severity. *J. Neurosci.* 21, 559–69.
276. Kontani, H., and Hayashi, K. (1997). Urinary bladder response to hypogastric nerve stimulation after bilateral resection of the pelvic nerve or spinal cord injury in rats. *Int. J. Urol.* 4, 394–400.
277. Mimata, H., Satoh, F., Tanigawa, T., Nomura, Y., and Ogata, J. (1993). Changes of rat urinary bladder during acute phase of spinal cord injury. *Urol. Int.* 51, 89–93.
278. Deveaud, C.M., Macarak, E.J., Kucich, U., Ewalt, D.H., Abrams, W.R., and Howard, P.S. (1998). Molecular analysis of collagens in bladder fibrosis. *J. Urol.* 160, 1518–27.
279. Watanabe, T., Rivas, D.A., and Chancellor, M.B. (1996). Urodynamics of spinal cord injury. *Urol. Clin. North Am.* 23, 459–73.
280. Nagatomi, J., DeMiguel, F., Torimoto, K., Chancellor, M.B., Getzenberg, R.H., and Sacks, M.S. (2005). Early molecular-level changes in rat bladder wall tissue following spinal cord injury. *Biochem. Biophys. Res. Commun.* 334, 1159–1164.
281. Gloeckner, D.C., Sacks, M.S., Fraser, M.O., Somogyi, G.T., de Groat, W.C., and Chancellor, M.B. (2002). Passive biaxial mechanical properties of the rat bladder wall after spinal cord injury. *J. Urol.* 167, 2247–52.
282. Wognum, S., Lagoa, C.E., Nagatomi, J., Sacks, M.S., and Vodovotz, Y. (2009). An exploratory pathways analysis of temporal changes induced by spinal cord injury in the rat bladder wall: insights on remodeling and inflammation. *PLoS One* 4, e5852.

283. Steers, W.D., Kolbeck, S., Creedon, D., and Tuttle, J.B. (1991). Nerve growth factor in the urinary bladder of the adult regulates neuronal form and function. *J. Clin. Invest.* 88, 1709–1715.
284. Ochodnický, P., Cruz, C.D., Yoshimura, N., and Cruz, F. (2012). Neurotrophins as regulators of urinary bladder function. *Nat. Rev. Urol.* 9, 628–637.
285. Ochodnický, P., Cruz, C.D., Yoshimura, N., and Michel, M.C. (2011). Nerve growth factor in bladder dysfunction: Contributing factor, biomarker, and therapeutic target. *Neurourol. Urodyn.* 30, n/a-n/a.
286. Gabella, G., and Uvelius, B. (1993). Effect of decentralization or contralateral ganglionectomy on obstruction-induced hypertrophy of rat urinary bladder muscle and pelvic ganglion. *J. Neurocytol.* 22, 827–34.
287. Gabella, G., Berggren, T., and Uvelius, B. (1992). Hypertrophy and reversal of hypertrophy in rat pelvic ganglion neurons. *J. Neurocytol.* 21, 649–62.
288. Yoshimura, N. (1999). Bladder afferent pathway and spinal cord injury: possible mechanisms inducing hyperreflexia of the urinary bladder. *Prog. Neurobiol.* 57, 583–606.
289. Hamburger, V., and Levi-Montalcini, R. (1949). Proliferation, differentiation and degeneration in the spinal ganglia of the chick embryo under normal and experimental conditions. *J. Exp. Zool.* 111, 457–501.
290. Davies, A.M. (1994). Neurotrophic Factors: Switching neurotrophin dependence. *Curr. Biol.* 4, 273–276.
291. Francis, N.J., and Landis, S.C. (1999). Cellular and molecular determinants of sympathetic neuron development. *Annu. Rev. Neurosci.* 22, 541–566.
292. Shadiack, A.M., Sun, Y., and Zigmond, R.E. (2001). Nerve growth factor antiserum

- induces axotomy-like changes in neuropeptide expression in intact sympathetic and sensory neurons. *J. Neurosci.* 21, 363–71.
293. Zigmond, R.E. (1997). LIF, NGF, and the Cell Body Response to Axotomy. *Neurosci.* 3, 176–185.
294. Zigmond, R.E., Hyatt-Sachs, H., Mohny, R.P., Schreiber, R.C., Shadiack, A.M., Sun, Y., and Vaccariello, S.A. (1996). Changes in neuropeptide phenotype after axotomy of adult peripheral neurons and the role of leukemia inhibitory factor. *Perspect. Dev. Neurobiol.* 4, 75–90.
295. Verge, V.M., Richardson, P.M., Wiesenfeld-Hallin, Z., and Hökfelt, T. (1995). Differential influence of nerve growth factor on neuropeptide expression in vivo: a novel role in peptide suppression in adult sensory neurons. *J. Neurosci.* 15, 2081–96.
296. Ruit, K.G., Osborne, P.A., Schmidt, R.E., Johnson, E.M., and Snider, W.D. (1990). Nerve growth factor regulates sympathetic ganglion cell morphology and survival in the adult mouse. *J. Neurosci.* 10, 2412–9.
297. Foditsch, E.E., Roider, K., Patras, I., Hutu, I., Bauer, S., Janetschek, G., and Zimmermann, R. (2017). Structural Changes of the Urinary Bladder After Chronic Complete Spinal Cord Injury in Minipigs. *Int. Neurourol. J.* 21, 12–19.
298. Miller, F.D., Speelman, A., Mathew, T.C., Fabian, J., Chang, E., Pozniak, C., and Toma, J.G. (1994). Nerve Growth Factor Derived from Terminals Selectively Increases the Ratio of p75 to trkA NGF Receptors on Mature Sympathetic Neurons. *Dev. Biol.* 161, 206–217.
299. Trapnell, C., Roberts, A., Goff, L., Pertea, G., Kim, D., Kelley, D.R., Pimentel, H., Salzberg, S.L., Rinn, J.L., and Pachter, L. (2012). Differential gene and transcript expression analysis of RNA-seq experiments with TopHat and Cufflinks. *Nat. Protoc.* 7,

- 562–578.
300. Anders, S., and Huber, W. (2010). Differential expression analysis for sequence count data. *Genome Biol.* 11, R106.
 301. Huang, D.W., Sherman, B.T., and Lempicki, R.A. (2009). Systematic and integrative analysis of large gene lists using DAVID bioinformatics resources. *Nat. Protoc.* 4, 44–57.
 302. Huang, D.W., Sherman, B.T., and Lempicki, R.A. (2009). Bioinformatics enrichment tools: paths toward the comprehensive functional analysis of large gene lists. *Nucleic Acids Res.* 37, 1–13.
 303. Krämer, A., Green, J., Pollard, J., Tugendreich, S., and Tugendreich, S. (2014). Causal analysis approaches in Ingenuity Pathway Analysis. *Bioinformatics* 30, 523–30.
 304. Schmittgen, T.D., and Livak, K.J. (2008). Analyzing real-time PCR data by the comparative C(T) method. *Nat. Protoc.* 3, 1101–8.
 305. Schindelin, J., Arganda-Carreras, I., Frise, E., Kaynig, V., Longair, M., Pietzsch, T., Preibisch, S., Rueden, C., Saalfeld, S., Schmid, B., Tinevez, J.-Y., White, D.J., Hartenstein, V., Eliceiri, K., Tomancak, P., and Cardona, A. (2012). Fiji: an open-source platform for biological-image analysis. *Nat. Methods* 9, 676–682.
 306. Rose, R.D., and Rohrlich, D. (1988). Counting sectioned cells via mathematical reconstruction. *J. Comp. Neurol.* 272, 365.
 307. Ramer, M.S., Bradbury, E.J., and McMahon, S.B. (2001). Nerve growth factor induces P2X3 expression in sensory neurons. *J. Neurochem.* 77, 864–875.
 308. Hüttemann, M., Lee, I., Samavati, L., Yu, H., and Doan, J.W. (2007). Regulation of mitochondrial oxidative phosphorylation through cell signaling. *Biochim. Biophys. Acta - Mol. Cell Res.* 1773, 1701–1720.

309. Leonard, D.G., Gorham, J.D., Cole, P., Greene, L.A., and Ziff, E.B. (1988). A nerve growth factor-regulated messenger RNA encodes a new intermediate filament protein. *J. Cell Biol.* 106, 181–93.
310. DeCouto, S.A., Jones, E.E., Kudwa, A.E., Shoemaker, S.E., Shafer, A.J., Brieschke, M.A., James, P.F., Vaughn, J.C., and Isaacson, L.G. (2003). The effects of deafferentation and exogenous NGF on neurotrophins and neurotrophin receptor mRNA expression in the adult superior cervical ganglion. *Brain Res. Mol. Brain Res.* 119, 73–82.
311. Bronfman, F.C., Tcherpakov, M., Jovin, T.M., and Fainzilber, M. (2003). Ligand-induced internalization of the p75 neurotrophin receptor: a slow route to the signaling endosome. *J. Neurosci.* 23, 3209–20.
312. Kuwako, K., Hosokawa, A., Nishimura, I., Uetsuki, T., Yamada, M., Nada, S., Okada, M., and Yoshikawa, K. (2005). Disruption of the paternal *necdin* gene diminishes TrkA signaling for sensory neuron survival. *J. Neurosci.* 25, 7090–9.
313. Lee, X., Yang, Z., Shao, Z., Rosenberg, S.S., Levesque, M., Pepinsky, R.B., Qiu, M., Miller, R.H., Chan, J.R., and Mi, S. (2007). NGF regulates the expression of axonal LINGO-1 to inhibit oligodendrocyte differentiation and myelination. *J. Neurosci.* 27, 220–5.
314. Meabon, J.S., De Laat, R., Ieguchi, K., Wiley, J.C., Hudson, M.P., and Bothwell, M. (2015). LINGO-1 protein interacts with the p75 neurotrophin receptor in intracellular membrane compartments. *J. Biol. Chem.* 290, 9511–20.
315. Meabon, J.S., de Laat, R., Ieguchi, K., Serbzhinsky, D., Hudson, M.P., Huber, B.R., Wiley, J.C., and Bothwell, M. (2016). Intracellular LINGO-1 negatively regulates Trk neurotrophin receptor signaling. *Mol. Cell. Neurosci.* 70, 1–10.

316. Coggeshall, R.E., and Carlton, S.M. (1999). Evidence for an inflammation-induced change in the local glutamatergic regulation of postganglionic sympathetic efferents. *Pain* 83, 163–8.
317. Doherty, P., and Walsh, F.S. (1987). Control of Thy-1 glycoprotein expression in cultures of PC12 cells. *J. Neurochem.* 49, 610–6.
318. Hou, X.E., and Dahlström, A. (1996). Synaptic vesicle proteins in cells of the sympathoadrenal lineage. *J. Auton. Nerv. Syst.* 61, 301–12.
319. Kataoka, M., Kuwahara, R., Iwasaki, S., Shoji-Kasai, Y., and Takahashi, M. (2000). Nerve growth factor-induced phosphorylation of SNAP-25 in PC12 cells: a possible involvement in the regulation of SNAP-25 localization. *J. Neurochem.* 74, 2058–66.
320. Vickers, J.C., Chiu, F.C., and Costa, M. (1992). Selective distribution of the 66-kDa neuronal intermediate filament protein in the sensory and autonomic nervous system of the guinea-pig. *Brain Res.* 585, 205–11.
321. Ren, B., Li, X., Zhang, J., Fan, J., Duan, J., and Chen, Y. (2015). PDLIM5 mediates PKC ϵ translocation in PMA-induced growth cone collapse. *Cell. Signal.* 27, 424–35.
322. Herrick, S., Evers, D.M., Lee, J.-Y., Udagawa, N., and Pak, D.T.S. (2010). Postsynaptic PDLIM5/Enigma Homolog binds SPAR and causes dendritic spine shrinkage. *Mol. Cell. Neurosci.* 43, 188–200.
323. Prato, V., Taberner, F.J., Hockley, J.R.F., Callejo, G., Arcourt, A., Tazir, B., Hammer, L., Schad, P., Heppenstall, P.A., Smith, E.S., and Lechner, S.G. (2017). Functional and Molecular Characterization of Mechanoinsensitive “Silent” Nociceptors. *Cell Rep.* 21, 3102–3115.
324. Salvatierra, J., Castro, J., Erickson, A., Li, Q., Braz, J., Gilchrist, J., Grundy, L., Rychkov,

- G.Y., Deiteren, A., Rais, R., King, G.F., Slusher, B.S., Basbaum, A., Pasricha, P.J., Brierley, S.M., and Bosmans, F. (2018). NaV1.1 inhibition can reduce visceral hypersensitivity. *JCI insight* 3.
325. Paravicini, U., Stoeckel, K., and Thoenen, H. (1975). Biological importance of retrograde axonal transport of nerve growth factor in adrenergic neurons. *Brain Res.* 84, 279–91.
326. Hendry, I.A. (1975). The response of adrenergic neurones to axotomy and nerve growth factor. *Brain Res.* 94, 87–97.
327. Weihe, E., Schäfer, M.K., Erickson, J.D., and Eiden, L.E. (1994). Localization of vesicular monoamine transporter isoforms (VMAT1 and VMAT2) to endocrine cells and neurons in rat. *J. Mol. Neurosci.* 5, 149–64.
328. Peter, D., Liu, Y., Sternini, C., de Giorgio, R., Brecha, N., and Edwards, R.H. (1995). Differential expression of two vesicular monoamine transporters. *J. Neurosci.* 15, 6179–88.
329. Schütz, B., Schäfer, M.K., Eiden, L.E., and Weihe, E. (1998). Vesicular amine transporter expression and isoform selection in developing brain, peripheral nervous system and gut. *Brain Res. Dev. Brain Res.* 106, 181–204.
330. Niu, J., Ding, L., Li, J.J., Kim, H., Liu, J., Li, H., Moberly, A., Badea, T.C., Duncan, I.D., Son, Y.-J., Scherer, S.S., and Luo, W. (2013). Modality-based organization of ascending somatosensory axons in the direct dorsal column pathway. *J. Neurosci.* 33, 17691–709.
331. Jackson, T.C., Manole, M.D., Kotermanski, S.E., Jackson, E.K., Clark, R.S.B., and Kochanek, P.M. (2015). Cold stress protein RBM3 responds to temperature change in an ultra-sensitive manner in young neurons. *Neuroscience* 305, 268–278.
332. Liu, J., Xue, J., Zhang, H., Li, S., Liu, Y., Xu, D., Zou, M., Zhang, Z., and Diao, J. (2015).

- Cloning, expression, and purification of cold inducible RNA-binding protein and its neuroprotective mechanism of action. *Brain Res.* 1597, 189–195.
333. Zhou, M., Yang, W.-L., Ji, Y., Qiang, X., and Wang, P. (2014). Cold-inducible RNA-binding protein mediates neuroinflammation in cerebral ischemia. *Biochim. Biophys. Acta - Gen. Subj.* 1840, 2253–2261.
334. Zhou, R.-B., Lu, X.-L., Zhang, C.-Y., and Yin, D.-C. (2017). RNA binding motif protein 3: a potential biomarker in cancer and therapeutic target in neuroprotection. *Oncotarget* 8, 22235–22250.
335. Huang, D.W., Sherman, B.T., Tan, Q., Collins, J.R., Alvord, W.G., Roayaei, J., Stephens, R., Baseler, M.W., Lane, H.C., and Lempicki, R.A. (2007). The DAVID Gene Functional Classification Tool: a novel biological module-centric algorithm to functionally analyze large gene lists. *Genome Biol.* 8, R183.
336. Gu, Y., Chen, Y., Zhang, X., Li, G.-W., Wang, C., and Huang, L.-Y.M. (2010). Neuronal soma-satellite glial cell interactions in sensory ganglia and the participation of purinergic receptors. *Neuron Glia Biol.* 6, 53–62.
337. Huang, W.L., Robson, D., Liu, M.C., King, V.R., Averill, S., Shortland, P.J., and Priestley, J. V. (2006). Spinal cord compression and dorsal root injury cause up-regulation of activating transcription factor-3 in large-diameter dorsal root ganglion neurons. *Eur. J. Neurosci.* 23, 273–278.
338. Brumovsky, P., Watanabe, M., and Hökfelt, T. (2007). Expression of the vesicular glutamate transporters-1 and -2 in adult mouse dorsal root ganglia and spinal cord and their regulation by nerve injury. *Neuroscience* 147, 469–490.
339. Wang, S., Elitt, C.M., Malin, S.A., and Albers, K.M. (2008). Effects of the neurotrophic

- factor artemin on sensory afferent development and sensitivity. *Sheng Li Xue Bao* 60, 565–70.
340. Grothe, C., Meisinger, C., and Claus, P. (2001). In vivo expression and localization of the fibroblast growth factor system in the intact and lesioned rat peripheral nerve and spinal ganglia. *J. Comp. Neurol.* 434, 342–57.
341. Grothe, C., Meisinger, C., Hertenstein, A., Kurz, H., and Wewetzer, K. (1997). Expression of fibroblast growth factor-2 and fibroblast growth factor receptor 1 messenger RNAs in spinal ganglia and sciatic nerve: regulation after peripheral nerve lesion. *Neuroscience* 76, 123–35.
342. Hausott, B., Rietzler, A., Vallant, N., Auer, M., Haller, I., Perkhofer, S., and Klimaschewski, L. (2011). Inhibition of fibroblast growth factor receptor 1 endocytosis promotes axonal branching of adult sensory neurons. *Neuroscience* 188, 13–22.
343. Hausott, B., Vallant, N., Hochfilzer, M., Mangger, S., Irschick, R., Haugsten, E.M., and Klimaschewski, L. (2012). Leupeptin enhances cell surface localization of fibroblast growth factor receptor 1 in adult sensory neurons by increased recycling. *Eur. J. Cell Biol.* 91, 129–38.
344. Hausott, B., Schlick, B., Vallant, N., Dorn, R., and Klimaschewski, L. (2008). Promotion of neurite outgrowth by fibroblast growth factor receptor 1 overexpression and lysosomal inhibition of receptor degradation in pheochromocytoma cells and adult sensory neurons. *Neuroscience* 153, 461–73.
345. Hadjab, S., Franck, M.C.M., Wang, Y., Sterzenbach, U., Sharma, A., Ernfors, P., and Lallemand, F. (2013). A local source of FGF initiates development of the unmyelinated lineage of sensory neurons. *J. Neurosci.* 33, 17656–66.

346. Furusho, M., Dupree, J.L., Bryant, M., and Bansal, R. (2009). Disruption of fibroblast growth factor receptor signaling in nonmyelinating Schwann cells causes sensory axonal neuropathy and impairment of thermal pain sensitivity. *J. Neurosci.* 29, 1608–14.
347. Haenzi, B., and Moon, L.D.F. (2017). The Function of FGFR1 Signalling in the Spinal Cord: Therapeutic Approaches Using FGFR1 Ligands after Spinal Cord Injury. *Neural Plast.* 2017, 2740768.
348. Frias, B., Santos, J., Morgado, M., Sousa, M.M., Gray, S.M.Y., McCloskey, K.D., Allen, S., Cruz, F., and Cruz, C.D. (2015). The Role of Brain-Derived Neurotrophic Factor (BDNF) in the Development of Neurogenic Detrusor Overactivity (NDO). *J. Neurosci.* 35, 2146–2160.
349. King, V.R., Bradbury, E.J., McMahon, S.B., and Priestley, J. V. (2000). Changes in truncated trkB and p75 receptor expression in the rat spinal cord following spinal cord hemisection and spinal cord hemisection plus neurotrophin treatment. *Exp. Neurol.* 165, 327–41.
350. Widenfalk, J., Lundströmer, K., Jubran, M., Brene, S., and Olson, L. (2001). Neurotrophic factors and receptors in the immature and adult spinal cord after mechanical injury or kainic acid. *J. Neurosci.* 21, 3457–75.
351. Liebl, D.J., Huang, W., Young, W., and Parada, L.F. (2001). Regulation of Trk receptors following contusion of the rat spinal cord. *Exp. Neurol.* 167, 15–26.
352. Deppmann, C.D., Mihalas, S., Sharma, N., Lonze, B.E., Niebur, E., and Ginty, D.D. (2008). A model for neuronal competition during development. *Science* 320, 369–73.
353. Kumer, S.C., and Vrana, K.E. (1996). Intricate regulation of tyrosine hydroxylase activity and gene expression. *J. Neurochem.* 67, 443–62.

354. Keast, J.R. (1995). Visualization and immunohistochemical characterization of sympathetic and parasympathetic neurons in the male rat major pelvic ganglion. *Neuroscience* 66, 655–62.
355. Girard, B.M., Galli, J.R., Young, B.A., Vizzard, M.A., and Parsons, R.L. (2010). PACAP expression in explant cultured mouse major pelvic ganglia. *J. Mol. Neurosci.* 42, 370–7.
356. Minis, A., Dahary, D., Manor, O., Leshkowitz, D., Pilpel, Y., and Yaron, A. (2014). Subcellular transcriptomics-dissection of the mRNA composition in the axonal compartment of sensory neurons. *Dev. Neurobiol.* 74, 365–81.
357. Beaudet, M.M., Braas, K.M., and May, V. (1998). Pituitary adenylate cyclase activating polypeptide (PACAP) expression in sympathetic preganglionic projection neurons to the superior cervical ganglion. *J. Neurobiol.* 36, 325–36.
358. May, V., and Vizzard, M.A. (2010). Bladder dysfunction and altered somatic sensitivity in PACAP^{-/-} mice. *J. Urol.* 183, 772–9.
359. Girard, B.M., Malley, S.E., Braas, K.M., May, V., and Vizzard, M.A. (2010). PACAP/VIP and receptor characterization in micturition pathways in mice with overexpression of NGF in urothelium. *J. Mol. Neurosci.* 42, 378–89.
360. Hansson, S.R., Mezey, E., and Hoffman, B.J. (1998). Ontogeny of vesicular monoamine transporter mRNAs VMAT1 and VMAT2. II. Expression in neural crest derivatives and their target sites in the rat. *Brain Res. Dev. Brain Res.* 110, 159–74.
361. Weihe, E., Tao-Cheng, J.H., Schäfer, M.K., Erickson, J.D., and Eiden, L.E. (1996). Visualization of the vesicular acetylcholine transporter in cholinergic nerve terminals and its targeting to a specific population of small synaptic vesicles. *Proc. Natl. Acad. Sci. U. S. A.* 93, 3547–52.

362. Matthews, M.R. (1989). Small, intensely fluorescent cells and the paraneuron concept. *J. Electron Microsc. Tech.* 12, 408–16.
363. Meeker, R., and Williams, K. (2014). Dynamic nature of the p75 neurotrophin receptor in response to injury and disease. *J. Neuroimmune Pharmacol.* 9, 615–28.
364. Caroleo, M.C., Costa, N., Bracci-Laudiero, L., and Aloe, L. (2001). Human monocyte/macrophages activate by exposure to LPS overexpress NGF and NGF receptors. *J. Neuroimmunol.* 113, 193–201.
365. Minnone, G., De Benedetti, F., and Bracci-Laudiero, L. (2017). NGF and Its Receptors in the Regulation of Inflammatory Response. *Int. J. Mol. Sci.* 18, 1028.
366. Roberson, M.D., Toews, A.D., Bouldin, T.W., Weaver, J., Goines, N.D., and Morell, P. (1995). NGFR-mRNA expression in sciatic nerve: a sensitive indicator of early stages of axonopathy. *Brain Res. Mol. Brain Res.* 28, 231–8.
367. Wyatt, S., and Davies, A.M. (1995). Regulation of nerve growth factor receptor gene expression in sympathetic neurons during development. *J. Cell Biol.* 130, 1435–46.
368. Zhou, J., Valletta, J.S., Grimes, M.L., and Mobley, W.C. (2002). Multiple Levels for Regulation of TrkA in PC12 Cells by Nerve Growth Factor. *J. Neurochem.* 65, 1146–1156.
369. Miller, F.D., Mathew, T.C., and Toma, J.G. (1991). Regulation of nerve growth factor receptor gene expression by nerve growth factor in the developing peripheral nervous system. *J. Cell Biol.* 112, 303–12.
370. Zigmond, R.E., and Sun, Y. (1997). Regulation of neuropeptide expression in sympathetic neurons. Paracrine and retrograde influences. *Ann. N. Y. Acad. Sci.* 814, 181–97.
371. Gizang-Ginsberg, E., and Ziff, E.B. (1990). Nerve growth factor regulates tyrosine

- hydroxylase gene transcription through a nucleoprotein complex that contains c-Fos. *Genes Dev.* 4, 477–91.
372. Ramer, M.S., Bradbury, E.J., Michael, G.J., Lever, I.J., and McMahon, S.B. (2003). Glial cell line-derived neurotrophic factor increases calcitonin gene-related peptide immunoreactivity in sensory and motoneurons in vivo. *Eur. J. Neurosci.* 18, 2713–21.
373. Davis, B.M., Wang, H.S., Albers, K.M., Carlson, S.L., Goodness, T.P., and McKinnon, D. (1996). Effects of NGF overexpression on anatomical and physiological properties of sympathetic postganglionic neurons. *Brain Res.* 724, 47–54.
374. Goodness, T.P., Albers, K.M., Davis, F.E., and Davis, B.M. (1997). Overexpression of nerve growth factor in skin increases sensory neuron size and modulates Trk receptor expression. *Eur. J. Neurosci.* 9, 1574–85.
375. Elitt, C.M., McIlwrath, S.L., Lawson, J.J., Malin, S.A., Molliver, D.C., Cornuet, P.K., Koerber, H.R., Davis, B.M., and Albers, K.M. (2006). Artemin overexpression in skin enhances expression of TRPV1 and TRPA1 in cutaneous sensory neurons and leads to behavioral sensitivity to heat and cold. *J. Neurosci.* 26, 8578–87.
376. de Groat, W.C., Kawatani, M., Hisamitsu, T., Cheng, C.L., Ma, C.P., Thor, K., Steers, W., and Roppolo, J.R. (1990). Mechanisms underlying the recovery of urinary bladder function following spinal cord injury. *J. Auton. Nerv. Syst.* 30 Suppl, S71-7.
377. Dupont, M.C., Persson, K., Spitsbergen, J., Tuttle, J.B., and Steers, W.D. (1995). *The Neuronal Response to Bladder Outlet Obstruction, a Role for NGF.* Springer, Boston, MA, pps. 41–54.
378. Steers, W.D., Ciambotti, J., Etzel, B., Erdman, S., and de Groat, W.C. (1991). Alterations in afferent pathways from the urinary bladder of the rat in response to partial urethral

- obstruction. *J. Comp. Neurol.* 310, 401–410.
379. Tuttle, J.B., and Steers, W.D. (1992). Nerve growth factor responsiveness of cultured major pelvic ganglion neurons from the adult rat. *Brain Res.* 588, 29–40.
380. Suzuki, T., and Ushiyama, T. (2001). Vesicoureteral reflux in the early stage of spinal cord injury: a retrospective study. *Spinal Cord* 39, 23–25.
381. Ozsoy, O., Ozsoy, U., Stein, G., Semler, O., Skouras, E., Schempf, G., Wellmann, K., Wirth, F., Angelova, S., Ankerne, J., Ashrafi, M., Schönau, E., Papamitsou-Sidoropolou, T., Jaminet, P., Sarikcioglu, L., Irintchev, A., Dunlop, S., Angelov, D., and Angelov, D.N. (2012). Functional deficits and morphological changes in the neurogenic bladder match the severity of spinal cord compression. *Restor. Neurol. Neurosci.* 30, 363–381.
382. Motulsky, H.J., and Brown, R.E. (2006). Detecting outliers when fitting data with nonlinear regression - a new method based on robust nonlinear regression and the false discovery rate. *BMC Bioinformatics* 7, 123.
383. David, B.T., and Steward, O. (2010). Deficits in bladder function following spinal cord injury vary depending on the level of the injury. *Exp. Neurol.* 226, 128–135.
384. Hancock, M.B., and Peveto, C.A. (1979). A preganglionic autonomic nucleus in the dorsal gray commissure of the lumbar spinal cord of the rat. *J. Comp. Neurol.* 183, 65–72.
385. Kepper, M.E., and Keast, J.R. (1998). Specific targeting of ganglion cell sprouts provides an additional mechanism for restoring peripheral motor circuits in pelvic ganglia after spinal nerve damage. *J. Neurosci.* 18, 7987–7995.
386. Holets, V., and Elde, R. (1982). The differential distribution and relationship of serotonergic and peptidergic fibers to sympathoadrenal neurons in the intermediolateral cell column of the rat: a combined retrograde axonal transport and immunofluorescence

- study. *Neuroscience* 7, 1155–74.
387. Sun, Y., Rao, M.S., Zigmond, R.E., and Landis, S.C. (1994). Regulation of vasoactive intestinal peptide expression in sympathetic neurons in culture and after axotomy: The role of cholinergic differentiation factor/leukemia inhibitory factor. *J. Neurobiol.* 25, 415–430.
388. Schotzinger, R., Yin, X., and Landis, S. (1994). Target determination of neurotransmitter phenotype in sympathetic neurons. *J. Neurobiol.* 25, 620–39.
389. Sun, Y., and Zigmond, R.E. (1996). Involvement of leukemia inhibitory factor in the increases in galanin and vasoactive intestinal peptide mRNA and the decreases in neuropeptide Y and tyrosine hydroxylase mRNA in sympathetic neurons after axotomy. *J. Neurochem.* 67, 1751–60.
390. Geissen, M., Heller, S., Pennica, D., Ernsberger, U., and Rohrer, H. (1998). The specification of sympathetic neurotransmitter phenotype depends on gp130 cytokine receptor signaling. *Development* 125, 4791–801.
391. Dail, W.G., Minorsky, N., Moll, M.A., and Manzanares, K. (1986). The hypogastric nerve pathway to penile erectile tissue: histochemical evidence supporting a vasodilator role. *J. Auton. Nerv. Syst.* 15, 341–9.
392. Shin, T.-Y., Ryu, J.-K., Jin, H.-R., Piao, S., Tumurbaatar, M., Yin, G.N., Shin, S.H., Kwon, M.-H., Song, K.-M., Fang, Z.-H., Han, J.-Y., Kim, W.J., and Suh, J.-K. (2011). Increased Cavernous Expression of Transforming Growth Factor- β 1 and Activation of the Smad Signaling Pathway Affects Erectile Dysfunction in Men with Spinal Cord Injury. *J. Sex. Med.* 8, 1454–1462.
393. Keast, J.R., and Kepper, M.E. (2001). Differential regulation of trkA and p75 in

- noradrenergic pelvic autonomic ganglion cells after deafferentation of their cholinergic neighbours. *Eur. J. Neurosci.* 13, 211–20.
394. Max, S.R., Rohrer, H., Otten, U., and Thoenen, H. (1978). Nerve growth factor-mediated induction of tyrosine hydroxylase in rat superior cervical ganglia in vitro. *J. Biol. Chem.* 253, 8013–5.
395. Ma, Y., Campenot, R.B., and Miller, F.D. (1992). Concentration-dependent regulation of neuronal gene expression by nerve growth factor. *J. Cell Biol.* 117, 135–41.
396. Verdi, J.M., and Anderson, D.J. (1994). Neurotrophins regulate sequential changes in neurotrophin receptor expression by sympathetic neuroblasts. *Neuron* 13, 1359–72.
397. Zhou, X.F., Rush, R.A., and McLachlan, E.M. (1996). Differential expression of the p75 nerve growth factor receptor in glia and neurons of the rat dorsal root ganglia after peripheral nerve transection. *J. Neurosci.* 16, 2901–11.
398. Tyagi, P., Kadekawa, K., Kashyap, M., Pore, S., and Yoshimura, N. (2016). Spontaneous Recovery of Reflex Voiding Following Spinal Cord Injury Mediated by Anti-inflammatory and Neuroprotective Factors. *Urology* 88, 57–65.
399. Lewis, S.E., Rao, M.S., Symes, A.J., Dauer, W.T., Fink, J.S., Landis, S.C., and Hyman, S.E. (1994). Coordinate regulation of choline acetyltransferase, tyrosine hydroxylase, and neuropeptide mRNAs by ciliary neurotrophic factor and leukemia inhibitory factor in cultured sympathetic neurons. *J. Neurochem.* 63, 429–38.
400. Damon, D.H. (2008). TH and NPY in sympathetic neurovascular cultures: role of LIF and NT-3. *Am. J. Physiol. Cell Physiol.* 294, C306-12.
401. Parrish, D.C., Alston, E.N., Rohrer, H., Nkadi, P., Woodward, W.R., Schütz, G., and Habecker, B.A. (2010). Infarction-induced cytokines cause local depletion of tyrosine

- hydroxylase in cardiac sympathetic nerves. *Exp. Physiol.* 95, 304–14.
402. Shi, X., and Habecker, B.A. (2012). gp130 cytokines stimulate proteasomal degradation of tyrosine hydroxylase via extracellular signal regulated kinases 1 and 2. *J. Neurochem.* 120, 239–47.
403. Adam, R.M., Eaton, S.H., Estrada, C., Nimgaonkar, A., Shih, S.-C., Smith, L.E.H., Kohane, I.S., Bāgli, D., and Freeman, M.R. (2004). Mechanical stretch is a highly selective regulator of gene expression in human bladder smooth muscle cells. *Physiol. Genomics* 20, 36–44.
404. Guo, X., Chandrasekaran, V., Lein, P., Kaplan, P.L., and Higgins, D. (1999). Leukemia inhibitory factor and ciliary neurotrophic factor cause dendritic retraction in cultured rat sympathetic neurons. *J. Neurosci.* 19, 2113–21.
405. Panni, M.K., Atkinson, J., and Sofroniew, M. V. (1999). Leukaemia inhibitory factor prevents loss of p75-nerve growth factor receptor immunoreactivity in medial septal neurons following fimbria-fornix lesions. *Neuroscience* 89, 1113–21.
406. Al Taweel, W., and Seyam, R. (2015). Neurogenic bladder in spinal cord injury patients. *Res. Reports Urol.* , 85.
407. Sherrington, C.S. (1892). Notes on the Arrangement of some Motor Fibres in the Lumbo-Sacral Plexus. *J. Physiol.* 13, 621–772.
408. Vahabi, B., and Drake, M.J. (2015). Physiological and pathophysiological implications of micromotion activity in urinary bladder function. *Acta Physiol.* 213, 360–370.
409. Heppner, T.J., Tykocki, N.R., Hill-Eubanks, D., and Nelson, M.T. (2016). Transient contractions of urinary bladder smooth muscle are drivers of afferent nerve activity during filling. *J. Gen. Physiol.* 147, 323–35.

410. Iijima, K., Igawa, Y., and Wyndaele, J.J. (2009). Mechanosensitive Primary Bladder Afferent Activity in Rats With and Without Spinal Cord Transection. *J. Urol.* 182, 2504–2510.
411. Lagou, M., Drake, M.J., and Gillespie, J.I. (2004). Volume-induced effects on the isolated bladder: a possible local reflex. *BJU Int.* 94, 1356–1365.
412. Drake, M.J., Hedlund, P., Harvey, I.J., Pandita, R.K., Andersson, K.-E., and Gillespie, J.I. (2003). Partial Outlet Obstruction Enhances Modular Autonomous Activity in the Isolated Rat Bladder. *J. Urol.* 170, 276–279.
413. Kruse, M.N., Belton, A.L., and de Groat, W.C. (1993). Changes in bladder and external urethral sphincter function after spinal cord injury in the rat. *Am. J. Physiol.* 264, R1157-63.
414. Pikov, V., Gillis, R.A., Jasmin, L., and Wrathall, J.R. (1998). Assessment of lower urinary tract functional deficit in rats with contusive spinal cord injury. *J. Neurotrauma* 15, 375–86.
415. Ikeda, Y., and Kanai, a. (2008). Urotheliogenic modulation of intrinsic activity in spinal cord-transected rat bladders: role of mucosal muscarinic receptors. *Am. J. Physiol. Renal Physiol.* 295, F454-61.
416. Yoshiyama, M., and de Groat, W.C. (2002). Effect of Bilateral Hypogastric Nerve Transection on Voiding Dysfunction in Rats with Spinal Cord Injury. *Exp. Neurol.* 175, 191–197.
417. Hou, S., Carson, D.M., Wu, D., Klaw, M.C., Houlé, J.D., and Tom, V.J. (2016). Dopamine is produced in the rat spinal cord and regulates micturition reflex after spinal cord injury. *Exp. Neurol.* 285, 136–146.

418. Pollock, D.M., Butterfield, M.I., Ader, J.L., and Arendshorst, W.J. (1986). Dissociation of urinary kallikrein activity and salt and water excretion in the rat. *Am. J. Physiol. - Ren. Physiol.* 250.
419. Samson, G., and Cardenas, D.D. (2007). Neurogenic bladder in spinal cord injury. *Phys. Med. Rehabil. Clin. N. Am.* 18, 255–74, vi.
420. Schmid, A., Huonker, M., Barturen, J.-M., Stahl, F., Schmidt-Trucksäss, A., König, D., Grathwohl, D., Lehmann, M., and Keul, J. (1998). Catecholamines, heart rate, and oxygen uptake during exercise in persons with spinal cord injury. *J. Appl. Physiol.* 85.
421. Schmid, A., Huonker, M., Stahl, F., Barturen, J.M., König, D., Heim, M., Lehmann, M., and Keul, J. (1998). Free plasma catecholamines in spinal cord injured persons with different injury levels at rest and during exercise. *J. Auton. Nerv. Syst.* 68, 96–100.
422. Gu, X., Simons, F.E., and Simons, K.J. (1999). Epinephrine absorption after different routes of administration in an animal model. *Biopharm. Drug Dispos.* 20, 401–5.
423. Persyn, S., Gillespie, J., Eastham, J., and De Wachter, S. (2016). Possible role of the major pelvic ganglion in the modulation of non-voiding activity in rats. *Auton. Neurosci.* 198, 33–37.
424. Schmid, A., Halle, M., Stütze, C., König, D., Baumstark, M.W., Storch, M.J., Schmidt-Trucksäss, A., Lehmann, M., Berg, A., and Keul, J. (2000). Lipoproteins and free plasma catecholamines in spinal cord injured men with different injury levels. *Clin. Physiol.* 20, 304–10.
425. Munro, A.F., and Robinson, R. (1960). The catecholamine content of the peripheral plasma in human subjects with complete transverse lesions of the spinal cord. *J. Physiol.* 154, 244–53.

426. Goldstein, D.S., McCarty, R., Polinsky, R.J., and Kopin, I.J. ([date unknown]). Relationship between plasma norepinephrine and sympathetic neural activity. *Hypertens.* (Dallas, Tex. 1979) 5, 552–9.
427. McCarty, R. (1983). Stress, behavior and experimental hypertension. *Neurosci. Biobehav. Rev.* 7, 493–502.
428. Fujimura, T., Tamura, K., Tsutsumi, T., Yamamoto, T., Nakamura, K., Koibuchi, Y., Kobayashi, M., and Yamaguchi, O. (1999). Expression and possible functional role of the beta3-adrenoceptor in human and rat detrusor muscle. *J. Urol.* 161, 680–5.
429. Seguchi, H., Nishimura, J., Zhou, Y., Niuro, N., Kumazawa, J., and Kanaide, H. (1998). Expression of beta3-adrenoceptors in rat detrusor smooth muscle. *J. Urol.* 159, 2197–201.
430. Michel, M.C., and Vrydag, W. (2006). α_1 -, α_2 - and β -adrenoceptors in the urinary bladder, urethra and prostate. *Br. J. Pharmacol.* 147, S88–S119.
431. Michel, M.C. (2015). Therapeutic modulation of urinary bladder function: multiple targets at multiple levels. *Annu. Rev. Pharmacol. Toxicol.* 55, 269–87.
432. Miyamoto, T., Mochizuki, T., Nakagomi, H., Kira, S., Watanabe, M., Takayama, Y., Suzuki, Y., Koizumi, S., Takeda, M., and Tominaga, M. (2014). Functional Role for Piezo1 in Stretch-evoked Ca^{2+} Influx and ATP Release in Urothelial Cell Cultures. *J. Biol. Chem.* 289, 16565–16575.
433. Michishita, M., Yano, K., Tomita, K., Matsuzaki, O., and Kasahara, K. (2016). Piezo1 expression increases in rat bladder after partial bladder outlet obstruction. *Life Sci.* 166, 1–7.
434. Lai, H., Gardner, V., Vetter, J., and Andriole, G.L. (2015). Correlation between psychological stress levels and the severity of overactive bladder symptoms. *BMC Urol.*

- 15, 14.
435. Lai, H.H., Rawal, A., Shen, B., and Vetter, J. (2016). The Relationship Between Anxiety and Overactive Bladder or Urinary Incontinence Symptoms in the Clinical Population. *Urology* 98, 50–57.
436. Wood, S.K., Baez, M.A., Bhatnagar, S., and Valentino, R.J. (2009). Social stress-induced bladder dysfunction: potential role of corticotropin-releasing factor. *AJP Regul. Integr. Comp. Physiol.* 296, R1671–R1678.
437. Ryken, T.C., Hurlbert, R.J., Hadley, M.N., Aarabi, B., Dhall, S.S., Gelb, D.E., Rozzelle, C.J., Theodore, N., and Walters, B.C. (2013). The acute cardiopulmonary management of patients with cervical spinal cord injuries. *Neurosurgery* 72 Suppl 2, 84–92.
438. Inoue, T., Manley, G.T., Patel, N., and Whetstone, W.D. (2014). Medical and surgical management after spinal cord injury: vasopressor usage, early surgerys, and complications. *J. Neurotrauma* 31, 284–91.
439. Streijger, F., So, K., Manouchehri, N., Gheorghe, A., Okon, E.B., Chan, R.M., Ng, B., Shortt, K., Sekhon, M.S., Griesdale, D.E., and Kwon, B.K. (2018). A Direct Comparison between Norepinephrine and Phenylephrine for Augmenting Spinal Cord Perfusion in a Porcine Model of Spinal Cord Injury. *J. Neurotrauma* 35, 1345–1357.
440. de Groat, W.C. (1993). Anatomy and physiology of the lower urinary tract. *Urol. Clin. North Am.* 20, 383–401.
441. Hou, S., Rabchevsky, A.G., Hou, S., and Rabchevsky, A.G. (2014). Autonomic Consequences of Spinal Cord Injury., in: *Comprehensive Physiology*. Hoboken, NJ, USA: John Wiley & Sons, Inc., pps. 1419–1453.
442. Keast, J.. (2004). Remodelling of connections in pelvic ganglia after hypogastric nerve

- crush. *Neuroscience* 126, 405–414.
443. Doxakis, E. (2014). RNA binding proteins: a common denominator of neuronal function and dysfunction. *Neurosci. Bull.* 30, 610–626.
444. Liu, Y., Beyer, A., and Aebersold, R. (2016). On the Dependency of Cellular Protein Levels on mRNA Abundance. *Cell* 165, 535–50.
445. Luckensmeyer, G.B., and Keast, J.R. (1995). Immunohistochemical characterisation of sympathetic and parasympathetic pelvic neurons projecting to the distal colon in the male rat. *Cell Tissue Res.* 281, 551–9.
446. Buettner, F., Natarajan, K.N., Casale, F.P., Proserpio, V., Scialdone, A., Theis, F.J., Teichmann, S.A., Marioni, J.C., and Stegle, O. (2015). Computational analysis of cell-to-cell heterogeneity in single-cell RNA-sequencing data reveals hidden subpopulations of cells. *Nat. Biotechnol.* 33, 155–160.
447. Potter, S.S. (2018). Single-cell RNA sequencing for the study of development, physiology and disease. *Nat. Rev. Nephrol.* , 1–14.
448. Monjotin, N., Farrié, M., Vergnolle, N., Le Grand, B., Gillespie, J., and Junquero, D. (2017). Bladder telemetry: A new approach to evaluate micturition behavior under physiological and inflammatory conditions. *Neurourol. Urodyn.* 36, 308–315.
449. Balsara, Z.R., Ross, S.S., Dolber, P.C., Wiener, J.S., Tang, Y., and Seed, P.C. (2013). Enhanced susceptibility to urinary tract infection in the spinal cord-injured host with neurogenic bladder. *Infect. Immun.* 81, 3018–26.
450. Lucin, K., Sanders, V., Jones, T., Malarkey, W., and Popovich, P. (2007). Impaired antibody synthesis after spinal cord injury is level dependent and is due to sympathetic nervous system dysregulation. *Exp. Neurol.* 207, 75–84.

451. Hougland, M.T., Harrison, B.J., Magnuson, D.S.K., Rouchka, E.C., and Petruska, J.C. (2013). The Transcriptional Response of Neurotrophins and Their Tyrosine Kinase Receptors in Lumbar Sensorimotor Circuits to Spinal Cord Contusion is Affected by Injury Severity and Survival Time. *Front. Physiol.* 3, 478.
452. Liu, H.-T., Chancellor, M.B., and Kuo, H.-C. (2009). Urinary Nerve Growth Factor Levels are Elevated in Patients with Detrusor Overactivity and Decreased in Responders to Detrusor Botulinum Toxin-A Injection. *Eur. Urol.* 56, 700–707.
453. Yokoyama, T., Kumon, H., and Nagai, A. (2008). Correlation of urinary nerve growth factor level with pathogenesis of overactive bladder. *Neurourol. Urodyn.* 27, 417–420.
454. Seki, S., Sasaki, K., Fraser, M.O., Igawa, Y., Nishizawa, O., Chancellor, M.B., de Groat, W.C., and Yoshimura, N. (2002). Immunoneutralization of nerve growth factor in lumbosacral spinal cord reduces bladder hyperreflexia in spinal cord injured rats. *J. Urol.* 168, 2269–74.
455. Harrison, S.C., Hunnam, G.R., Farman, P., Ferguson, D.R., and Doyle, P.T. (1987). Bladder instability and denervation in patients with bladder outflow obstruction. *Br. J. Urol.* 60, 519–22.
456. Hughes, F.M., Hill, H.M., Wood, C.M., Edmondson, A.T., Dumas, A., Foo, W.-C., Oelsen, J.M., Rac, G., and Purves, J.T. (2016). The NLRP3 Inflammasome Mediates Inflammation Produced by Bladder Outlet Obstruction. *J. Urol.* 195, 1598–1605.
457. Gabella, G., and Uvelius, B. (1990). Urinary bladder of rat: fine structure of normal and hypertrophic musculature. *Cell Tissue Res.* 262, 67–79.
458. Zhang, Y., Guan, Z., Reader, B., Shawler, T., Mandrekar-Colucci, S., Huang, K., Weil, Z., Bratasz, A., Wells, J., Powell, N.D., Sheridan, J.F., Whitacre, C.C., Rabchevsky, A.G.,

- Nash, M.S., and Popovich, P.G. (2013). Autonomic dysreflexia causes chronic immune suppression after spinal cord injury. *J. Neurosci.* 33, 12970–81.
459. Capella, P., Ghasemzadeh, M.B., Adams, R.N., Wiedemann, D.J., and Wightman, R.M. (1993). Real-time monitoring of electrically stimulated norepinephrine release in rat thalamus: II. Modeling of release and reuptake characteristics of stimulated norepinephrine overflow. *J. Neurochem.* 60, 449–53.
460. Michel, M.C., and Vrydag, W. (2006). Alpha1-, alpha2- and beta-adrenoceptors in the urinary bladder, urethra and prostate. *Br. J. Pharmacol.* 147 Suppl 2, S88-119.
461. Gold, M.S., Dastmalchi, S., and Levine, J.D. (1997). Alpha 2-adrenergic receptor subtypes in rat dorsal root and superior cervical ganglion neurons. *Pain* 69, 179–90.
462. Nicholson, R., Dixon, A.K., Spanswick, D., and Lee, K. (2005). Noradrenergic receptor mRNA expression in adult rat superficial dorsal horn and dorsal root ganglion neurons. *Neurosci. Lett.* 380, 316–321.
463. Shi, T.S., Winzer-Serhan, U., Leslie, F., and Hökfelt, T. (2000). Distribution and regulation of alpha(2)-adrenoceptors in rat dorsal root ganglia. *Pain* 84, 319–30.
464. Pongratz, G., and Straub, R.H. (2014). The sympathetic nervous response in inflammation. *Arthritis Res. Ther.* 16, 504.

Appendix

Complete RNA sequencing tables from Chapter 2

As referred to in Chapter 2, below are the complete list of differentially expressed genes from the DRGs (Appendix Tables 1 and 2) and PGs (Appendix Tables 3 and 4) determined with DESeq of RNA sequencing results. The complete results from the Canonical Pathway Analysis of the DRG differentially expressed genes are in Appendix Table 5.

Appendix Table 1: Complete list of annotated genes upregulated in the DRG one month post-T3x sorted by fold change

Gene ID	Gene description	Fold change	Adj. p-value
ENSRNOG00000003809	spermidine/spermine N1-acetyl transferase 1	1.540	7.61E-12
ENSRNOG00000005387	RNA binding motif (RNP1, RRM) protein 3	1.519	8.58E-11
ENSRNOG000000039203	ribosomal protein S9; similar to 40S ribosomal protein S9; hypothetical protein LOC681065	1.410	5.70E-05
ENSRNOG000000047194	ADP-ribosylation factor like GTPase 13B	1.376	0.000348
ENSRNOG000000033697	caspase 4, apoptosis-related cysteine peptidase	1.374	0.00108
ENSRNOG000000022871	similar to zinc finger protein 84 (HPF2)	1.370	0.00701
ENSRNOG000000018069	neuroguidin, EIF4E binding protein	1.368	0.000220
ENSRNOG000000008075	intraflagellar transport 74 homolog (Chlamydomonas)	1.359	0.00360
ENSRNOG000000013078	zinc finger, CCHC domain containing 7	1.350	4.56E-05
ENSRNOG000000014463	URI1, prefoldin-like chaperone	1.350	5.70E-05
ENSRNOG000000036592	zinc finger protein 518A	1.342	0.000231
ENSRNOG000000020464	mitochondrial ribosomal protein L54; similar to mitochondrial ribosomal protein L54	1.339	0.00180
ENSRNOG000000002835	cisplatin resistance-associated overexpressed protein	1.335	1.49E-05
ENSRNOG000000016581	serine (or cysteine) proteinase inhibitor, clade B, member 1a	1.332	0.000220
ENSRNOG000000014789	dendrin	1.332	0.0114
ENSRNOG000000014380	zinc finger protein 788	1.327	0.00119
ENSRNOG000000012929	WD repeat and SOCS box-containing 1	1.322	4.56E-05
ENSRNOG000000010050	StAR-related lipid transfer domain containing 9	1.319	0.0123
ENSRNOG000000013738	glutaredoxin-like protein	1.318	0.0167
ENSRNOG000000019659	aspartoacylase	1.317	0.0257
ENSRNOG000000020264	dehydrogenase/reductase (SDR family) member 1	1.316	1.19E-05
ENSRNOG000000007159	chemokine (C-C motif) ligand 2	1.313	0.0188
ENSRNOG000000010248	serine (or cysteine) peptidase inhibitor, clade I, member 1	1.312	6.18E-06
ENSRNOG000000029841	cadherin 19, type 2	1.306	0.00844
ENSRNOG000000017959	coiled-coil domain containing 37	1.306	0.0290

Appendix Table 1: Complete list of annotated genes upregulated in the DRG one month post-T3x sorted by fold change (continued I)

Gene ID	Gene description	Fold change	Adj. p-value
ENSRNOG00000004268	zinc finger protein 386 (Kruppel-like)	1.303	0.0127
ENSRNOG000000036802	small nucleolar RNA host gene 11	1.296	1.49E-05
ENSRNOG000000011440	coiled-coil domain containing 39	1.293	0.00517
ENSRNOG00000000640	early growth response 2	1.293	0.0448
ENSRNOG000000029886	hemoglobin alpha, adult chain 2	1.293	0.0305
ENSRNOG000000011258	mannan-binding lectin serine peptidase 2	1.293	0.0132
ENSRNOG000000049259	zinc finger protein 91-like	1.291	0.0150
ENSRNOG000000015220	cartilage acidic protein 1	1.290	0.0176
ENSRNOG000000027990	cysteine-rich intestinal protein	1.289	0.0310
ENSRNOG000000015999	cold inducible RNA binding protein	1.289	0.000283
ENSRNOG000000038202	calmodulin-like 4	1.282	0.00408
ENSRNOG000000038319	aldo-keto reductase family 1, member C19	1.282	0.0172
ENSRNOG000000002036	PAX3 and PAX7 binding protein 1	1.278	0.00119
ENSRNOG000000021176	myotubularin related protein 11; OTU domain containing 7B	1.276	0.0273
ENSRNOG000000014660	ubiquitin specific peptidase 53	1.272	0.0151
ENSRNOG000000047321	hemoglobin alpha, adult chain 2	1.271	0.0398
ENSRNOG000000008782	splicing factor, arginine/serine-rich 18	1.270	4.56E-05
ENSRNOG000000030302	cold shock domain containing E1, RNA binding	1.269	0.0344
ENSRNOG000000020605	similar to phosphoseryl-tRNA kinase	1.268	0.0181
ENSRNOG000000004553	COX20 cytochrome C oxidase assembly factor	1.268	5.58E-05
ENSRNOG000000017784	ligand dependent nuclear receptor interacting factor 1	1.268	0.0151
ENSRNOG000000033615	NADH-ubiquinone oxidoreductase chain 3	1.264	0.0104
ENSRNOG000000028688	cystinosis, nephropathic	1.264	0.00340
ENSRNOG000000019406	zinc finger protein 61	1.263	0.0101
ENSRNOG000000037227	Yamaguchi sarcoma viral (v-yes) oncogene homolog 1	1.263	0.0136
ENSRNOG000000004737	Cd48 molecule	1.263	1.59E-06
ENSRNOG000000021776	centromere protein C 1	1.263	0.009386
ENSRNOG000000008440	cortactin binding protein 2	1.262	0.00354
ENSRNOG000000006684	zinc finger protein 317	1.262	0.0259
ENSRNOG000000008360	polycomb group ring finger 1	1.261	0.000484
ENSRNOG000000037661	thymosin beta 15B2	1.260	0.0193
ENSRNOG000000024142	arginine and glutamate rich 1	1.260	0.000283
ENSRNOG000000011647	S100 calcium binding protein A6	1.259	0.00430

Appendix Table 1: Complete list of annotated genes upregulated in the DRG one month post-T3x sorted by fold change (continued II)

Gene ID	Gene description	Fold change	Adj. p-value
ENSRNOG00000001861	YdjC homolog (bacterial)	1.259	0.0299
ENSRNOG000000042224	cytochrome P450, family 2, subfamily j, polypeptide 10	1.258	0.0349
ENSRNOG000000032946	PDZ domain containing 7	1.258	0.0481
ENSRNOG000000004001	O-sialoglycoprotein endopeptidase-like 1	1.258	0.00962
ENSRNOG000000011675	zinc finger protein 40	1.257	0.0353
ENSRNOG000000004273	interferon induced transmembrane protein 1	1.257	0.0433
ENSRNOG000000004521	pre-mRNA processing factor 39	1.256	0.0181
ENSRNOG000000043204	harbinger transposase derived 1	1.254	0.0470
ENSRNOG000000012099	PAP associated domain containing 4	1.254	0.0168
ENSRNOG000000023338	tetraspanin 2	1.249	0.00387
ENSRNOG000000024863	family with sequence similarity 76, member B	1.249	0.0304
ENSRNOG000000005486	PHD finger protein 20-like 1	1.248	0.0310
ENSRNOG000000050067	AABR07026058.1	1.248	0.00730
ENSRNOG000000001142	protein kinase, AMP-activated, beta 1 non-catalytic subunit	1.248	0.0181
ENSRNOG000000012492	similar to 60S ribosomal protein L7	1.246	0.0386
ENSRNOG000000040279	ankyrin repeat domain 32	1.245	0.0368
ENSRNOG000000019875	matrin 3	1.245	0.0229
ENSRNOG000000011821	S100 calcium-binding protein A4	1.244	0.0244
ENSRNOG000000015230	similar to chromosome 6 open reading frame 70	1.244	0.0368
ENSRNOG000000014173	structural maintenance of chromosomes 3	1.243	0.000348
ENSRNOG000000007336	churchill domain containing 1	1.243	0.0440
ENSRNOG000000016619	unconventional SNARE in the ER 1	1.242	0.0117
ENSRNOG000000002270	heterogeneous nuclear ribonucleoprotein D-like	1.239	9.26E-05
ENSRNOG000000036913	similar to hypothetical protein FLJ10652	1.239	0.0414
ENSRNOG000000021013	syntaxin 3	1.238	0.0287
ENSRNOG000000005513	splicing factor, arginine/serine-rich 5	1.237	2.62E-06
ENSRNOG000000022502	coiled-coil domain containing 55	1.235	0.0304
ENSRNOG000000021255	similar to polyamine oxidase isoform 2; spermine oxidase	1.235	0.0406
ENSRNOG000000004288	peptidyl-tRNA hydrolase 2	1.234	0.0199
ENSRNOG000000021267	hypothetical protein LK44	1.234	0.000810
ENSRNOG000000002618	influenza virus NS1A binding protein	1.232	6.82E-06

Appendix Table 1: Complete list of annotated genes upregulated in the DRG one month post-T3x sorted by fold change (continued III)

Gene ID	Gene description	Fold change	Adj. p-value
ENSRNOG00000006487	caspase 8 associated protein 2	1.231	0.0433
ENSRNOG00000004061	pinin, desmosome associated protein	1.230	0.00714
ENSRNOG000000045698	lin-7 homolog C, crumbs cell polarity complex component	1.230	0.0229
ENSRNOG000000038933	similar to signal peptidase complex subunit 3 homolog	1.230	0.0353
ENSRNOG000000031038	glycosyltransferase-like domain containing 1	1.230	0.00614
ENSRNOG000000005021	origin recognition complex, subunit 4-like (yeast)	1.229	0.0310
ENSRNOG000000025145	family with sequence similarity 82, member B	1.229	0.0341
ENSRNOG000000038012	COMM domain containing 6	1.229	0.0312
ENSRNOG000000002280	SH3 domain binding glutamic acid-rich protein like	1.228	0.00725
ENSRNOG000000009310	NMD3 ribosome export adaptor	1.228	0.0179
ENSRNOG000000009116	integrin beta 3 binding protein (beta3-endonexin)	1.228	0.0327
ENSRNOG000000003116	DPH1 homolog (<i>S. cerevisiae</i>)	1.228	0.0259
ENSRNOG000000002630	CCR4-NOT transcription complex, subunit 8	1.227	6.82E-06
ENSRNOG000000006241	membrane-associated ring finger (C3HC4) 7	1.227	0.0124
ENSRNOG000000016454	nuclear autoantigenic sperm protein (histone-binding); similar to nuclear autoantigenic sperm protein	1.226	0.0305
ENSRNOG000000008423	G protein-coupled receptor 22	1.226	0.0426
ENSRNOG000000030572	structural maintenance of chromosomes 5	1.226	0.00932
ENSRNOG000000031032	high mobility group nucleosomal binding domain 3	1.226	0.0124
ENSRNOG000000049819	DnaJ heat shock protein family (Hsp40) member C19	1.226	0.0199
ENSRNOG000000017309	similar to chromosome 1 open reading frame 63	1.225	0.000452
ENSRNOG000000014501	zinc finger, matrin-like	1.224	0.00828
ENSRNOG000000012994	pseudouridylate synthase 3	1.224	0.0368
ENSRNOG000000002874	RNA binding motif protein 25; similar to RNA binding motif protein 25	1.224	0.00812
ENSRNOG000000019630	2-hydroxyacyl-CoA lyase 1	1.224	0.0138

Appendix Table 1: Complete list of annotated genes upregulated in the DRG one month post-T3x sorted by fold change (continued IV)

Gene ID	Gene description	Fold change	Adj. p-value
ENSRNOG00000018642	leukocyte receptor cluster (LRC) member 8	1.223	0.00403
ENSRNOG00000002296	similar to nuclear transcription factor, X-box binding-like 1	1.222	0.0296
ENSRNOG00000042233	ribosomal protein L41	1.221	0.0388
ENSRNOG00000017404	protein-L-isoaspartate (D-aspartate) O-methyltransferase domain containing 2	1.221	0.0273
ENSRNOG00000034246	similar to ribosomal protein S27a; ribosomal protein S27a	1.221	0.0119
ENSRNOG00000031579	ribosomal protein S24; similar to ribosomal protein S24	1.221	0.0293
ENSRNOG00000046420	AABR07006458.1	1.220	0.0305
ENSRNOG00000015552	peptidylprolyl isomerase (cyclophilin)-like 4	1.219	0.0136
ENSRNOG00000018246	Traf and Tnf receptor associated protein	1.219	0.0161
ENSRNOG00000050960	AABR07040864.1	1.219	0.0194
ENSRNOG00000008362	zinc finger protein 775	1.219	0.0110
ENSRNOG00000047052	caseinolytic mitochondrial matrix peptidase proteolytic subunit	1.218	0.0329
ENSRNOG00000013121	mesoderm induction early response 1, family member 3	1.218	0.0379
ENSRNOG00000005710	RNA binding motif protein 7	1.218	0.0388
ENSRNOG00000005842	similar to suppressor of hairy wing homolog 4 isoform 1	1.218	0.0120
ENSRNOG00000021270	similar to CGI-09 protein; tRNA methyltransferase 6 homolog (<i>S. cerevisiae</i>)	1.217	0.0456
ENSRNOG00000004874	fibronectin leucine rich transmembrane protein 3	1.217	0.03425
ENSRNOG00000009345	UDP glycosyltransferase 8	1.217	0.0346
ENSRNOG00000022325	structural maintenance of chromosomes 2	1.217	0.0343
ENSRNOG00000004967	similar to U2 small nuclear ribonucleoprotein B; small nuclear ribonucleoprotein polypeptide B"	1.216	0.0259
ENSRNOG00000018211	uroporphyrinogen decarboxylase	1.214	0.0244
ENSRNOG00000009749	WD repeat domain 45	1.214	0.0254
ENSRNOG00000011621	heterogeneous nuclear ribonucleoprotein C (C1/C2)	1.213	0.0429
ENSRNOG00000046383	AABR07030156.2	1.212	0.0376

Appendix Table 1: Complete list of annotated genes upregulated in the DRG one month post-T3x sorted by fold change (continued V)

Gene ID	Gene description	Fold change	Adj. p-value
ENSRNOG00000049067	IgA-inducing protein	1.212	0.0368
ENSRNOG00000009057	SEC62 homolog, preprotein translocation factor	1.212	0.00182
ENSRNOG00000006796	zinc finger protein OZF-like	1.211	0.0409
ENSRNOG00000027049	ATP synthase membrane subunit f	1.211	0.0433
ENSRNOG00000007117	clusterin associated protein 1	1.211	0.00812
ENSRNOG00000008399	WD repeat domain 21	1.210	0.0476
ENSRNOG00000030371	mitochondrially encoded cytochrome c oxidase II	1.210	0.009582
ENSRNOG00000020763	U1 small nuclear ribonucleoprotein polypeptide A	1.210	0.000139
ENSRNOG00000017447	eukaryotic translation initiation factor 2, subunit 2 (beta)	1.210	0.00958
ENSRNOG00000047931	thymosin beta 4, X-linked	1.207	0.0353
ENSRNOG00000005705	glutaminyl-peptide cyclotransferase	1.207	0.0298
ENSRNOG00000033133	NEDD8 activating enzyme E1 subunit 1	1.205	0.0132
ENSRNOG00000019175	ERCC excision repair 6 like 2	1.203	0.0242
ENSRNOG00000039091	patatin-like phospholipase domain containing 8	1.202	0.0151
ENSRNOG00000008626	mannosidase, endo-alpha	1.202	0.0383
ENSRNOG00000012985	prefoldin subunit 5	1.202	0.0395
ENSRNOG00000003359	O-linked N-acetylglucosamine (GlcNAc) transferase (UDP-N-acetylglucosamine:polypeptide-N-acetylglucosaminyl transferase)	1.201	0.00812
ENSRNOG00000008455	transmembrane protein 87A	1.201	0.00812
ENSRNOG00000029592	splicing factor, arginine/serine-rich 11	1.201	0.000149
ENSRNOG00000033916	40S ribosomal protein S21	1.200	0.0494
ENSRNOG00000046621	AABR07043748.1	1.199	0.0229
ENSRNOG00000001317	zinc finger protein 68	1.199	0.0382
ENSRNOG00000012081	thioredoxin 1	1.199	0.0254
ENSRNOG00000008477	mitochondrial ribosomal protein L53	1.198	0.0386
ENSRNOG00000018671	COMM domain containing 4	1.198	0.0200
ENSRNOG00000005869	similar to transcription elongation factor A 1 isoform 2; transcription elongation factor A (SII) 1	1.198	0.00315
ENSRNOG00000017315	UCHL5 interacting protein	1.197	0.0477
ENSRNOG00000029885	stromal antigen 2	1.197	0.0443
ENSRNOG00000009990	zinc finger, RAN-binding domain containing 2	1.196	0.00418

Appendix Table 1: Complete list of annotated genes upregulated in the DRG one month post-T3x sorted by fold change (continued VI)

Gene ID	Gene description	Fold change	Adj. p-value
ENSRNOG00000018795	similar to 60S ribosomal protein L18a; ribosomal protein L18A	1.195	0.0257
ENSRNOG00000007065	RNA polymerase II associated protein 3	1.195	0.00344
ENSRNOG00000020495	eukaryotic translation initiation factor 3, subunit K	1.194	0.0242
ENSRNOG00000010418	NIMA (never in mitosis gene a)-related expressed kinase 1	1.194	0.00730
ENSRNOG00000009364	NADH dehydrogenase (ubiquinone) 1 beta subcomplex, 9	1.193	0.0424
ENSRNOG00000006432	tRNA nucleotidyl transferase, CCA-adding, 1; tRNA nucleotidyl transferase, CCA-adding, 1, pseudogene 1	1.193	0.0444
ENSRNOG00000012594	SGT1 homolog, MIS12 kinetochore complex assembly cochaperone	1.193	0.0166
ENSRNOG00000011057	mitofusin 1	1.193	0.00854
ENSRNOG00000047053	thymocyte nuclear protein 1	1.193	0.0310
ENSRNOG00000029667	tubulin folding cofactor E	1.192	0.0199
ENSRNOG00000022507	twinfilin actin-binding protein 1	1.191	0.0132
ENSRNOG00000010593	catenin (cadherin associated protein), alpha-like 1	1.191	0.0307
ENSRNOG00000036971	small integral membrane protein 26	1.191	0.0490
ENSRNOG00000006973	similar to RIKEN cDNA C430008C19	1.190	0.0405
ENSRNOG00000019986	protection of telomeres 1	1.189	0.0478
ENSRNOG00000034233	forty-two-three domain containing 1	1.189	0.0120
ENSRNOG00000015332	THO complex 1	1.188	0.0270
ENSRNOG00000005625	zinc finger, C4H2 domain containing	1.188	0.0132
ENSRNOG00000013618	ankyrin repeat domain 10	1.188	0.0332
ENSRNOG00000016516	myelin basic protein	1.187	0.0494
ENSRNOG00000008393	Tax1 (human T-cell leukemia virus type I) binding protein 1	1.187	0.0214
ENSRNOG00000033611	WD repeat domain 83 opposite strand	1.187	0.0471
ENSRNOG00000045844	impact RWD domain protein	1.186	0.0132
ENSRNOG00000018849	transcription elongation regulator 1	1.186	0.00831
ENSRNOG00000026171	Bardet-Biedl syndrome 4	1.185	0.0330
ENSRNOG00000031731	family with sequence similarity 216, member A	1.184	0.0455
ENSRNOG00000009278	intraflagellar transport 88	1.183	0.0204
ENSRNOG00000005123	tetratricopeptide repeat domain 35	1.183	0.0257
ENSRNOG00000029574	ribosomal protein S4, X-linked	1.183	0.0299

Appendix Table 1: Complete list of annotated genes upregulated in the DRG one month post-T3x sorted by fold change (continued VII)

Gene ID	Gene description	Fold change	Adj. p-value
ENSRNOG00000039496	proteolipid protein 2 (colonic epithelium-enriched); similar to proteolipid protein 2	1.181	0.0260
ENSRNOG00000006833	RB1-inducible coiled-coil 1	1.180	0.0354
ENSRNOG00000003825	WD repeat domain 75	1.178	0.0388
ENSRNOG00000011652	signal peptide peptidase-like 2A	1.178	0.0444
ENSRNOG00000024428	kinesin family member 20A	1.178	0.0478
ENSRNOG00000000519	serine/threonine kinase 38	1.177	0.0151
ENSRNOG00000010147	programmed cell death 10	1.177	0.0266
ENSRNOG00000007862	acetyl-coenzyme A acetyltransferase 1	1.177	0.00854
ENSRNOG00000004106	proline/serine-rich coiled-coil 2	1.176	0.0305
ENSRNOG00000023529	ribosomal protein L5	1.176	0.0374
ENSRNOG00000013052	BCL2-associated transcription factor 1	1.176	0.0358
ENSRNOG00000004085	tolerance-associated gene 1	1.173	0.0403
ENSRNOG00000012868	uveal autoantigen with coiled-coil domains and ankyrin repeats	1.173	0.0478
ENSRNOG00000019840	magnesium-dependent phosphatase 1	1.173	0.0402
ENSRNOG00000047960	RAB9B, member RAS oncogene family	1.172	0.0475
ENSRNOG00000011379	cyclin D-type binding-protein 1	1.171	0.0442
ENSRNOG00000007203	proteasome (prosome, macropain) 26S subunit, ATPase, 6; similar to Psmc6 protein	1.171	0.0209
ENSRNOG00000043388	interferon regulatory factor 3	1.171	0.0114
ENSRNOG00000020271	regulator of G-protein signaling 10; Tia1 cytotoxic granule-associated RNA binding protein-like 1	1.170	0.0146
ENSRNOG00000010184	similar to chromosome 3 open reading frame 10	1.169	0.00564
ENSRNOG00000028461	guanine nucleotide binding protein-like 3 (nucleolar); similar to guanine nucleotide binding protein-like 3 (nucleolar)	1.169	0.0370
ENSRNOG00000019020	Bardet-Biedl syndrome 2 homolog (human)	1.169	0.0239
ENSRNOG00000001090	StAR-related lipid transfer (START) domain containing 13	1.169	0.0259
ENSRNOG00000017791	Rho GTPase activating protein 12	1.169	0.0497
ENSRNOG00000029535	nuclear receptor binding protein 2	1.168	0.0338

Appendix Table 1: Complete list of annotated genes upregulated in the DRG one month post-T3x sorted by fold change (continued VIII)

Gene ID	Gene description	Fold change	Adj. p-value
ENSRNOG00000018075	signal peptidase complex subunit 1 homolog (<i>S. cerevisiae</i>)	1.168	0.0442
ENSRNOG00000030862	ATPase, H ⁺ transporting, lysosomal V1 subunit H	1.167	0.0255
ENSRNOG00000017444	neurensin 1	1.166	0.0143
ENSRNOG00000006810	LanC lantibiotic synthetase component C-like 2 (bacterial)	1.165	0.0409
ENSRNOG00000026236	microrchidia 3	1.164	0.0344
ENSRNOG00000000207	hypothetical gene supported by BC088468; NM_001009712	1.163	0.0480
ENSRNOG00000004681	enhancer of yellow 2 homolog (<i>Drosophila</i>)	1.161	0.0426
ENSRNOG00000008747	pleckstrin homology domain containing, family A member 5	1.161	0.0323
ENSRNOG00000002632	nascent-polypeptide-associated complex alpha polypeptide	1.160	0.0494
ENSRNOG00000018691	cyclin L2	1.159	0.0255
ENSRNOG00000009430	guanine nucleotide binding protein-like 2 (nucleolar)	1.159	0.0229
ENSRNOG00000011383	NADH dehydrogenase (ubiquinone) Fe-S protein 4	1.159	0.0259
ENSRNOG00000005641	F-box and leucine-rich repeat protein 4	1.158	0.0494
ENSRNOG00000006532	H3 histone family member 3B	1.158	0.0442
ENSRNOG00000010286	calpastatin	1.157	0.0235
ENSRNOG00000042195	poly(A) binding protein, nuclear 1	1.154	0.0296
ENSRNOG00000017695	AABR07012795.1	1.154	0.0458
ENSRNOG00000006001	LUC7-like 2 (<i>S. cerevisiae</i>)	1.153	0.0420
ENSRNOG00000016416	ribonuclease/angiogenin inhibitor 1	1.153	0.0132
ENSRNOG00000021233	inosine triphosphatase (nucleoside triphosphate pyrophosphatase)	1.153	0.0382
ENSRNOG00000024322	shroom family member 2	1.152	0.0453
ENSRNOG00000017895	enolase 1	1.151	0.0305
ENSRNOG00000010827	polypyrimidine tract binding protein 2	1.150	0.0310
ENSRNOG00000006779	carnitine O-octanoyltransferase	1.147	0.0433
ENSRNOG00000008630	proteasome (prosome, macropain) subunit, alpha type 7	1.147	0.0442
ENSRNOG00000001488	proteasome (prosome, macropain) subunit, beta type 1	1.146	0.0448
ENSRNOG00000009478	similar to RIKEN cDNA 3110043O21	1.144	0.0453
ENSRNOG00000013930	ring finger protein 4	1.142	0.0194
ENSRNOG00000018676	similar to cDNA sequence BC031181	1.142	0.0439

Appendix Table 1: Complete list of annotated genes upregulated in the DRG one month post-T3x sorted by fold change (continued IX)

Gene ID	Gene description	Fold change	Adj. p-value
ENSRNOG00000012738	similar to Dendritic cell protein GA17	1.141	0.0440
ENSRNOG00000007241	formin binding protein 4	1.141	0.0452
ENSRNOG00000010105	S100 calcium binding protein A11	1.139	0.0494
ENSRNOG000000036742	ubiquinol cytochrome c reductase core protein 2	1.139	0.0433
ENSRNOG000000031475	collagen, type XVI, alpha 1	1.138	0.0290
ENSRNOG00000010117	eukaryotic translation initiation factor 3, subunit 10 (theta)	1.138	0.0455
ENSRNOG000000006751	proteasome (prosome, macropain) 26S subunit, non-ATPase, 6	1.137	0.0428
ENSRNOG000000008673	actin related protein 2/3 complex, subunit 3	1.136	0.0417
ENSRNOG000000027860	gametogenetin binding protein 2	1.134	0.0312
ENSRNOG000000003071	vesicle-associated membrane protein 4	1.134	0.0214
ENSRNOG000000007283	similar to hypothetical protein CL25084	1.132	0.0305
ENSRNOG00000013516	splicing factor 3b, subunit 1	1.129	0.0420
ENSRNOG00000012481	protein phosphatase 1J	1.128	0.0468
ENSRNOG00000015540	SAPS domain family, member 3	1.128	0.0270
ENSRNOG00000017781	DnaJ (Hsp40) homolog, subfamily C, member 7	1.123	0.0373
ENSRNOG000000042821	CD59 molecule	1.116	0.0489
ENSRNOG000000006380	splicing factor, arginine/serine-rich 6	1.115	0.0267

Appendix Table 2: Complete list of annotated genes downregulated in the DRG one month post-T3x sorted by fold change

Gene ID	Gene description	Fold change	Adj. p-value
ENSRNOG00000020369	insulin-like growth factor 2	0.6290	3.09E-05
ENSRNOG00000006548	mannose receptor, C type 2	0.6965	0.00244
ENSRNOG000000031801	Eph receptor B3	0.7207	0.00225
ENSRNOG000000013954	alkaline phosphatase, liver/bone/kidney	0.7325	0.000615
ENSRNOG000000020263	ATPase, Na ⁺ /K ⁺ transporting, alpha 3 polypeptide	0.7334	0.00154
ENSRNOG000000019955	oxoglutarate dehydrogenase-like	0.7363	0.00225
ENSRNOG000000005148	scratch homolog 2, zinc finger protein	0.7494	0.000452
ENSRNOG000000025612	similar to Seizure 6-like protein precursor	0.7532	0.0149
ENSRNOG000000009446	retinoid X receptor alpha	0.7603	0.0181
ENSRNOG000000049944	solute carrier family 25 member 22	0.7616	0.000275
ENSRNOG000000020918	cyclin D1	0.7617	0.000739
ENSRNOG000000017154	ATPase, class VI, type 11A	0.7697	0.00340
ENSRNOG000000008471	kinesin family member 21B	0.7733	0.0353
ENSRNOG000000001621	similar to RIKEN cDNA 5830404H04	0.7746	0.00874
ENSRNOG000000009967	otoferlin	0.7755	0.0299
ENSRNOG000000005076	BCL6 co-repressor-like 1	0.7772	0.0103
ENSRNOG000000016050	Fibroblast growth factor receptor 1	0.7787	2.62E-06
ENSRNOG000000012546	FERM and PDZ domain containing 1	0.7795	0.000673
ENSRNOG000000048043	coagulation factor II (thrombin) receptor	0.7799	0.0172
ENSRNOG000000028580	pecanex-like 2 (Drosophila)	0.7821	0.00859
ENSRNOG000000042855	AT hook, DNA binding motif, containing 1	0.7826	0.00958
ENSRNOG000000009629	carbonic anhydrase II	0.7832	0.00999
ENSRNOG000000018251	mannose receptor, C type 1	0.7858	0.0255
ENSRNOG000000020339	neuralized homolog (Drosophila)	0.7870	0.00883
ENSRNOG000000000955	ligand of numb-protein X 2	0.7873	0.0151
ENSRNOG000000021824	DnaJ (Hsp40) homolog, subfamily B, member 1	0.7876	0.000673
ENSRNOG000000029570	family with sequence similarity 222, member B	0.7880	0.00517
ENSRNOG000000026238	similar to RIKEN cDNA 6030419C18 gene	0.7891	0.00102
ENSRNOG000000019735	DPH2 homolog (S. cerevisiae)	0.7894	0.0259
ENSRNOG000000017659	heparan sulfate (glucosamine) 3-O-sulfotransferase 2	0.7894	0.0116
ENSRNOG000000050057	ATP binding cassette subfamily A member 3	0.7897	0.0346
ENSRNOG000000023208	myogenesis regulating glycosidase	0.7902	5.58E-05

Appendix Table 2: Complete list of annotated genes downregulated in the DRG one month post-T3x sorted by fold change (continued I)

Gene ID	Gene description	Fold change	Adj. p-value
ENSRNOG00000018561	peroxisome proliferator-activated receptor gamma, coactivator-related 1	0.7913	0.000371
ENSRNOG00000007338	fibulin 2	0.7917	0.0128
ENSRNOG00000016110	potassium channel, subfamily K, member 12	0.7918	0.0257
ENSRNOG00000025083	protein kinase C and casein kinase substrate in neurons 1	0.7933	0.000371
ENSRNOG00000010428	bromo adjacent homology domain containing 1	0.7935	0.0128
ENSRNOG000000032618	macrophage stimulating 1 receptor (c-met-related tyrosine kinase)	0.7952	0.0368
ENSRNOG00000013681	potassium voltage-gated channel, delayed-rectifier, subfamily S, member 1	0.7968	0.00958
ENSRNOG00000014658	zinc finger protein 423	0.7977	0.0477
ENSRNOG000000045636	fatty acid synthase	0.7984	0.00539
ENSRNOG00000026748	DENN/MADD domain containing 2A	0.7992	0.00883
ENSRNOG00000011380	potassium voltage gated channel, Shaw-related subfamily, member 1	0.7997	0.0490
ENSRNOG00000005569	phosphatase, orphan 1	0.8005	0.0114
ENSRNOG00000014230	microtubule-associated protein 1A	0.8009	0.0219
ENSRNOG00000012730	leucine-rich repeat kinase 1	0.8012	0.0312
ENSRNOG00000023781	plectin 1	0.8017	0.0179
ENSRNOG00000021130	ATP-binding cassette, sub-family C (CFTR/MRP), member 8	0.8019	0.0310
ENSRNOG00000017409	wingless-type MMTV integration site family, member 6	0.8021	0.0235
ENSRNOG00000019645	oxysterol binding protein 2	0.8031	0.00387
ENSRNOG00000011646	RAS (RAD and GEM) like GTP binding 2	0.8038	0.0423
ENSRNOG00000002265	calcium-sensing receptor	0.8044	0.0426
ENSRNOG00000012989	serine incorporator 2	0.8044	0.0310
ENSRNOG00000003741	neuronal pentraxin 1	0.8048	0.0255
ENSRNOG00000050090	solute carrier family 6 member 17	0.8055	0.00790
ENSRNOG00000009949	protocadherin 18	0.8059	0.0280
ENSRNOG00000027264	diacylglycerol lipase, alpha	0.8060	0.00757
ENSRNOG00000016023	ankyrin repeat domain 15	0.8079	0.00728
ENSRNOG00000002832	solute carrier family 16, member 2 (monocarboxylic acid transporter 8)	0.8082	0.0362
ENSRNOG00000012356	solute carrier family 36 (proton/amino acid symporter), member 1	0.8085	0.0199

Appendix Table 2: Complete list of annotated genes downregulated in the DRG one month post-T3x sorted by fold change (continued II)

Gene ID	Gene description	Fold change	Adj. p-value
ENSRNOG00000020372	histone deacetylase 4	0.8089	0.0257
ENSRNOG00000008716	neurofilament, heavy polypeptide	0.8090	0.00119
ENSRNOG00000022967	solute carrier family 35 (UDP-glucuronic acid/UDP-N-acetylgalactosamine dual transporter), member D1	0.8092	0.0439
ENSRNOG00000002588	C-type lectin domain family 16, member A	0.8100	0.0161
ENSRNOG00000014243	platelet endothelial aggregation receptor 1	0.8101	0.0496
ENSRNOG00000005574	ADAM metallopeptidase with thrombospondin type 1 motif, 8	0.8105	0.0368
ENSRNOG00000016204	leucine rich repeat containing 24	0.8106	0.0114
ENSRNOG00000007427	ectonucleoside triphosphate diphosphohydrolase 6	0.8118	0.000495
ENSRNOG00000002636	4-aminobutyrate aminotransferase	0.8120	0.0368
ENSRNOG00000019140	Btg3 associated nuclear protein	0.8128	0.0184
ENSRNOG000000047219	ubiquitin protein ligase E3B	0.8130	0.00279
ENSRNOG00000017974	G protein-regulated inducer of neurite outgrowth 1	0.8132	0.0343
ENSRNOG00000012568	MAP-kinase activating death domain	0.8132	0.00403
ENSRNOG000000047307	ciliary neurotrophic factor receptor	0.8136	0.00854
ENSRNOG000000033663	procollagen-proline, 2-oxoglutarate 4-dioxygenase (proline 4-hydroxylase), alpha polypeptide II	0.8152	0.0382
ENSRNOG00000019564	spectrin, beta, non-erythrocytic 2	0.8159	0.00874
ENSRNOG000000025815	cerebellar degeneration-related protein 2-like	0.8168	0.00584
ENSRNOG00000002229	adenylate cyclase 5	0.8174	0.00962
ENSRNOG000000004019	pleckstrin homology-like domain, family A, member 1	0.8180	0.0310
ENSRNOG000000046497	BRCA1 associated protein	0.8184	0.00536
ENSRNOG000000005053	egl-9 family hypoxia-inducible factor 3	0.8187	0.0442
ENSRNOG00000010649	catenin (cadherin-associated protein), delta 2 (neural plakophilin-related arm-repeat protein)	0.8187	0.0310
ENSRNOG00000013694	netrin G2	0.8192	0.0443
ENSRNOG000000028545	AC141959.1	0.8197	0.0429
ENSRNOG000000049019	transmembrane protein 170A	0.8198	0.0257

Appendix Table 2: Complete list of annotated genes downregulated in the DRG one month post-T3x sorted by fold change (continued III)

Gene ID	Gene description	Fold change	Adj. p-value
ENSRNOG00000021671	leucine zipper, down-regulated in cancer 1-like	0.8198	0.0379
ENSRNOG00000013030	phosphatidylinositol-5-phosphate 4-kinase, type II, beta	0.8207	0.0209
ENSRNOG00000019322	Notch homolog 1, translocation-associated (Drosophila)	0.8207	0.0349
ENSRNOG00000011517	tumor necrosis factor receptor superfamily, member 21	0.8209	4.56E-05
ENSRNOG00000025155	lemur tyrosine kinase 2	0.8219	0.0174
ENSRNOG00000000638	zinc finger protein 365	0.8225	0.0409
ENSRNOG00000049236	myosin heavy chain 9-like 1	0.8236	0.0273
ENSRNOG00000011886	myosin IE	0.8238	0.00258
ENSRNOG00000006062	HCLS1 binding protein 3	0.8243	0.0162
ENSRNOG00000018358	5'-nucleotidase domain containing 2	0.8244	0.0341
ENSRNOG00000020778	cholinergic receptor, nicotinic, beta 2 (neuronal)	0.8250	0.0114
ENSRNOG00000007133	plexin B2	0.8250	0.0151
ENSRNOG00000027098	seizure related 6 homolog (mouse)-like 2	0.8254	0.0219
ENSRNOG00000018241	ankyrin 1, erythrocytic	0.8254	0.0255
ENSRNOG00000012795	Cdk5 and Abl enzyme substrate 1	0.8256	0.0242
ENSRNOG00000005504	plakophilin 4	0.8257	0.0290
ENSRNOG00000002886	myosin, heavy chain 10, non-muscle	0.8262	0.0104
ENSRNOG00000012747	sparc/osteonectin, cwcv and kazal-like domains proteoglycan (testican) 1	0.8266	0.0102
ENSRNOG00000017671	RAS p21 protein activator 3	0.8272	0.0245
ENSRNOG00000008862	ATP-binding cassette, sub-family G (WHITE), member 4	0.8275	0.0287
ENSRNOG00000008146	granulosa cell HMG-box protein 1	0.8278	0.0116
ENSRNOG00000013717	bone morphogenetic protein 6	0.8279	0.0346
ENSRNOG00000030269	ATPase, Ca ⁺⁺ transporting, plasma membrane 2	0.8281	0.0470
ENSRNOG00000000949	fms-related tyrosine kinase 3	0.8281	0.0376
ENSRNOG00000007047	epidermal growth factor receptor pathway substrate 8	0.8282	0.0442
ENSRNOG00000007982	solute carrier family 9 (sodium/hydrogen exchanger), member 1	0.8282	0.0388
ENSRNOG00000018952	sema domain, immunoglobulin domain (Ig), short basic domain, secreted, (semaphorin) 3G	0.8288	0.00821

Appendix Table 2: Complete list of annotated genes downregulated in the DRG one month post-T3x sorted by fold change (continued VI)

Gene ID	Gene description	Fold change	Adj. p-value
ENSRNOG00000011156	calsyntenin 3	0.8291	0.0242
ENSRNOG00000014928	amyloid beta (A4) precursor protein-binding, family A, member 1	0.8296	0.0478
ENSRNOG00000048431	NYN domain and retroviral integrase containing	0.8299	0.0349
ENSRNOG00000018977	adaptor-related protein complex 3, delta 1 subunit	0.8307	0.00325
ENSRNOG00000000175	mesoderm induction early response 1, family member 2	0.8309	0.0290
ENSRNOG00000019575	RELT-like 2	0.8309	0.009579
ENSRNOG00000003469	microtubule associated serine/threonine kinase 1	0.8310	0.0184
ENSRNOG00000018971	MOB1, Mps One Binder kinase activator-like 2A (yeast)	0.8313	0.00340
ENSRNOG00000000121	phosphatidylinositol glycan anchor biosynthesis, class V	0.8319	0.0485
ENSRNOG00000042786	vesicle transport through interaction with t-SNAREs 1A	0.8321	0.0420
ENSRNOG00000007705	potassium inwardly-rectifying channel, subfamily J, member 10	0.8321	0.0271
ENSRNOG00000002251	SEC31 homolog A (<i>S. cerevisiae</i>)	0.8323	0.00730
ENSRNOG00000049862	ring finger protein 157	0.8326	0.0272
ENSRNOG00000025235	transmembrane protein 130	0.8338	0.0194
ENSRNOG00000019492	protein O-linked mannose N-acetylglucosaminyltransferase 2 (beta 1,4-)	0.8343	0.0410
ENSRNOG00000006952	phosphatidylinositol-3,4,5-trisphosphate-dependent Rac exchange factor 1	0.8344	0.0104
ENSRNOG00000010635	insulin-like growth factor binding protein 4	0.8345	0.0455
ENSRNOG00000025394	tetratricopeptide repeat, ankyrin repeat and coiled-coil containing 1	0.8348	0.0210
ENSRNOG00000036663	forkhead box K2	0.8356	0.0242
ENSRNOG00000011227	ATPase, Na ⁺ /K ⁺ transporting, beta 2 polypeptide	0.8358	0.0264
ENSRNOG00000019968	tripartite motif-containing 8	0.8360	0.0214
ENSRNOG00000017219	Vac14, PIKFYVE complex component	0.8366	0.0138
ENSRNOG00000002821	PH domain and leucine rich repeat protein phosphatase	0.8369	0.0199
ENSRNOG00000017439	cingulin-like 1	0.8374	0.0147

Appendix Table 2: Complete list of annotated genes downregulated in the DRG one month post-T3x sorted by fold change (continued V)

Gene ID	Gene description	Fold change	Adj. p-value
ENSRNOG00000007727	lipoma HMGIC fusion partner-like 4	0.8378	0.0332
ENSRNOG00000047281	histone deacetylase 6	0.8381	0.0132
ENSRNOG00000002122	leucine rich repeat containing 8 family, member C	0.8381	0.0382
ENSRNOG00000008443	family with sequence similarity 234, member B	0.8383	0.00854
ENSRNOG00000014132	Myb protein P42POP	0.8385	0.0462
ENSRNOG00000014030	synemin, intermediate filament protein	0.8385	0.0257
ENSRNOG00000011633	parvin, beta	0.8385	0.0259
ENSRNOG00000008790	ganglioside-induced differentiation-associated protein 1-like 1	0.8389	0.0131
ENSRNOG00000017922	similar to trophoblast glycoprotein	0.8393	0.0388
ENSRNOG00000006557	cytoplasmic FMR1 interacting protein 2	0.8395	0.0199
ENSRNOG00000005531	TYRO3 protein tyrosine kinase	0.8396	0.0225
ENSRNOG00000017290	zinc finger protein 335	0.8397	0.0160
ENSRNOG00000010161	myosin X	0.8397	0.0497
ENSRNOG00000004052	protein phosphatase 1, regulatory subunit 9B	0.8398	0.0160
ENSRNOG00000016031	bicaudal D homolog 2 (Drosophila)	0.8399	0.0104
ENSRNOG00000008194	zinc finger, NFX1-type containing 1	0.8405	0.00413
ENSRNOG00000010048	dynactin 1	0.8405	0.00730
ENSRNOG00000003386	RNA binding fox-1 homolog 3	0.8406	0.0176
ENSRNOG00000019799	protocadherin gamma subfamily C, 3; protocadherin gamma subfamily A, 12	0.8406	0.00939
ENSRNOG00000018231	BTB (POZ) domain containing 14A	0.8407	0.0242
ENSRNOG00000020650	solute carrier family 17 (sodium-dependent inorganic phosphate cotransporter), member 7	0.8408	0.0114
ENSRNOG00000000851	HLA-B-associated transcript 3	0.8409	0.0295
ENSRNOG00000017673	BR serine/threonine kinase 1	0.8413	0.00567
ENSRNOG00000020107	serine/threonine kinase 11 interacting protein	0.8414	0.0375
ENSRNOG00000028090	rho/rac guanine nucleotide exchange factor (GEF) 18	0.8414	0.0226
ENSRNOG00000011375	tuberous sclerosis 2	0.8415	0.0332
ENSRNOG00000009889	phosphoglucomutase 1	0.8416	0.00730
ENSRNOG00000020298	Bcl2-associated athanogene 3	0.8417	0.0406
ENSRNOG00000011726	glutamate receptor, ionotropic, N-methyl D-aspartate 1	0.8422	0.0138
ENSRNOG00000018788	BTB (POZ) domain containing 2	0.8427	0.0259

Appendix Table 2: Complete list of annotated genes downregulated in the DRG one month post-T3x sorted by fold change (continued VI)

Gene ID	Gene description	Fold change	Adj. p-value
ENSRNOG00000005130	oxoglutarate (alpha-ketoglutarate) dehydrogenase (lipoamide)	0.8431	0.0312
ENSRNOG00000021725	malectin	0.8435	0.0267
ENSRNOG00000010219	ral guanine nucleotide dissociation stimulator	0.8435	0.0226
ENSRNOG00000020407	ataxia, cerebellar, Cayman type	0.8438	0.00413
ENSRNOG00000018982	ectonucleoside triphosphate diphosphohydrolase 3	0.8440	0.00958
ENSRNOG00000001314	family with sequence similarity 20, member C	0.8440	0.0395
ENSRNOG00000019193	syntaxin 1B	0.8442	0.0307
ENSRNOG00000001227	adenosine deaminase, RNA-specific, B1	0.8444	0.0306
ENSRNOG00000020347	nucleoporin 98kDa	0.8445	0.00874
ENSRNOG00000008758	tetraspanin 18	0.8451	0.0376
ENSRNOG00000050834	family with sequence similarity 102, member A	0.8457	0.0305
ENSRNOG00000009000	forkhead box J2	0.8458	0.0275
ENSRNOG00000006787	24-dehydrocholesterol reductase	0.8459	0.0209
ENSRNOG00000009946	low density lipoprotein receptor	0.8460	0.0410
ENSRNOG00000009585	transcription factor 20	0.8465	0.0255
ENSRNOG00000001237	calcineurin binding protein 1	0.8469	0.0275
ENSRNOG00000003821	regulatory associated protein of MTOR, complex 1	0.8469	0.0259
ENSRNOG00000029784	p21 protein (Cdc42/Rac)-activated kinase 1	0.8475	0.0349
ENSRNOG00000001313	guanine nucleotide binding protein (G protein), alpha z polypeptide	0.8475	0.0179
ENSRNOG00000000816	similar to 2310014H01Rik protein	0.8478	0.0166
ENSRNOG00000026048	golgi-specific brefeldin A resistant guanine nucleotide exchange factor 1	0.8489	0.0423
ENSRNOG00000032293	polymerase (DNA directed), gamma	0.8489	0.0406
ENSRNOG00000018160	zinc finger, SWIM domain containing 5	0.8491	0.0259
ENSRNOG00000016846	phosphatidylinositol 3-kinase catalytic delta polypeptide	0.8494	0.0151
ENSRNOG00000001368	rabphilin 3A	0.8499	0.0478
ENSRNOG00000011725	ubiquitin-associated protein 2	0.8509	0.0259
ENSRNOG00000000129	PHD finger protein 24	0.8516	0.0325
ENSRNOG00000032828	mitogen-activated protein kinase 8 interacting protein 2	0.8520	0.0489
ENSRNOG00000017354	zyxin	0.8521	0.04653

Appendix Table 2: Complete list of annotated genes downregulated in the DRG one month post-T3x sorted by fold change (continued VII)

Gene ID	Gene description	Fold change	Adj. p-value
ENSRNOG00000000867	valyl-tRNA synthetase 2, mitochondrial (putative); valyl-tRNA synthetase	0.8522	0.0182
ENSRNOG00000020151	cadherin 1	0.8526	0.0104
ENSRNOG00000013154	splicing factor proline/glutamine rich (polypyrimidine tract binding protein associated)	0.8527	0.0194
ENSRNOG00000017431	similar to RIKEN cDNA 6430548M08	0.8528	0.0420
ENSRNOG00000002004	PR domain containing 8	0.8531	0.0371
ENSRNOG00000050404	prostate transmembrane protein, androgen induced 1	0.8532	0.0368
ENSRNOG00000014963	G protein-coupled receptor 56	0.8532	0.0176
ENSRNOG00000017532	testis-specific kinase 1	0.8536	0.0460
ENSRNOG00000015434	midnolin	0.8537	0.0424
ENSRNOG00000011431	malignant fibrous histiocytoma amplified sequence 1	0.8543	0.0417
ENSRNOG00000001866	phosphatidylinositol 4-kinase, catalytic, alpha	0.8543	0.0151
ENSRNOG00000050646	fem-1 homolog A	0.8543	0.0245
ENSRNOG00000014806	paroxysmal nonkinesigenic dyskinesia	0.8544	0.0425
ENSRNOG00000016670	phosphatidylinositol-5-phosphate 4-kinase, type II, alpha	0.8556	0.00714
ENSRNOG00000033568	mitogen-activated protein kinase 8 interacting protein 3	0.8556	0.0475
ENSRNOG00000002645	gem (nuclear organelle) associated protein 5	0.8559	0.0485
ENSRNOG00000050748	dipeptidyl peptidase 9	0.8563	0.0171
ENSRNOG00000005452	protein phosphatase 2 (formerly 2A), regulatory subunit B, gamma isoform	0.8570	0.0332
ENSRNOG00000025296	leucine rich repeat containing 8 family, member A	0.8572	0.0271
ENSRNOG00000001228	protein O-fucosyltransferase 2	0.8572	0.0353
ENSRNOG000000032473	sodium channel, voltage-gated, type X, alpha subunit	0.8577	0.0344
ENSRNOG00000014986	ubiquitination factor E4B	0.8581	0.0132
ENSRNOG00000017069	MAP/microtubule affinity-regulating kinase 4	0.8581	0.0494
ENSRNOG00000010064	ATP binding cassette subfamily C member 4	0.8586	0.0349
ENSRNOG00000011931	SWI/SNF related, matrix associated, actin dependent regulator of chromatin, subfamily a, member 2	0.8591	0.0332

Appendix Table 2: Complete list of annotated genes downregulated in the DRG one month post-T3x sorted by fold change (continued VIII)

Gene ID	Gene description	Fold change	Adj. p-value
ENSRNOG00000018097	ER membrane protein complex subunit 1	0.8593	0.0422
ENSRNOG00000042464	F-box protein 25 (Fbxo25), transcript variant 3, mRNA	0.8594	0.0259
ENSRNOG00000046424	mitofusin-2-like	0.8595	0.0388
ENSRNOG00000050841	acetylcholinesterase	0.8596	0.0257
ENSRNOG00000003812	neuroligin 3	0.8597	0.0464
ENSRNOG00000019832	Bardet-Biedl syndrome 1	0.8598	0.0310
ENSRNOG00000019374	c-src tyrosine kinase	0.8605	0.0369
ENSRNOG00000019587	protein tyrosine phosphatase, receptor type, N	0.8612	0.0390
ENSRNOG00000020812	glycogen synthase 1, muscle	0.8612	0.0254
ENSRNOG00000003234	mahogunin, ring finger 1	0.8615	0.0447
ENSRNOG00000020269	splicing factor, arginine/serine-rich 14	0.8619	0.00391
ENSRNOG00000015153	integrator complex subunit 3	0.8619	0.0148
ENSRNOG00000001436	tyrosine 3-monooxygenase/ tryptophan 5-monooxygenase activation protein, gamma polypeptide	0.8624	0.00285
ENSRNOG00000012240	SPT6 homolog, histone chaperone	0.8630	0.0388
ENSRNOG00000010765	vinculin	0.8634	0.00337
ENSRNOG00000018823	nischarin	0.8639	0.0332
ENSRNOG00000003905	N-ethylmaleimide-sensitive factor	0.8640	0.0272
ENSRNOG00000013658	neurofilament, light polypeptide	0.8642	0.00482
ENSRNOG00000017022	ceramide kinase	0.8650	0.0251
ENSRNOG00000014371	cadherin 13	0.8656	0.0104
ENSRNOG00000025463	hypothetical protein LOC100125362	0.8660	0.03682
ENSRNOG00000012844	TOX high mobility group box family member 4	0.8663	0.00365
ENSRNOG00000003721	progesterone and adiponectin receptor family member IV	0.8670	0.0299
ENSRNOG00000010944	hypoxia up-regulated 1	0.8674	0.0250
ENSRNOG00000010646	transmembrane protein 229B	0.8679	0.0297
ENSRNOG00000019372	pyruvate carboxylase	0.8679	0.0255
ENSRNOG00000013916	neurofilament, medium polypeptide	0.8681	0.0257
ENSRNOG00000018145	carnitine acetyltransferase	0.8685	0.0468
ENSRNOG000000032152	RAB11 family interacting protein 3	0.8685	0.0228
ENSRNOG000000036814	ATPase, H ⁺ transporting, lysosomal V0 subunit A1	0.8689	0.0349
ENSRNOG00000025832	zyg-11 related, cell cycle regulator	0.8690	0.0290
ENSRNOG00000019325	ring finger protein 185	0.8693	0.0382

Appendix Table 2: Complete list of annotated genes upregulated in the DRG one month post-T3x sorted by fold change (continued IX)

Gene ID	Gene description	Fold change	Adj. p-value
ENSRNOG00000004159	FLII, actin remodeling protein	0.8695	0.00958
ENSRNOG00000008830	nuclear factor, erythroid derived 2,-like 1	0.8695	0.0244
ENSRNOG00000010396	EYA transcriptional coactivator and phosphatase 3	0.8695	0.0437
ENSRNOG00000017930	lysophosphatidylcholine acyltransferase 1	0.8696	0.0386
ENSRNOG00000000437	1-acylglycerol-3-phosphate O-acyltransferase 1 (lysophosphatidic acid acyltransferase, alpha)	0.8701	0.0452
ENSRNOG00000005058	lysophosphatidylcholine acyltransferase 4	0.8707	0.0349
ENSRNOG00000027194	small G protein signaling modulator 2	0.8709	0.0345
ENSRNOG00000010303	tripartite motif-containing 32	0.8711	0.0259
ENSRNOG00000002347	ral guanine nucleotide dissociation stimulator,-like 1	0.8715	0.0199
ENSRNOG00000004099	R3H domain containing 1	0.8725	0.0462
ENSRNOG00000019534	adaptor-related protein complex 2, alpha 2 subunit	0.8729	0.0388
ENSRNOG00000049531	ubiquitin specific peptidase 19	0.8734	0.0259
ENSRNOG00000009862	olfactomedin 1	0.8745	0.0213
ENSRNOG00000015236	MYB binding protein (P160) 1a	0.8747	0.0132
ENSRNOG00000009198	RAB6B, member RAS oncogene family	0.8750	0.0333
ENSRNOG00000013659	testis expressed 2	0.8755	0.0376
ENSRNOG00000003495	PRP8 pre-mRNA processing factor 8 homolog (S. cerevisiae)	0.8757	0.0332
ENSRNOG00000017193	leucine rich repeat and Ig domain containing 1	0.8772	0.0429
ENSRNOG00000021691	coiled-coil domain containing 92	0.8780	0.0440
ENSRNOG00000003990	growth factor receptor bound protein 2	0.8782	0.0341
ENSRNOG00000007732	solute carrier family 35, member C1	0.8787	0.0382
ENSRNOG00000002142	CDP-diacylglycerol synthase 1	0.8800	0.01513
ENSRNOG00000017209	tubulin, beta 3	0.8804	0.0182
ENSRNOG00000020433	actinin alpha 4	0.8809	0.0310
ENSRNOG00000016122	3-hydroxy-3-methylglutaryl-Coenzyme A reductase	0.8817	0.0153
ENSRNOG00000013194	ribosomal protein S6 kinase polypeptide 2	0.8821	0.0368
ENSRNOG00000002746	follistatin-like 1	0.8829	0.0151

Appendix Table 2: Complete list of annotated genes upregulated in the DRG one month post-T3x sorted by fold change (continued X)

Gene ID	Gene description	Fold change	Adj. p-value
ENSRNOG00000007400	sterol regulatory element binding transcription factor 2	0.8836	0.0426
ENSRNOG00000013603	DNA fragmentation factor, alpha subunit	0.8840	0.0280
ENSRNOG00000002949	phosphatidylglycerophosphate synthase 1	0.8843	0.0255
ENSRNOG00000025000	glycine-, glutamate-, thienylcyclohexylpiperidine-binding protein	0.8849	0.0332
ENSRNOG00000019282	ubiquilin 1	0.8854	0.0136
ENSRNOG00000018404	alanyl-tRNA synthetase	0.8856	0.0214
ENSRNOG00000049975	zinc finger protein 46	0.8869	0.0483
ENSRNOG00000009761	tropomodulin 1	0.8874	0.00614
ENSRNOG00000007912	chromogranin A	0.8880	0.0397
ENSRNOG00000002575	SAP30-like	0.8881	0.0368
ENSRNOG00000016923	CLPTM1-like	0.8881	0.0476
ENSRNOG00000032884	sodium channel, voltage-gated, type XI, alpha	0.8884	0.0388
ENSRNOG00000007496	myotubularin related protein 4	0.8885	0.0110
ENSRNOG00000008802	DnaJ (Hsp40) homolog, subfamily C, member 11	0.8900	0.0333
ENSRNOG00000009625	dihydropyrimidinase-like 2	0.8905	0.0398
ENSRNOG00000018704	nucleolar and coiled-body phosphoprotein 1	0.8910	0.0254
ENSRNOG00000022216	active BCR-related gene	0.8922	0.0420
ENSRNOG00000016924	ATP citrate lyase	0.8931	0.0422
ENSRNOG00000000902	heat shock 105kDa/110kDa protein 1	0.8943	0.0290
ENSRNOG00000007710	ubiquitin specific peptidase 20	0.8949	0.0453
ENSRNOG00000019742	signal transducer and activator of transcription 3	0.8958	0.0280
ENSRNOG00000049681	AABR07031491.2	0.9009	0.0398
ENSRNOG00000024501	regulator of G-protein signaling 3	0.9016	0.0404
ENSRNOG00000020336	enhancer of zeste 1 polycomb repressive complex 2 subunit	0.9020	0.0485
ENSRNOG00000011511	serine/threonine kinase 24 (STE20 homolog, yeast)	0.9021	0.0477
ENSRNOG00000011572	kinesin light chain 1	0.9087	0.0379
ENSRNOG00000018255	cleft lip and palate associated transmembrane protein 1	0.9087	0.0382
ENSRNOG00000047179	amyloid beta precursor like protein 2	0.9128	0.0435
ENSRNOG00000022392	heat shock protein 8	0.9154	0.0388

Appendix Table 3: Complete list of annotated genes upregulated in the PG one month post-T3x sorted by fold change

Gene ID	Gene description	Fold change	Adj. p-value
ENSRNOG00000015999	cold inducible RNA binding protein	1.316	3.71E-05
ENSRNOG00000015685	major facilitator superfamily domain containing 3	1.310	0.00683
ENSRNOG00000014350	cysteine-rich, angiogenic inducer, 61	1.308	0.0352
ENSRNOG00000026447	patched domain containing 2	1.308	0.00701
ENSRNOG00000005392	nerve growth factor receptor (TNFR superfamily, member 16)	1.283	2.73E-06
ENSRNOG00000033402	similar to Glutathione S-transferase A1 (GTH1) (HA subunit 1) (GST-epsilon) (GSTA1-1) (GST class-alpha)	1.246	0.0248
ENSRNOG00000017752	methylcrotonoyl-Coenzyme A carboxylase 2 (beta)	1.241	0.0164
ENSRNOG00000000967	acetoacetyl-CoA synthetase	1.238	0.00299
ENSRNOG00000003809	spermidine/spermine N1-acetyl transferase 1	1.232	0.00235
ENSRNOG00000003217	lectin, galactoside-binding, soluble, 3 binding protein	1.224	0.00431
ENSRNOG00000042691	armadillo repeat containing 7	1.223	0.0416
ENSRNOG00000000974	zinc finger protein 358	1.221	0.0367
ENSRNOG00000015643	peripherin	1.220	1.59E-05
ENSRNOG00000012439	BH3 interacting domain death agonist	1.219	0.0365
ENSRNOG00000049944	solute carrier family 25 member 22, mitochondrial glutamate carrier	1.217	0.00487
ENSRNOG00000020881	FERM domain containing 8	1.211	2.07E-05
ENSRNOG00000032902	Y box binding protein 1	1.209	0.0378
ENSRNOG00000012260	DEAD-box helicase 25, GRTH; putative RNA helicases	1.202	0.0409
ENSRNOG00000019869	leucine rich repeat and fibronectin type III domain containing 1	1.199	0.0409
ENSRNOG00000010535	cadherin 18, type 2	1.199	0.0380
ENSRNOG00000021150	phospholipase C, beta 3 (phosphatidylinositol-specific)	1.192	0.00683
ENSRNOG00000004377	lipin 1	1.190	0.0221
ENSRNOG00000009872	potassium voltage-gated channel, subfamily H (eag-related), member 2	1.185	0.0164
ENSRNOG00000005905	phosphodiesterase 4B, cAMP specific	1.181	0.0175
ENSRNOG00000000476	zinc finger and BTB domain containing 22	1.181	0.0328
ENSRNOG00000013953	neurotrophic tyrosine kinase, receptor, type 1	1.178	0.0297

Appendix Table 3: Complete list of annotated genes upregulated in the PG one month post-T3x sorted by fold change (continued)

Gene ID	Gene description	Fold change	Adj. p-value
ENSRNOG00000010712	telomeric repeat binding factor 2, interacting protein	1.176	0.0111
ENSRNOG00000010617	signal peptide, CUB domain, EGF-like 1	1.176	0.00287
ENSRNOG00000007367	septin 4	1.175	0.00480
ENSRNOG00000016550	doublecortin-like kinase 2	1.168	0.0227
ENSRNOG00000019560	phosphodiesterase 2A	1.167	0.0409
ENSRNOG00000000975	mucolipin 1	1.165	0.0367
ENSRNOG00000015558	zinc finger protein 512B	1.162	0.0256
ENSRNOG000000033615	mitochondrially encoded NADH dehydrogenase 3	1.160	0.0431
ENSRNOG00000001629	tryptophan rich basic protein	1.159	0.00279
ENSRNOG000000006241	membrane associated ring-CH-type finger 7	1.159	0.0392
ENSRNOG00000019485	branched chain ketoacid dehydrogenase kinase	1.155	0.0391
ENSRNOG00000010146	necdin homolog (mouse)	1.152	0.0219
ENSRNOG00000017193	leucine rich repeat and Ig domain containing 1	1.152	0.0493
ENSRNOG00000007583	phosphorylase, glycogen; brain	1.148	0.00825
ENSRNOG000000009783	calcium/calmodulin-dependent protein kinase II gamma	1.148	0.00457
ENSRNOG00000001888	armadillo repeat gene deleted in velo-cardio-facial syndrome	1.135	0.0112
ENSRNOG00000012347	GATA binding protein 2	1.132	0.0238
ENSRNOG000000029941	glutamate receptor, ionotropic, N-methyl D-aspartate-associated protein 1 (glutamate binding)	1.128	0.0297
ENSRNOG00000019240	adenosine monophosphate deaminase 2 (isoform L)	1.126	0.0365
ENSRNOG00000014963	adhesion G protein coupled receptor G1	1.118	0.0493
ENSRNOG00000001295	S100 calcium binding protein B	1.113	0.0380
ENSRNOG00000018454	apolipoprotein E	1.110	0.0392
ENSRNOG00000016896	ribosomal protein L3; similar to 60S ribosomal protein L3 (L4)	1.102	0.0312
ENSRNOG00000029574	ribosomal protein S4, X-linked	1.093	0.0138

Appendix Table 4: Complete list of annotated genes downregulated in the PG one month post-T3x sorted by fold change

Gene ID	Gene description	Fold change	Adj. p-value
ENSRNOG00000015957	coagulation factor XIII, A1 polypeptide	0.6880	1.19E-05
ENSRNOG00000049882	adenylate cyclase activating polypeptide 1	0.7406	0.00121
ENSRNOG00000011992	solute carrier family 18 (vesicular monoamine), member 1	0.7453	0.00287
ENSRNOG00000003221	myocilin	0.7539	0.0223
ENSRNOG00000019140	Btg3 associated nuclear protein	0.7569	0.00487
ENSRNOG00000002810	glutamine-fructose-6-phosphate transaminase 2	0.7589	0.00806
ENSRNOG00000018808	vasoactive intestinal peptide	0.7764	0.000324
ENSRNOG00000020410	Tyrosine Hydroxylase	0.7780	0.00121
ENSRNOG00000016437	transmembrane 4 L six family member 4	0.7861	0.000299
ENSRNOG00000019622	chemokine (C-X-C motif) receptor 7	0.7933	0.0363
ENSRNOG00000008415	Ngfi-A binding protein 2	0.7949	3.71E-05
ENSRNOG00000001607	ADAM metallopeptidase with thrombospondin type 1 motif, 1	0.7989	0.00205
ENSRNOG00000000924	solute carrier family 7 (cationic amino acid transporter, y ⁺ system), member 1	0.8034	0.0332
ENSRNOG00000011823	transcription factor AP-2 beta	0.8041	0.00287
ENSRNOG00000007597	rhopilin, Rho GTPase binding protein 1	0.8066	0.0382
ENSRNOG00000012959	Ngfi-A binding protein 1	0.8069	0.00115
ENSRNOG000000038784	piezo-type mechanosensitive ion channel component 2	0.8082	0.0150
ENSRNOG000000021198	histone cluster 1, H2bl; similar to H2B histone family	0.8119	0.0181
ENSRNOG000000023778	glucosaminyl (N-acetyl) transferase 2, I-branching enzyme	0.8120	0.00784
ENSRNOG000000050655	prolyl 4-hydroxylase subunit alpha 1	0.8163	0.0468
ENSRNOG000000027016	Cobl-like 1	0.8167	0.00758
ENSRNOG00000015232	phosphatidylinositol-4-phosphate 5-kinase type 1 beta	0.8174	0.0391
ENSRNOG00000004048	leucine-rich repeat kinase 2	0.8192	0.000863
ENSRNOG00000002580	similar to C1orf25	0.8196	0.0297
ENSRNOG000000021824	DnaJ (Hsp40) homolog, subfamily B, member 1	0.8246	0.0294
ENSRNOG00000016419	PDZ and LIM domain 5	0.8286	0.0409
ENSRNOG00000004026	ATPase, Ca ⁺⁺ transporting, plasma membrane 1	0.8315	0.000324

Appendix Table 4: Complete list of annotated genes downregulated in the PG one month post-T3x sorted by fold change (continued I)

Gene ID	Gene description	Fold change	Adj. p-value
ENSRNOG00000001069	ELAV (embryonic lethal, abnormal vision, <i>Drosophila</i>)-like 1 (Hu antigen R)	0.8342	0.0164
ENSRNOG00000020918	cyclin D1	0.8366	0.00204
ENSRNOG00000011891	ATPase, H transporting, lysosomal V1 subunit B2	0.8368	0.00144
ENSRNOG00000033280	peptidylglycine alpha-amidating monooxygenase	0.8382	0.00118
ENSRNOG00000011977	sema domain, seven thrombospondin repeats (type 1 and type 1-like), transmembrane domain (TM) and short cytoplasmic domain, (semaphorin) 5A	0.8406	0.0373
ENSRNOG00000020871	latent transforming growth factor beta binding protein 4	0.8427	0.00577
ENSRNOG00000018982	ectonucleoside triphosphate diphosphohydrolase 3	0.8435	0.0447
ENSRNOG00000022999	protein phosphatase 2 (formerly 2A), regulatory subunit B", alpha	0.8447	0.00457
ENSRNOG00000012881	fibrinogen-like 2	0.8453	0.00968
ENSRNOG00000012826	cAMP responsive element binding protein 3-like 2	0.8456	0.0238
ENSRNOG00000001613	zinc finger and BTB domain containing 11	0.8473	0.0367
ENSRNOG00000012499	retinoic acid receptor, gamma	0.8475	0.00968
ENSRNOG00000012942	SATB homeobox 1	0.8493	0.0332
ENSRNOG00000016617	WW domain containing transcription regulator 1	0.8504	0.0392
ENSRNOG00000010819	heat shock protein 4 like	0.8529	0.0218
ENSRNOG00000007029	DnaJ (Hsp40) homolog, subfamily A, member 1	0.8572	0.00715
ENSRNOG00000008012	ATP-binding cassette, subfamily B (MDR/TAP), member 1B	0.8575	0.0416
ENSRNOG00000020726	signal-induced proliferation-associated 1	0.8605	0.0479
ENSRNOG00000010872	creatine kinase, brain	0.8612	0.000155
ENSRNOG00000015288	disco-interacting protein 2 homolog C	0.8613	0.0405
ENSRNOG00000012311	solute carrier family 35, member D3	0.8617	0.0319
ENSRNOG00000006576	BMS1 ribosome biogenesis factor	0.8625	0.0486
ENSRNOG00000004908	SMC6 structural maintenance of chromosomes 6-like 1 (yeast)	0.8626	0.0328

Appendix Table 4: Complete list of annotated genes downregulated in the PG one month post-T3x sorted by fold change (continued II)

Gene ID	Gene description	Fold change	Adj. p-value
ENSRNOG00000020248	internexin neuronal intermediate filament protein, alpha	0.8671	0.0164
ENSRNOG00000020347	nucleoporin 98kDa	0.8701	0.0164
ENSRNOG00000007808	nucleosome assembly protein 1-like 5	0.8738	0.0283
ENSRNOG00000006037	synaptosomal-associated protein 25	0.8773	0.0107
ENSRNOG00000026704	dystrophin related protein 2	0.8780	0.0409
ENSRNOG00000002079	mitogen activated protein kinase 10	0.8796	0.0373
ENSRNOG00000006604	Thy-1 cell surface antigen	0.8809	0.0409
ENSRNOG00000021681	early endosome antigen 1	0.8816	0.0382
ENSRNOG00000011305	SRY box 10	0.8847	0.0491
ENSRNOG00000004337	family with sequence similarity 20, member B	0.8884	0.0181

Appendix Table 5: Complete list of canonical pathway analysis of differentially expressed DRG genes, complete table with all z-scores

Canonical pathway	p-value	Ratio	z-score	genes
Actin cytoskeleton signaling	0.000248	0.066 (15/227)	-2.324	ACTN4, ARPC3, BRK1, CSK, F2R, FGFR1, GRB2, MYH9, MYH10, PAK1, PIK3CD, PIP4K2B, SLC9A1, TMSB10, VCL
Phosphatidylglycerol biosynthesis II (non-plastidic)	0.000271	0.192 (5/26)	-2.236	AGPAT1, CDS1, LPCAT1, LPCAT4, PGS1
TR/RXR activation	0.000414	0.092 (9/98)		ENO1, FASN, FGFR1, GRB2, LDLR, PIK3CD, RXRA, SLC16A2, SREBF2
AMPK signalling	0.000479	0.065 (14/216)	-0.632	CCND1, CHRNB2, FASN, GRB2, GYS1, HMGCR, PIK3CD, PPM1J, PRKAB1, RAB9B, RPTOR, SMARCA2, TSC2
Epithelial adherens junction signaling	0.000549	0.075 (11/146)		ACTN4, ARPC3, CDH1, FGFR1, MYH9, MYH10, NOTHCH1, TUBB3, VCL, YES1, ZYX
CDP-diacylglycerol biosynthesis I	0.002	0.167 (4/24)	-2.000	AGPAT1, CDS1, LPCAT1, LPCAT4
ILK signaling	0.00201	0.061 (12/197)	-1.732	ACTN4, CCND1, FGFR1, GRB2, MYH9, MYH10, NACA, PIK3CD, PPM1J, TMSB10, VCL
Spermine and spermidine degradation I	0.00304	0.5 (2/4)		SAT1, SMOX
CNTF signaling	0.0034	0.094 (6/64)	-2.449	CNTFR, FGFR1, GRB2, PIK3CD, RPS6KA2, STAT3
Remodeling of epithelial adherens junctions	0.00494	0.087 (6/69)		ACTN4, ARPC3, CDH1, TUBB3, VCL, ZYX
Aldosterone signaling in epithelial cells	0.00543	0.06 (10/168)	-2.236	DNAJB1, DNAJC7, DNAJC11, FGFR1, GRB2, HSPB8, HSPH1, PIK3CD, PIP4K2B, SLC9A1,
Rac signaling	0.0055	0.068 (8/117)	-1.134	ANK1, ARPC3, BRK1, FGFR1, GRB2, PAK1, PIK3CD, PIP4K2B
mTOR signaling	0.00677	0.055 (11/201)	-2.121	EIF3A, EIF3K, EIF3M, FGFR1, GRB2, PIK3CD, PPM1J, PRKAB1, RPS6KA2, RPTOR, TSC2

Appendix Table 5: Complete list of canonical pathway analysis of differentially expressed DRG genes, complete table with all z-scores (continued I)

Canonical pathway	p-value	Ratio	z-score	genes
Protein ubiquitination pathway		(13/265)		DNAJB1, DNAJC7, DNAJC11, HAPB8, HSPH1, PSMB1, PSMC6, PSMD6, SUGT1, UBE3B, UBE4B, USP19, USP20
Melanoma signaling	0.00835	0.091 (5/55)	-2.000	EIF3A, EIF3K, EIF3M, FGFR1, GRB2, PIK3CD, PPM1J, PRKAB1, RPS6KA2, RPTOR, TSC2
Regulation of cellular mechanics by calpain protease	0.00968	0.088(5/57)		ACTN4, CAST, CCND1, GRB2, VCL
Macropinocytosis signaling	0.0106	0.074 (6/81)	-2.000	ACTN4, FGFR1, GRB2, MRC1, PAK1, PIK3CD
Huntington's disease signaling	0.0129	0.048 (12/250)	-2.000	AP2A2, CASP4, DCTN1, DNAJB1, FGFR1, GRB2, HDAC4, NSF, PIK3CD, RPH3A, TCERG1, VTI1A
EIF2 signaling	0.0132	0.05 (11/221)	-0.378	CCDN1, EIF2S2, EIF3A, EIF3M, FGFR1, GRB2, PIK3CD, RPL5, RPL41, RPL18A,
Growth hormone signaling	0.0133	0.071 (6/85)	-2.236	FGFR1, GRB2, IGF2, PIK3CD, RPS6KA2, STAT3
Signaling by Rho Family GTPases	0.0137	0.048 (12/252)	-2.111	ARHGEF18, ARPC3, CDH1, CDH13, CDH19, FGFR1, GNAZ, GRB2, PAK1, PIK3CD, PIP4K2B, SLC9A1
NRF2-mediated oxidative stress response	0.0137	0.052 (10/193)		ABCC4, CLPP, DNAJB1, DNAJC7, FGFR1, GRB2, HSPB8, PIK3CD, TXN,
Amyotrophic lateral sclerosis signaling	0.0139	0.063 (7/111)	-2.236	FGFR1, GRB2, GRIN1, NEFH, NEFL, PAK1, PIK3CD
Paxillin signaling	0.0152	0.062 (7/113)	-1.89	ACTN4, CSK, FGFR1, GRB2, PAK1, PIK3CD, VCL
Endometrial cancer signaling	0.0155	0.078 (5/64)	-1.342	CCND1, CDH1, FGFR1, GRB2, PIK3CD
Axonal guidance signaling	0.0172	0.04 (18/453)		ADAMTS8, ARPC3, BMP6, DPYSL2, EPHB3, FGFR1, GNAZ, GRB2, KLC1, LINGO1, NTNG2, PAK1, PIK3CD, PLXNB2, RGS3, SEMA3G, TUBB, WNT6
Germ cell-sertoli cell junction signaling	0.0184	0.052 (9/173)		ACTN4, CDH1, FGFR1, GRB2, PAK1, PIK3CD, TUBB3, VCL, ZYX
Reelin signaling in neurons	0.0190	0.065 (6/92)		FGFR1, GRB2, MAPK8IP2, MAPK8IP3, PIKCD, YES1

Appendix Table 5: Complete list of canonical pathway analysis of differentially expressed DRG genes, complete table with all z-scores (continued II)

Canonical pathway	p-value	Ratio	z-score	genes
IL-9 signaling	0.0192	0.089 (4/45)	-2.000	FGFR1, GRB2, PIK3CD, STAT3
Pancreatic adenocarcinoma signaling	0.0205	0.058 (7/120)	-2.646	CCND1, FGFR1, GRB2, NOTCH1, PIK3CD, RALGDS, STAT3
ErbB2-ErbB3 signaling	0.0208	0.072 (5/69)	-2.236	CCND1, FGFR1, GRB2, PIK3CD, STAT3
RhoGD1 signaling	0.0210	0.051 (9/177)	0.707	ARHGAP12, ARHGEF18, ARPC3, CDH1, CDH13, CDH19, GNAZ, PAK1, PIP4K2B
Acetyl-CoA biosynthesis III (from citrate)	0.0292	1 (1/1)		ACLY
MSP-RON signaling pathway	0.0245	0.069 (5/72)		FGFR1, GRB2, MST1R, PIK3CD, RPS6KA2
PI3K/AKT signaling	0.025	0.056 (7/125)	-1.89	CCND1, GRB1, GYS1, PIK3CD, PPM1J, TSC2, YWHAG
IL-15 production	0.0255	0.107 (3/28)		IRF3, MST1R, TWF1
Superpathway of cholesterol biosynthesis	0.0255	0.107 (3.28)		ACAT1, DHCR24, HMGCR
GM-CSF signaling	0.0259	0.068 (5/73)	-2.236	CCND1, FGFR1, GRB2, PIK3CD, STAT3
FAK signaling	0.0262	0.061 (6/99)		CSK, FGFR1, GRB2, PAK1, PIK3CD, VCL
Regulation of eIF4 and p70S6K signaling	0.0283	0.051 (8/157)	-2.000	EIF2S2, EIF3A, EIF3K, EIF3M, FGFR1, GRB2, PIK3CD, PPM1J
VEGF signaling	0.0310	0.058 (6/103)	-1.342	ACTN4, EIF2S2, FGRF1, GRB2, PIK3CD, VCL
Non-small cell lung cancer signaling	0.0316	0.065 (5/77)	-2.000	CCND1, FGFR1, GRB2, PIK3CD, RXRA
IGF-1 signaling	0.035	0.057 (6/106)	-2.000	FGFR1, GRB2, IDFBP4, PIK3CD, STAT3, YWHAG
Ga12/13 signaling	0.0358	0.052	-1.134	CDH1, CDH13, CDH19, F2R, FGFR1, GRB2, PIK3CD
Oxidative phosphorylation	0.0393	0.055 (6/109)	2.449	ATP5MF, MT-CO2, MT-ND3, NDUFB9, NDUFS4, UQCRC2
IL-3 signaling	0.0417	0.06 (5/83)	-2.236	FGFR1, GRB2, PAK1, PIK3CD, STAT3

Appendix Table 5: Complete list of canonical pathway analysis of differentially expressed DRG genes, complete table with all z-scores (continued III)

Canonical pathway	p-value	Ratio	z-score	genes
Renal cell carcinoma signaling	0.0417	0.06 (5/83)	-2.000	EGLN3, FGFR1, GRB2, PAK1, PIK3CD
Tec kinase signaling	0.0422	0.047 (8/170)	-1.89	FGFR1, GNAZ, GRB2, PAK1, PIK3CD, STAT3, TNFRSF21, YES1
3-phosphoinositide biosynthesis	0.0422	0.045 (9/201)	-2.333	ALPL, FGFR1, GRB2, MDP1, MTMR4, PHOSPHO1, PIK3CD, PIP4K2B, PTPRN
Telomerase signaling	0.0423	0.054 (6/111)	-2.000	FGFR1, GRB2, HDAC4, PIK3CD, POT1, PPM1J
Insulin receptor signaling	0.0436	0.05 (7/141)	-1.89	ACLY, FGFR1, GRB2, GYS1, PIK3CD, RPTOR, TSC2
B-alanine degradation I	0.0452	0.5 (1/2)		ABAT
Palmitate biosynthesis I	0.0452	0.5 (1/2)		FASN
Fatty acid biosynthesis initiation II	0.0452	0.5 (1/2)		FASN
Cardiolipin	0.0452	0.5 (1/2)		FASN
Small cell lung cancer signalling	0.0454	0.059 (5/85)	-2.000	CCDN1, FGFR1, GRB2, PIK3CD, RXRA
Breast cancer regulation by stathmin1	0.0468	0.044 (9/205)		ADCY5, ARHGEF18, FGFR1, GRB2, PAK1, PIK3CD, PPM1J, RB1CC1, TUBB3
Leptin signaling in obesity	0.0473	0.058 (5/86)	-2.000	ADCY5, FGFR1, GRB2, PIK3CD, STAT3
Ephrin A signaling	0.0484	0.067 (4/60)		FGFR1, GRB2, PAK1, PIK3CD
Ephrin B signaling	0.0485	0.046 (8/175)	-1.134	ARPC3, EPHB3, GNAZ, GRB2, GRIN1, PAK1, RGS3, STAT3
HGF signaling	0.0488	0.052 (6/115)	-2.449	CCND1, FGFR1, GRB2, PAK1, PIK3CD, STAT3
FLT3 signaling in hematopoietic progenitor cells	0.0493	0.057 (5/87)	-2.236	FGFR1, GRB2, PIK3CD, RPS6KA2, STAT3

Rows highlighted in green or red have z-scores $>|2|$ and are found in Table 2.7